Limbic Generators of Incentive Motivation and Aversive Motivation

by

Hannah M. Baumgartner

A dissertation submitted in partial fulfillment
of the requirements for the degree of
Doctor of Philosophy
(Psychology)
in the University of Michigan
2021

Doctoral Committee:

Professor Kent C. Berridge, Chair
Assistant Professor Ada Eban-Rothschild
Associate Professor Shelly B. Flagel
Associate Professor Natalie C. Tronson

Hannah M. Baumgartner

hmbaum@umich.edu

ORCID iD: 0000-0002-8385-9229

Dedication

This dissertation is dedicated to my aunt Una Mae Hargrave, a pioneer for community action and civil rights in south Louisiana.

Acknowledgements

Thank you to my advisor, Dr. Kent Berridge, who through mentorship and example has taught me what a scientist should strive to become. It was a privilege to be in your lab. I would also like to thank my committee members Drs. Shelly Flagel, Ada Eban-Rothschild, and Natalie Tronson. These impressive and brilliant women have supported me through many stages of my graduate career with much advice and enthusiasm. Thank you to the various scientific mentors and colleagues I have had throughout my career, especially Drs. Jay Schulkin, Terry Robinson, Paul Currie, and Michael Pitts.

I would like to acknowledge the various family members, mentors, and friends who fought tirelessly to give me educational opportunities beyond what seemed remotely attainable, allowing me to pave my own path. I owe these women and more, including Debbie Hargrave, Melinda Mangham, my late aunt Una Mae Hargrave, and my grandmother Marian Hargrave, for helping me along this path from a rice farmer's family to a PhD.

Of course, none of this would have been possible without the love and support from my parents, Molly Baumgartner and George Baumgartner, who did everything within their power to provide the best educational opportunities for Nina and me. Thank you both for instilling a limitless sense of curiosity and confidence in us, and love along the way. Thank you to my new parents Donna Vukelich and Claudio Selva, who provided so much excitement (and winter clothing) at every stage of my graduate career. And despite our best efforts, thank you to Nina Baumgartner whose parallel path has been an anchor for me from the beginning.

Throughout my PhD I have been lucky enough to be surrounded by a thoughtful and supportive community of scholars. I specifically want to acknowledge Erin Naffziger, who may be the single biggest factor in my completion of this dissertation, and Ileana Morales, who I have been able to look up to and grow with for nearly a decade of our scientific careers. I also want to thank the other wonderful members of the Berridge lab who always made research a joy, including Shayan Abtahi and Drs. Shelley Warlow, Shannon Cole, Jeffrey Olney, David Nguyen, Kevin Urstadt, Yan Xiong, and Koshi Murata. The support and brilliance of these colleagues were a major driver in my scientific growth. I want to thank Madeliene Ayoub who has been a critical factor in nearly my entire PhD research, as a research assistant, thesis student, lab manager, and a scientific colleague, as well as my other amazing thesis students throughout the years including Elizabeth Hubbard, Laura Huerta Sanchez, Alex Baum, and Tayah Schuette. Finally, nothing in the Berridge lab would have been remotely possible without the tireless work

done by our lab managers throughout the years, including Josh Goldman, Nina Mostovoi, Marco Liera, and Madeliene Ayoub, nor without the diligent and integral work provided by our ULAM staff, including Scarlett Dulisch and many more wonderful animal care technicians that I have been able to work with throughout the years. An additional thank you to Justin Roeloff, for fixing and creating the various technical parts of my experiments as well as the pleasant presence he always provides.

To the wonderful peers in my program and beyond, thank you for creating a supportive and collaborative scientific environment. In particular, thank you to my amazing cohort, Cassandra Avila, Sofia Carrera, Caitlin Posillico, Jacqueline Quigley, and Anne Sabol. I was incredibly lucky to have these brilliant scholars and welcoming friends throughout my graduate career and associated medical emergencies. Thank you to Sarah Westrick, whose dissertation and career growth I had the privilege of watching between interrupting her work at our adjacent desks. And a truly big thank you to the phenomenal community of Biopsychology and Neuroscience graduate students past and present I have been lucky enough to be surrounded by, particularly Amanda Iglesias, Mena Davidson, Patricia Delacey, Rosemary Bettle, Christopher Turner, Carlos Vivaldo, Harini Suri, Eryn Donovan, Ivette Gonzalez, and Sharena Rice. And thank you to the impressive former students I have had the privilege of looking up to, including Drs. Crystal Carr, Kyra Phillips, Katie Yoest, and Natalie Nevarez.

To my wonderful husband Joaquín, the single biggest supporter of my career and personal growth. Even the intellectual journey of completing my PhD was never solitary, as your selflessness and encouragement was an integral piece of the story beyond any other.

Finally, I would like to acknowledge the funding and support that made this work possible from the National Institute of Health, including my Ruth L. Kierschtein National Research Service Award (F31 DA047738) and the University of Michigan NIDA training grant (T32 DA007281).

Table of Contents

Dedication ii
Acknowledgements iii
List of Tables vii
List of Figures viii
Abstract ix

CHAPTER I. Introduction 1

CHAPTER II. 'Desire' and 'Dread' From Nucleus Accumbens Inhibitions: Reversed by Same-Site Optogenetic Excitations. 13
Introduction 13
Materials and Methods 16
Results 26
Discussion 44
Figures 50
Tables 57

CHAPTER III. Corticotropin Releasing Factor Systems in Nucleus Accumbens, Amygdala, and Bed Nucleus of Stria Terminalis: Incentive Motivation Versus Aversive Roles. 60
Introduction 60
Materials and methods 63
Results 67
Discussion 75
Figures 81
Tables 96

CHAPTER IV. Corticotropin Releasing Factor (CRF) Systems Promoting Cocaine Pursuit: Through Distress or Incentive Motivation? 98
Introduction 98
Methods 101
Results 108
Discussion 115
Figures 121
Tables 131

CHAPTER V. General Discussion **132**

Appendix A: Chapter III Supplementary information 150
References 167

List of Tables

2.1 Structures of interest for distributed Fos analysis 57
2.2 Unilateral vs bilateral alignment of fiber/cannula tips for within-subjects groups 58
2.3 Between-subjects alignment of fiber/cannula tips for ChR2 animals only 59
3.1 Histological placements of experimental animals 96
3.2 Brain regions assessed for laser-recruited changes in Fos expression 97
4.1 Histological placements of experimental animals 131
A.1 Brain-wide Fos activation from CRF system excitation in NAc, CeA, or BNST 166

List of Figures

2.1 Representative fiber-cannula alignment, virus, and Fos expression in NAc shell..... 50
2.2 Same-site laser reverses distant Fos activation induced by NAc DNQX microinjections 51
2.3 Aligned ChR2 laser reverses DNQX increases in food intake 52
2.4 NAc maps of increases induced by DNQX microinjections and reversals by laser..... 53
2.5 ChR2 laser reverses caudal 'fear' as well as rostral 'desire' from DNQX microinjections 54
2.6 NAc maps of DNQX-induced caudal 'fear' and rostral 'desire' and laser reversals 55
2.7 Alignment of fiber and cannula tips required to reverse DNQX-elicited motivation..... 56
3.1 Localization of function maps 81
3.2 Virus expression and local Fos plumes..... 82
3.3 CRF and Cre colocalization verification through fluorescence in situ hybridization..... 84
3.4 Laser-enhancements in distant Fos expression..... 85
3.5 CRF-containing neuron stimulation in NAc biases and amplifies sucrose motivation 87
3.6 CRF-containing neuron stimulation in CeA biases and amplifies sucrose motivation 89
3.7 BNST CRF-containing neuron stimulation is avoided and suppresses sucrose motivation.. 91
3.8 Laser spout self-stimulation by NAc and CeA *Crh*-Cre+ rats, not BNST 93
3.9 Place-based self-stimulation and aversion of CRF-containing neuron stimulation..... 94
4.1 Photomicrograph of virus expression and local Fos plumes. 122
4.2 Localization of function maps 123
4.3 Distant Fos recruitment from NAc, CeA, or BNST CRF-containing neuron excitation..... 125
4.4 NAc CRF-containing neuronal stimulation biases and amplifies cocaine motivation 126
4.5 CeA CRF-containing neuronal stimulation biases and amplifies cocaine motivation 127
4.6 BNST CRF system stimulation fails to direct or enhance escalation of cocaine pursuit 128
4.7 Differences in cocaine escalation for NAc and CeA versus BNST ChR2 groups..... 129
4.8 Spout self-stimulation of NAc and CeA CRF-containing neurons, not BNST 130
A.1 Female and male groups across behavioral tests 158
A.2 Two-choice extended data 159
A.3 Progressive ratio extended data..... 160
A.4 Spout self-stimulation extended data 161
A.5 Place-based self-stimulation extended data 162
A.6 Halorhodopsin pilot data..... 163

Abstract

Striatal-level structures such as the nucleus accumbens (NAc) and central amygdala (CeA) are capable of generating intense incentive and aversive motivated behaviors (Baumgartner et al. 2020; Warlow et al. 2020). NAc may have two modes for motivation, as inhibition and excitation of NAc can both produce motivated behaviors. For example, NAc medial shell inhibition through AMPA receptor antagonist (DNQX) microinjections can produce both intense eating and defensive behaviors (Baumgartner et al., 2020). Chapter 2 of this dissertation investigates the inhibition hypothesis of accumbens motivation generation by testing whether local pairing of optogenetic excitation can disrupt 'desire' and 'dread' behaviors generated by DNQX microinjections.

Incentive and aversive motivation generated by NAc and other limbic structures are flexible and able to respond to external stressors. Chapter 3 therefore investigates a previously untested neuronal population in NAc that expresses corticotropin-releasing factor (CRF), a stress-related peptide heavily implicated in aversive motivation and distressing drug-withdrawal states in CeA and bed nucleus of stria terminalis (BNST). Like NAc, the CeA is also capable of producing intense positive and negative motivated behaviors and we investigate the flexibility of incentive or aversive motivation in CRF neurons using new *Crh*-Cre+ rats to optogenetically stimulate NAc, CeA, or BNST CRF-containing neurons. This work finds that excitation of CRF-expressing neurons is capable of biasing and amplifying motivation for sucrose rewards in both NAc shell and lateral CeA (Baumgartner et al. 2021). Conversely, it also demonstrates that optogenetic excitation of pallidal-like bed nucleus of stria terminalis (BNST) CRF-containing

neurons produces only negative affect and aversive motivation, filling the traditional role that CRF has been hypothesized to play in aversive withdrawal and affect (Koob 2013).

Following the demonstrated positive role of NAc and CeA CRF-containing neurons for sucrose rewards, Chapter 4 of this dissertation examines whether this influence on incentive motivation also applies to drug rewards. CRF in CeA and BNST is posited to underlie aversive withdrawal states, causing negative distress that leads to addictive relapse through attempts at hedonic self-medication to relieve this state (Koob 2013). Chapter 4 therefore tests whether optogenetic excitation of CRF neurons in NAc, CeA, and BNST are capable of biasing and amplifying motivation for self-administered intravenous cocaine infusions. Understanding whether CRF-mediated incentive motivation also can drive drug motivation is therefore integral. We find that NAc and CeA CRF-expressing neurons are indeed capable of biasing motivation for cocaine infusions, while rats given the option between BNST CRF-containing neuron-paired cocaine and cocaine alone show no drug escalation or preferences between cocaine options.

Altogether this dissertation demonstrates the limbic generation of intense motivation in structures such as NAc and CeA, and how both incentive and aversive motivation can be modulated by stress and brain CRF systems. The neural mechanisms underlying these different motivational valences provide important insight into cases where motivation can become pathological, such as in addiction, schizophrenia, and other psychological disorders.

CHAPTER I. Introduction

"Is emotion a magic product, or is it a physiologic process which depends on an anatomic mechanism?" posed James Papez as he described a circuit of emotion that formed the basis of the limbic system (Papez 1995). While the specific structures and corresponding "streams" for feeling, thought, and top-down emotion have been refined from the original Papez circuit, the notion of a limbic system framework has long withstood time. These ideas greatly influenced Maclean in his contributions in both structure and function to this theoretical limbic system, leading to a hypothesized evolutionary origin of an emotional brain (Maclean 1949). Further, he made a distinction between the advanced mammalian brain and a primitive "visceral" brain, the latter of which proposed to be the basis of evolved emotional functioning (Maclean 1949). This collection of communicating structures was named the "limbic system", coined from "le grand lobe limbique" described by Broca (Broca 1978; Maclean 1949). While the usefulness of this theoretical framework has since been debated (LeDoux 1993; Ledoux 1991), the existence of interconnected neural systems that regulate affective states and motivated behaviors is certain.

The range of positively- and negatively-valenced motivated behaviors, from eating to escaping, are produced by limbic system structures largely preserved across species. Striatal-level structures in particular are heavily implicated in generating these motivated behaviors and affective states (DiFeliceantonio and Berridge 2016; DiFeliceantonio et al. 2012; Meredith et al.

2008; Robinson et al. 2014; Stratford and Kelley 1997; Swanson 2005; Warlow et al. 2020). Striatal-level structures such as the ventral striatum, central amygdala, and dorsal striatum are thought to have similar morphological, developmental, and neuroanatomical characteristics within a cortico-striatal-pallidal macrosystem framework, and may potentially play similar roles in motivation (Alheid and Heimer 1988; Alheid 2003; Heimer and Van Hoesen 2006; Heimer et al. 2007; Swanson 2005; Zahm 2006). For example, the nucleus accumbens (NAc) and ventral striatum dopamine have long been seen as a key mediator of reward-related behaviors and incentive motivation, following original designations as a "limbic-motor interface" (Herrick 1926; Meredith et al. 2008; Mogenson et al. 1980). Alternatively, stress-mediated aversive motivation is heavily associated with the striatal-level central amygdala and its connections with the pallidal-level bed nucleus of the stria terminalis (Alheid and Heimer 1988; Erb et al. 2001a; Koob et al. 2014; Minami 2019; Pomrenze et al. 2019b; Ventura-Silva et al. 2020). In particular, corticotropin releasing factor (CRF) systems in these extended amygdala nuclei are thought to underlie brain stress responses and associated negative affective states (Asok et al. 2018; Fadok et al. 2017; Koob and Schulkin 2019; Koob et al. 2014; Pomrenze et al. 2019b, 2019a; Ventura-Silva et al. 2020). Therefore, NAc and brain CRF systems provide powerful neural mechanisms for generating both positively- and negatively-valenced motivated behaviors, respectfully.

However, the ability for an organism to adapt for different survival needs implies that the neural mechanisms underlying incentive and aversion motivation must interact in response to changing internal and external states. This evolutionary necessity therefore raises the question of how limbic generators of motivated behaviors can maintain this flexibility of affective states?

Nucleus accumbens generation of incentive motivation

The early evidence that supported a role for the ventral striatum and accumbens dopamine in the initiation of movement, additionally implicated accumbens dopamine as key mediators of appetitive motivation. For example, the observation that 6-OHDA lesions of dopamine in NAc can block amphetamine-induced locomotion could alternatively be interpreted to suggest that NAc dopamine is necessary for the rewarding effects caused by amphetamine, thus reducing subsequent behavioral effects (Kelly 1975). Early anatomical and behavioral observations caused Mogenson and colleagues to propose that NAc may act as a "limbic-motor" interface, particularly through inputs from ventral tegmentum (VTA) and hypothesized motor information outputs to the globus pallidus (Haber and Knutson 2010; Herrick 1926; Mogenson et al. 1980). While original observations were interpreted through a locomotor control perspective, the identification of VTA to NAc projections as being integral to limbic function laid a foundation for future incentive motivation investigations. Eventually, the possibility of NAc being integral to affective states and reward-motivated behaviors grew widespread, strongly supported by electrode self-stimulation work (Mogenson et al. 1979; Phillips 1984; Van Ree and Otte 1980; Rolls 1971). The NAc is now understood to have a critical and comprehensive role in motivated behaviors and positive affective states, such as eating, reward-seeking, and pleasure (Berridge and Robinson 1998; Carlezon and Wise 1996; Castro and Bruchas 2019; Kalivas and Duffy 1990; Peciña and Berridge 2000, 2005; Wang et al. 2016).

Attempts to delineate the mechanisms through which the accumbens can generate the range of affective states and motivated behaviors have had some degree of success. For instance, separate components of nucleus accumbens shell and core have been linked to different aspects of reward cue learning, motivated behavior, and incentive salience, and can be distinguished by different anatomical and morphological profiles (Corbit et al. 2001; Heimer et al. 1991; Jongen-

Rělo et al. 1993; Kelley and Swanson 1997; Meredith et al. 1989, 2008; Parkinson et al. 1999; Voorn et al. 1989; Záborszky et al. 1985). The NAc medial shell in particular is heavily implicated in incentive motivation, and its wide range of connections has previously caused it to been called the "viscero-endocrine striatum" (Kelley 1999). The medial shell also receives the densest dopaminergic inputs from the ventral tegmentum (Voorn et al. 1986; Zahm 1992), therefore anatomically supporting its strong role in mediating incentive motivation through integral dopamine signaling. However, it is actually the heterogeneity of neuronal populations that has been proposed to be critical to the versatility of NAc-mediated motivated behaviors, relying on substantial non-dopaminergic mechanisms (Meredith et al. 2008). Indeed many other neural systems have been implicated in the generation of appetitive motivation by accumbens medial shell, such as cortical glutamatergic inputs, GABAergic medial spiny neurons (MSNs), mμ opioid receptor activation, and cholinergic interneurons (Bals-Kubik et al. 1993; Castro and Berridge 2014; Castro and Bruchas 2019; Faure et al. 2010; Kelley and Swanson 1997; Richard and Berridge 2011a; Richard et al. 2013b, 2013a).

Accumbens shell motivational mechanisms

NAc medial shell, as a striatal-level structure in a macrosystem framework (Alheid and Heimer 1988; Heimer and Van Hoesen 2006; Heimer et al. 2007; Zahm 2006), is a powerful mediator of both positively- and negatively-valenced 'wanting' modes throughout the rostral-caudal axis. NAc may also have two major modes for initiation of these behaviors, as both *inhibition* and *excitation* of NAc can both produce motivated behaviors (O'Donnell and Grace 1995; O'Donnell et al. 1999). For example, original electrode self-stimulation studies support the finding that excitation of NAc is reinforcing and positively-valenced (Mogenson et al. 1979; Phillips 1984; Van Ree and Otte 1980; Rolls 1971). Further, countless modern pharmacology

and optogenetic studies demonstrate that NAc activation can generate intense motivation (Cole et al. 2018; Koo et al. 2014; Lex and Hauber 2008; Lobo et al. 2010; Schmidt et al. 2006).

However, a long history of research instead provides support for an alternative hypothesis that NAc generates motivation via relative neurophysiological *inhibition* of NAc MSNs (Carlezon and Wise 1996; Carlezon and Thomas 2009; Cheer et al. 2005; Krause et al. 2010; Meredith et al. 2008; Roitman et al. 2005, 2008, 2010; Taha et al. 2006; Wheeler et al. 2008). For example, while inhibition of NAc medial shell through AMPA receptor antagonist (e.g., DNQX) microinjections can produce intense eating and appetitive behaviors, these same manipulations can also elicit fearful defensive treading in rats (Reynolds and Berridge 2008; Richard and Berridge 2011b; Richard et al. 2013b). Microinjections of $GABA_A$ agonist muscimol show similar incentive and aversive effects, further supporting the notion of an inhibitory NAc motivational mode (Covelo et al. 2014; Faure et al. 2010; Reynolds and Berridge 2001, 2002, 2008; Richard and Berridge 2011b; Richard et al. 2013b; Stratford and Kelley 1997; Stratford and Wirtshafter 2012).

The proposed mechanism for these muscimol and DNQX effects is through the largely supported disinhibition hypothesis of motivation generated by NAc shell. Based on both pharmacological and electrophysiological evidence, this theory posits that NAc neuronal inhibition causes *disinhibition* of structures downstream from NAc, such as lateral hypothalamus (LH), VTA, and ventral pallidum (Heimer et al. 1991; Humphries and Prescott 2010; Lu et al. 1998; Mogenson et al. 1983; Usuda et al. 1998; Zahm and Heimer 1990; Zhou et al. 2003). Thus, it is hypothesized that releasing these targets from tonic GABAergic suppression therefore releases related motivated behaviors. However, while the disinhibition theory remains largely popular, it has not been directly tested previously.

Examining NAc disinhibition hypothesis

NAc DNQX- and muscimol-elicited 'desire' and 'dread' effects have been hypothesized to act through this disinhibition hypothesis, but this has never been explicitly tested. In Chapter 2, we tested whether local neuronal inhibition is *necessary* for microinjections of the glutamate AMPA antagonist DNQX in the rostral medial shell of nucleus accumbens, to generate intense appetitive motivation to consume food reward (i.e., 'desire'), or in caudal NAc shell, to generate behavioral antipredator reactions that reflect intense defensive motivation (i.e., 'dread'). To do this we added optogenetic ChR2 excitation at the same NAc site as concurrent DNQX microinjections, to test whether local neuronal excitation prevents glutamate AMPA blockade from generating robust appetitive or defensive behaviors. Finally, we also investigated whether NAc relative inhibition by DNQX produces GABAergic disinhibition of downstream limbic structures into excitation as predicted by the disinhibition hypothesis, by assessing distant Fos activation in those structures.

Chapter 2 provides direct support for an inhibition-based mechanism for motivation in NAc shell, and further demonstrates that these neural mechanisms underlying incentive and aversive motivation can be overlapping and even occur by the same brain manipulations. Here we also show how a stressful environment can change appetitive manipulations to become aversive, supporting the flexibility of limbic control of affective valence. However, while stress is typically assumed to be aversive and a negatively-valenced driver of motivation, is that universally the case?

Aversive motivation neural mechanisms

The psychological drives underlying incentive motivation are intuitively straightforward. An organism must have the ability to direct motivation to external stimuli to obtain resources

necessary for survival, and the attribution of incentive salience to these stimuli can enhance the success of these abilities. Aversive motivation has also been hypothesized to elicit motivation, though often through separate psychological mechanisms. Drive-reduction theories posit that motivation to pursue a goal is elicited to relieve an aversive state, thus making the act of *reducing the drive* the reward, rather than the object of the directed motivation (Hull 1951; Miller 1971). In modern psychological theories of drive-reduction, this aversive state elicited by an increasing motivational drive is often described as *distressing*, suggesting an integral role of brain stress systems in these aversive experiences (Koob and Volkow 2010; Koob et al. 2014).

When investigating brain stress systems and neural mechanisms underlying aversive motivation, perhaps the most evoked neural mediator is corticotropin-releasing factor (CRF). CRF is a 41-amino acid peptide, also known as corticotropin-releasing hormone in the peripheral nervous system for its role in initiation of the hypothalamic-pituitary-adrenal axis (Sutton et al. 1982; Vale et al. 1981). CRF release is triggered in the brain by a diverse range of external stressors to initiate behavioral and physiological stress responses, and CRF is therefore viewed as one of the most integral brain stress molecules (Koob et al. 2014). CRF is densely expressed in the paraventricular nucleus of the hypothalamus to initiate peripheral stress responses, though CRF-containing neurons and CRF1 and CRF2 receptors are widely distributed throughout the brain (Dabrowska et al. 2016, 2013; Lemos et al. 2019; Makino et al. 1994a, 1994b; Merchenthaler 1984; Merchenthaler et al. 1984; Peng et al. 2017; Schulkin 2017; Swanson et al. 1983).

Decades of research have now linked extra-hypothalamic CRF systems to a full range of affective and physiological negative *distress* states. For example, activation of CRF systems through intraventricular microinjections in mice and rats mimic arousal and anxiety-like

responses to natural stressors and can enhance "emotionality" as predicted in aversive distress states (Dunn and Berridge 1990; Heinrichs and Joppa 2001; Hupalo et al. 2019; Koob and Bloom 1985). CRF-containing neuronal populations are additionally linked to a wide spectrum of negatively-valenced affective behaviors, including anxiety, pain, fear and fear learning, and drug withdrawal (Asok et al. 2018, 2016; Fadok et al. 2017; Funk et al. 2006; Minami 2019; Pomrenze et al. 2019b, 2019a; Sahuque et al. 2006; Takahashi et al. 2019; Tran et al. 2014). With the wide range of aversive motivational states that CRF could potentially initiate through activation, alterations in brain CRF systems have been hypothesized to play a role in many neuropsychiatric conditions including depression, generalized anxiety disorder, post-traumatic stress disorder, and most prominently, addiction (Dunlop et al. 2017; Epstein et al. 2016; Erb and Brown 2006; Koob 2010, 2013; Koob et al. 2014; Schwandt et al. 2016; Simms et al. 2014; Spierling and Zorrilla 2017; Tollefson et al. 2017; Zorrilla and Koob 2004).

Opponent-process theory of addiction

Perhaps the most notable drive-reduction theory in modern neuroscience builds upon this hypothesized role of CRF in mediating aversive *distress*, positing that drive-reduction can spur motivation to overcome these negative states. The allostatic theory of addiction, also known as the opponent-process, hedonic homeostatic dysregulation, or hyperkatifeia theory of addiction, further hypothesizes that distress states are key to explaining continued drug use and addictive relapse (Koob and Le Moal 1997, 2008; Koob and Schulkin 2019; Koob 2010, 2013). The original opponent-process theory of Solomon and Corbit described a motivational *a*-process which causes an A-state that is positive and euphoric, though slowly decreases in strength over time (Solomon and Corbit 1978; Solomon 1980). The *a*-process also initiates a *b*-process, which causes a nasty, aversive B-state that increases over time. Koob and colleagues modify this

theory into a neuroscientific theory of addiction, where taking addictive drugs activates the *a*-process leading to a euphoric, pleasant state (i.e., the "high" a drug causes), though the strength of this A-state decreases over time due to drug tolerance (Koob and Le Moal 1997, 2008). However, what is posited to drive continued drug use is that the *a*-process also activates the opponent *b*-process and the subsequent negative aversive B-state, in this case linked to distressing withdrawal from drug use. Just as the A-state wanes over repeated drug use, the opponent B-state grows over time and causes continued drug pursuit and consumption through attempts at self-medicating this escalating aversive withdrawal state. Neurochemically, this withdrawal-induced distressing B-state is posited to be driven largely by enhancement and activation of brain CRF systems, particularly in the extended amygdala (Funk et al. 2006; Koob and Le Moal 1997, 2008; Koob and Schulkin 2019; Koob 2010, 2013; Olive et al. 2002; Park et al. 2013; Zorrilla et al. 2014).

Traditionally CRF's role in aversive motivation is heavily implicated in the extended amygdala regions of the central amygdala (CeA) and bed nucleus of stria terminalis (BNST), which contain dense extra-hypothalamic CRF neuron populations (Erb et al. 2001a; Heinrichs et al. 1995; Pomrenze et al. 2019b, 2019a; Rinker et al. 2017; Sahuque et al. 2006). However, the evoked concept of the extended amygdala in the opponent-process theory of addiction also includes transitional parts of the medial accumbens shell, which contains a population of sparse and relatively unexamined CRF-containing neurons (Koob and Schulkin 2019; Koob 2010, 2013; Lemos et al. 2012, 2019). While many negatively-valenced states driven by CRF systems have been documented, a role in *positive* motivational mechanisms remains relatively unexplored (Lemos and Alvarez 2020). Given the integral role that these CRF-neuronal populations are

posited to have in addictive behaviors and a variety of other affective neuropsychiatric disorders, investigating potential incentive motivation mechanisms is critical.

CRF-mediated incentive and aversive motivation for sucrose rewards

As an integral stress-related neurotransmitter, CRF-containing neurons offer potential mechanisms for amplifying incentive motivation, such as a surge in incentive salience and reward consumption following a positively experienced stressor. In line with this, NAc CRF microinjections cause surges in cue-triggered 'wanting' in a Pavlovian Instrumental Transfer (PIT) task, equivalent to dopamine-stimulating amphetamine microinjections (Peciña et al. 2006). Similarly, NAc CRF microinjections cause conditioned place-preferences and stimulate local dopamine release in unstressed mice (Lemos et al. 2012).

CRF-containing neurons in the CeA and BNST have long been implicated in motivated behaviors. While CRF in CeA and BNST has largely been assumed to drive negative and aversive motivational effects such as anxiety and distress (Asok et al. 2018; Fadok et al. 2017; Funk et al. 2007; Koob 2013; Partridge et al. 2016; Pomrenze et al. 2019b; Sahuque et al. 2006; Tran et al. 2014), there is some evidence that CeA CRF-containing neurons at least may also contribute to positive incentive effects as well. Specifically, mice will self-stimulate for optogenetic excitation of CRF-containing neurons in this striatal-level structure (Kim et al. 2017).

Chapter 3 of this dissertation therefore examines the potential incentive and aversive motivational roles of CRF-containing neurons in NAc, CeA, and BNST using new transgenic *Crh*-Cre rats. These rats underwent operant tasks to test how excitation of CRF-containing neurons in these structures may amplify or bias incentive motivation for sucrose rewards and underwent self-stimulation tests to assess the potential positive or negative valence of stimulation

by itself. Finally, we compared activation patterns of recruited downstream structures following excitation of CRF-containing neurons in NAc, CeA, and BNST through distant Fos analysis, and used Fluorescent *in Situ Hybridization* (FISH) to quantify and compare CRF systems in NAc, CeA, and BNST in this transgenic BAC rat line.

CRF-containing neurons and cocaine motivation.

While the role of CRF-containing neurons in incentive motivation for natural rewards such as sucrose is informative, CRF has largely been implicated as the cause of aversive distress from withdrawal symptoms following cessation of drug-use (Koob and Volkow 2016; Koob et al. 2014; Merlo Pich et al. 1995; Olive et al. 2002; Park et al. 2013; Zorrilla et al. 2014). Indeed, the allostatic model of addiction, based on the opponent-process theory, posits that CRF in CeA and BNST are elevated during drug-withdrawal and causes negative aversive distress, thus leading to relapse through attempts at hedonic self-medication (Koob and Le Moal 1997, 2008; Koob and Schulkin 2019; Koob 2013; Koob et al. 2014; Solomon and Corbit 1978; Zorrilla et al. 2014). However, it is also plausible that CRF-systems could contribute to relapse and addiction through *positive* incentive mechanisms, such as promoting drug intake due to stress-induced surges in incentive salience. Therefore, Chapter 4 of this dissertation probes how optogenetic stimulation of CRF-containing neurons in NAc, CeA, and BNST may bias or amplify motivation for cocaine-rewards, using transgenic rats and a modified self-administration two-choice task (Warlow et al. 2017).

Summary

Overall, this dissertation examines the generation and amplification of incentive motivation and aversive motivation by limbic structures. It investigates how stressful experiences and stress-related neural systems may enhance and direct these motivational

modes, particularly through striatal-level limbic structures including the nucleus accumbens medial shell and central amygdala.

CHAPTER II. 'Desire' and 'Dread' From Nucleus Accumbens Inhibitions: Reversed by Same-Site Optogenetic Excitations.

Introduction

Localized neuropharmacological glutamate blockade at sites in the medial shell of nucleus accumbens (NAc), by microinjections of the glutamate AMPA antagonist, DNQX, produce either intense appetitive behavior or fearful behavior. Valence depends partly on site placement along a rostro-caudal gradient. Rostral shell microinjections of DNQX produce increased appetitive motivation, such as increased eating and food intake, and establish conditioned place preferences (Maldonado-Irizarry et al. 1995; Reynolds and Berridge 2003). By contrast, caudal shell DNQX microinjections can instead elicit active-coping forms of 'fearful' behaviors, such as anti-predator defensive treading-burying, fearful vocalizations to touch, and establish conditioned place avoidance (Faure et al. 2010; Reynolds and Berridge 2001, 2002, 2008; Richard and Berridge 2011b; Richard et al. 2013b). Beyond anatomical determinants, the motivational valence produced by DNQX microinjections at many shell sites can be shifted by changes in the emotional ambience or stress-levels of the external environment (Reynolds and Berridge 2008; Richard and Berridge 2011b).

What underlying neurobiological mechanisms are responsible for this NAc-generated 'desire' or 'dread'? A major neurobiological hypothesis has been that reward motivation is

generated via relative neurophysiological inhibition of NAc medium spiny neurons (MSNs) (Carlezon and Wise 1996; Carlezon and Thomas 2009; Cheer et al. 2005; Krause et al. 2010; Meredith et al. 2008; Roitman et al. 2008; Taha et al. 2006; Wheeler et al. 2008). By this hypothesis, NAc neuronal inhibition of MSNs shuts off axonal GABA release from projections to anatomical targets in lateral hypothalamus (LH), ventral pallidum (VP), and ventral tegmental area (VTA), releasing those targets from tonic GABAergic suppression, and disinhibiting them into relative excitation to generate intense motivation (Heimer et al. 1991; Humphries and Prescott 2010; Lu et al. 1998; Mogenson et al. 1983; Usuda et al. 1998; Zahm and Heimer 1990; Zhou et al. 2003).

This NAc-inhibition hypothesis also has plausibility when applied to DNQX microinjections, to the extent that local AMPA blockade suppresses the ability of excitatory glutamate signals from cortex, hippocampus, or basolateral amygdala to produce local excitatory post-synaptic potentials in MSNs. This would produce at least relative inhibition of those local MSNs, by suppressing activity below normal levels.

However, as yet, there is no direct evidence that neuronal inhibition is actually *necessary* NAc for DNQX microinjections to generate either appetitive or fearful motivations. Alternatively, other pharmacologically-induced post-synaptic neurochemical and second messenger effects of the drugs induced in parallel with electrophysiological changes, as well as presynaptic antagonist effects, might cause the motivated behaviors (Lee et al. 2010; Menuz et al. 2007; Tarazi et al. 1998a, 1998b).

Here with colleagues Dr. Shannon Cole and Dr. Jeffrey Olney, we directly tested the hypothesis that *local neuronal inhibition* is *necessary* for DNQX microinjections in NAc to

induce intense motivated behaviors. This was done by *locally opposing* putative DNQX-inhibition of NAc neurons at the microinjection site by adding optogenetic channelrhodopsin (ChR2) excitation *at the same NAc site*. Our results indicate that localized ChR2 excitation at the same site of a DNQX microinjection reverses both positively-valenced desire and negatively-valenced dread induced by DNQX microinjections at their corresponding rostrocaudal sites in NAc medial shell. Both motivational reversals occurred only if ChR2 optic fiber tip and DNQX microinjector tip were within 0.5mm (or at least 0.8mm) of each other in shell, but not if fiber tip and microinjector tip are spaced further apart. Laser-induced behavioral reversals of DNQX effects were also accompanied by neurobiological reversal of recruitment of Fos increases in LH, VP, VTA, and other limbic structures, that were otherwise induced by NAc DNQX microinjections. These results help confirm the necessity of relative NAc inhibition, and support the release of downstream targets into excitation, for NAc DNQX microinjections to generate appetitive or defensive motivations.

Materials and Methods

Subjects

Forty-nine rats (Sprague Dawley or Long Evans obtained Envigo, Indianapolis, IN or bred in-house; $n = 5$ females and $n = 43$ males; 300-500g) were implanted with bilateral NAc cannula for drug microinjection, and received bilateral virus microinfusions (ChR2 or eYFP) and bilateral optic fibers implanted at the same individualized sites in medial shell of NAc. Sites were bilaterally identical within an individual, but were staggered across individuals so that the group as a whole filled most of the NAc medial shell. Rats were housed in same-sex pairs or groups of three on a 12:12-hour reverse light/dark cycle at ~21°C with *ad libitum* access to food (Purina Rat Chow) and water. All experimental procedures were approved by the University Committee on the Use and Care of Animals (UCUCA) at the University of Michigan and carried out in accordance with the guidelines on animal care and use by the National Institutes of Health.

Experimental groups

1. *Standard lab – Within subject Group:* 14 total (Sprague-Dawley = all male)
2. *Stressful environment – Within subject group*: 11 total (Long-Evans = 5 female, 6 male)
3. *Standard Lab Fos mapping – Between-subject group*: 24 total (Sprague Dawley = all male)

Three separate groups of rats were run. Two groups compared within-subject behavior of the same individuals after four different NAc microinjection/laser conditions (*Within-subject comparison groups*): DNQX microinjection alone, DNQX microinjection plus laser illumination during test, vehicle microinjection alone, and vehicle microinjections plus laser illumination during test. These two within-subject groups differed in the rat strain and emotional ambience of their external environment used to test behavior after NAc microinjections. The first within-

subject group used Sprague-Dawley rats tested in a standard laboratory environment (*standard lab environment groups*). The second within-subject group added loud sound to the behavioral test environment, in the form of raucous music, intended to raise potential stress levels to facilitate DNQX-elicitation of defensive treading-burying behavior as a 'fearful' anti-predator reaction, and used Long-Evans rats, as they may potentially have greater emotional-reactivity to stress than Sprague-Dawley rats (de Boer et al. 2003) (*stressful environment group*). The third group provided between-subject behavioral comparisons, and allowed measurement of the size of local Fos plumes in NAc induced by each microinjection/laser condition, and changes in distant Fos expression in other limbic structures accompanying those conditions (*Fos mapping*; *between-subject condition*). Because repetition of microinjections can induce local gliosis or necrosis at a microinjection site that impedes drug spread, potentially reducing Fos plume size of a final drug microinjection and reducing behavioral effects elicited by the drug microinjection (Castro and Berridge 2017; Richard and Berridge 2011b), each rat in this between-subject group was tested behaviorally only once with a single microinjection/optogenetic condition (individuals assigned in counterbalanced numbers to each of the four conditions). Brains were processed for Fos expression immediately afterwards. This avoided underestimation of NAc Fos plume sizes, which would have distorted assessment of whether DNQX microinjection plumes and ChR2 laser illumination plumes anatomically overlapped in a given rat.

Cranial cannulation and fiber implantation surgery

Rats were anesthetized using isoflurane (5% induction, maintenance at 1-2%), and pretreated with atropine (.05 mg/kg, i.p.) to prevent respiratory distress. Carprofen (5.0 mg/kg, s.c.) was additionally administered for post-surgical analgesia, and cefazolin (75 mg/kg, s.c.) was administered to prevent infection. Rats were positioned in a stereotaxic apparatus (David Kopf

Instruments, Tujunga, CA, USA), with the mouth bar set to 5.0 mm above intra-aural for cannula insertion, with the head flat using a lateral 16 degree angle for optic fiber insertion to avoid the cannula path and not penetrate lateral ventricles, and to achieve positioning of fiber/cannula tips closely together (Figure 2.1). Bilateral stainless-steel microinjection guide cannulae (14 mm, 23-gauge) and bilateral optic fibers (approximately 8-9 mm in length) were aimed at matching NAc sites. Guide cannula ended 2 mm above optic tips, because microinjector tips extended 2.0 mm beyond the end of the guide cannulae, and sites for optic fiber tip and microinjector tip were intended to be identical (7.6 mm on the dorsoventral plane). Bilateral sites were also identical for a given rat. However, site coordinates were staggered across rats so that the group's collective sites filled the entire rostrocaudal extent of NAc medial shell (ranging between antero-posterior AP +2.2+3.0; medio-lateral ML ± 0.8+1.2mm, and dorso-ventral DV-7.6mm; all relative to bregma).

During the surgery, the microinjector was inserted into the guide cannula, and each rat received bilateral 0.5 μL microinfusions of either AAV5-hSYN-ChR2-eYFP virus (UNC Vector Core, Chapel Hill, NC, USA; rate = 0.1 μL per min; 5-min duration; ChR2 rats) or optically inactive control virus that lacked ChR2 (AAV5-HSYN-eYFP, UNC Vector Core; control eYFP rats). After microinfusions, virus was allowed to diffuse for 10 minutes before withdrawing microinjector cannula.

Next, optic fiber implants were inserted in a flat-skull position at a 16° lateral angle, triangulating the aim of the optic fiber tip to closely approach the microinjector cannula tip without following the same track. Optic fiber implants were always aimed at coordinates approximately 0.3mm above the microinjector tip, so that illumination would overlap with tissue containing the drug (AP +1.0 to +2.5 ML ± 3.0 to ± 3.5 mm; DV-6.5 to -7.2; at 16 degree lateral

angle). External ends of microinjection guide cannula and fiber implants were secured to the skull with four surgical screws and dental acrylic. Stainless-steel stylets (28-gauge) were inserted into the guide cannulae to prevent infection and clotting.

Rats were monitored daily post-operatively for 7 days. Each rat received another dose of carprofen for additional pain relief after 24 hours, and received topical reapplications of antibiotic ointment around the skullcap every day for the week. Approximately 4 weeks was allowed before behavioral testing to allow virus incubation and adequate ChR2 expression.

Post-test site verification

All optic fiber and microinjection sites were verified histologically after the experiments were completed. Any rat that had fiber optic tips and microinjector tips within <1 mm of each other on at least one side of in medial shell was considered to have potentially *overlapping* or *aligned* NAc sites for optogenetic stimulation and drug microinjections (aligned fiber/microinjector tips; see Fos plume results below). Any rat with fiber optic tips more distant than 1.0 mm away from microinjector tip was considered to have *misaligned* tips. Aligned versus misaligned groups were statistically compared separately to assess if behavioral effects for laser modulation of DNQX-induced motivations differed depending on proximity of fiber tips to microinjector tips.

Handling and Habituation

For 2-3 days before behavioral testing began, rats were handled for at least 15 minutes per day for acclimation. Then for four additional habituation days, rats were connected to optogenetic laser delivery cables and placed in the test chamber for 1 hour per day. The behavioral test chamber permitted *ad libitum* access to food and water, and contained cob bedding as a substrate to support potential defensive treading/burying. Laser power supplies

were turned on during these habituation sessions, so rats became accustomed to their ambient sound, but laser output to cables was turned off. On the fourth day of chamber habituation, rats received an intra-accumbens microinjection of vehicle solution prior to being placed into the test chamber, to habituate them to all aspects of receiving a microinjection and handling procedures.

Intracranial Microinjections for behavioral testing

Drug microinjections were administered bilaterally. Rats received either the AMPA antagonist DNQX dissolved in vehicle (220ng/0.5μL/side; Sigma-Aldrich Corporation, St. Louis, MO, USA) or vehicle alone (50% DMSO and 50% 0.15M saline). Vehicle/DNQX conditions counterbalanced across days for within-subject rats. Microinjections of 0.5-μL-per-side were spaced 48 hours apart on test days for within-subject groups to ensure that there were no lingering drug effects. A standard dose of DNQX at 220 ng/0.5 μL per side was selected based on results of a previous study in our laboratory (Richard and Berridge 2013), which indicated this DNQX dose to produce moderate levels of either appetitive behavior or defensive behavior, depending on rostro-caudal site in NAc medial shell.

To administer NAc microinjections, rats were individually taken out of their home cages and the experimenter removed the stylet protecting the guide cannulae. Rats were gently held in the experimenter's lap while microinjectors (16 mm, 29-gauge) connected to PE-20 delivery tubing were inserted into each guide cannula, and microinjections were made. Microinjections were administered at a rate of 0.3 μL/minute using a microinjection syringe pump to deliver a total 0.5 μL volume per side of NAc (Hamilton Company, Reno, NV, USA). After a DNQX or vehicle microinjection, microinjectors were left in place ~1 minute to allow for drug diffusion. Stylets were replaced in guide cannulae after microinjectors were removed, fiber optic cables were attached, and rats were immediately put into the testing chamber.

Optogenetic Laser Stimulation

Prior to all tests, two fiber optic cables were attached to a rat's bilateral fiber implants, so that laser could be bilaterally delivered to NAc. Laser power supplies were always turned on to keep fan sound constant, though laser was activated only during particular test sessions, as described below Fiber optic implant output was measured to be >85% efficiency, and laser intensity was kept between 8-10 mW at tips. Laser illumination was programmed to deliver 5s bins of 25 Hz (5 ms ON, 25 ms OFF) blue (473 nm) laser stimulation with 15 s in between the laser bins, and ON-OFF bins were cycled repeatedly throughout the whole 1-hr test.

Behavioral Testing

DNQX and laser effects on appetitive eating behavior and defensive behavior were measured in 1-hr daily tests on four test days with the following conditions counterbalanced in order: (i) baseline condition (vehicle microinjection, no laser), (ii) Laser-alone condition (Laser stimulation, vehicle microinjection), (iii) DNQX-alone condition (DNQX but no laser), and (iv) combined DNQX-Laser condition (DNQX microinjection, laser stimulation). Tests were conducted in a transparent chamber (25.5 x 46 x 46 cm) containing at least 3 cm of granular corncob bedding on the floor, plus a water cup taped to the bottom on one side, and a pre-weighed amount of rat chow (25-30 g of Purina rat chow). The cob bedding provided material that rats could kick forward, as a substrate to support defensive treading/burying behavior. The room contained standard white ambient illumination (400-500 lux). Ambient sound levels were 50-60 decibels measured in test chamber. A video camera in front of each test chamber recorded behavior for subsequent slow-motion analysis.

Behavioral testing in Sensory Stressful Environment

A separate group of rats (n = 11) underwent testing conditions described above, except in

a laboratory environment with elevated levels of sound (rock music soundtrack: Iggy Pop, Hippodrome Paris 77; 80-87 decibels measured in chamber), intended to create a potentially more stressful ambience. Ambient light levels were identical to those in standard testing environment (400-500 lux).

Behavioral scoring of defensive reactions during retrieval at end of test

At the end of the testing session, the experimenter retrieved the rat with a gloved hand using a standardized set of slow-approach movement similar to previous studies (Richard and Berridge 2011b): a) the experimenter approached the chamber with slow steps (taking approximately 3s), b) reached with one gloved hand inside the chamber to slowly approach the rat and stroke its side once (taking~3 sec), c) inserted 4 fingers beneath the rat with palm up, and then d) gently lifted the rat out of the chamber (taking~3s). Any audible distress calls, escape attempts or bite attempts directed at the experimenter were recorded during the retrieval process. A bite attempt was counted if a rat attempted to contact the experimenter's hand with teeth. Escape attempts were counted if a rat rapidly moved away from a hand or attempted to climb the wall upon initial touch or lifting. Distress calls were noted any if audible vocalizations were made during the retrieval procedure.

Behavioral Scoring of Video-records

Video-recorded behavior during tests was scored in slow motion (1/8-1/2 speed; Observer software, Noldus), by observers blind to experimental condition. Eating (actively chewing and swallowing food), defensive treading/burying, escape attempts (subject tries to move away from the experimenter's reach), were all measured as cumulative duration in seconds of each behavior. Bouts of eating (counted as the number of times eating was initiated after a pause of >0.5 sec), bouts of treading (counted as the number of times treading was initiated after

a pause of >0.5 sec) and distress vocalizations were all counted as discrete events or bouts each time they occurred.

Brain Histology

Thirty minutes after the end of the final behavioral testing session for within-subject groups, or after the single behavioral test session for the between-subject group, rats received an overdose of sodium pentobarbital (0.8 mL), and were transcardially perfused (i.e., 90 min after final DNQX or vehicle microinjection for all groups). Brains were post-fixed in paraformaldehyde for two days at 4°C, then stored in a 25% sucrose solution at 4°C until later processing.

For immunohistochemistry, brains were sliced into 40 μm sections using a cryostat (Leica, Wetzlar, Germany). Tissue was rinsed for 10 min in 0.1M sodium phosphate buffer (NaPB) three times, then blocked with 5% normal donkey serum for 30 minutes. Tissue was incubated overnight at room temperature in rabbit anti-cFos (1:1000; Catalog #: ABE457; Lot #: 3142408; Millipore, Burlington, MA). Slices were rinsed three times for 10 minutes in 0.1M NaPB before incubation with donkey anti-rabbit Alexa Fluor 594 (1:300; Code #: 711-585-152; Lot #: 1827674; Jackson Immunoresearch, West Grove, PA) for 120 minutes. Tissue was again rinsed for 10 minutes in 0.1M NaPB three times and mounted onto slides. Images of the fiber and cannula tip were taken using a digital camera (QImaging, Surrey, BC, Canada) attached to a fluorescence microscope (Leica, Wetzlar, Germany). Sites of optic fibers and of microinjection cannulae were identified and mapped onto coronal slices from a rat brain atlas (Paxinos and Watson, 2007), and positions were extrapolated and transferred onto a sagittal slice (see Fig 2.1 for example).

Fos plume analysis

Local Fos plumes surrounding a fiber optic tip that was illuminated 90 minutes before perfusion, or surrounding the microinjector tip 90 minutes after a DNQX microinjection, reflect local changes in neuronal transcription induced by direct ChR2 photoexcitation or by DNQX neurochemical impact (compared to eYFP baseline or vehicle-microinjection baseline as control groups). The diameter of a Fos plume provides an objective indicator of how far changes in neuronal activity induced by optogenetic stimulation or drug microinjection extend from the tips of fiber or cannula. Fos expression was measured with a fluorescent microscopy filter and excitation band at 515–545 nm to identify Fos-positive cells. Numbers of Fos-expressing cells were counted at 10x magnification within successive blocks (50 x 50 μm) of tissue emanating along eight radial arms centered at the optic fiber tip or microinjector tip. Counts continued outward along an arm until at least two sequential blocks contained zero Fos-labeled cells, which was taken as marking the terminal radius of the Fos plume along that arm. Intensities of Fos elevation in an illuminated ChR2 brain were calculated in terms of percent change from a control baseline measured in rats receiving vehicle microinjections alone and/or illuminated eYFP inactive-virus control rats. That is, equivalent block locations from NAc of eYFP control rats that received laser illumination prior to perfusion similarly to ChR2 rats. Fos elevations in ChR2 blocks were denoted in increments of > 200% elevation or higher > 300% elevation above the baseline. Similarly, changes induced by DNQX microinjections were computed by comparison a vehicle-microinjection baseline. For that, Fos was measured in equivalent sites in rats that received vehicle microinjections 90 minutes before perfusion (Castro and Berridge 2017; Cole et al. 2018; Warlow et al. 2017).

Distant Fos expression

Recruitment of distant changes in Fos expression in other brain structures was also

assessed to determine functional connectivity expressed in anatomical patterns of limbic Fos elevation following microinjection or optogenetic manipulations that altered motivated behaviors (see Table 2.1 for list of structures). Within each structure or subregion, Fos expressing neurons were counted in 2-3 separate sample boxes, placed roughly equidistantly within the structure, and at approximately the same locations across different rats. The size of sample boxes was specifically adjusted to each brain structure, so that each sample box contained approximately 10 Fos-expressing neurons in control rats that received vehicle microinjections in NAc. The number of Fos expressing neurons within each box was counted separately for each NAc drug/laser condition as above and compared to the vehicle microinjection baseline, each measured in that particular corresponding brain structure or subregion in separate rats.

Experimental Design and Statistical Analysis

To evaluate behavioral data, effects of drug microinjections, ChR2 laser stimulation, drug-laser interactions, anatomical site effects, and sex differences when necessary were assessed initially via mixed model ANOVAs and subsequent pair-wise post hoc comparisons with Bonferroni corrections. For non-normally distributed data (i.e., time spent treading), non-parametric Kruskal-Wallis and follow up Wilcoxon tests were used. Planned comparisons were used to compare Fos expression. For statistical analysis of anatomical sites, the NAc medial shell was divided into rostral and caudal halves: rats with AP coordinates > 1.2 mm ahead of bregma were placed in the rostral group, and those with sites < 1.2 mm ahead of bregma in the caudal group. Effects were considered statistically significant if $p<.05$, two-tailed. Cohen's *d*, and $r = \frac{Z}{\sqrt{N_1 + N_2}}$ for non-parametric tests, were used to calculate the magnitude of effect sizes.

Results

Anatomical placements of optic fibers & microinjections in NAc

Standard lab – Within subject group (Group 1). NAc sites of optic fibers and microinjection cannulae were confirmed to be in the rostral half of medial shell for 11 of 14 rats, and in the caudal half of medial shell for 3 remaining rats. To assess potential interaction between laser and drug at a given site, placements in one side of NAc shell that had optic fiber and microinjector tips anatomically aligned together (i.e., both tips <0.5 to 0.8 mm apart, based on Fos plume sizes below) were distinguished from placements that were not aligned (i.e., fiber tip >1 mm from cannula tip, even if both in medial shell) (Tables 2.2, 2.3). Rats that had <0.5 mm aligned tips on both sides of NAc were considered bilaterally aligned (n=7). Rats that had unilateral <0.5 mm alignment on one side of NAc and 0.5 mm to 0.8 mm alignment on the contralateral side (n=2) were considered provisionally aligned, and explicitly compared to bilaterally aligned rats for ChR2 laser effects on DNQX-elicited behaviors. Because these two groups showed comparable levels of laser-induced ChR2 suppression (laser ChR2 suppression for bilateral <0.5mm group = 62.0 $\pm$ 13.6%; suppression for unilateral <0.5mm and contralateral 0.5 to 0.8 mm group = 59.1 $\pm$ 11.9%), they were combined in subsequent statistical analyses. No rats had unilateral <0.5 mm alignment but non-aligned >1 mm placements on the contralateral side of NAc. Remaining rats had bilaterally non-aligned placements, with tips >1 mm apart on both sides of NAc (n = 5) and were considered separately in statistical analyses.

Local Fos plumes – zones of impact for DNQX microinjections and ChR2 laser stimulations

DNQX microinjections and ChR2 fiber illumination both produced local Fos plumes of increased Fos expression immediately surrounding the cannula/fiber tips in NAc medial shell (Figure 2.1). DNQX microinjections by themselves (without laser during the subsequent test)

produced Fos plumes with >300% intense increases in Fos over control levels measured at the same sites (i.e., after vehicle microinjections without laser) in a plume center of 94 ± 51 μm radius, and moderate >200% increases in a middle plume of 288 ± 63 μm radius, and an outer plume of 392 ± 58 μm radius of 125% elevation over control levels (effect of DNQX on plume radius versus vehicle non-laser group: $F_{1,14} = 7.740$, $p = 0.015$, $d = 3.93$). Optogenetic excitation by itself, or laser illumination of NAc ChR2 neurons with vehicle microinjection, produced an intense inner plume with >300% elevation of 38 ± 13 μm radius, a middle plume of 206 ± 49 μm radius of >200%, and an outer plume of 300 ± 53 SEM μm radius of 25% elevation over control levels. Therefore, the diameter of Fos plumes suggested that an aligned fiber tip placed within <0.5mm to <0.8mm of a microinjector tip, would create a zone of overlapping impact for both manipulations on neurons in medial shell.

Adding aligned laser ChR2 stimulation to a DNQX microinjection trended toward shrinking the size of the resulting inner, middle, and outer Fos plumes by 67 ± 20% SEM, 31 ± 22% SEM, and 18 ± 18% SEM, respectively, although variance was high, from sizes produced by DNQX microinjection alone (DNQX alone: inner plume = 94 ± 51 SEM μm, middle plume = 288 ± 63 μm; outer plume = 392 ± 58 μm; Combined laser ChR2 + DNQX: inner plume = 31 ± 19 μm, middle plume = 200 ± 63 μm; outer plume = 325 + 72 μm; Figure 2.1). This trend toward reduction nearly reversed the level of laser ChR2 + DNQX local Fos elevation back to vehicle levels after laser excitation alone without DNQX (Laser alone: inner plume = 38 ± 13 μm, middle plume = 206 ± 49 μm; outer plume = 300 ± 53 SEM μm), so that they no longer differed from vehicle plumes ($F_{1,14} = 1.358$, $p = 0.263$). This suggests that laser ChR2 stimulation opposed neurobiological effects of DNQX microinjection that controlled Fos increases in local neurons.

We note DNQX induction of increased local NAc Fos may seem confusing given that DNQX should suppress neuronal firing. However, Fos reflects 3rd-messenger genomic transcription signals, in response in 2nd messenger intra-neuronal signals, and so can depart from electrophysiological activation (Herdegen and Leah 1998). Whether DNQX-induced Fos reflects changes in receptor signal, or lateral GABAergic disinhibition from suppressed neighboring MSNs, or other factors is unknown. We do not take Fos plumes as a proxy for electrophysiological activation, but merely as a proxy for spread of drug action or spread of laser/ChR2 action on local neurons.

NAc Laser reverses DNQX-elicited Fos increases in distant brain structures

DNQX microinjections by themselves in NAc shell, without laser, also recruited distant increases in Fos expression in several other limbic brain structures distributed across the brain, consistent with the idea of downstream circuitry being released into excitation to generate motivated behaviors (Figure 2.2). Fos expression was more than doubled by DNQX microinjections in several structures that directly receive NAc shell output projections, such as LH, VP and VTA, compared to control baselines measured in rats that received vehicle microinjection without laser: anterior ventral pallidum (aVP; 457 ± 94 % increase, $t(10) = 3.103$, $p = 0.011$, $d = 2.31$), posterior VP (pVP; 359 ± 65 % increase, $t(9) = 3.269$, $p = 0.010$, $d = 2.36$), anterior lateral hypothalamus (aLH; 228 ± 11 % increase, $t(9) = 7.381$, $p < 0.001$, $d = 4.44$), posterior LH (pLH; 257 ± 9 % increase, $t(11) = 10.872$, $p < 0.001$, $d = 6.03$) and VTA (214 ± 8 % increase, $t(8) = 8.403$, $p < 0.001$, $d = 5.37$). Fos expression was similarly increased by NAc DNQX in structures belonging to the extended amygdala macrosystem: anterior bed nucleus of stria terminalis (aBNST; 245 ± 23 % increase, $t(10) = 4.198$, $p = 0.002$, $d = 2.85$), posterior BNST (pBNST; 250 ± 29 % increase, $t(10) = 4.046$, $p = 0.002$, $d = 2.67$), medial amygdala

(MeA; 186 ± 24 % increase, t(11) = 3.200, $p = 0.008$, $d = 2.07$), central amygdala (CeA; 281 ± 20 % increase, t(10) = 5.872, $p < 0.001$, $d = 3.40$). Finally, NAc shell DNQX increased in another NAc component, the core (NAcC; 288 ± 36 % increase, t(9) = 3.769, $p = 0.004$, $d = 3.19$). However, trends toward increases did not reach statistical significance in several other structures: in anterior infralimbic (aIF; 101 ± 9 % increase, t(10) = 0.046, $p = 0.964$), posterior infralimbic (pIF; 103 ± 11 % increase, t(10) = 0.122, $p = 0.906$), basolateral amygdala (BLA; 144 ± 24 % increase, t(10) = 0.850, $p = 0.415$), or perifornical hypothalamus (PFA; 136 ± 15 % increase, t(11) = 1.766, $p = 0.105$; Figure 2.2).

Adding aligned laser illumination in ChR2 rats to DNQX microinjections in NAc shell also successfully attenuated the recruitment of increases in distant Fos expression over vehicle control levels in most structures listed above. Accordingly, ChR2 rats that had aligned NAc shell laser illumination plus DNQX microinjections had significantly lower Fos in several limbic structures than ChR2 rats that received DNQX microinjections alone: DNQX-induced Fos was suppressed by ChR2 laser illumination in direct target subregions of VP, LH and VTA: pVP (73 ± 7 % suppression, t(7) = 2.696, $p = 0.031$, $d = 2.59$), aLH (52 ± 11 % suppression, t(7) = 5.274, $p = 0.001$, $d = 3.46$), pLH (54 ± 6 % suppression, t(8) = 8.070, $p < 0.001$, $d = 5.58$), and VTA (48 ± 7 % suppression, t(6) = 6.091, $p = 0.001$, $d = 4.81$). DNQX-induced Fos was similarly suppressed by ChR2 laser illumination in extended amygdala structures: aBNST (54 ± 8 % suppression, t(8) = 2.878, $p = 0.021$, $d = 2.37$), pBNST (63 ± 5 %, t(8) = 3.411, $p = 0.009$, $d = 3.23$), CeA (65 ± 18 % suppression, t(7) = 5.719, $p = 0.001$, $d = 4.39$). Finally, DNQX-induced Fos was also suppressed by ChR2 laser illumination in the core of NAc (NAcC 58 ± 7 % suppression from DNQX alone; t(8) = 2.871, $p = 0.021$, $d = 2.63$). However, no significant suppression was found in aVP or MeA, though there was a trend in this direction (aVP: 75 ± 6 %

suppression, t(8) = 2.281, $p = 0.052$, $d = 2.33$; MeA: 40 ± 5 % suppression, t(8) = 1.976, $p = 0.084$, $d = 1.93$). Similarly, there was no laser-induced change in structures that did not show a DNQX-recruited enhancement in Fos such as aIF (1 ± 2 % suppression, t(6) = 0.079, $p = 0.940$), pIF (11% suppression, t(5) = 0.285, $p = 0.787$), BLA (18 ± 12 % suppression, t(7) = 0.634, $p = 0.546$), and PFA (34 ± 3 % suppression, t(8), $p = 0.110$).

One ChR2 rat that received DNQX with laser illumination had only a unilateral NAc cannula aligned with fiber optic (with contralateral cannulae in ventral pallidum). Nonetheless, this rat demonstrated a similar laser-induced attenuation of distant Fos activation compared to rats that received DNQX alone: aVP (70% suppression), pVP (66% suppression), aLH (30% suppression), pLH (43% suppression), VTA (56% suppression), aBNST (47% suppression), pBNST (59% suppression), CeA (54% suppression), NAcC (68% suppression).

By contrast with ChR2 rats, laser was ineffective in control rats with inactive eYFP virus in altering DNQX-elicited Fos levels, at all sampled structures throughout the brain: eYFP rats that received DNQX plus laser did not differ from eYFP rats that received DNQX alone without laser (aVP (t(7) = 0.988, $p = 0.356$), pVP (t(6) = 1.183, $p = 0.282$), aLH (t(6) = 0.988, $p = 0.361$), pLH (t(7) = 4.745, $p = 0.201$), VTA (t(5) = 0.721, $p = 0.503$), aBNST (t(7) = 0.723, $p = 0.493$), pBNST (t(7) = 0.254, $p = 0.806$), MeA (t(7) = 0.835, $p = 0.431$), CeA (t(6) = 1.028, $p = 0.344$), NAcC (t(7) = 1.877, $p = 0.103$), aIF (t(5) = 1.524, $p = 0.188$), pIF (t(5) = 0.007, p = 0.995), BLA (t(6) = 0.562, $p = 0.594$), and PFA (t(7) 1.223, $p = 0.261$).

ChR2 rats that received laser alone in NAc, with vehicle but not DNQX microinjections, trended toward Fos changes in distant brain structures, but these did not reach statistical significance given the few subjects in this group (n=3). That is, ChR2 rats that received NAc laser plus vehicle microinjections aVP (20 ± 59 % suppression below vehicle microinjections

alone, t(7) = 1.117, $p = 0.301$), pVP (138 ± 72 % enhancement, t(6) = 1.183, $p = 0.282$), aLH (132 ± 52 % enhancement, t(5) = 0.918, $p = 0.401$), pLH (147 ± 32 % enhancement, t(7) = 2.354, $p = 0.051$), VTA (106 ± 48% enhancement, t(4) = 0.207, $p = 0.846$), aBNST (132 ± 93 % enhancement, t(5) = 0.620, $p = 0.563$), pBNST (104 ± 38 % enhancement, t(6) = 0.119, $p = 0.909$), MeA (145 ± 40 % enhancement, t(7) = 1.558, $p = 0.163$), CeA (132 ± 90 % enhancement, t(7) = 0.583, $p = 0.578$), NAcC (141 ± 51 % enhancement, t(5) = 0.782, $p = 0.470$), aIF (102% enhancement, t(5) = 1.027, $p = 0.351$), pIF (8% suppression, t(5) = 1.034, $p = 0.349$), BLA (144 ± 21 % enhancement, t(7) = 1.221, $p = 0.262$), PFA (103 ± 19 % enhancement, t(7) = 0.114, $p = 0.912$). We note that other studies have reported distant increases in Fos in VP, LH, and VTA to be induced by ChR2 stimulation of NAc MSNs (Cole et al. 2018; Soares-Cunha et al. 2016).

Behavioral effects: DNQX in shell increased food intake in standard lab environment

Overall, DNQX microinjections in NAc shell increased food intake measured as grams consumed and similarly increased cumulative time spent eating (two-way ANOVA main effect of drug on food intake: $F_{1,13} = 30.857$, $p < 0.001$; two-way ANOVA main effect of drug on time spent eating: $F_{1,13} = 28.665$, $p < 0.001$; Figures 2.3 & 2.4). Anatomical comparison of rostral versus caudal sites of DNQX microinjection in medial shell produced similar increases in food in the standard lab environment here, and the anatomical halves did not differ in magnitude of eating increase (ANOVA drug x laser conditions by anatomical placement on food intake: $F_{1,12} = 0.742$, $p = 0.406$; on time spent eating: $F_{1,12} = 0.185$, $p = 0.675$; on eating bouts: $F_{1,12} = 0.421$, $p = 0.529$).

Overall here, DNQX microinjections in NAc shell caused rats to increase food consumption >300% compared to vehicle microinjection baselines in the same rats (grams of

chow eaten 1.5g± 0.4g after vehicle; 4.8± 0.5 g after DNQX; t(13) = 5.464, $p < 0.001$, Cohen's d = 1.46; Fig 2.3), a result consistent with many previous studies with DNQX sites mostly in rostral shell (Faure et al. 2010; Reynolds and Berridge 2008, 2003; Richard and Berridge 2011b; Richard et al. 2013b). In behavioral duration of eating bouts, DNQX microinjections also increased bout duration by >250% relative to vehicle baselines (mean DNQX/no laser: 480.0 ± 67.2 seconds in the hour-long session; vehicle/no laser: 181.6 ± 51.3 seconds; t(13) < 4.70, p = 0.001, d = 1.26). A bout was defined as continuous eating with no pause for at least 0.5 sec, separated from other bouts by pauses of >0.5sec. DNQX similarly increased the number or frequency of emitted eating bouts by >250%, (t(13) = 3.02, p = 0.010, d = 0.81).

Same-site optogenetic stimulation reversed DNQX increases in food intake

Adding laser ChR2 excitation reversed the ability of DNQX microinjections in medial shell to cause increases in food intake, at least for rats with bilaterally aligned fiber and cannula tips at the same NAc site (i.e., both within 1 mm of microinjector tip), (t(13) = 2.771, p = 0.016, d = 0.74; see Figure 2.3 and 2.7). Rats with bilaterally aligned fiber/cannula tips consumed 5.5 ± 0.6 grams after DNQX microinjection alone, but adding laser ChR2 stimulation to DNQX cut in half their intake to only 2.3± 0.7 grams (t(8) = 6.57, $p < 0.001$, d = 2.19). This reduced level of intake after combining ChR2 laser illumination with DNQX no longer differed significantly from control baseline levels of the same rats after vehicle microinjection alone without laser (DNQX + laser = 2.3 grams; vehicle = 1.5 grams; t(8) = 1.05, p = 0.325). Behaviorally, adding ChR2 laser-stimulation to DNQX correspondingly reduced cumulative duration of time spent eating by 40% in rats with bilaterally aligned placement (t(8) = 2.77, p = 0.024, d = 0.92). However, this laser-induced reduction in time spent eating was only partial, as there was still a marginal trend towards more time eating after laser + DNQX combination (mean: 333.0 ± 90.5 seconds) than

after vehicle microinjection without laser (mean: 168.9 ± 52.5 seconds; t(8) = 2.23, $p = 0.056$). Similarly, adding ChR2 laser stimulation to DNQX sites did not significantly decrease the number of eating bouts (DNQX/no laser vs DNQX/laser on number of eating bouts: t(8) = 1.29, $p = 0.234$), though the number of eating bouts also no longer differed between DNQX + laser stimulation and control vehicle baselines or (t(8) = 0.646, $p = 0.536$).

The 5 sec Laser ON, 15 sec OFF cycle was repeated throughout the 1-hr test, but we did not see differences in behaviors during the ON portions versus OFF portions of the cycle (normalized eating laser-ON: 528.7 ± 290.5 sec) vs laser-OFF (462.9 ± 221.4 sec; t(2) = 0.939, $p = 0.447$). This suggests that behavioral suppression of DNQX is not tightly time-linked on the order of single seconds. In other words, 5-sec laser ON bins appeared to exert a depressive effect on DNQX behaviors even during the 15 sec period of laser OFF, at least as long as the ON/OFF bins were continuously cycled.

Separation >1mm between tips renders laser impotent to reverse DNQX eating increase

A separate subgroup of 5 rats had bilaterally nonaligned sites, with fiber tips and cannulae tips spaced >1mm apart (no rats in this group had a unilaterally aligned site but contralaterally nonaligned site). In bilaterally nonaligned rats, addition of ChR2 laser stimulation failed to reduce at all the DNQX-elevation of food intake (DNQX/laser: 4.3 ± 1.0 grams; DNQX alone: 3.5 ± 0.9 grams; t(4) = 1.68, $p = 0.168$; Figure 2.7). Similarly, in time spent eating, adding laser to DNQX-induced failed to impede the amount of eating behavior in bilaterally nonaligned rats (t(4) = 1.87, $p = 0.135$). Thus, spatial separation of the optic fiber tip from microinjector cannula tip by a distance greater than 1 mm appeared to render optogenetic excitation ineffective, so that ChR2 laser was no longer able to counteract DNQX-induced increases in eating behavior or food intake. This need for <1mm proximity suggests that laser

must excite ChR2 neurons in a location that anatomically overlaps with that directly impacted by DNQX in order reverse behavioral effects of the NAc drug, a conclusion supported by Fos plume analyses above. Consistent with the conclusion that NAc ChR2 excitation *per se* was not a strong suppressor of intake, ChR2 laser stimulation on its own (i.e., after vehicle microinjection) did not suppress chow consumption below baseline levels after vehicle alone here (bilaterally aligned group: $t(8) = 0.607$, $p = 0.561$; bilaterally nonaligned $t(4) = 0.005$, $p = 0.996$).

We note that the homogenous appetitive pattern for NAc DNQX microinjections at all sites in medial shell was different from our previous studies, which found DNQX at caudal sites typically suppressed food intake in standard lab and instead generated active-coping fearful reactions, such as defensive burying (Reynolds and Berridge 2001, 2008; Richard and Berridge 2011b, 2013). Here, by contrast, few defensive behaviors were observed under any conditions, although we note that 11 of 14 rats here had sites in rostral shell, and only 3 rats had caudal sites. Thus, DNQX vs vehicle conditions did not differ ($F_{1,12} = 0.352$; $p = 0.564$), nor did rostral and caudal halves differ significantly ($F_{1,12} = 0.058$; $p = 0.814$). For this reason, and because DNQX produced similar increases in food intake in the 3 rats with caudal sites as in the larger rostral group, subsequent analyses of laser and DNQX effects on food intake below combined all sites together.

Single-test between-subject group local ChR2 laser reverses DNQX-stimulation of eating

In the bilaterally-aligned ChR2 rats of group 2 (between-subjects comparison), each rat was behaviorally tested only in one of the four microinjection/laser conditions (balanced across different rats: vehicle-no laser; DNQX-no laser; DNQX-laser; vehicle-laser), and then immediately euthanized for Fos processing afterwards. In this group, DNQX similarly elicited appetitive increases in intake when tested in a standard lab environment, and ChR2 laser

stimulation at the same site similarly reversed DNQX-induced increases in appetitive motivation (Figure 2.3). Although a between-subjects comparison might be less sensitive than a within-subjects comparison, most effects described above were reproduced here. Rats with NAc DNQX microinjections alone ate more grams of food than rats that received vehicle microinjections alone (main effect of drug on intake: $F_{1,5} = 66.517$, $p < 0.001$). Again as in the within-subjects comparison above, rats with DNQX-alone sites in either rostral or caudal halves of medial shell had higher food intakes than rats with corresponding vehicle-alone sites, and rostral and caudal halves did not differ in magnitude of intake enhancement (main effect of site: $F_{1,5} = 3.755$, $p < 0.110$; site × valence interaction: $F_{1,5} = 3.755$, $p < 0.110$). Similarly, no defensive behavior was elicited at any site. For these reasons, rostral and caudal sites were again combined for subsequent statistical analyses of laser modulating effects on feeding behavior.

Combined, rats that received DNQX microinjections without laser ate >700% more chow than rats that received vehicle microinjections without laser (DNQX: 7.4 ± 1.5 g; Vehicle: 1.0 ± 0.8 g, $p = 0.028$, $d = 3.14$). DNQX rats without laser similarly ate more than rats that received vehicle microinjections with laser (0.3 ± 0.2 g, $p = 0.007$, $d = 4.27$).

Adding concurrent laser ChR2 stimulation during test reduced the magnitude of food intake elicited by DNQX microinjections back to vehicle baseline levels, so that intake did not differ from that of control rats that received vehicle (without laser; 1.0 ± 0.8g. $p > 0.05$). Thus, intake of ChR2 rats with DNQX plus simultaneous laser illumination was roughly only 10% of intake levels of ChR2 rats that received DNQX alone (without laser) (ChR2 DNQX alone = 7.4 ± 1.5g; ChR2 DNQX + Laser = 0.8 ± 0.4g; Main effect of drug = $F_{1,8} = 9.448$, $p = 0.015$; Main effect of laser = $F_{1,8} = 10.377$, $p = 0.012$; drug × laser interaction = $F_{1,8} = 6.615$, $p = 0.033$). ChR2 rats that received vehicle microinjections plus laser illumination ate the lowest amount of

all (0.3 ± 0.2g), consistent with a main suppressive effect of laser, but this did not differ statistically from the ~1 g amounts eaten by vehicle eYFP control rats.

Among rats with bilaterally aligned optic fiber tips and DNQX microinjection tips (n=19 of 24), those that concurrently received additional ChR2 laser excitation combined with DNQX ate far less chow (0.8 ± 0.4 g) than those that received DNQX microinjections alone without laser (7.4 ± 1.5 g*;* $p = 0.012$, $d = 3.54$). The intake level of the rats with combined aligned ChR2 laser stimulation plus DNQX microinjection did not differ from control baseline intake levels of rats that received vehicle microinjections alone without laser ($p > 0.05$). Similarly, in terms of behavioral time spent eating, ChR2 rats that received DNQX microinjections alone spent 896 ± 282 sec in cumulative duration of eating, whereas eating duration of ChR2 rats that had laser illumination added to DNQX microinjection was roughly half that amount, 374 ± 299 sec, though these were not statistically different ($t(6) = 1.27$, $p = 0.250$). By comparison, ChR2 rats that received vehicle microinjections alone spent only 154 ± 117 sec engaging in eating, and ChR2 rats that received laser illumination added to vehicle microinjections trended toward reducing further to only 33 ± 30 sec ($t(3) = 1.258$, $p = 0.298$).

One ChR2 rat that received DNQX with laser illumination had only a unilateral NAc cannula aligned with fiber optic tip, whereas the contralateral cannula missed the NAc shell entirely and was in ventral pallidum (Table 2.3). This DNQX + laser rat with unilateral NAc shell cannula and ChR2 virus displayed nearly equivalent levels of laser-induced suppression DNQX-elicited feeding relative to rats that received DNQX with laser excitation with bilateral ChR2 expression (78% versus 94 ± 5%, $p = 0.221$). All other rats in the between-subject group had bilaterally aligned fiber and cannula tips (i.e., <1.0 mm separation between optic fiber tip and microinjector tip).

Control rats with optically-inactive eYFP virus that received DNQX microinjections similarly ate more than rats that received vehicle microinjections alone (DNQX: 5.5 ± 1.6 g; vehicle: 0.7 ± 0.3 g; Main effect of drug: $F_{1,8} = 9.582$, $p = 0.015$). However, laser illumination did not reduce the DNQX-induced increases in intake in eYFP rats, which remained comparable to intake of eYFP rats that received DNQX alone ($F_{1,8} = 0.113$, $p = 0.745$). Similarly, laser illumination of the NAc shell did not impact intake in eYFP rats (no laser: 3.1 ± 1.2 g, laser: 2.2 ± 1.6 g; Main effect of laser: $F_{1,8} = 0$ .290, $p = 0.605$).

Stressful environment – Within subject group: ChR2 laser reverses caudal DNQX-induced 'fear' as well as rostral 'desire'

Why caudal DNQX sites produced more appetitive eating and less defensive treading/burying above than in our earlier studies remains unknown, but suggests a more positive bias in affective valence in our current rats. As potential contributing factors, we note that rats in the present study had a history of greater environmental enrichment in rearing and housing conditions than rats in previous studies in our lab roughly (e.g., more toys, climbing features and related environmental enrichment are now provided in home cages than was typical in earlier years), and also were group housed throughout their lives, ensuring social interactions. Possibly having enriched and social environments encourages a more positive valence bias in rats. Alternatively, genetic drift across generations may have altered affective dispositions, or the change could be due to other unknown causes.

In any case, the relatively positive affective bias here prompted us to repeat the within-subject experiment here, but using Long-Evans rats ($n = 11$), which may be more emotionally reactive than Sprague-Dawley rats, and imposing a moderately stressful environment. A stressfully louder and brighter environment has been found to facilitate the induction of

negatively-valenced fearful behaviors by DNQX microinjections in NAc medial shell (Reynolds and Berridge, 2008; Richard and Berridge, 2011). Inducing fearful defensive treading-burying, a natural rodent anti-predator reaction, by NAc DNQX microinjections in rats tested in a stressfully loud environment therefore allowed us to assess if aligned ChR2 laser illumination in medial shell reverses defensive motivation, just as it reversed appetitive motivation in the experiments above.

Results showed that, as expected in the stressfully loud environment, NAc DNQX microinjections without laser at caudal sites in medial shell (defined as < +1.2mm anterior to bregma; $n = 6$), elicited negatively-valenced defensive treading-burying behavior (two-way repeated measures ANOVA valence x site interaction, $F_{1,9} = 5.359$, $p = 0.046$; Figures 2.5 & 2.6). Defensive treading-burying consisted of rhythmic forward-and backward thrusts of the forepaws (1-3 cm extension) with paw palm oriented forward. The treading-burying movements served to kick granules of corncob bedding forward in front of the rat, which if sufficiently persistent and appropriately directed, can form an elevated mound as barrier between the rat and a perceived threat, and sometimes even bury a threatening object (Reynolds and Berridge, 2001; Treit et al., 1981).

Lack of sex differences in DNQX+laser effects

Overall, females with caudal DNQX placements tended to emit more defensive treading/burying (mean: 10.7 ± 3.9 sec) than males (mean: 3.5 ± 3.9 sec), although this sex difference was not significant given the small sample size ($F_{1,4} = 1.665$, $p = 0.226$). However, females and males showed equal percentage levels of laser-induced ChR2 reduction of treading in the DNQX+Laser condition (Females: 49% reduction from DNQX-alone; mean: 12.4 ± 12.2 sec; Males: 62% reduction from DNQX-alone: 4.3 ± 2.3) ($F_{1,4} = 0.736$, $p = 0.439$).

For rats with rostral NAc sites, males tended to eat more at baseline and after DNQX (baseline: 2.4 ± 0.4 g; DNQX: 5.8 ± 1.2 g) than females (baseline: 1.8 ± 0.5; DNQX; 3.9 ± 0.7 g), though this was not significant for the current sample ($F_{1,3} = 4.97$, $p = 0.112$). However, females and males showed equal percentage levels of laser-induced ChR2 reduction of food intake from the DNQX-alone condition (Males: 71 % reduction from DNQX-alone; mean: 1.7 ± 1.0 g; Females: 87% reduction from DNQX-alone; 0.5 ± 0.3 g). For these reasons, males and females were combined for subsequent statistical analyses of the effects of DNQX on appetitive vs defensive behavior, and for the modulating effects of adding laser to DNQX.

Anatomical segregation of DNQX motivational valence: rostral desire vs caudal fear

Here, the 3 rats with unilateral tips <0.5mm apart and contralateral tips between 0.5 - 0.8mm apart showed levels of laser-induced suppressions of eating that were similar to suppression levels of rats with bilateral <0.5 mm placements (unilateral = 93.8% reduction; bilateral = 72.2 ± 11.1% reduction). Unilaterally <0.5mm aligned rats with sites in caudal shell (n=2) also showed similar levels of laser-induced suppressions of defensive behavior as bilaterally aligned rats (unilateral <0.5mm = 56.4 ± 13.6%; bilateral < 0.5mm = 65.0 ± 20.4%). Therefore, unilaterally-aligned and bilaterally-aligned groups were combined together in subsequent statistical analyses.

Defensive treading-burying behavior was elicited by DNQX alone in the loud environment only at sites in the caudal half of NAc shell, and never at rostral sites (Kruskal-Wallis Test: Chi-Square: 15.225, $p = 0.002$; Figures 2.5 & 2.6). Defensive treading-burying was oriented typically (67%) to throw cob bedding forward specifically towards the front of the transparent chamber facing the open room, which was relatively bright and where the human experimenter occasionally moved. DNQX alone at caudal sites increased 'fearful' treading-

burying behavior >750 % over vehicle/no laser control levels in the same rats (DNQX cumulative time spent treading: 17.8 ± 6.3 seconds per session; vehicle: 1.3 ± 0.9 seconds; Wilcoxon Z = 2.201, $p = 0.028$, r = 0.90). Similarly, DNQX at caudal sites caused a >500% increase in the number of discrete bouts of defensive treading-burying over vehicle control levels of the same rats (bout = continuous treading-burying with no pause > 0.5 sec; DNQX bout number: 7.0 ± 1.0; vehicle: 1.3 ± 0.9; t(10) = 3.96, $p = 0.011$, $d = 1.62$). The same caudal DNQX microinjections without laser did not increase food intake in the stressful environment (t(5) = 1.97, p = 0.106).

Conversely, at rostral sites in medial shell (> +1.2mm bregma; $n = 5$), DNQX microinjections alone elicited 400% increases in food intake above vehicle baseline levels of the same rats, similar to groups above (DNQX: 5.0 ± 1.8 grams; vehicle/no laser: 1.3 ± 0.9 grams; t(4) = 3.83, $p = 0.019$, $d = 1.71$), and >300% increases in time spent eating (DNQX: 635.8 ± 125.0 seconds; vehicle: 191.6 ± 73.3 seconds; t(4) = 3.004, $p = 0.040$, $d = 1.34$). Anatomically, all appetitive eating increases were produced only by sites in the rostral half of medial shell in this stressfully loud environment (t(9) = 2.642, $p = 0.027$, $d = 1.60$). We note that one ChR2 rat had a unilateral microinjection site in rostral shell, with the contralateral cannula in the bed nucleus of stria terminalis. Its unilateral DNQX NAc microinjection still caused an >800% increase in food intake; however, because it was only a unilateral NAc site, this rat was considered separately in the analysis of laser modulation effects below.

Simultaneous laser ChR2 stimulation reversed DNQX-induced caudal fear and rostral desire

In ChR2 rats with aligned fiber-cannula tips at caudal sites in medial shell, adding laser illumination reduced DNQX-elicited the amount of defensive behavior to about 50% compared to levels of the same rats after DNQX-alone (DNQX+laser: 9.0 ± 5.9 seconds cumulative

duration; DNQX alone: 17.8 ± 6.3 seconds; Wilcoxon, Z = 2.201, p = 0.028, r = 0.90; caudal vs rostral sites: Kruskal-Wallis Test: Chi-Square: 14.425, p = 0.002). Levels of defensive behavior after combined laser + DNQX microinjection at caudal sites no longer statistically differed from control baseline levels measured after vehicle microinjections in the same rats, although still trending to remain nominally higher, suggesting at least a partial reversal that was very substantial (laser + DNQX mean: 9.0 ± 5.9; vehicle mean: 1.3 ± 0.9; Wilcoxon, Z = 1.214, p = 0.225). Laser illumination here appeared primarily to reduce the average length of bouts of defensive treading-burying (DNQX/no laser mean: 2.3 ± 0.4 seconds; DNQX/laser mean: 1.0 ± 0.4 seconds; Wilcoxon, Z = 2.201, p = 0.028, r = 0.90), as the number of defensive bouts emitted during the session was not changed (DNQX/no laser: 7.0 ± 1.3; DNQX/laser: 5.2 ± 2.8; t(5) = 0.921, p = 0.399). In this sense, ChR2 excitation may have reduced the maintenance of fear-motivated behavior promoted by caudal DNQX microinjections, more than its initiation. Comparing the 5 sec Laser ON bins vs 15 sec OFF bins as the cycle was repeated, similar levels of defensive treading/burying behavior were seen in both ON and OFF portions of the cycle (normalized treading/burying laser-ON: 12.0 ± 7.1 sec; laser-OFF: 9.5 ± 5.9; t(3) = 1.608, p = 0.20). This again suggests that 5-sec laser ON bins exerted a depressive effect on DNQX behaviors even during the 15 sec period of laser OFF while ON/OFF bins were continuously cycled.

After vehicle microinjections in ChR2 rats, defensive behavior was at near-zero levels even in the loud environment, and adding laser had no further effect (Vehicle/no laser: 1.4 ± 1.0; Vehicle/laser: 0.2 ± 0.2; Wilcoxon, Z = 1.069, p = 0.285).

One caudal ChR2 rat had bilateral NAc sites of caudal microinjection/fiber placement, but the tips were aligned within <1mm only on one unilateral side, whereas on the contralateral

side spacing was further apart. However, laser illumination in this unilaterally-aligned rat still reduced DNQX-elicited defensive treading behavior (from DNQX/no laser condition = 12 seconds treading; Figure 2.7), suggesting again that a unilateral ChR2 neuronal depolarization which overlaps with its DNQX-induced Fos plume can successfully reduce DNQX generation of motivated behavior even when the contralateral DNQX microinjection in NAc goes locally unopposed.

In ChR2 rats with rostral sites, adding simultaneous aligned laser illumination in the stressful environment again prevented DNQX from increasing food intake (drug x laser interaction, $F_{1,4} = 8.696$, $p = 0.042$; Figures 2.5 & 2.6). Laser illumination to DNQX markedly decreased food consumption below DNQX/no laser levels of the same rats (DNQX/laser: 1.2 ± 1.4 gram; DNQX/no laser: 5.2 ± 1.8 grams; t(4) = 4.634, $p = 0.010$, $d = 2.07$), and similarly reduced DNQX-induced time spent eating (DNQX/laser 187.8 ± 182.1 seconds; DNQX/no laser condition: 635.8 ± 125.0; t(4) = 3.11, $p = 0.036$, $d = 1.39$). There were no differences in eating suppression between laser-ON bins (215.0 ± 20.1 sec) and laser-OFF bins (mean: 221.3 ± 24.1 sec; t(2) = 1.462, $p = 0.281$) within the laser ON/OFF cycle during the DNQX/Laser test. Laser by itself in absence of DNQX did not alter eating in this group, as there was no difference in food intake between vehicle/laser and vehicle alone conditions for either rostral (vehicle/laser: 1.2 ± 0.3 g; vehicle alone: 1.3 ± 0.4 g; t(4) = 0.212, $p = 0.843$) or caudal sites (vehicle/laser: 2.0 ± 0.5 g; vehicle alone : 1.4 ± 0.6 g; t(5) = 1.027, $p = 0.352$).

For the ChR2 rat with unilateral cannula/fiber sites in rostral shell but contralateral sites in BNST, adding laser illumination still reversed the increase in eating otherwise produced by DNQX (DNQX alone: 3.5g; Combined laser + DNQX = 1.5 g; Figure 2.7). Similarly, another rostral rat with unilaterally aligned tips but contralaterally nonaligned tips (both sides in medial

shell), still showed laser reversal of DNQX-induction of eating. These observations further support the suggestion that overlapping alignment of ChR2 excitation with DNQX microinjection on one side of NAc is sufficient to reverse effects of DNQX, even when the contralateral DNQX microinjection site is nonaligned (Table 2.2). That suggests cross-hemisphere interaction could be involved in optogenetic modulation of DNQX-elicited motivations, although we note that lateralization also exists for NAc inhibition effects in generating motivated behavior (Stratford and Wirtshafter, 2012).

Discussion

Our findings demonstrate that optogenetic ChR2 excitation at same sites of DNQX microinjections in NAc medial shell can attenuate neurobiological recruitment of limbic circuitry, and reduce or reverse generation of intense appetitive or defensive behaviors otherwise elicited by those microinjections (Echo et al. 2001; Reynolds and Berridge 2008, 2003; Richard and Berridge 2011b, 2013; Stratford and Kelley 1997).

Optogenetic reversals of DNQX-elicited motivation appeared to require that ChR2-laser excitation be at the same local NAc site as the DNQX microinjection. That is, reversals occurred only if the optic fiber tip was within 0.5 mm (or at least 0.8 mm) of the DNQX microinjector tip, otherwise the laser became less effective. This suggests that optogenetic depolarization does not simply produce an opposing motivational signal in NAc shell circuitry to counteract DNQX effects. Rather, ChR2 excitation of neurons presumably reverses the relative neuronal inhibitions caused locally by blockade of glutamate AMPA signals in the same NAc site.

Support for NAc-inhibition hypothesis of motivation generation

To our knowledge, these results provide the first direct evidence for the hypothesis that relative inhibition of localized NAc shell neurons is *necessary* for DNQX microinjections to induce appetitive or 'fearful' motivations. Similar NAc neuronal inhibitions have been suggested to mediate appetitive and defensive behaviors elicited microinjections of a $GABA_A$ agonist, such as muscimol in NAc shell (Stratford and Kelley, 1997; Stratford and Wirtshafter, 2012; Covelo et al., 2014; (Faure et al. 2010; Reynolds and Berridge 2001, 2002, 2008; Richard and Berridge 2011b; Richard et al. 2013b). NAc neuronal inhibitions may release downstream VP, LH and VTA targets into relative excitation, by decreasing their tonic suppression by NAc GABA inputs (Baldo et al. 2004; Bromberg-Martin and Hikosaka 2009; Ljungberg et al. 1991;

Smith et al. 2011; Stratford 2005; Tindell et al. 2009). Target excitation was supported here by observing Fos increases in VP, LH, VTA, and other limbic structures after NAc DNQX microinjections that caused intense motivated behaviors. Those distant neurobiological recruitments were also impeded here by the same NAc ChR2 excitations that produced behavioral reversals, supporting the hypothesis that released limbic target activation mediated the generation of motivated behaviors.

Conceivably, a role for NAc shell inhibition in generating motivations could help explain why optogenetic excitation of NAc D1-MSNs or BLA projections to NAc is reported to stop ingestive motivation (O'Connor et al. 2015). Here, however, we did not detect a significant reduction in spontaneous food intake from NAc laser ChR2 stimulation in rats with vehicle microinjections, although there was a trend toward reduced consumption. Still, our ChR2 depolarization was effective for blocking the intense eating otherwise produced by DNQX microinjections.

Our results extend the NAc inhibition hypothesis to include NAc generation of negative-valenced 'fear' motivation, as well as positive-valenced appetitive motivation. Defensive treading is an active-coping type of antipredator reaction to perceived threats (Owings and Coss 1977; Treit et al. 1981). Defensive treading was reversed here by laser-induced ChR2 excitation at caudal NAc sites in a stressfully loud environment. Thus, the hypothesis that NAc inhibition is required for DNQX-generation applies to motivated behaviors of both positive and negative valence. Given that ChR2 effects were identified here with hSyn promoter that infected all local neurons, it will be of interest for future studies to target specific subtypes of NAc neurons (e.g., D1 dopamine receptor-expressing MSNs; D2 receptor-expressing MSNs; etc.) to parse their relative contributions to these effects.

Alternative pharmacological DNQX effects insufficient to cause motivations

Besides relative inhibition of NAc neurons, other plausible hypotheses could have explained how DNQX microinjections in NAc shell generate motivations. For example, pharmacological effects of AMPA blockade on neuronal function, which occur in parallel with relative inhibition, could have been more important than neuronal inhibition *per se*. Such parallel effects might include post-synaptic second messenger signals and gene transcription changes in MSNs. Alternatively, though DNQX is generally viewed as an AMPA post-synaptic receptor antagonist, it has been also reported to excite postsynaptic neurons (Lee et al. 2010; Menuz et al. 2007). Additionally, DNQX can act as a competitive antagonist for kainate receptors on presynaptic axon terminals, which might further alter signals in NAc (Tarazi et al. 1998a, 1998b). Such effects could have been a primary mechanism for DNQX generation of motivation, but might not have been effectively opposed by laser ChR2 excitation of local neurons. However, our finding that ChR2 laser depolarization of local NAc neurons successfully reversed DNQX-induction of appetitive and defensive motivations suggests that local neural inhibition is indeed required, and that other alternative neurobiological effects are not sufficient in absence of NAc neuronal inhibition.

Anatomical valence gradient and environmental switching of site valence

In standard laboratory conditions here, DNQX microinjections at both rostral and caudal shell sites generated increases in appetitive eating behavior. However, a test environment with stressfully loud noise (rock music) caused DNQX at caudal shell sites instead to generate negatively-valenced 'fearful' motivation (i.e., defensive treading). The difference between anatomical sites replicates our previous reports of a rostrocaudal valence gradient of desire vs dread in NAc medial shell for DNQX effects (Reynolds and Berridge, 2001, 2002, 2008; Richard

and Berridge, 2011; Richard et al., Berridge, 2013). That anatomical difference also fits related reports of different affective functions or neurobiological features in rostral/caudal halves of NAc medial shell (Reed et al. 2018; Thompson and Swanson 2010; Trouche et al. 2019; Zahm et al. 2013).

Similarly, the ability of changes in environment ambience to switch between appetitive versus defensive effects replicates our previous reports that switching from standard lab to a stressfully noisy-bright environment switches the valence of DNQX-induced motivation at NAc sites to negatively 'fearful' (Reynolds and Berridge, 2008; Richard and Berridge, 2011). However, results here differed from our previous DNQX reports as our current cohort of rats appeared more strongly biased overall towards positive valence. Specifically, DNQX microinjections elicited appetitive food intake even at caudal sites in the standard lab environment, whereas our previous studies found that caudal DNQX evoked mostly defensive behavior. Further, in the stressfully loud environment, only caudal sites generated defensive treading behavior here, whereas in previous studies many rostral shell sites additionally switched to defensive valence. As caveat, we note that only louder sound was added to our stressful environment here, whereas previous studies of stress-induced switching also included brighter lights. We did not compare combinations of light and sound here, but it is possible that adding brighter light or other stressful stimuli might have expanded the fear-generating zone further into the rostral medial shell, as in previous studies (Reynolds and Berridge, 2008; Richard and Berridge, 2011).

Still, the lack of defensive behavior at caudal sites in standard lab suggests a difference in affective reactivity between current rats versus previous studies. Although the reason for the difference remains unclear, several explanations seem possible. For example, our current cohort

was raised in a more enriched environment than previous cohorts. Current housing conditions include additional toys in home cages and always being housed in social groups, which might conceivably decrease chronic stress levels (Manouze et al. 2019) and reduce fearful reactivity (Clark and Galef 1980). Also, behavioral test chambers here had taller walls to accommodate optogenetic cables, which might be perceived as more sheltering and less anxiogenic. Finally, genetic drift in rat colonies may have altered emotional reactivity over several years. To know which factors are actually responsible for modulating the affective valence of NAc DNQX effects would require further investigation.

Contrary role of NAc depolarizations in motivation

Despite ample evidence for the NAc *inhibition* hypothesis for motivation described above, we note there is also evidence to support a paradoxically opposite hypothesis: that neuronal *excitations* in the NAc shell can elicit appetitive motivation. For example, decades of electrode self-stimulation studies suggested that neuronal excitations in NAc are reinforcing (Mogenson et al. 1979; Phillips 1984; Van Ree and Otte 1980; Rolls 1971). Optogenetic studies similarly show that NAc MSN excitation can generate intense incentive motivation, reflected in either consummatory intake or appetitive instrumental measures (Koo et al. 2014; Lobo et al. 2010). How can NAc excitation effects be reconciled with NAc inhibition effects in generating appetitive and defensive motivations?

There are several possibilities. For example, NAc excitations may excite lateral inhibition, via inhibitory GABAergic interneurons that produce local inhibitions of other NAc neurons. Indeed, ChR2 excitation of MSNs does inhibit at least some local NAc neurons (Kravitz and Kreitzer, 2011). Alternatively, NAc neurons might have multiple excitatory and inhibitory modes for motivational functions, through bimodal “up” versus “down” states that

gate cortical and mesolimbic inputs (O'Donnell and Grace 1995; O'Donnell et al. 1999). Finally, excitation and inhibition might recruit different NAc neuronal ensembles, defined as subsets with coordinated firing patterns, which have distinct downstream consequences (O'Donnell and Grace 1995; O'Donnell et al. 1999; Pennartz et al. 1994).

Conclusion

Our results indicate that local NAc neuronal inhibition is a *necessary* mechanism for DNQX microinjections in medial shell to generate either appetitive or defensive motivation. Together, these findings support the hypothesis that inhibition of NAc medial shell neurons is an important mechanism for generating intense motivation states of both positive and negative valence.

Figures

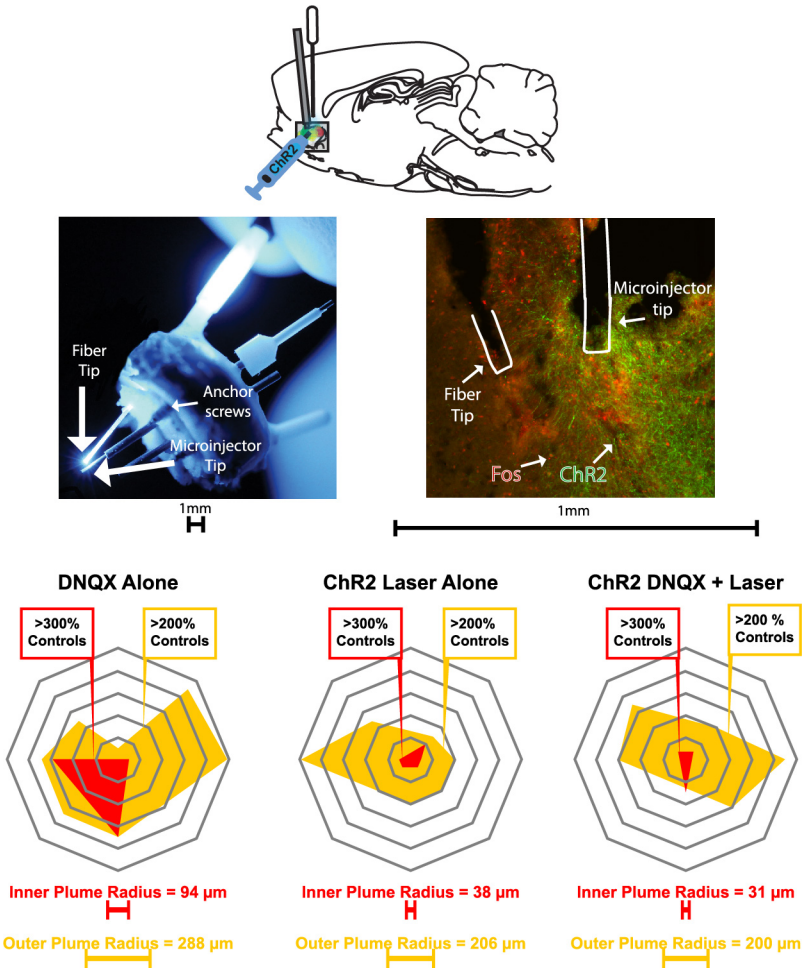

2.1 Representative fiber-cannula alignment, virus, and Fos expression in NAc shell
(Top) Sagittal schematic of simultaneous DNQX microinjection and optogenetic stimulation procedure. (Middle Left) Example of alignment (<1mm apart) between tips of optic fiber and microinjection cannula (injector cannula protrudes below guide cannula). (Middle Right) Coronal slice of NAc medial shell showing spread of virus expression (green), Fos expression (red), and fiber and cannula placements. (Bottom) Examples of mapped Fos plumes, comparing DNQX microinjection alone, Laser + vehicle, and DNQX + Laser conditions.

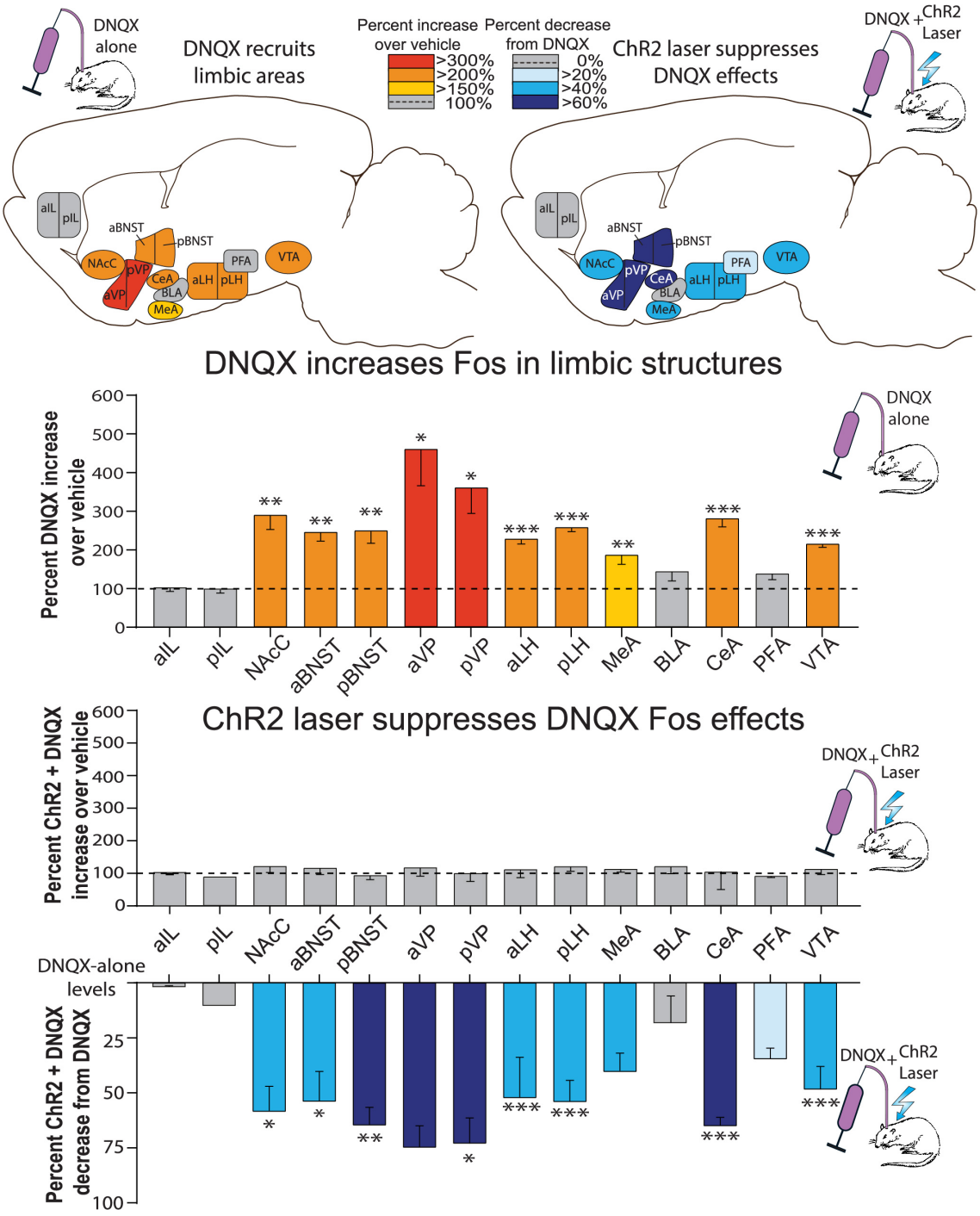

2.2 Same-site laser reverses distant Fos activation induced by NAc DNQX microinjections
(Top) Sagittal brain maps show recruitment of limbic Fos elevations by DNQX microinjections in NAc shell in comparison to vehicle (left; red/orange). ChR2 laser induced reversals of DNQX-induced Fos is shown as suppressions from DNQX-alone levels (right; blue). (Middle) Bar graphs depict the quantitative percent increase of DNQX-induced Fos elevations in limbic structures over vehicle control levels; dashed line at 100% = vehicle levels (red/orange bars). Center uncolored bars show Laser + DNQX levels compared to vehicle levels. Bottom bars (blue) show suppression of Laser + DNQX levels compared to DNQX-alone levels. *p<0.05, **p<0.01, ***p<0.001

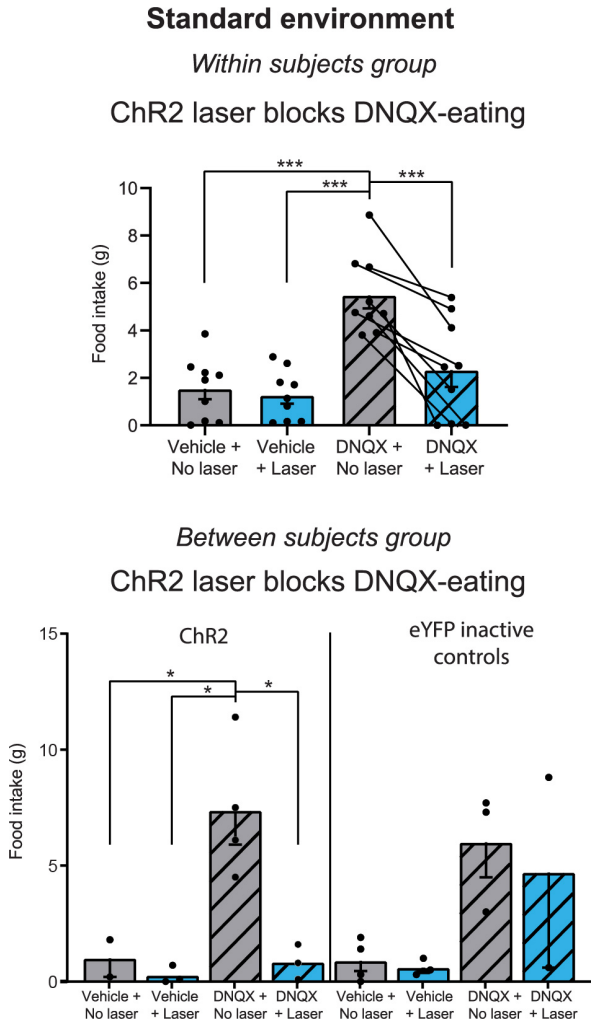

2.3 Aligned ChR2 laser reverses DNQX increases in food intake
DNQX microinjections alone without laser caused increases in food intake for both the within-subjects group 1 (top) and between-subjects group 2 (bottom) for NAc shell sites in standard lab conditions. Aligned laser illumination in ChR2 rats (<1mm apart) reduced DNQX-levels of intake by approximately 50%, reducing intake to baseline vehicle levels (top). Laser illumination had no effect on vehicle or DNQX intake in control rats with inactive eYFP virus (bottom right). Grey bars alone=no laser vehicle, blue bars alone = laser alone, grey bars with stripes=DNQX alone, and blue bars with stripes=DNQX+laser. *p<.05, ***p<0.001

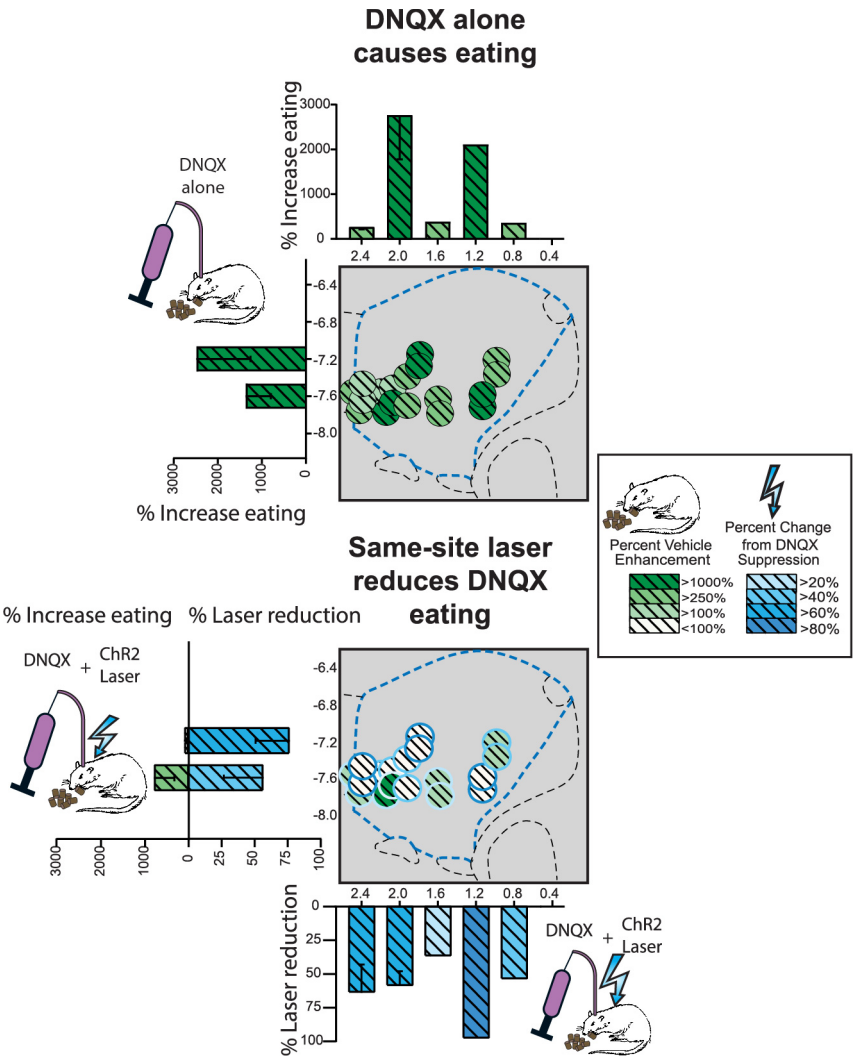

2.4 NAc maps of increases induced by DNQX microinjections and reversals by laser
(Top) Sagittal placements show % changes in food intake change from vehicle baseline induced by DNQX microinjections alone (green) in standard lab conditions for within-subjects group 1. (Bottom) Percentage suppressions of intake from DNQX-levels induced by adding aligned laser illumination (blue).

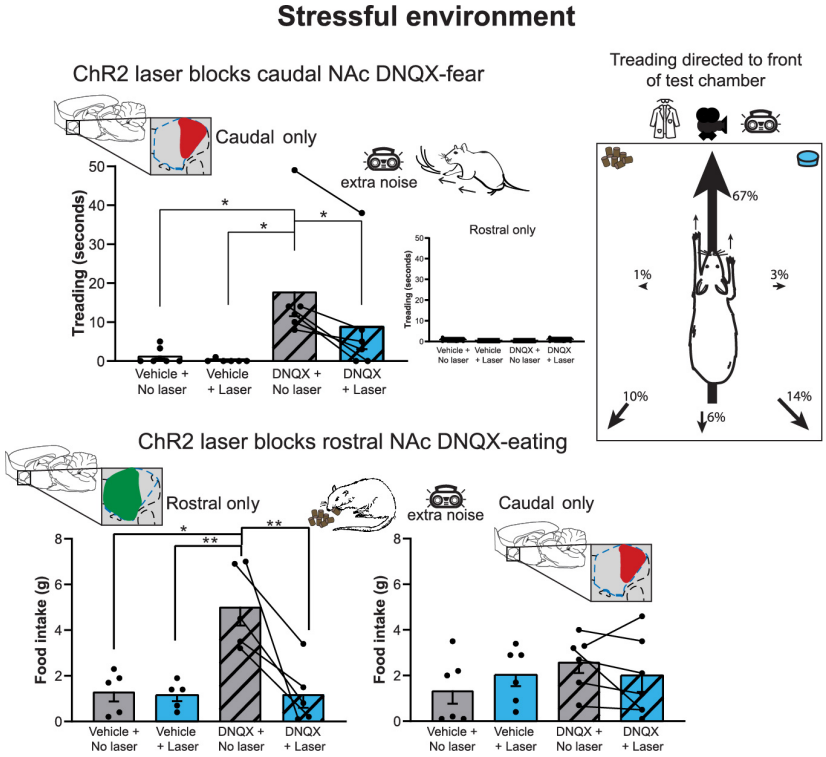

2.5 ChR2 laser reverses caudal 'fear' as well as rostral 'desire' from DNQX microinjections
At caudal sites in NAc shell DNQX microinjections alone elicited defensive treading-burying behavior when ChR2 rats were tested in a stressfully loud environment (top left). Defensive behavior was typically directed toward the transparent front of the cage and view of the room beyond (top right). Adding aligned laser illumination substantially reversed DNQX ability to elicit defensive behavior at caudal sites. At rostral sites, DNQX elicited increases in food intake in the loud environment (bottom left). Laser illumination again reversed appetitive intake elicited by DNQX at rostral sites. *p<0.05, **p<0.01

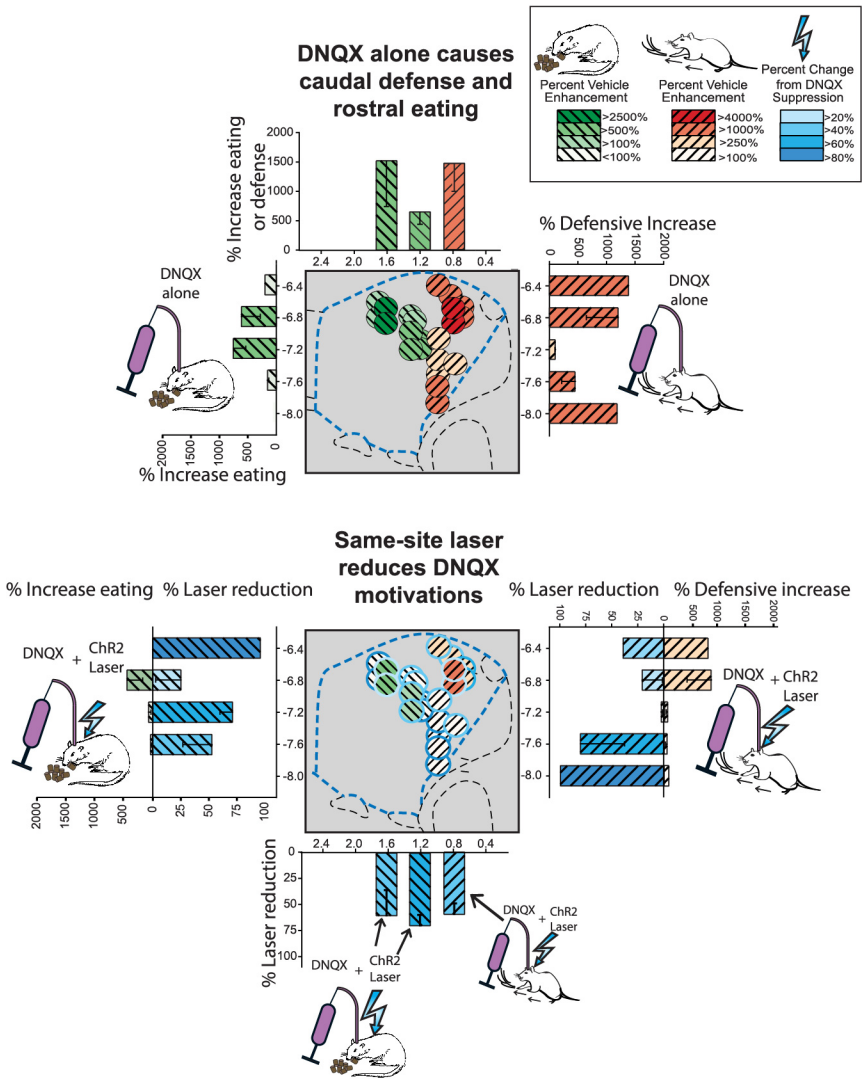

2.6 NAc maps of DNQX-induced caudal 'fear' and rostral 'desire' and laser reversals
(Top) Sagittal placements show % increases in defensive behavior (orange) and in appetitive behavior (green) induced at sites in NAc shell by DNQX microinjections alone in the loud environment. (Bottom) Placements show suppressions from DNQX-levels (blue) of motivated behavior induced by adding aligned laser illumination in the same ChR2 rats.

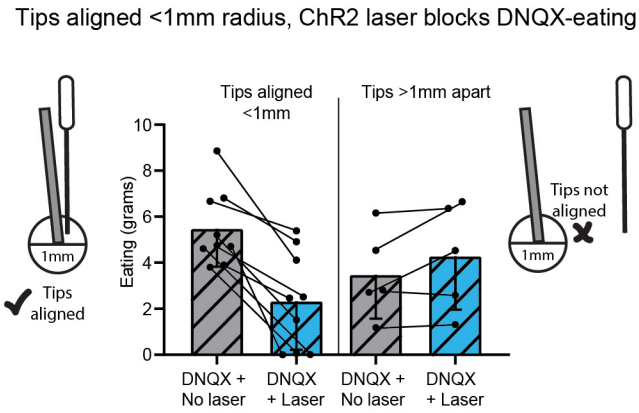

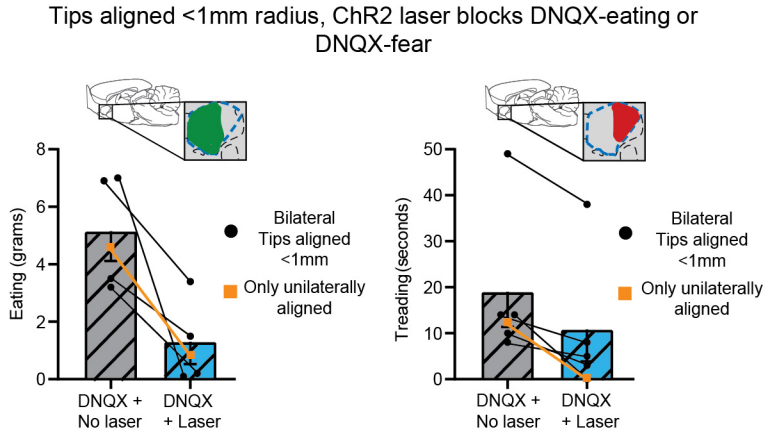

2.7 Alignment of fiber and cannula tips required to reverse DNQX-elicited motivation
Laser illumination reversed DNQX-elicited motivations in ChR2 **r**ats with closely aligned tips of optic fiber and microinjection cannula (<1mm apart in NAc shell, bilaterally aligned). By contrast, laser was ineffective at reducing motivated behavior if fiber/cannula tips were spaced more than 1 mm apart bilaterally. Appetitive intake of within-subjects group 1 in standard lab shown at top. Rostral appetitive behavior and caudal defensive behavior of within-subjects group 3 tested in stressfully loud environment shown at bottom. Having even one aligned fiber-cannula tip pairing appeared sufficient to reverse DNQX effects in the stressful environment for both rostral eating (bottom left) and caudal fear behaviors (bottom right).

Tables

Limbic brain structures in which distant Fos recruitment was assessed	
BLA	MeA
BNST	NAcC
CeA PFA	PFA
IF	VP
LH	VTA

2.1 Structures of interest for distributed Fos analysis
Fos was separately quantified in both anterior and posterior subregions of infralimbic cortex, and in bed nucleus of stria terminalis, lateral hypothalamus, and ventral pallidum.

Test environment	Placement	Cannulae	Fiber	*N*	DNQX increase, %	Laser suppression, %	Missed target
Standard	All combined	Bilateral	Bilateral aligned	9	Yes 300	Yes >50	—
			Unilateral aligned	0	—	—	—
			Misaligned	4	Yes 200	No	AcbSh; VP; DS (fibers)
		Unilateral	Unilateral aligned	0	—	—	—
			Misaligned	1	Yes 500	No	LS (cannula); DS (fibers)
Stressful	Rostral	Bilateral	Bilateral aligned	3	Yes 400	Yes >75	—
			Unilateral aligned	1	Yes 250	Yes >80	DS (fiber)
			Misaligned	0	—	—	—
		Unilateral	Unilateral aligned	1	Yes 1500	Yes >50	BNST (cannula/fiber)
			Misaligned	0	—	—	—
	Caudal	Bilateral	Bilateral aligned	5	Yes 700	Yes >50	—
			Unilateral aligned	1	Yes 1200	Yes 100	DS (fiber)
			Misaligned	0	—	—	—
		Unilateral	Unilateral aligned	0	—	—	—
			Misaligned	0	—	—	—

In the current study, ChR2 laser reversed DNQX effects even in rats with aligned fiber-cannula tips on only one side of the NAc fiber. AcbSh, Nucleus accumbens shell; DS, dorsal striatum; LS, lateral septum.

2.2 Unilateral vs bilateral alignment of fiber/cannula tips for within-subjects groups

Test environment	Placement	Cannulae	Fiber	*N*	DNQX increase, % (vs vehicle group)	Laser suppression, % (vs DNQX only group)	Missed target
Standard (Fos)	All combined	Bilateral	Bilateral aligned	7	1488	94	—
			Unilateral aligned	0	—	—	—
			Misaligned	0	—	—	—
			Unilateral virus	3	804	—	—
		Unilateral	Unilateral aligned	2	—	78	VP; MS
			Misaligned	0	—	—	—

In the current study, ChR2 laser reversed DNQX effects even in rats with aligned fiber-cannula tips on only one side of NAc fiber. MS, Medial septum.

2.3 Between-subjects alignment of fiber/cannula tips for ChR2 animals only

CHAPTER III. Corticotropin Releasing Factor Systems in Nucleus Accumbens, Amygdala, and Bed Nucleus of Stria Terminalis: Incentive Motivation Versus Aversive Roles.

Introduction

Corticotropin releasing factor (CRF) is triggered by diverse aversive stressors to initiate behavioral and physiological stress responses (Bale and Vale 2003; Dallman et al. 2003; Dunn and Berridge 1990; Hupalo et al. 2019; Koob and Bloom 1985; McEwen and Akil 2020; Merali et al. 1998, 2004; Schulkin 2017; Stewart 2000; Vale et al. 1981). CRF-expressing neurons are concentrated in the hypothalamic paraventricular nucleus (PVN), but also occur in the nucleus accumbens (NAc), and in extended amygdala components such as the central amygdala (CeA) and bed nucleus of the stria terminalis (BNST)(Dabrowska et al. 2016; Giardino et al. 2018; Gray and Magnuson 1992; Itoga et al. 2019; Kim et al. 2017; Lemos and Alvarez 2020; Lemos et al. 2012, 2019; Makino et al. 1994a, 1994b; Peciña et al. 2006; Pomrenze et al. 2015; Swanson and Simmons 1989).

Stress can trigger relapse in addiction or eating disorders (Grilo et al. 2012; Koob and Schulkin 2019; Mantsch et al. 2016). Traditional views suggest that CRF-containing systems increase reward consumption primarily by mediating the negative-valence of stress, creating unpleasant states that promote drug relapse or eating for hedonic self-medication (Koob and Schulkin 2019; Koob 2013; Roberto et al. 2017). In the opponent-process theory of addiction

(Koob and Le Moal 1997; Solomon and Corbit 1978; Solomon 1980) taking addictive drugs activates a pleasant a-process, which is posited to trigger underlying longer-lasting aversive b-processes to create an unpleasant opponent B-state of withdrawal. In particular, opponent-process neuroscience models of addiction have posited that activation of CeA and BNST CRF-containing systems generates unpleasant withdrawal symptoms, again leading to relapse via hedonic self-medication (de Guglielmo et al. 2019; Funk et al. 2006; Koob and Le Moal 1997; Koob and Schulkin 2019; Koob 2013; Roberto et al. 2017; Zorrilla et al. 2014).

However, CRF systems may also activate to changing events that mobilize biobehavioral responses, whether or not stressful (Merali et al. 1998, 2004; Schulkin 2017). For example, CRF-containing neurons can be activated by positive reward stimuli (Kim et al. 2017; Lemos and Alvarez 2020; Lemos et al. 2012; Lim et al. 2007; Merali et al. 1998, 2004; Peciña et al. 2006). Some CRF systems may have positively-valenced roles in promoting appetitive incentive motivation without inducing negative distress or withdrawal. For instance, NAc CRF microinjections in rats increase cue-triggered 'wanting' for sucrose during Pavlovian Instrumental Transfer testing, comparable to dopamine-stimulating amphetamine microinjections (Peciña et al. 2006). NAc CRF microinjections can also establish positive conditioned place-preference and increase NAc dopamine release in mice, only becoming aversive roles following severe stress (Lemos et al. 2012). Additionally, mice self-stimulate for optogenetic excitation of CeA CRF-expressing neurons, suggesting incentive motivation (Kim et al. 2017). CRF in rats does mediate stress-induced reinstatement for addictive drugs, but does not require either withdrawal or corticosterone (Erb et al. 2006; Shaham and Stewart 1995; Shaham et al. 1997). Overall, CRF seems not simply tied to an aversive affective dimension, but instead has a larger

regulatory role in affective valence and organization of behaviors (Refojo et al. 2011; Vranjkovic et al. 2018; Wang et al. 2005).

Here we examined potential positively-valenced versus negatively-valenced roles of CRF-expressing neurons in either NAc, CeA, or BNST, using BAC transgenic *Crh*-Cre+ rats (Pomrenze et al. 2015) to optogenetically stimulate CRF-containing neurons in each structure. During two-choice incentive motivation tests, rats could choose between earning sucrose paired with laser stimulations and another sucrose option without laser (Robinson et al. 2014). In progressive ratio breakpoint tests, laser stimulation effects on incentive motivation magnitude for sucrose was assessed. Finally, laser self-stimulation tests assessed whether CRF-containing neuronal stimulation was rewarding on its own. We found that NAc and CeA CRF-containing neuron stimulation enhanced sucrose incentive motivation, was reinforcing, and recruited activation of mesolimbic circuitry. Conversely, BNST CRF-containing neuronal stimulation was avoided, suppressed sucrose pursuit, and recruited pain-related circuitry.

Materials and methods

Animals

Female (n=37) and male (n=34) *Crh*-Cre+ Wistar rats (>250g at surgery) (Pomrenze et al. 2015), were bred and phenotyped in-house. Same-sex groups were housed on a 12-hour reverse light-cycle (~21°C) with *ad libitum* food (Purina) and water. All experimental procedures were approved by the University of Michigan Institutional Animal Care & Use Committee in accordance with NIH animal care and use guidelines.

Surgery

Surgeries followed previous methods (see Appendix A) (Baumgartner et al. 2020; Robinson et al. 2014; Warlow et al. 2020). Bilateral 1.0µl infusions in NAc, CeA, or BNST contained either active AAV-DIO-ChR2-eYFP virus (n=33) or optically-inactive control virus AAV-DIO-eYFP (n=19) to infect only neurons containing Cre-recombinase. We note that the *Crh*-Cre BAC rats used here express Cre primarily in CRF neurons that are also GABAergic (Pomrenze et al. 2015). This makes them suitable for our study, given that CeA, BNST, and NAc CRF-expressing neurons predominantly co-express GABA. A separate group received halorhodopsin AAV-DIO-NpHR-eYFP (n=19) virus for CRF-containing neuronal inhibition. NAc shell, lateral CeA, or dorsolateral BNST sites were staggered across individuals (Fig. 3.1, Table 3.1) and optic fibers were secured with surgical screws and acrylic.

Stimulation parameters

ChR2 laser-illumination (2-3mW; 473nm) was tested at 10Hz and 40Hz (Fadok et al. 2017; Soares-Cunha et al. 2016; Torruella-Suárez et al. 2020). Inhibitory halorhodopsin testing used constant-illumination (8-10mW; yellow 592nm) (Warlow et al. 2017).

Two-choice sucrose

An instrumental two-choice task evaluated whether pairing CRF-expressing neuronal stimulation in NAc, CeA, or BNST with one sucrose reward made it more or less desirable than an identical sucrose reward delivered without laser (Appendix A)(Robinson et al. 2014). Briefly, rats learned that presses on one lever earned sucrose pellets plus 8-sec laser illuminations and an 8-sec tone or white-noise *(Laser+Sucrose).* Presses on a different lever earned sucrose and noise/tone but no laser (*Sucrose-alone).* Lever and tone/noise assignments were balanced across rats, but remained permanent for each rat.

Reinforcement schedules increased across 8 test days: FR1 (days 1-3), FR4 (4), RR4 (5), RR6 (6-8). Each day rats were required to earn rewards twice from each lever presented alone, before free-choice. The alternate laser frequency (10Hz/40Hz) was tested on three subsequent RR6 days. Separate halorhodopsin rats underwent identical procedures with yellow laser.

Progressive ratio

Progressive ratio tests assessed whether ChR2 stimulation of CRF-containing neurons affects magnitude of sucrose incentive motivation (Appendix A) (Robinson et al. 2014). Briefly, rats were tested one day with only the *Laser+Sucrose* (10Hz/40Hz) lever available, another day with *Sucrose-alone,* and a third *Laser+Sucrose* day with the alternate frequency. Within each session, the responses required to earn the next reward increased after each reward, and breakpoint or ratio reached during 30min sessions was assessed. Separate halorhodopsin rats underwent testing with inhibition.

Spout-touch laser self-stimulation

Incentive properties of laser alone without sucrose were tested in instrumental spout-touch self-stimulation tests. With two empty waterspouts available, each touch on a designated *Laser-spout* provided stimulation (3-sec; 10Hz/40Hz; 30min). Touches on the other *Inactive-*

spout earned nothing, as a baseline exploration measure. Rats were classified on Day 1 as robust, low, or non-self-stimulators and Days 2-3 evaluated consistency of self-stimulation (Appendix A) (Warlow et al. 2020).

Place-based self-stimulation

In a different place-based self-stimulation test, rats could earn laser self-stimulations by remaining in a designated *Laser-delivering* chamber within a 3-chamber apparatus (2-major, 1-smaller center, see Supplementary Methods) after an initial session without laser evaluated baseline preference. For 3 test days, *Laser-delivering* chamber entries triggered laser (3-sec-on/4-sec-off), which continued cycling as long as rats remained, terminating upon exit. Time in *Laser-delivering* minus time in alternative *No-laser* chamber difference-scores were assessed.

Histology

Briefly, laser-stimulations preceded lethal doses of sodium pentobarbital and transcardial perfusions for Fos assessment (see Appendix A) (Baumgartner et al. 2020). Brains were extracted, post-fixed, sectioned into 40μm slices via cryostat (Leica), processed for GFP and cFos immunohistochemistry (Fig. 3.2), and imaged using a digital camera (Qimaging) and fluorescence microscope (Leica).

Coronal sections were imaged (10x magnification) to quantify distributed Fos using Paxinos & Watson atlas (Paxinos and Watson 2007). Laser-recruited changes in Fos expression in NAc/CeA/BNST groups were compared to eYFP-control levels in several mesocorticolimbic structures (Table 3.2).

CRF and Cre expression assessed by RNAScope® Fluorescent In Situ Hybridization (FISH)

Colocalization of Cre and CRF in infected neurons was verified with FISH (see Appendix A) (Lemos et al. 2019; Wang et al. 2012). Cells containing *Cre* and *Crh* mRNAs were

manually counted in 100x100x17µm volumes from core samples in NAc, CeA, and BNST (n=6).

Statistical Analyses

Mixed-model ANOVAs evaluated within-group (e.g., laser-pairings) and between-group effects (e.g., ChR2/eYFP) followed by post-hoc comparisons with Bonferroni corrections. Distant Fos was evaluated by unpaired *t*-tests. Effect sizes are Cohen's D. For all analyses, significance level was p=0.05, two-tailed.

Results

Cre and CRF colocalization

Crh and *Cre* mRNAs were visualized using FISH in slices from *Crh*-Cre+ rats (n=6) and found to typically occur together in the same neurons. CRF+ and Cre+ co-expressing neurons were densely concentrated within the lateral CeA (10.1±0.9 co-labeled neurons per 100x100x17µm volume) and dorsolateral BNST (10.0±0.7). In NAc, CRF+ neurons were sparsely distributed throughout medial shell (6.0±0.7 co-labeled neurons, or nearly one-half CeA/BNST density; Fig. 3.3, Appendix A).

NAc and CeA CRF-expressing neurons recruit similar structures, BNST shows distinct activation

Recruitment of Fos elevation in distant brain circuitry was assessed following CRF-expressing neuron excitation in NAc, CeA or BNST (Tables 3.2, A.1).

Laser ChR2 excitation of CRF-containing neurons in NAc shell (NAcSh) recruited 150-200% increases in distant Fos expression over eYFP control levels in reward-related mesocorticolimbic structures including NAc core, CeA, ventral tegmentum (VTA), ventral pallidum (VP), lateral hypothalamus (LH), etc. (Fig. 3.4A). Similarly, CeA stimulation of CRF-expressing neurons excitation increased Fos expression 150-250% in NAcSh, VTA, VP, LH, etc. (Fig. 3.4B).

Conversely in BNST ChR2 rats, CRF-containing neuron excitation recruited distant Fos 150-200% elevation in several structures related to pain, aversion, fear, or satiety: midbrain periaqueductal gray (PAG), PVN, and basolateral amygdala (BLA), in addition to 150% elevation in some mesocorticolimbic structures (Fig. 3.4C).

NAc and CeA CRF-expressing neuronal stimulation enhances paired-sucrose value

NAc CRF-containing neuron incentive enhancement. Pairing ChR2 stimulation of CRF-containing neurons in NAc (n=8) with earning sucrose rewards in the two-choice tasks caused rats to pursue that paired *Laser+Sucrose* option nearly exclusively over the other identical *Sucrose-alone* option without laser ($F_{1,6}$=46.700, p<0.001; Fig. 3.5A). Rats reached a 7:1 ratio preference by final day 8 (t_7=5.846, p=0.001, 95%CI:[208,491], d=2.66). Both female and male ChR2 Crh-cre+ rats showed strong preferences for NAc *Laser+Sucrose* lever over *Sucrose-alone* lever (females: 5:1±1 ratio, males: 7:1±1; Fig. A.1A). Both 10Hz (n=5; $F_{1,4}$=24.540, p=0.008) and 40Hz frequencies of NAc laser excitation (n=7; $F_{1,6}$=39.209, p=0.001) supported similar *Laser+Sucrose* preference, with no difference between them ($F_{1,10}$=1.186, p=0.302; Fig. A.2C). By contrast, NAc eYFP controls with inactive virus chose randomly between *Laser+Sucrose* and *Sucrose-alone* options (n=6; $F_{1,5}$=0.014, p=0.911; Fig. 3.5B).

NAc CRF-containing neuron inhibition paired-avoidance. Separate inhibition rats, with halorhodopsin (NpHR) in NAc, developed strong avoidance of the paired *Laser+Sucrose* option and instead preferred *Sucrose-alone* by a 20:1 ratio (n=6; $F_{1,5}$=25.741, p=0.004; Fig. 3.5C).

CeA CRF-containing neuron incentive enhancement. In CeA, ChR2 stimulation of CRF-containing neurons induced similar near-exclusive pursuit of the paired *Laser+Sucrose* option (n=9; $F_{1,7}$=19.227, p=0.003; Fig. 3.6A), growing to a >10:1 ratio over *Sucrose-alone* by day 8 (t_8=5.110, p=0.001, 95%CI:[241,638], d=3.09). Female and male ChR2 *Crh*-Cre+ rats had similar preference ratios for CeA *Laser+Sucrose* over *Sucrose-alone* (females: 13:1±2, males:

10:1±2; Fig. A.1A). Both 10Hz (n=9; $F_{1,8}$=59.101, p<0.001; Fig. A.2D) and 40Hz frequencies of CeA laser excitation (n=5; $F_{1,4}$=90.572, p=0.001) supported comparable levels of preference ($F_{1,12}$=0.534, p=0.479). By contrast, control CeA eYFP rats chose equally between sucrose options (n=7; $F_{1,6}$=0.003, p=0.959) and so differed significantly from CeA ChR2 rats ($F_{1,14}$=4.853, p=0.045; Fig. 3.6B).

CeA CRF-containing neuron inhibition paired-avoidance. NpHR CeA inhibition of CRF-containing neurons (n=7) produced avoidance of the laser-paired sucrose option, instead causing a 10:1 ratio preference for *Sucrose-alone* ($F_{1,6}$=72.960, p<0.001; Fig. 3.6C).

NAc and CeA CRF-expressing neuronal excitation increases breakpoint

Progressive ratio (PR) breakpoint tests assessed whether CRF-containing neuron stimulation changed the intensity of incentive motivation to obtain sucrose reward. NAc ChR2 rats (n=6) worked twice as hard in the PR task on their *Laser+Sucrose* day, and achieved 200% higher effort breakpoints, than on the *Sucrose-alone* day (t_5=6.010, p=0.002, 95%CI:[23,58], d=2.6; Fig. 3.5D). Both female (210±16%) and male rats doubled their breakpoints in *Laser+Sucrose* condition (170±24%; Fig. A.1B). Similarly, 10Hz (t_3=4.841, p=0.017, n=4) and 40Hz (t_5=6.010, p=0.002, n=6; Fig. A.3D) laser frequencies supported similar doubling of breakpoint. NAc eYFP controls showed no breakpoint differences between *Laser+Sucrose* and *Sucrose-alone* days (n=5; t_4=0.533, p=0.62; Fig. 3.5D), and so differed significantly from ChR2 rats ($F_{1,9}$=6.689, p=0.029).

In CeA, excitation of CRF-containing neurons also increased *Laser+Sucrose* breakpoint by >200% over *Sucrose-alone* (n=7; t_6=6.712, p=0.001, 95%CI:[34,73], d=3.58; Fig. 3.6D). CeA stimulation doubled breakpoint in both females (250±56%) and males (250 ±25% males; Fig. A.1B), and at both 10Hz (n=7, t_6=4.992, p=0.002) and 40Hz frequencies (n=5, t_4=4.3981,

p=0.012; Fig. A.3D). Control CeA eYFP rats (n=5) showed no laser effect on breakpoint (t_4=0.314, p=0.769; Fig. 3.6D), and significantly differed from ChR2 rats ($F_{1,10}$=9.590, p=0.011).

BNST CRF-containing neuron excitation induces laser-paired sucrose avoidance.

In the two-choice task, BNST ChR2 rats avoided their *Laser+Sucrose* option and instead preferred *Sucrose-alone* (n=8; $F_{1,6}$=13.927, p=0.010; Fig. 3.7A), reaching an 8:1 *Sucrose-alone* preference by day 8 (n=8; t_7=6.059, p=0.001, 95%CI:[214,488], d=4.72). ChR2 males showed numerically stronger avoidance of BNST *Laser+Sucrose,* (10:1±3 preference for *Sucrose-alone*) than females (5:1±1), but the small group sizes were not adequately powered to statistically evaluate sex differences here (Fig. A.1). Both 10Hz (n=7; $F_{1,6}$=30.241, p=0.002) and 40Hz frequencies supported similar *Laser+Sucrose* avoidance (n=5; $F_{1,4}$=9.474, p=0.037), with no difference in magnitude ($F_{1,10}$=0.996, p=0.342). In contrast, BNST eYFP control rats chose equally between the two sucrose options (n=6; $F_{1,5}$=0.054, p=0.826; Fig. 3.7B).

BNST NpHR two-choice. BNST NpHR rats (n=6) showed no statistical difference in choice between sucrose options ($F_{1,5}$=0.167, p=0.700; Fig. 3.7C), although there was a nonsignificant trend toward preferring the *Laser+Sucrose* option paired with halorhodopsin inhibition.

BNST CRF-containing neuron excitation suppresses sucrose incentive motivation. Excitation of BNST CRF-containing neurons suppressed incentive motivation to earn sucrose, reducing *Laser+Sucrose* breakpoint effort to half that of *Sucrose-alone* (t_7=5.492, p=0.001, 95%CI: [20,49], d=2.25; Fig. 3.7D). Both female (49±27%) and male rats (54±14%) showed

similar breakpoint reductions, and both 10Hz (t_7=6.178, p<0.001, n=8) and 40Hz frequencies were comparably effective (t_3=5.333, p=0.013, n=4). By contrast, BNST eYFP controls showed no breakpoint laser-effects (n=5; t_4=0.441, p=0.682; Fig. 3.7D), and so differed from BNST ChR2 rats ($F_{1,11}$=5.874, p=0.034).

Opposite breakpoint effects for CRF-expressing neuronal inhibition

Halorhodopsin inhibition of CRF-containing neurons in NAc (n=6, Fig. 3.5D) or CeA (n=7; Fig. 3.6D) suppressed *Laser+Sucrose* breakpoint to ~50% that of *Sucrose-alone* (NAc: t_5=5.308, p=0.003, 95%CI:[19,53], d=2.58; CeA: t_6=4.032, p=0.007, 95%CI:[13,55], d=2.33). BNST CRF-containing neuronal inhibition did not significantly alter breakpoint effort, though there was a nonsignificant trend toward a higher breakpoint for *Laser+Sucrose* (n=6; t_5=0.717, p=0.506; Fig. 3.7D).

Spout Self-stimulation: NAc and CeA stimulation of CRF-expressing neurons by itself is a moderate reward

In the instrumental self-stimulation task, each touch on the designated *Laser-spout* earned 3-sec of laser excitation, while *Inactive-spout* touches delivered nothing. No NAc ChR2 rats met criterion for robust self-stimulation of >50 touches on *Laser-spout* on Day 1 (Warlow et al. 2020). However, 7 of 8 NAc ChR2 rats demonstrated low-level self-stimulation, meeting a lesser criterion of only >10 *Laser-spout* touches and >2x touches on *Laser-spout as on Inactive-spout*. On Days 2-3, those 7 NAc rats achieved 25-35 self-stimulations per 30min session, roughly 4x more than *Inactive-spout* touches (n=7; $F_{1,5}$=7.823, p=0.038; Fig.8A), and~1.5x more *Laser-spout* touches than eYFP control rats ($F_{1,9}$=9.949, p=0.012). Female and male NAc ChR2 rats showed similar levels of self-stimulation (males: 29±16 illuminations; females: 29±8), and

10Hz and 40Hz frequencies both supported self-stimulation (10Hz: 25±10, n=3; 40Hz: 32±10, n=4).

CeA self-stimulation. Two of eight CeA ChR2 rats met the >50 illuminations criterion for robust self-stimulation, while 7 met the lower >10 self-stimulation criterion. These 7 CeA ChR2 rats self-stimulated ~25-35 times on days 2-3, >3x more than *Inactive-spout* ($F_{1,5}$=12.009, p=0.018; Fig. 3.8B), and earned >3x more illuminations than eYFP control rats ($F_{1,9}$=17.576, p=0.002). The 2 most robust self-stimulators were both females and reached 40±3 self-stimulations per day (males n=5, 23±7). Both 10Hz (n=4) and 40Hz (n=3) frequencies supported similar levels of CeA self-stimulation (10Hz: 27±10 self-stimulations; 40Hz: 29±8).

BNST fails to support self-stimulation. No BNST ChR2 rats met any criteria for self-stimulation of CRF-containing neurons, responding equally at low rates on both spouts (n=8, $F_{1,6}$=0.006, p=0.939, Fig. 3.8C).

CeA and NAc self-stimulation does not account for laser effects on sucrose motivation.

Did laser self-stimulation in CeA and NAc substantially drive laser's ability to control sucrose pursuit in two-choice or PR tasks? The answer appears to be 'no': there was no correlation between self-stimulation values, which were generally low, and control of sucrose pursuit in the two-choice test (n=6 NAc: r=0.624, p=0.098; n=7 CeA: r=-0.024, p=0.926). Nor was there a correlation between self-stimulation and enhancement of PR breakpoint, which was relatively strong in most NAc or CeA ChR2 rats (Pearson's correlation, n=6 NAc: r=-0.349, p=0.498; n=7 CeA: r=0.605, p=0.280). Finally, even CeA (n=1) and NAc (n=1) rats that failed to self-stimulate showed ~200% laser-induced enhancements of breakpoint, and control of *Laser+Sucrose* preference (11:1 ratio) as strong as in self-stimulators (~200%, 9:1).

NAc and CeA place-based self-stimulation, BNST place-avoidance

Rats were additionally tested for self-stimulation using a second place-based task, where entering and staying in a designated chamber earned laser (cycling 3-sec-on/4-sec-off; 15min).

NAc and CeA place-based self-stimulation. NAc ChR2 rats spent >150% more time in *Laser-delivering* chamber than in *No-laser* chamber ($F_{1,6}$=6.664, p=0.042; Fig. 3.9A). NAc ChR2 rats also spent 150% longer in *Laser-delivering* chamber than they had during previous baseline tests without laser (t_7=3.376, p=0.012, 95%CI:[56,318], d=1.21), and more time in their *Laser-delivering* chamber than inactive eYFP controls (t_{11}=2.318, p=0.041, 95%CI: [9,353], d=1.05). Both female (n=2) and male (n=6) NAc ChR2 rats spent comparably more time in the *Laser-delivering* chamber (female: 160±20%; males: 140±10%), and both 10Hz (n=3; 160±20%) and 40Hz (n=5; 160±20%) frequencies were equally effective.

CeA ChR2 rats (n=8) demonstrated robust place-based self-stimulation of CeA CRF-containing neurons, spending ~200% more time in *Laser-delivering* than the *No-laser* chamber ($F_{1,6}$=21.085, p=0.004). CeA ChR2 rats also spent 200% longer in *Laser-delivering* chamber than they had during previous baseline tests without laser (t_7=3.038, p=0.019, 95%CI:[63,509], d=1.41), and more than CeA eYFP controls (t_{11}=2.062, p=0.011, 95%CI:[57,484], d=1.20). Both female (n=2; 160±20% more *Laser-delivering* time) and male (n=3; 200±20%) CeA ChR2 rats showed place-based self-stimulation, and 10Hz (n=5) and 40Hz (n=3) laser frequencies were both effective (10Hz: 200±10%; 40Hz: 150±30%).

BNST induces place-avoidance. BNST ChR2 rats mildly avoided the *Laser-delivering* chamber that stimulated CRF-containing neurons in BNST, spending only <75% as much time

there as in the *No-laser* chamber (n=10; $F_{1,8}$=6.593, p=0.033; Fig. 3.9C). ChR2 BNST rats also spent less time in their *Laser-delivering* chamber than they had during baseline tests without laser (t_9=3.188, p=0.011, 95%CI:[67,397], d=1.25), and less time than eYFP control rats (t_{13}=2.737, p=0.017, 95%CI:[49,415], d=1.76). Both female (n=5) and male (n=5) BNST ChR2 rats showed avoidance of the *Laser-delivering* chamber (female: <85±10%; males: <50±10%), and both 10Hz (n=6; <65±10%) and 40Hz (n=4; <70±10%) frequencies induced place-based avoidance.

Discussion

Our results demonstrate that optogenetic excitation of CRF-containing neural systems in both CeA and NAc shell focused and increased incentive motivation for sucrose and carried positive valence by itself. ChR2 stimulation of CRF-containing neurons in CeA and NAc 1) focused intense incentive motivation on the *Laser+Sucrose* option over an alternative *Sucrose-alone* option in the two-choice task, 2) amplified incentive motivation and breakpoint effort for sucrose reward, and 3) was actively sought by itself as laser self-stimulation. Simultaneously, ChR2 stimulation of CRF-expressing neurons in CeA and NAc recruited reward-related mesolimbic circuitry, reflected as Fos increases in VTA, NAc, VP, LH, etc.

By contrast, only BNST optogenetic excitation of CRF-containing neurons produced aversive motivation. BNST CRF-containing neuronal excitation here caused avoidance of the *Laser+Sucrose* option and of laser by itself, suppressed breakpoint of sucrose motivation, and recruited increased Fos in PVN and PAG, structures associated with negative-avoidance or distress.

Our NAc and CeA incentive effects are consistent with previous reports that CRF systems in CeA or NAc can contribute positively to reward motivation (Kim et al. 2017; Lemos and Alvarez 2020; Lemos et al. 2012; Lim et al. 2007; Merali et al. 1998; Peciña et al. 2006). NAc CRF microinjections increase bursts of cue-triggered 'wanting' for sucrose rewards in rats, and cause conditioned place-preference and increase NAc dopamine release in non-stressed mice (Lemos and Alvarez 2020; Lemos et al. 2012; Peciña et al. 2006).

CRF systems mobilize bio/behavioral responses to changing events (Merali et al. 1998, 2004; Schulkin 2017), and can be responsive to either positive or negative events. For instance, it has long been known that CRF systems in CeA respond to positive reward stimuli such as food

cues, not only to aversive stimuli (Merali et al. 1998). Indicating positively-valenced roles, mice optogenetically self-stimulate CRF-containing neurons in CeA (Kim et al. 2017). Our results confirm CeA CRF-containing neuronal self-stimulation in rats and extend CRF neuronal self-stimulation to NAc. They further demonstrate that NAc and CeA activations potentiate and focus incentive motivation for natural sucrose reward. Conversely, CRF-containing neuronal stimulation in BNST produced opposite negative motivational effects.

Future studies could identify the specific projections from CeA, NAc and BNST that mediate these effects. For example, CeA CRF-containing neurons project to LH, VP, VTA, and BNST (Asok et al. 2018; Erb et al. 2001a; Pomrenze et al. 2015, 2019b; Rodaros et al. 2007; Ventura-Silva et al. 2020). CeA-BNST CRF-containing projections may reliably mediate aversive motivation (Asok et al. 2018; de Guglielmo et al. 2019; Pomrenze et al. 2019b; Ventura-Silva et al. 2020), implying that projections to LH, VP, VTA or elsewhere may mediate incentive motivation effects. ChR2 stimulation here likely activated these CeA-BNST projections too, implying that other positively-valenced CeA-outputs may overpower BNST aversive effects when simultaneously activated. For NAc, local connections of CRF-containing neurons may mediate incentive motivation effects, such as intra-NAc connections to cholinergic interneurons, which may modulate dopamine release in NAc (Lemos and Alvarez 2020; Lemos et al. 2012, 2019). Neuroanatomically, it would be of interest to additionally investigate the motivational effects of dense CRF-containing neuronal projections from hypothalamic PVN. However, PVN CRF-containing neurons may co-release glutamate, whereas the *Crh*-Cre rat line used here may primarily target CRF-expressing neurons that co-release GABA (Dabrowska et al. 2013; Pomrenze et al. 2015).

Neurochemically, it would be useful in future studies to examine the roles in these motivational effects of CRF release versus other neurotransmitters co-released by CRF-expressing neurons, such as GABA, dynorphin, neurotensin, and somatostatin (Partridge et al. 2016; Pomrenze et al. 2015, 2019a; Shimada et al. 1989; Torruella-Suárez et al. 2020). Co-release might be related to why CRFR1 antagonists may fail to block stress-induced craving in clinical models (Grillon et al. 2015; Kwako et al. 2015; Schwandt et al. 2016; Shaham and de Wit 2016).

Positive NAc and CeA vs negative BNST: Anatomical differences in motivational valence

Why did CRF-containing neuron activations have positively-valenced effects in NAc and CeA but negatively-valenced effects in BNST? NAc and CeA are both striatal-level structures in cortico-striatal-pallidal macrosystem frameworks of telencephalon organization, having neuronal, connectivity, neurochemical, and embryological features shared with neostriatum (Heimer et al. 2007; Swanson 2005; Zahm 2006). For example, CeA and NAc contain mostly GABAergic neurons that receive descending cortical-type glutamatergic inputs and ascending mesotelencephalic dopaminergic inputs, and both send GABAergic outputs to pallidal-level structures of BNST or VP (Heimer and Van Hoesen 2006; Heimer et al. 2007; Swanson 2005; Zahm 2006). In the same frameworks, BNST is a pallidal-level structure with descending outputs to hypothalamus and brainstem, plus ascending re-entrant projections back to thalamo-cortico-striatal-pallidal loops (Dabrowska et al. 2016; Giardino et al. 2018; Gray and Magnuson 1992; Heimer and Van Hoesen 2006; Heimer et al. 2007; Swanson 2005; Zahm 2006).

Hypothesized roles of CRF-containing systems in addiction

Traditionally, CRF-containing neurons have been hypothesized to generate aversive states like anxiety and drug withdrawal, although CRF systems also have wider roles in affective appraisals of incentives that mobilize motivational states (Merali et al. 1998, 2004; Schulkin 2017). Our study helps puts this in perspective.

Regarding the role of CRF in anxiety and addiction, the allostatic theory of addiction posits that CRF-containing neuronal activation in CeA and BNST components of extended amygdala cause aversive drug withdrawal, which is hypothesized to promote relapse through efforts to hedonically self-medicate via consumption of drug rewards (Funk et al. 2006; Koob and Le Moal 1997; Koob and Schulkin 2019; Koob 2013; Roberto et al. 2017; Zorrilla et al. 2014).

Our results call into question some of these assumptions. Indeed, the hypothesis that CRF-containing neurons in CeA and BNST necessarily generate negatively-valenced states may not apply to CeA. Instead, our results indicate that CRF-expressing neuronal activation in both CeA and NAc increases reward pursuit and produces positively-valenced incentive states which rats actively worked to induce. Conversely, in partial support of the allostatic model, BNST CRF-containing neural activation did cause aversive motivational states. However, the aversive state induced by stimulating BNST CRF-expressing neurons failed to increase reward-seeking, instead suppressing sucrose pursuit.

This suggests that hedonic self-medication of aversion may not be the primary mechanism by which CRF-containing neurons promote reward pursuit and consumption for any of these structures. Instead, CRF-expressing neurons in CeA and NAc amplify 'wanting' to pursue and consume rewards without aversive states, while BNST CRF-expressing neuronal excitation may actually impede reward pursuit and consumption. This may be why drug

withdrawal is not as effective for reinstatement of drug taking as stress or drug priming (Erb et al. 2006; Mantsch et al. 2016; Shaham and Stewart 1995; Shaham et al. 1997). Although brain-wide CRF activation may cause aversive withdrawal states through BNST CRF-containing neurons, our results suggest that any accompanying increases in reward pursuit or addictive relapse might predominantly be due to co-activation of CRF incentive motivation systems in NAc and CeA.

Valence flips

Motivational valence induced by CeA optogenetic stimulation can switch depending on environmental situation, and therefore the valence of our CRF-containing neuron stimulation could potentially switch in certain circumstances (Lemos et al. 2012; Warlow et al. 2020). If so, CRF systems could be quite labile in their functional role in motivated behaviors depending upon context and need, which deserves further investigation.

Clinical implications

Activation of CRF systems during stress or emotional excitement may promote relapse in addiction, binge-eating, and other excessive consumption. The dominant perspective relied solely on the postulated aversiveness of CRF-expressing neural activation. However, our results indicate that incentive motivation roles of CRF-containing neurons in NAc and CeA predominate under tested conditions, and promote intense reward pursuit without aversive distress (Kim et al. 2017; Lemos et al. 2012; Peciña et al. 2006). This could explain why even positively-valenced stressors (i.e., new relationships, winning the lottery) can be triggers of addictive relapse and binge-eating (Annis and Graham 1995; Kaundal et al. 2016; Larimer et al. 1999; Maisto et al.

1988a). Conversely, aversive motivation induced by BNST CRF-containing neurons contributed little to reward pursuit. Ultimately, CRF-containing systems have diverse motivational roles. Further clarification of negatively-valenced versus positively-valenced motivation roles of CRF systems will be important to understand how they promote excessive consumption in addiction and related disorders.

Figures

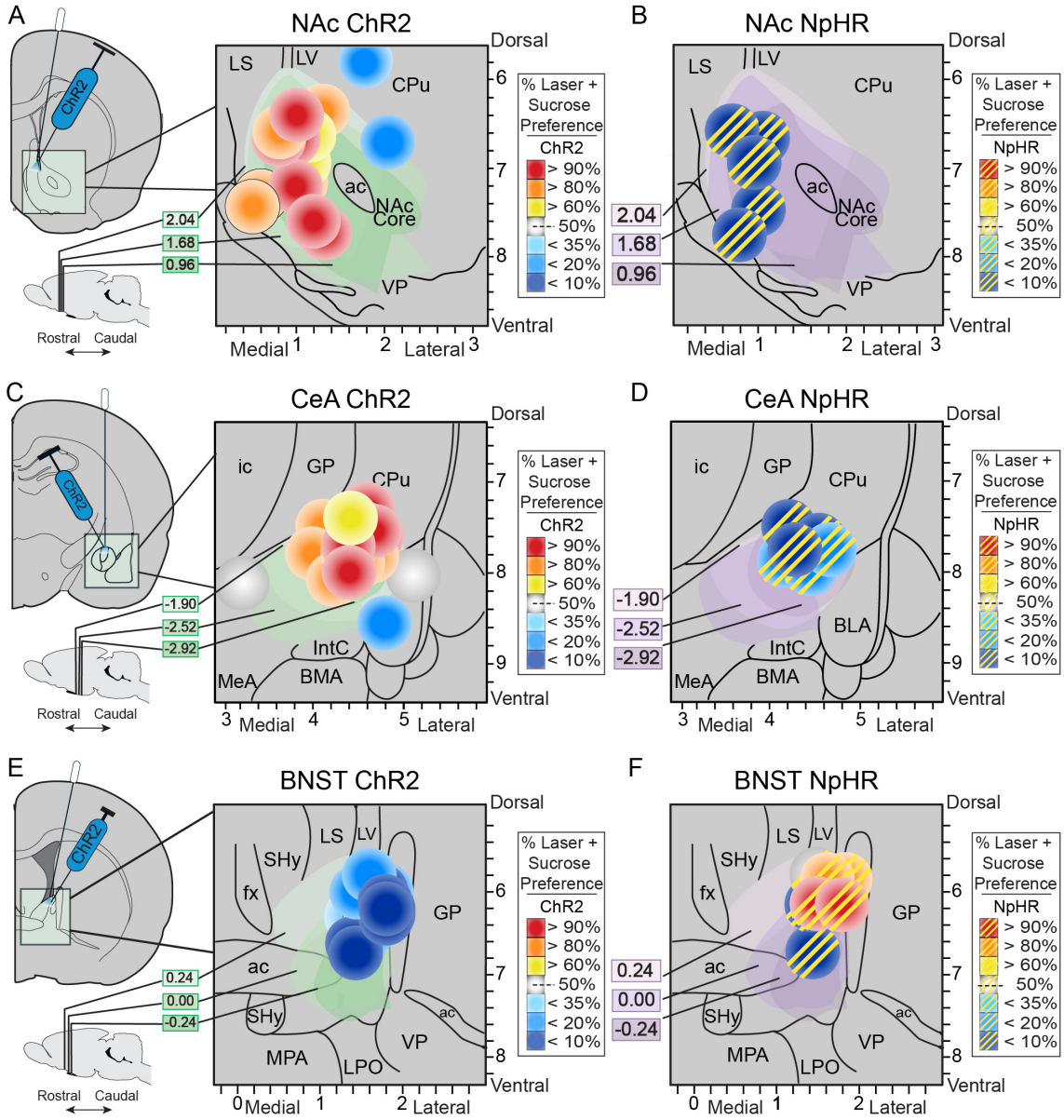

3.1 Localization of function maps

Function maps of effects on sucrose preference in two-choice task of ChR2 stimulation of CRF-expressing neurons in **A)** NAc, **C)** CeA, and **E)** BNST. Maps for inhibitory halorhodopsin effects of laser illumination on CRF-expressing neurons shown in **B)** NAc, **D)** CeA, and **F)** BNST (striped symbols). Symbol sizes reflect size of optogenetic Fos plumes (see Fig. 3.2 and Appendix A). Yellow, orange, or red symbol colors show intensity of enhancement of laser-induced preference for *Laser+Sucrose* option over *Sucrose-alone* option produced at that site (effects shown for days 6-8 of two-choice task). Conversely, blue colors show intensity of avoidance of *Laser+Sucrose* (i.e., preference instead for *Sucrose-alone*). Also see Table 3.1. CPu, caudate putamen; LV, lateral ventricle; LS, lateral septum; VP, ventral pallidum; ac, anterior commissure; ic, internal capsule; GP, globus pallidus; MeA, medial amygdala; IntC, intercalated amygdala; BMA, basomedial amygdala; BLA, basolateral amygdala; fx, fornix; SHy, septohypothalamic nucleus; MPA, medial preoptic area; LPO, lateral preoptic area.

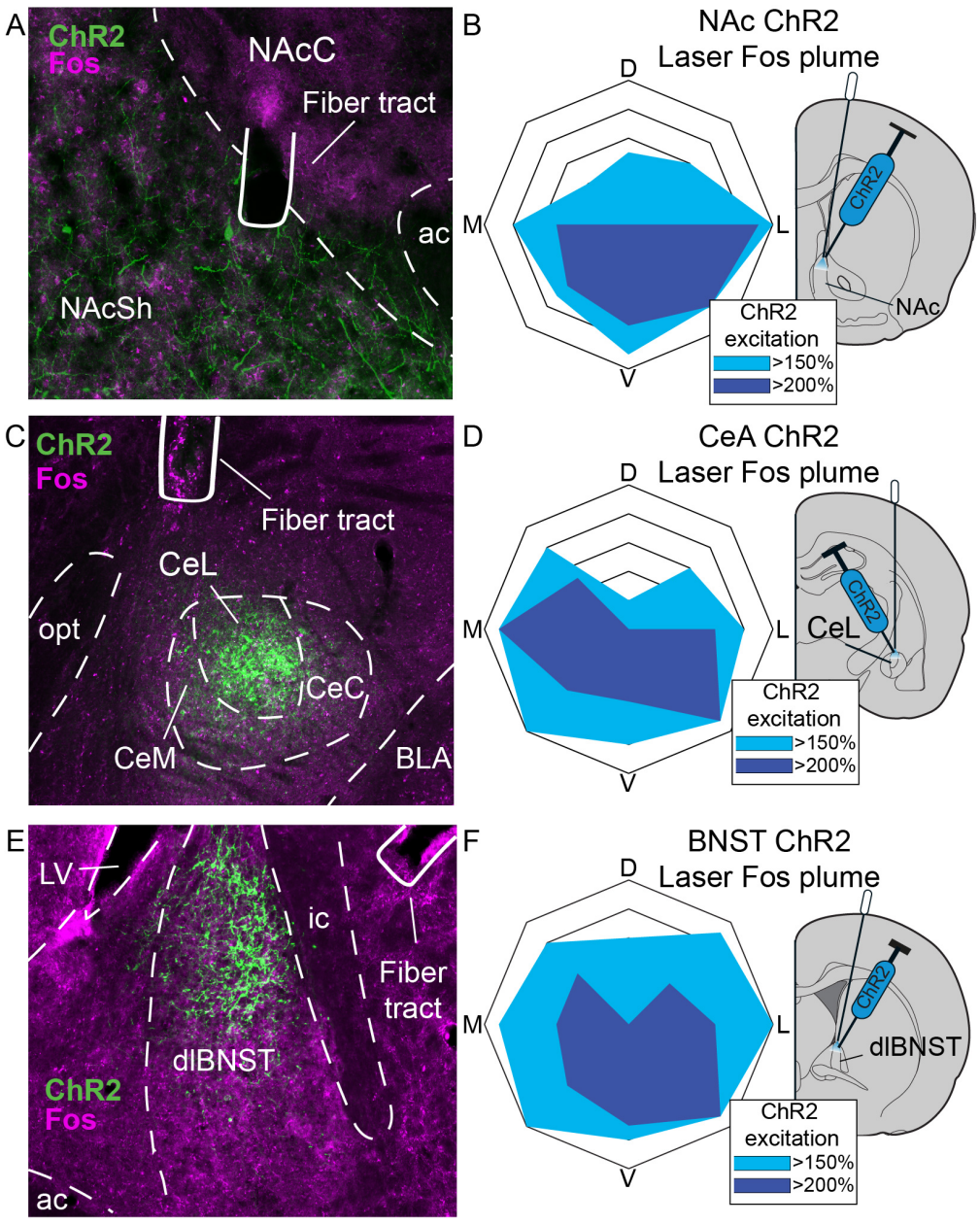

3.2 Virus expression and local Fos plumes

Photomicrograph (×10 magnification) shows channelrhodopsin virus expression (ChR2; green), and neuronal Fos protein expression (magenta) immediately surrounding optic fiber tips for *Crh*-Cre+ rats in **A)** nucleus accumbens (NAc) shell, **C)** lateral division of central nucleus of amygdala (CeA) and **E)** dorsolateral division of bed nucleus of stria terminalis (BNST). Blue diagrams at right show maps displaying size and intensity of local Fos plumes produced in each structure by laser stimulation of CRF-containing neurons expressing ChR2 (i.e., zones of >150% Fos elevation and >200% Fos elevation over baselines (100%) measured in laser-illuminated eYFP control rats. Average Fos plume diameters are shown for *Crh*-Cre+ ChR2 rats after laser illumination in **B)** NAc, **D)** CeA, and **F)** BNST CRF-containing neurons. D: dorsal, M: medial, L: lateral, V: ventral to fiber tip; ac, anterior commissure; NAcC, nucleus accumbens core; NAcSh, nucleus accumbens shell; CeC, capsular central amygdala; CeL, lateral central amygdala; CeM, medial central amygdala; dlBNST, dorsolateral bed nucleus of stria terminalis; ic, internal capsule; LV, lateral ventricle.

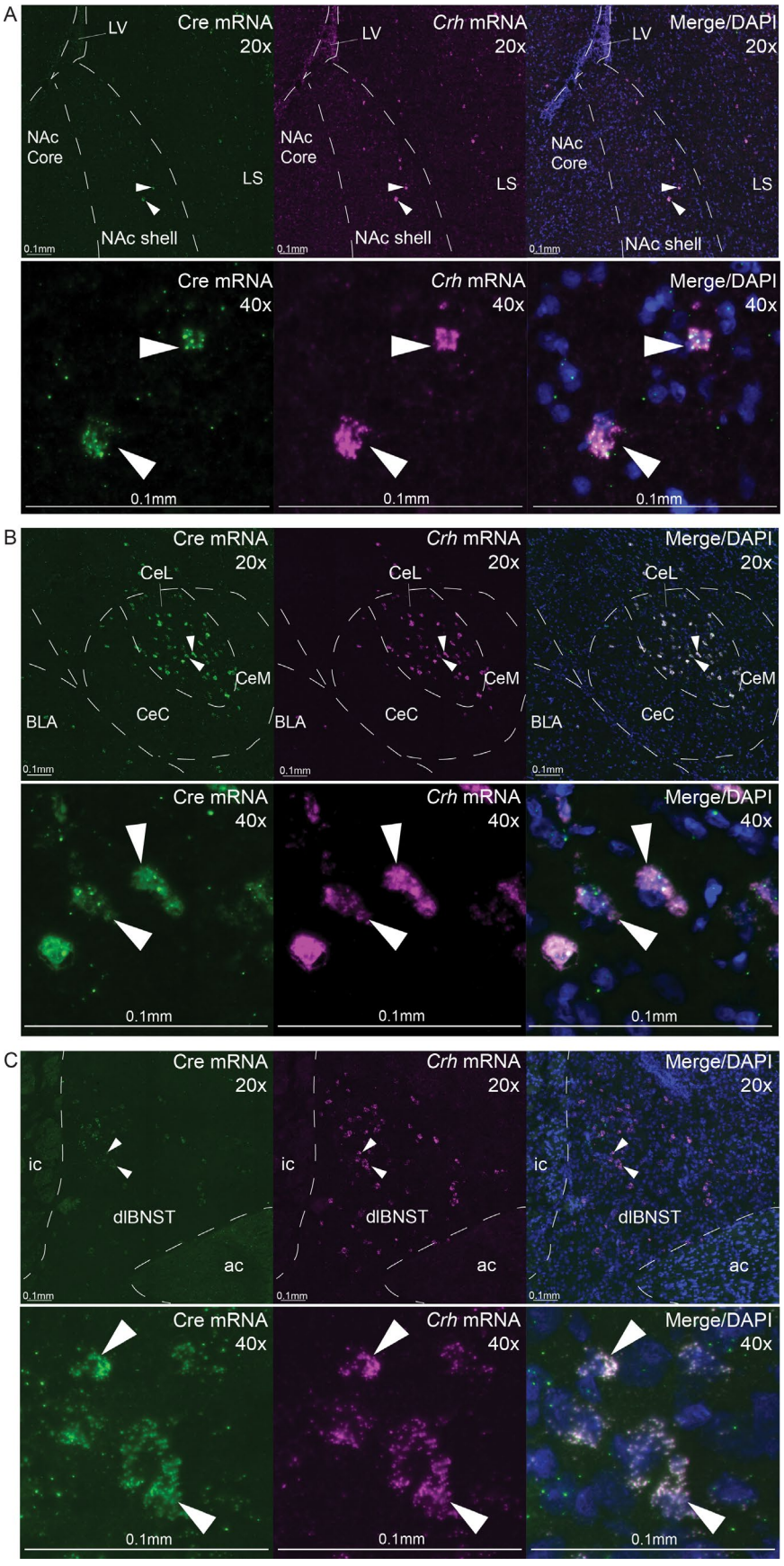
A
Cre mRNA 20x
Crh mRNA 20x
Merge/DAPI 20x
LV
NAc Core
LS
NAc shell
0.1mm
Cre mRNA 40x
Crh mRNA 40x
Merge/DAPI 40x
B
CeL
CeM
CeC
BLA
C
ic
dlBNST
ac

3.3 CRF and Cre colocalization verification through fluorescence in situ hybridization
Representative images for Cre mRNA expression and *Crh* mRNA expression in A) nucleus accumbens (NAc) shell, B) lateral division of CeA (CeL), and C) dorsolateral division of bed nucleus of stria terminalis (dlBNST) in *Crh*-Cre+ rats (n=6). Low-power (20x) and high-power (40x) images show localization of neurons expressing Cre mRNA (green) or *Crh* mRNA (magenta), and Cre/*Crh* colocalization with cell bodies stained with DAPI (blue). Arrows point to examples of cells coexpressing Cre and *Crh* mRNAs. Scale bars denote 0.1mm at both 20x and 40x. See Supplementary methods and results. LV, lateral ventricle; LS, lateral septum; BLA, basolateral amygdala; CeC, capsular central amygdala, medial central amygdala; ic, internal capsule; ac, anterior commissure.

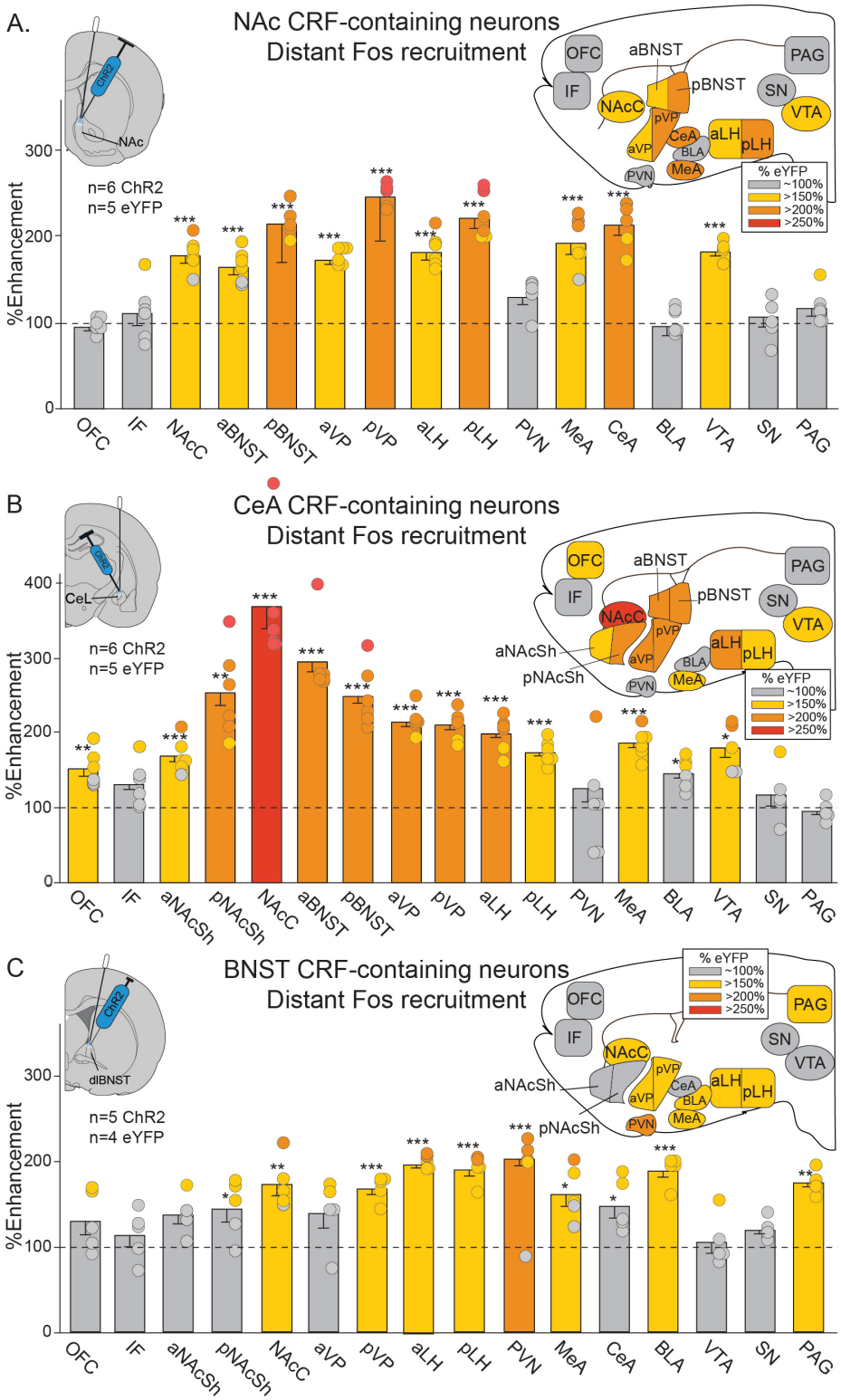

3.4 Laser-enhancements in distant Fos expression

Brain maps show recruitment of distant Fos elevation in mesocorticolimbic structures following CRF-containing neuron ChR2 stimulation in NAc, CeA or BNST (colors denote percent Fos elevation vs. eYFP controls, all two-way unpaired *t*-tests). **A)** NAc ChR2 stimulation (n=3 female, n=3 male): NAc core (NAcC), ventral tegmentum (VTA), anterior ventral pallidum (aVP), posterior VP (pVP), anterior

lateral hypothalamus (aLH), pLH, medial amygdala (MeA), CeA, aBNST, pBNST. **B)** CeA ChR2 stimulation (n=3 female, n=3 male): orbitofrontal cortex (OFC), aNAcSh, pNAcSh, NAcC, aVP, pVP, aLH, pLH, MeA, VTA, aBNST, pBNST, and minor increases in basolateral amygdala (BLA; <150%). **C)** BNST ChR2 stimulation (n=2 female, n=3 male): BLA, periaqueductal gray (PAG), hypothalamic paraventricular nucleus (PVN), NAcC, pVP, aLH, pLH, MeA, and minor increases in pNAcSh (<150%) and CeA (<150%). See Table A.1. infralimbic cortex (IF); substantia nigra (SN). Means and SEM reported. *p<0.05,**p<0.01,***p<0.001

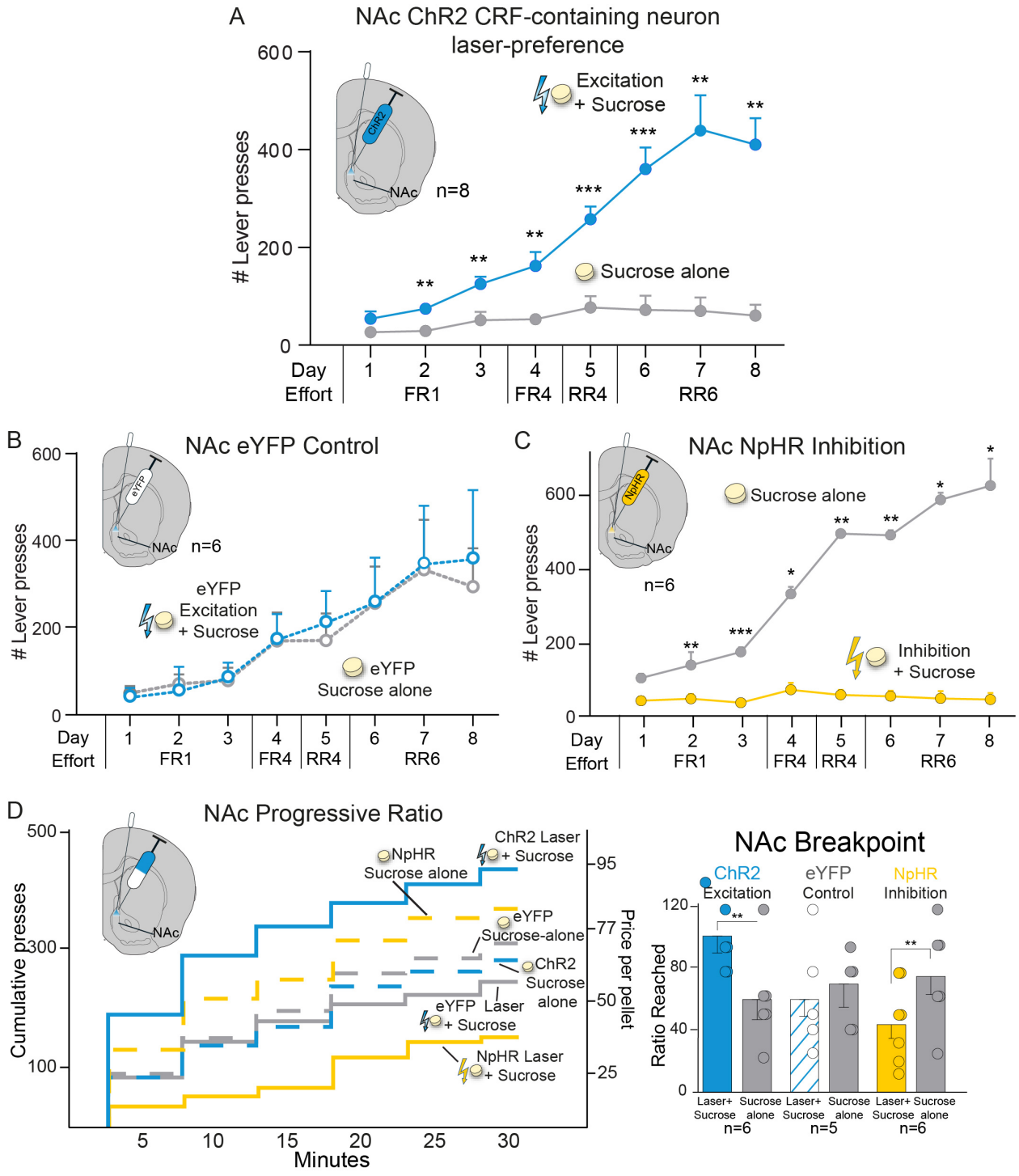

3.5 CRF-containing neuron stimulation in NAc biases and amplifies sucrose motivation
ChR2 excitation of CRF-containing neurons in NAc shell caused preference for paired *Laser+Sucrose* over *Sucrose Alone* in **A)** two-choice test (n=3 female, n=5 male), reaching a 7:1 ratio by day 8. By contrast **B)** control NAc eYFP rats chose equally between options. **C)** NpHR inhibition of CRF-containing neurons in NAc shell (n=3 female, n=3 male) caused avoidance of *Laser+Sucrose* and *Sucrose-alone* preference. **D)** In a progressive ratio test, NAc ChR2 CRF-containing neuron excitation enhanced incentive motivation breakpoint *Laser+Sucrose* over *Sucrose Alone* (n=2 female, n=4 male).

ChR2 rats had higher *Laser+Sucrose* breakpoints than eYFP controls (n=5). Laser did not affect NAc eYFP control breakpoint between progressive ratio test days. NAc NpHR inhibition of CRF-containing neurons reduced *Laser+Sucrose* breakpoint motivation (n=3 female, n=3 male). Means and SEM reported. *$p<0.05$,**$p<0.01$,***$p<0.001$

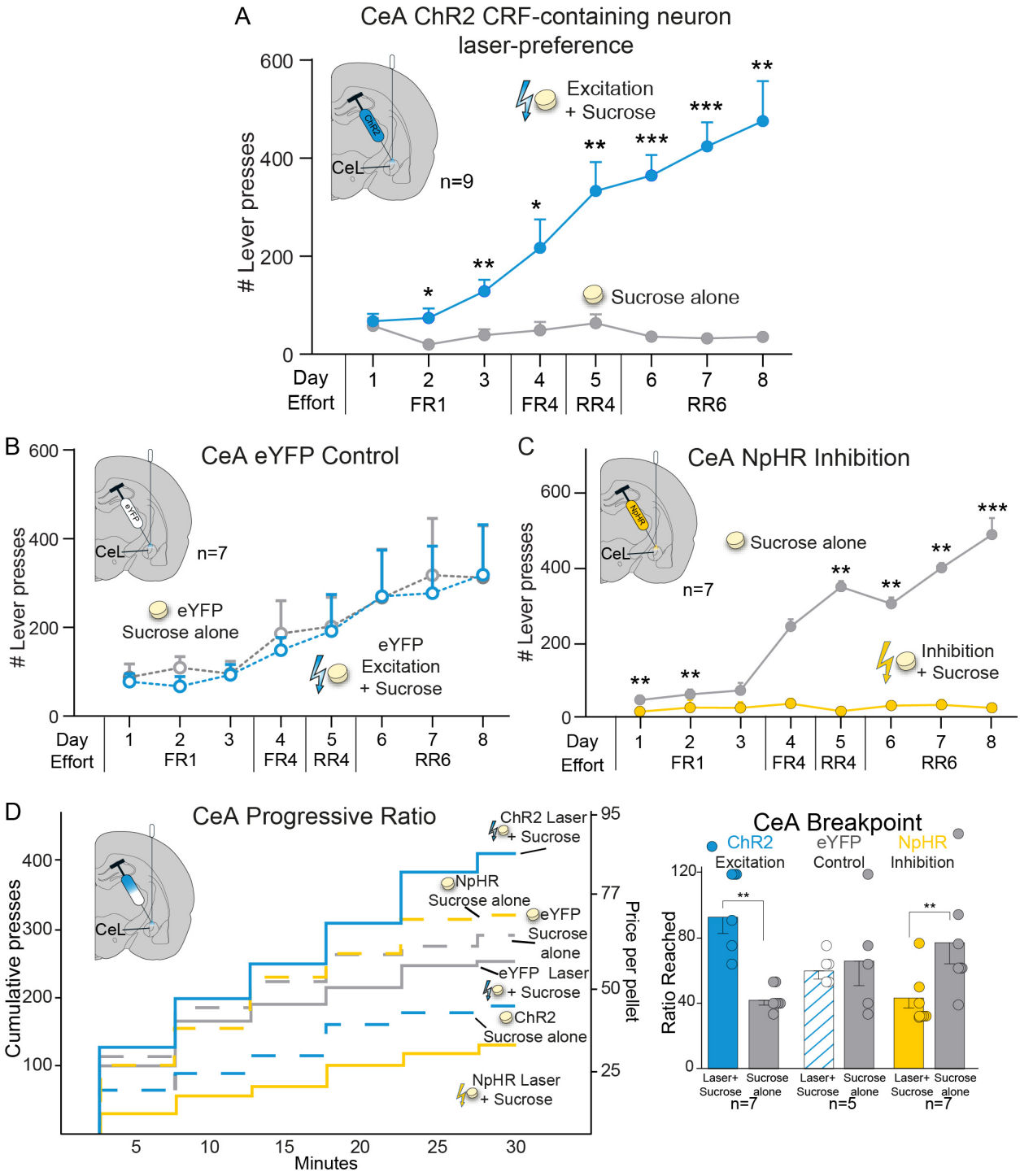

3.6 CRF-containing neuron stimulation in CeA biases and amplifies sucrose motivation
CeA ChR2 excitation of CRF-containing neurons caused near-exclusive preference for *Laser+Sucrose* over *Sucrose-alone* rewards in two-choice test (n=4 female, n=5 male), **A)** reaching a 10:1 ratio by day 8. **B)** CeA eYFP controls chose equally between sucrose options (n=7) and differed from CeA ChR2 rats. **C)** CeA NpHR inhibition of CRF-containing neurons caused *Laser+Sucrose* avoidance and *Sucrose-alone* preference (n=2 female, n=5 male). **D)** In progressive ratio test, CeA CRF-containing neuron excitation enhanced incentive motivation for sucrose breakpoint (n=3 female, n=4 male). Laser did not affect CeA eYFP control breakpoint (n=5), which differed from ChR2 rats. CeA NpHR inhibition of

CRF-containing neurons reduced *Laser+Sucrose* breakpoint (n=2 female, n=5 male). Means and SEM reported. *$p<0.05$,**$p<0.01$,***$p<0.001$

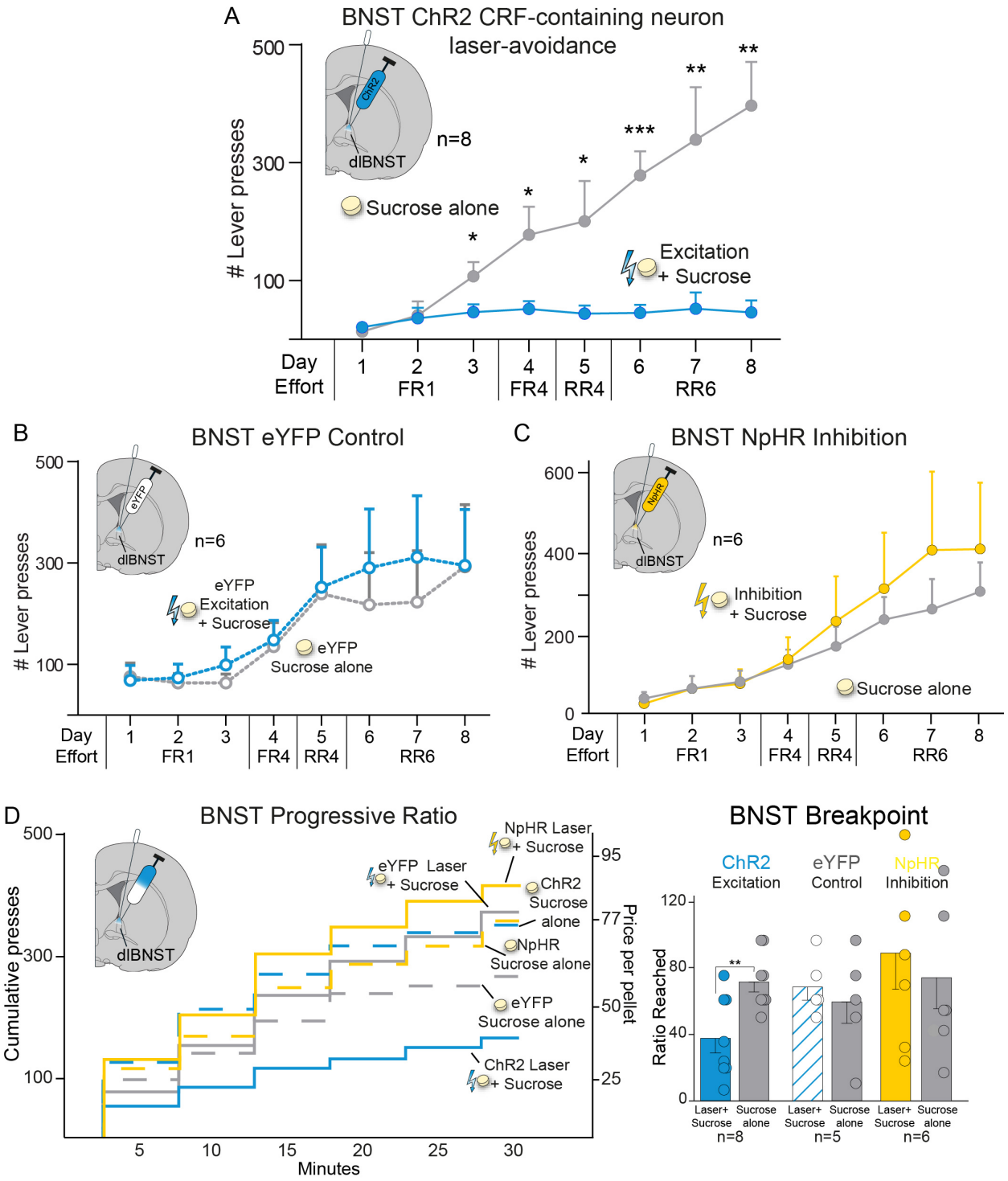

3.7 BNST CRF-containing neuron stimulation is avoided and suppresses sucrose motivation ChR2 rats avoided *Laser+Sucrose* that stimulated CRF-expressing neurons in BNST in **A)** two-choice test (n=5 female, n=3 male). BNST ChR2 *Laser+Sucrose* avoidance rose to an 8:1 opposite preference for *Sucrose-alone* by day 8. **B)** Control eYFP BNST rats chose equally between sucrose options (n=6). **C)** BNST NpHR rats (n=3 female, n=3 male) showed no significant difference between inhibitory *Laser+Sucrose* and *Sucrose-alone*. **D)** BNST ChR2 excitation of CRF-containing neurons suppressed breakpoint effort for sucrose in progressive ratio tests (n=5 female, n=3 male). Laser did not affect BNST

eYFP control breakpoint, and so eYFP rats significantly differed from BNST ChR2 rats in laser effects on breakpoint. NpHR inhibition of BNST CRF-containing neurons did not statistically alter sucrose breakpoint, despite a nonsignificant trend toward increased motivation (n=3 female, n=3 male). Means and SEM reported. *p<0.05,**p<0.01,***p<0.001

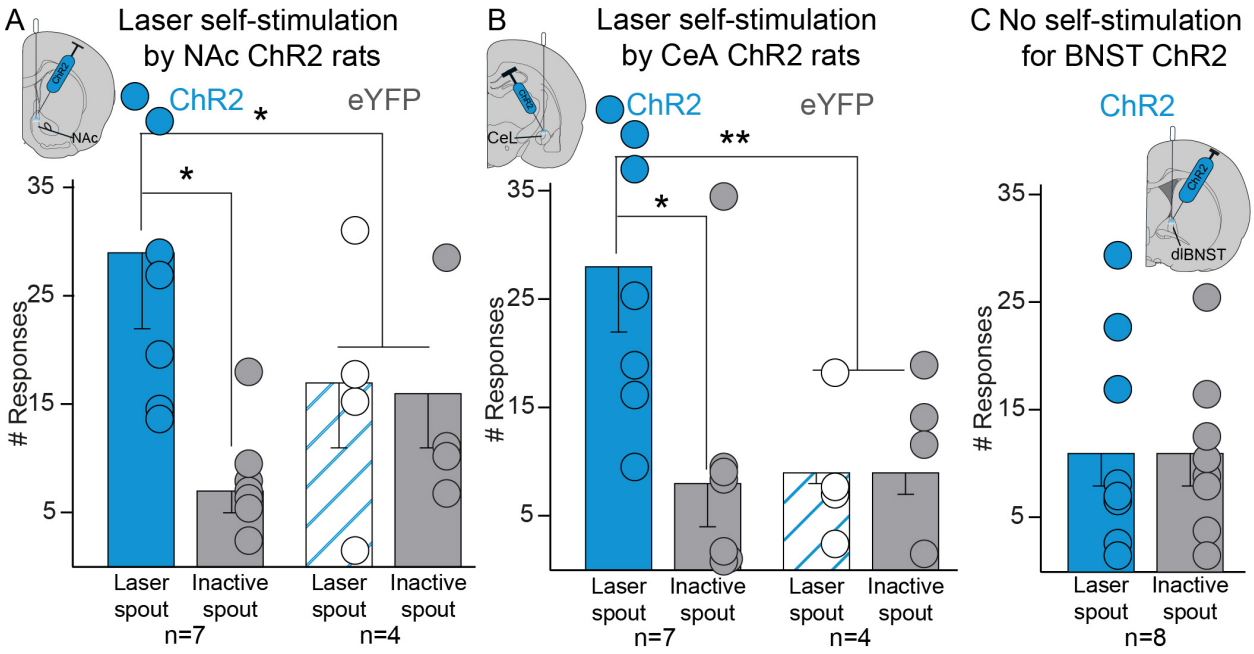

3.8 Laser spout self-stimulation by NAc and CeA *Crh*-Cre+ rats, not BNST
A) NAc ChR2 rats self-stimulated ~25-35 times on average (n=5 female, n=2 male), whereas NAc eYFP control rats (n=4) touched both spouts equally about 15 times. **B)** CeA ChR2 rats similarly self-stimulated (n=2 female, n=5 male), whereas eYFP control rats did not (n=4). **C)** BNST ChR2 rats failed to self-stimulate for laser in BNST CRF-containing neurons (n=3 female, n=5 male). Also see Fig. A.4 and Fig. A.6D. Means ± SEM, and individual scores shown. *p<0.05,**p<0.01

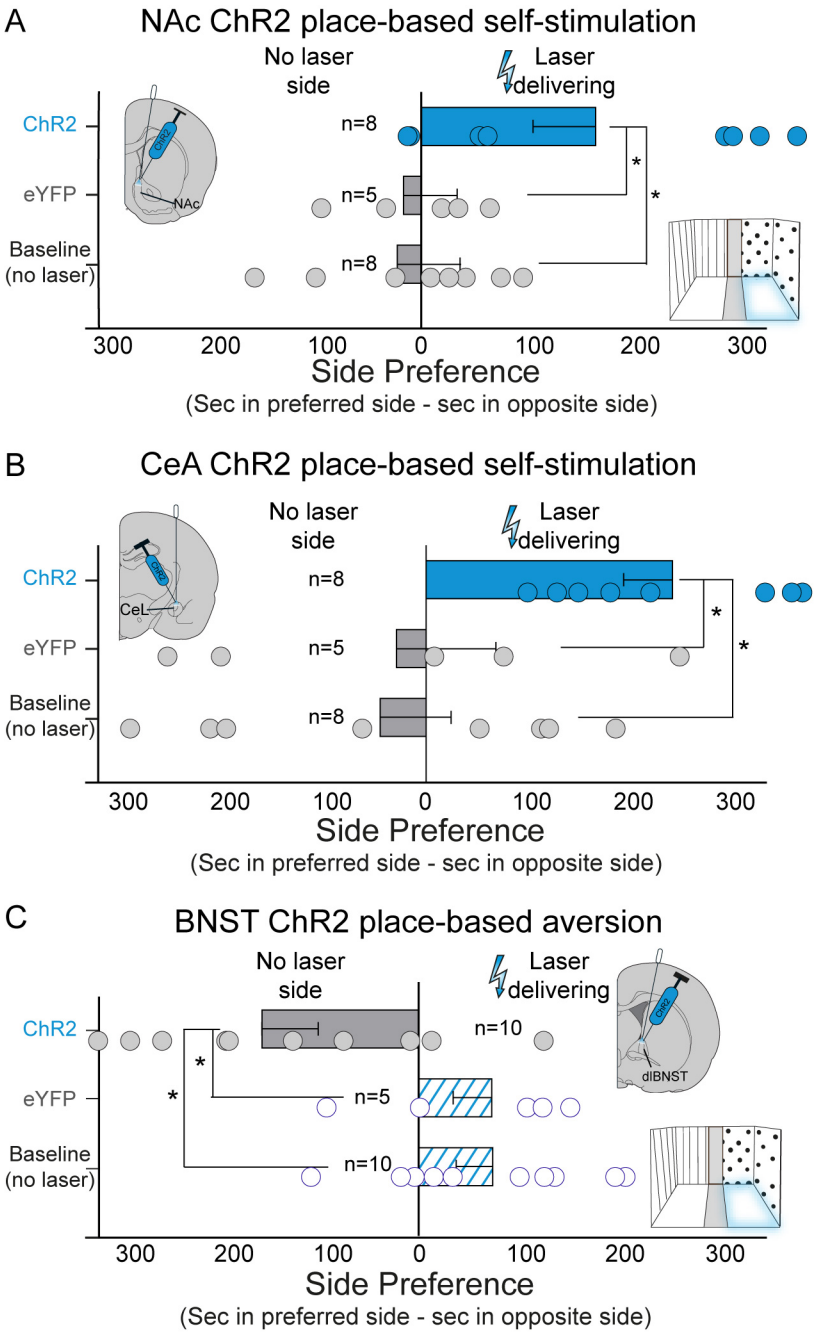

3.9 Place-based self-stimulation and aversion of CRF-containing neuron stimulation
A) NAc supported ChR2 place-based laser self-stimulation of CRF-containing neurons. NAc ChR2 rats (n=2 female, n=6 male) spent more time in *Laser-delivering* chamber than in *No-laser* chamber, more time in *Laser-delivering* chamber than NAc eYFP controls (n=5), and more than they previously spent in same chamber during no-laser baseline preference tests. **B)** CeA also supported place-based self-stimulation of CRF-containing neurons. CeA ChR2 rats (n=5 female, n=3 male) spent more time in *Laser-delivering* chamber than in no-laser chamber, more time in *Laser-delivering* chamber than CeA eYFP controls (n=5), and more than they previously spent in identical chamber during no-laser baseline tests. **C)** Conversely, BNST produced avoidance the *Laser-delivering* chamber. BNST ChR2 rats (n=5 female, n=5 male) spent less time in *Laser-delivering* chamber than eYFP controls (n=5), and less time

than they spent in the same chamber during no-laser baseline tests. Also see Fig. A.5 and Fig. A.6E. Means and SEM reported. *$p<0.05$

Tables

Target	Confirmed placement ranges (mm from Bregma)			ChR2 N's		eYFP N's		NpHR N's		Contralateral misses, locations
	A/P	M/L	D/V	Uni	Bil	Uni	Bil	Uni	Bil	
CeA	-2.16 to -3.00	± 4.2 to 4.7	-7.0 to -7.6	3	7	2	5	3	4	BLA, MeA, optic tract
NAc	+1.44 to 0.96	± 0.8 to 1.6	-6.3 to -7.6	4	5	3	4	3	3	DS, MS, NAcC
BNST	+0.24 to -0.24	±1.6 to 2.0	-5.8 to -6.4	4	6	3	4	2	4	ac, GP

3.1 Histological placements of experimental animals
Table shows anatomical confirmed placement ranges for experimental animals targeting either lateral central amygdala (CeA), nucleus accumbens (NAc) shell, or dorsolateral bed nucleus of stria terminalis (BNST). Confirmed placement ranges are determined from Paxinos and Watson brain atlas (Paxinos and Watson 2007) and display anterior/posterior (A/P), medial/lateral (M/L), and dorsal/ventral (D/V) coordinates in mm from bregma. N-values for excitatory channelrhodopsin (ChR2), inactive control eYFP virus, and inhibitory halorhodopsin (NpHR) groups include those with bilateral fiber and virus placements (Bil) or unilateral virus/fiber placements in one hemisphere, with a contralateral miss in the other hemisphere (Uni). For CeA rats (top), contralateral miss sites were located in either basolateral amygdala (BLA), medial amygdala (MeA), or optic tract, with no substantial virus expression found in these missed hemispheres. For NAc rats (middle), placements for unilateral misses were located in dorsal striatum (DS), medial septum (MS), or nucleus accumbens core (NAcC) and no viral expression in these structures was observed. For BNST rats (below) sites of unilateral misses in either the anterior commissure (ac) or globus pallidus (GP) without substantial virus expression. See Fig. 3.1.

Regions	
Orbitofrontal cortex (OFC)	Anterior lateral hypothalamus (aLH)
Infralimbic cortex (IF)	Posterior lateral hypothalamus (pLH)
Nucleus accumbens core (NAcC)	Paraventricular nucleus hypothalamus (PVN)
Anterior nucleus accumbens shell (aNAcSh)	Medial amygdala (MeA)
Posterior nucleus accumbens shell (pNAcSh)	Central amygdala (CeA)
Anterior bed nucleus of stria terminalis (aBNST)	Basolateral amygdala (BLA)
Posterior bed nucleus of stria terminalis (pBNST)	Ventral tegmentum (VTA)
Anterior ventral pallidum (aVP)	Substantia nigra (SN)
Posterior ventral pallidum (pVP)	Midbrain periaqueductal gray (PAG)

3.2 Brain regions assessed for laser-recruited changes in Fos expression
Laser-induced enhancements were assessed in the listed mesocorticolimbic brain regions, following CRF-expressing neuronal excitation in NAc, CeA, or BNST. Distant Fos levels in ChR2 animals were compared to levels assessed in inactive eYFP control rats that underwent identical Fos induction procedures.

CHAPTER IV. Corticotropin Releasing Factor (CRF) Systems Promoting Cocaine Pursuit: Through Distress or Incentive Motivation?

Introduction

Stress can exacerbate addictive relapse and consumption of sensory rewards (Erb et al. 2001b; Koob et al. 2014; Mantsch et al. 2016; Shalev et al. 2010). Neurobiologically, activation of brain corticotropin releasing factor (CRF) systems in limbic brain structures has been posited to drive stress-induced relapse and overconsumption in addiction via aversive distress states (Dallman 2010; Dunn and Berridge 1990; Koob and Le Moal 2008; Koob and Schulkin 2019; Koob and Volkow 2010; McEwen and Akil 2020; Merali et al. 1998, 2004; Shaham et al. 1997; Stewart 2000; Sutton et al. 1982; Vale et al. 1981).

For example, the allostatic theory of addiction (also called the opponent-process, hedonic dysregulation, hedonic homeostasis, or hyperkatifeia theory), posits that increases in activity of CRF neuronal systems in central amygdala (CeA) and bed nucleus of stria terminalis (BNST) drive negative distress feelings associated with withdrawal from addictive drugs, which in turn is posited to lead to relapse and overconsumption of pleasant rewards as attempts at hedonic self-medication to counter the aversion (de Guglielmo et al. 2019; Koob and Le Moal 1997, 2008; Koob and Schulkin 2019; Koob 2013, 2021). In that model, relapse and drug intake is thought to be driven by distress caused by the activation of CRF neural systems in CeA and BNST.

However, other evidence suggests that CRF neural systems in both CeA and nucleus accumbens (NAc) may instead mediate incentive motivation mechanisms to pursue rewards, somewhat similar to the role of mesolimbic dopamine systems, without necessarily causing distress (Kim et al. 2017; Lemos and Alvarez 2020; Lemos et al. 2012; Peciña et al. 2006; Wang et al. 2005). These mechanisms include incentive salience or cue-triggered 'wanting'.

In particular, we recently demonstrated that optogenetic stimulation of CRF-containing neurons in CeA and NAc of C*rh*-Cre+ rats produced positively-valenced incentive motivation to pursue and consume rewards, rather than causing negatively-valenced aversive motivation. (Baumgartner et al. 2021). For example, CRF-expressing neuronal excitation in CeA and NAc was itself sought out by rats, which worked to obtain laser self-stimulations. CRF-expressing neuronal stimulation also activated reward-related mesocorticolimbic circuitry to amplify incentive motivation to obtain and consume hedonic sucrose rewards in effort breakpoint tests, and focused intense motivation in a 2-choice task narrowly and specifically on the laser-paired sucrose reward, while the rats ignored an alternative sucrose reward that was not accompanied by CRF neuronal excitation (Baumgartner et al. 2021).

Conversely, in BNST we found that optogenetic excitation of CRF-containing neurons caused an aversive state that ChR2 rats avoided, partially consistent with the allostatic hypothesis for CRF motivational function (Baumgartner et al. 2021). However, rather than increase motivation to consume sucrose rewards as the hedonic self-medication hypothesis posits, the aversive state generated by activation of CRF-containing BNST neurons actually suppressed motivation to obtain hedonic sucrose rewards, rather than increasing it as postulated by opponent-process logic.

The results of Baumgartner et al. (2021) indicate that CRF neural systems cause pursuit and consumption of sweet rewards by activating incentive motivation processes, not by hedonic self-medication attempts to alleviate distress. But allostatic/hyperkatifeia hypotheses of CRF function have focused primarily on drug addiction, and it is not yet clear whether those sucrose-based conclusions will transfer to drugs of abuse, such as cocaine. Therefore, we examined here whether CRF neural mechanisms underlying pursuit and consumption of intravenous cocaine similarly operate by incentive motivation principles. In BAC transgenic *Crh*-Cre rats, we paired optogenetic excitation of CRF-containing neurons in either NAc, CeA, or BNST with opportunities to earn intrajugular infusions of cocaine. Using a 2-choice task (Warlow et al. 2017) we examined if those groups of CRF ChR2 rats preferred or avoided an i.v. cocaine option accompanied by CRF-containing neuronal stimulation compared to an alternative i.v. cocaine option without CRF ChR2 activation. Using a progressive ratio task to assess effort breakpoint, we also asked if ChR2 neural stimulation in *Crh*-Cre rats altered the intensity of incentive motivation to self-administer i.v. cocaine. Finally, to assess the motivational valence effects of CRF-expressing neuronal stimulation we assessed whether rats would self-administer laser stimulation in NAc, CeA or BNST CRF systems by itself. The results of these experiments provide insight into the incentive versus aversive motivational roles of particular CRF neural systems, and indicate that CRF neural systems may control cocaine pursuit and intake primarily by incentive motivation mechanisms, not by hedonic self-medication efforts to alleviate distress.

Methods

Animals

Female (n=24) and male (n=9) transgenic *Crh*-Cre+ rats were bred and genotyped in house, from breeders obtained from the Messing laboratory at the University of Texas (Pomrenze et al. 2015). Rats were housed in same-sex pairs at 21C under reverse light cycle with ad libitum access to food and water, until after intrajugular catheter implantation, when rats became single-housed and were subsequently maintained at 85-90% ad lib body weight levels on a restricted food schedule for the duration of cocaine experiments. All experimental procedures were approved by the University of Michigan Institutional Animal Care & Use Committee in accordance with NIH animal care and use guidelines.

Optogenetic virus and fiber surgery

Rats were anesthetized with isoflurane gas (induction: 4-5%, maintenance, 1-2%) and placed in a stereotaxic apparatus (David Kopf Instruments, Tujunga, CA) for surgery. Rats received atropine (0.05 mg/kg; i.p.; Henry Schein) at start of surgery and after received cefazolin (75 mg/kg, s.c.; Henry Schein) and carprofen (5 mg/kg; s.c.; Henry Schein) for postsurgical pain relief. Bilateral microinjections in either NAc, CeA, or BNST were made of either active AAV-DIO-ChR2-eYFP virus (n=21) with ChR2 or optically-inactive control virus AAV-DIO-eYFP (n=12). Both ChR2 virus and inactive eYFP-only virus are driven by an EF1a promoter to infect only Cre-recombinase+ neurons. This transgenic *Crh*-Cre BAC rat line may primarily express Cre-recombinase in CRF neurons that also co-express GABA, which made it suitable for targeting the largely GABAergic CRF neuron populations in NAc, CeA and BNST here (Pomrenze et al. 2015). Site coordinates for virus microinjections were bilaterally identical for individual rats, but staggered across rats in the following ranges so that the group's sites filled

most of each targeted structure (NAc medial shell; lateral CeA; dorsolateral BNST). *NAc medial shell* range (from bregma): A/P: +1.08 to +2.52, M/L: ±0.6 to 1.2, D/V: -6.0 to -7.07 (Angle used: 16 or 10 degrees, flat skull; n=10); *lateral CeA* range: A/P: -1.92 to -3.24, M/L: ± 3.8 to 4.6, D/V: -6.8 to -7.8 (flat skull; n=13); *dorsolateral BNST* range, A/P: 0.36 to -0.36, M/L: 1.0 to 1.8, D/V: -6.1 to -6.5, (Angle used: 16 degrees, flat skull; n=10). A 1.0 microliter volume of virus per hemisphere was microinjected at each bilateral site over a 10-minute period (0.1 microliter / minute), and microinjector was left in place an additional 10 minutes to allow diffusion. Optic fibers (200 micrometer) were implanted above each site so that the fiber tip was 0.3mm dorsal to virus microinjection site and secured with skull screws and dental cement. Rats were monitored one-week post-surgery and received additional carprofen injections for two-days post-surgery for pain relief. At least 3 weeks between stereotaxic surgeries and initial behavioral testing was provided for virus incubation and recovery from intrajugular catheter surgery.

Intrajugular catheter surgery

Approximately 2 weeks after stereotaxic surgeries, rats underwent an additional surgery to insert an intravenous catheter into the jugular vein for cocaine self-administration experiments (Warlow et al. 2017). Rats again received pre- and post-operative procedures as described above. Briefly, a subcutaneous anchor was secured in the mid-scapular region and the attached Silastic catheter was passed subcutaneously up the back and dorsal neck region, and threaded into the right jugular vein (Warlow et al. 2017). Following surgeries, rats received daily intra-catheter gentamicin infusions for 10 days to prevent infection, as well as daily intra-catheter heparinized saline infusions that continued throughout testing. Rats had 7-10 days for recovery and catheter patency was confirmed with brevital sodium injections (0.2ml, 20mg/ml) before

behavioral testing and again once testing was completed. Rats that failed to become ataxic within 10s were excluded from self-administration analyses.

Stimulation parameters

Optogenetic blue laser (592nm) laser excitation for ChR2 was delivered at 10Hz (10ms-ON-90ms-OFF; 2-3mW) using durations and pairing conditions described below (Fadok et al. 2017).

Two-choice cocaine self-administration

An instrumental two-choice task was used to test whether pairing laser excitation of CRF-containing neurons in NAc, CeA, or BNST with earning cocaine reward by making nosepokes into one particular porthole made that cocaine option more or less valuable than an alternative option of identical cocaine infusion delivered alone (without laser) earned by nosepokes into a different porthole (Warlow et al. 2017). Briefly, rats were trained on a fixed ratio 1 (FR1) schedule in a chamber containing two retractable portholes. *Crh*-Cre ChR2 rats learned that a nose poke into one particular port hole (*Laser+Cocaine* porthole) would deliver intrajugular infusions of cocaine (0.3mg/kg for each rat, 50ul volume dissolved in a sterile saline solution, 2.8sec per infusion, National Institute on Drug Abuse), accompanied by 8-sec of laser stimulation, plus a distinct associated sound (8sec, tone or white noise). Nosepokes into the other porthole earned identical cocaine infusions, plus the other sound cue, but no laser (*Cocaine-alone* porthole). For both portholes a 20s timeout was initiated after each cocaine infusion earned, which coincided with retraction of the inserted portholes so no nosepokes could be made.

Rats were allowed to freely choose between *Laser+Cocaine* or *Cocaine-alone* options over 10 daily test sessions, after brief refresher experiences with both outcomes. Each session

started with a single-choice trial: just one porthole was inserted into the chamber, and a nosepoke earned that porthole's customary reward (either *Laser+Cocaine* or *Cocaine-alone).* Then the first porthole was retracted, and the other porthole was inserted so the rat would experience its different reward (single-choice trial). Both single-choice trials were repeated a second time, and these trials ensured the rats were reminded each day of the difference between *Laser+Cocaine* versus *Cocaine-alone* options, prior to making free choices. Following completion of these 4 single-choice trials, repeated 2-choice trials followed for the remainder of the daily session. In 2-choice trials, both portholes were inserted simultaneously, and rats were allowed to choose freely between both portholes and their outcomes. These 2-choice trials continued for the remainder of the 60-min session, interrupted only by 20s timeout periods after each cocaine infusion. To be included in the experiment, rats were required to make a total of at least 5 daily cocaine infusions on days 1-3, and rats that failed to reach that requirement were excluded from analyses (3 of 27 rats were excluded for this reason).

Progressive ratio test of incentive motivation intensity

To test whether laser excitation of CRF-containing neurons changed the *magnitude* of incentive motivation for cocaine rewards, rats underwent two days of progressive ratio testing in 60 minutes sessions to identify effort breakpoints. On one day rats were tested with *Laser+Cocaine,* presenting its customary porthole alone. On another day (in balanced order), rats were tested with *Cocaine-alone,* presenting its customary porthole. Each day, after a cocaine infusion was received, the number of responses required to earn the next cocaine infusion increased on a progressive ratio schedule following the formula $PR=[5e^{(reward\ number\times 0.2)}]-5$. The breakpoint effort at which rats stopped responding for cocaine rewards, or ratio was reached, was compared across day conditions.

Spout-touch self-stimulation

Incentive properties of laser alone without cocaine were tested in instrumental spout-touch self-stimulation tests. Rats had the opportunity to touch either of two empty spouts: touches on a designated 'laser spout' delivered brief 3-sec laser illuminations (3sec, 10Hz), whereas touches on the other 'inactive' spout delivered nothing, serving as a control measure of baseline exploratory touches. Self-stimulation tests were repeated in 30-min sessions across 3 days of testing.

Histology

To identify CRF-recruited circuitry via Fos analysis, rats underwent a final laser stimulation for 30-min, preceding euthanasia (45-min post-stimulation session) by lethal sodium pentobarbital injection, followed by transcardial perfusion and brain extraction. A cryostat was used to slice brains into 40 micrometer slices (Leica, Wetzlar, Germany). Immunohistochemistry followed previously reported procedures to stain for Fos gene expression and GFP (Baumgartner et al. 2020). Briefly, tissue was rinsed three times for 10min in sodium phosphate buffer (NaPB) and blocked in 5% normal donkey serum (60min) before overnight incubation in rabbit anti-cFos (1:2500; Catalog#: 226 003; Lot #: 4-63; RRID:AB_2231974; Synaptic Systems, Göttingen, Germany) and chicken anti-GFP (1:2000; Catalog#: AB13970; Lot #: GR3190550-30; RRID:AB_300798; Abcam, Cambridge, MA). Slices were again rinsed 3x in NaPB for 10min and placed for 2 hours in biotinylated donkey anti-rabbit (1:300; Catalog #: AB2340593; Lot #: 128703; RRID: AB2340593; Jackson Immunoresearch, West Grove, PA) and donkey anti-chicken AlexaFluor 488 (1:300; Code #: AB2340375; Lot #: 144438; RRID:AB_2340375; Jackson Immunoresearch, West Grove, PA). Following 3 more rinses in NaPb, tissue was then incubated for 90min in tertiary containing Streptavidin Cy3 (1:300;

Catalog #: AB2337244, Lot #: 141873, RRID: AB_2337244; Jackson Immunoresearch, West Grove, PA), before three final 10min rinses. Slices were mounted onto slides (Fischer), coverslipped with Prolong-gold with DAPI (Invitrogen), and imaged using a digital camera (Qimaging, Surrey, BC, Canada) attached to a fluorescent microscope (Leica, Wetzlar, Germany). Viral expression of ChR2 virus was confirmed within NAc, CeA, or BNST targets (see Table 1), and visualized using filter cubes with excitation bands of 490-510nm.

Local Fos plumes

Local Fos plumes indicate the extent and degree of local neuronal activation immediately surrounding the fiber optic tip produced by ChR2 excitation of CRF-containing neurons. Fos plumes in NAc, CeA, or BNST were measured by counting the number of Fos+ neurons in 50x50um boxes placed along 8 radial axes emanating from the fiber optic tip after laser stimulation in CRF ChR2 rats (Baumgartner et al. 2020). Counting continued in 50x50um boxes along each axis until 2 consecutive boxes containing zero Fos+ cells were reached. Percent elevation in Fos expression compared to the same sites in eYFP control rats was calculated to determine the intensity of neuronal activation induced by CRF ChR2 laser stimulation in each box, and the radii of elevated plumes reflected the anatomical extent of local stimulation.

Distant Fos analysis

Functional connectivity, or recruitment of distant neural activity in other brain structures, was assessed by measuring by changes in Fos protein expression in coronal whole-brain images (10x magnification) within a number of mesocorticolimbic structures: anteromedial orbitofrontal cortex (OFC), infralimbic cortex (IF), anterior NAc shell (aNAcSh), posterior NAcSh (pNAcSh), NAc core (NAcC), anterior ventral pallidum (aVP), PVP, anterior BNST (aBNST), pBNST, anterior lateral hypothalamus (aLH), pLH, paraventricular nucleus of the hypothalamus (PVN), basolateral amygdala (BLA), CeA, medial amygdala (MeA), ventral tegmentum (VTA),

substantia nigra (SN), and midbrain periaqueductal grey (PAG). In each structure targeted, boxes for counting Fos+ neurons were sized to contain ~10 Fos+ neurons in naïve unoperated brain tissue, ranging from 6-49 μm^2. In each structure, Fos was counted in 3 boxes placed at approximately the same locations between rats for each structure, assessed using a Paxinos brain atlas (Paxinos and Watson 2007). Percent enhancement in Fos expression recruited in each structure by CRF-containing neuron laser stimulation in NAc, CeA, or BNST was calculated by comparison to equivalent sites in inactive eYFP control rats that received similar laser illuminations prior to euthanasia.

Statistical analysis

Behavioral data were analyzed using mixed-model ANOVAs with either between-subject (i.e., ChR2 vs. eYFP) or within-subject factors (i.e., days, laser effects), followed by two-tailed paired t-tests to assess within-subject post-hoc effects. Wilcoxon Z tests were used for data that did not fit assumptions of parametric testing. Independent pairwise comparisons were used for distant Fos analysis. For all analyses $p=0.05$, and Cohen's D was used to calculate effect sizes.

Results

Local Fos plumes

In NAc, ChR2 laser stimulation of CRF neurons rats produced 0.18-0.36mm radius local Fos plumes of 150-200% elevated expression immediately surrounding optic fiber tips, compared to NAc eYFP control levels at corresponding sites. In CeA, ChR2 stimulation of CRF-containing neurons produced 150-200% elevated Fos plumes of 0.17–0.34mm radius, and in BNST produced 150-200% Fos plumes of 0.18-0.34mm radius. These Fos plume sizes suggest that laser illumination of ChR2-infected CRF-containing neurons induced local zones of neural activation ~0.4-0.7mm in all three structures (Figure 4.1). Therefore 0.7mm diameter size was used for placement symbols in localization-of-function maps (Figure 4.2).

Distant Fos

Excitation of CRF-expressing neurons in NAc medial shell (n=4 ChR2 NAc, n=3 eYFP NAc; Figure 4.3A) elicited >150-350% increases in Fos expression in distant mesocorticolimbic structures including the nucleus accumbens core (NAcC; $t_5 = 3.447$, $p = 0.018$), anterior ventral pallidum (aVP; $t_5 = 7.109$, $p = 0.001$), posterior VP (pVP $t_5 = 8.243$, $p < 0.001$), posterior BNST ($t_5 = 3.065$, $p = 0.028$), anterior lateral hypothalamus (aLH; $t_5 = 2.833$, $p = 0.037$), posterior LH ($t_5 = 9.098$, $p < 0.001$), CeA ($t_5 = 6.939$, $p = 0.001$), and ventral tegmentum (VTA; $t_4 = 3.573$, $p = 0.023$), as well as marginal trends toward enhancements in medial amygdala (MeA; $t_5 = 2.568$, $p = 0.050$) and basolateral amygdala (BLA; $t_5 = 2.537$, $p = 0.052$).

Stimulation of CRF-containing neurons in lateral CeA (n=5 ChR2 CeA, n=2 eYFP CeA; Figure 4.3B) also recruited mesocorticolimbic structures into activation, causing >150-350% increases in Fos expression in NAcC ($t_5 = 2.727$, $p = 0.041$), NAc caudal shell ($t_5 = 5.529$, $p =$

0.003), aVP (t_5 = 2.893, p = 0.034), posterior BNST (t_5 = 2.859, p = 0.035), pVP (t_5 = 2.744, p = 0.041), anterior LH (t_5 = 6.291, p = 0.001), and VTA (t_5 = 2.7240 p = 0.041), with marginal trends in NAc rostral shell (t_5 = 2.408, p = 0.061) and MeA; t_5 = 2.258, p = 0.074).

In contrast, stimulation of CRF-containing neurons in dorsolateral BNST produced minimal significant changes in Fos activation in tested structures, at least in the current small sample size (n=5 ChR2 BNST, n=1 eYFP BNST; Figure 4.3C). Instead, excitation of this BNST CRF system solely produced a statistically significant change in the infralimbic cortex (IF) where Fos activation was suppressed with ChR2 stimulation (t_4 = 3.822, p = 0.019).

<u>NAc and CeA paired CRF neuronal excitation focuses and amplifies cocaine motivation.</u>

For NAc CRF stimulation, in the 2-choice task where rats could freely choose between earning either a cocaine i.v. infusion plus with laser excitation of NAc CRF-containing neurons (*Laser+Cocaine)* or an identical cocaine infusion without laser (*Cocaine alone)*, NAc ChR2 rats (n=6) primarily pursued only *Laser+Cocaine,* preferring that option by a 4:1 ratio over *Cocaine alone* by the final day ($F_{1,5}$ = 8.365, p = 0.034; Figure 4.4A). NAc ChR2 preference for *Laser+Cocaine* over *Cocaine alone* emerged as statistically significant by day 4 (t_5 = 3.162, p = 0.025). On average, NAc ChR2 rats nosepoked 14.3±2.9 times at the *Laser+Cocaine* porthole on day 10 versus only 3.3±0.6 at the *Cocaine alone* porthole (responses: t_5 = 3.307, p = 0.021). Consequently, NAc ChR2 rats earned nearly four times more *Laser+Cocaine* infusions (13.8±3.0) than *Cocaine alone* infusions (3.3±0.6; t_5 = 3.050, p = 0.028). Further, regarding absolute amounts of cocaine intake, NAc ChR2 rats consumed twice as much total cocaine than eYFP control rats even on the first day, indicating that NAc CRF stimulation quickly elevates overall consumption of cocaine (total infusions testing day 1; n=6 ChR2: 6.0±0.4; n=4 eYFP: 3.7±1.4; t_{11} = 3.552, p = 0.005). However, this difference in cocaine consumption disappeared

by day 2 and throughout day 10 of testing (total infusions day 10; n=6 ChR2: 17.2±2.6; n=3 eYFP: 16.8±6.2; $t_8 = 0.071$, $p = 0.945$).

Unlike NAc ChR2 rats, NAc eYFP control rats chose essentially equally between *Laser+Cocaine* and *Cocaine alone* options across test days (day 10 *Laser+Cocaine*: 8.3±3.5 infusions; *Cocaine alone*: 4.8±1.0; $F_{1,2} = 2.077$, $p = 0.286$; Figure 4.4B).

For CeA CRF stimulation, in the 2-choice task, CeA ChR2 rats (n=5) similarly pursued their *Laser+Cocaine* option nearly exclusively, by almost a 4:1 ratio of nosepokes over *Cocaine alone* ($F_{1,4} = 9.720$, $p = 0.036$; Figure 4.5A). This *Laser+Cocaine* preference emerged by testing day 6 for CeA ChR2 rats ($t_4 = 4.543$, $p = 0.010$). On day 10 CeA ChR2 rats earned 13.6±4.1 *Laser+Cocaine* infusions, versus only 3.8±1.6 *Cocaine alone* infusions ($t_4 = 2.790$, $p = 0.049$).

By contrast, CeA eYFP control rats chose equally between *Laser+Cocaine* and *Cocaine alone* options, earning 5.8±3.8 *Laser+Cocaine* infusions and 3.0±0.7 *Cocaine alone* infusions by testing day 10 (n=4; $F_{1,3} = 1.819$, $p = 0.270$; Figure 4.5B) and significantly differed from CeA ChR2 in *Laser+Cocaine* preference ($F_{1,7} = 5.845$, $p = 0.046$). On average, eYFP control rats consumed less total cocaine infusions as ChR2 rats on testing day 10, though this difference was not significant (eYFP rats: 9.0±5.0 total cocaine infusions; CeA ChR2 rats: 17.2±4.9; $t_6 = 1.152$, $p = 0.287$).

<u>CRF-containing neuron excitation in NAc and CeA amplifies motivation breakpoint for cocaine.</u>

A progressive ratio task measured the magnitude of incentive motivation, expressed as maximum effort or breakpoint that rats were willing to exert for cocaine. In either NAc or CeA, laser ChR2 stimulation of CRF neurons approximately doubled effort breakpoint to obtain cocaine. NAc ChR2 rats worked ~200% harder on the day when cocaine was accompanied by NAc laser than when cocaine was earned without laser (n=6; Wilcoxon Z = 2.023, $p = 0.043$;

Figure 4.4C), as NAc ChR2 effort breakpoints were 11.2±2.9 on *Laser+Cocaine* day versus only 5.7±1.4 on *Cocaine alone* day. Additionally, NAc ChR2 rats nosepoked 24.8±9.6 times (thus earning 4.5±0.8 infusions) on *Laser+Cocaine* day versus only 8.3±3.2 nosepokes and 2.7±0.6 infusions on *Cocaine alone* day ($Z = 2.023$, $p = 0.043$). In contrast, eYFP control rats with laser targeting NAc CRF neurons (n=4) did not differ in their breakpoints on *Laser+Cocaine* (6.0±2.2) versus *Cocaine alone* days (4.8±1.3; $Z = 0.535$, $p = 0.5935$), and eYFP effort on both days was similar to the lower NAc ChR2 effort on *Cocaine alone* day.

Similarly, CeA ChR2 rats reached breakpoints for cocaine that were >200% higher on *Laser+Cocaine* day (breakpoint: 8.4±1.8 ratio reached) than on *Cocaine alone* day (breakpoint: 3.2±1.5; n=5; Wilcoxon $Z = 2.060$, $p = 0.039$; Figure 4.5C). ChR2 rats nosepoked 16.4±4.1 times on the *Laser+Cocaine* day (earning 4.0±0.4 average infusions), which was >400% more than the 3.2±1.5 nosepokes (and subsequent average 1.4±0.6 infusions) earned on *Cocaine alone* day ($Z = 2.023$, $p = 0.043$). In contrast, CeA eYFP control rats (n=4) reached similar breakpoints between *Laser+Cocaine* (ratio reached: 7.3±2.0) and *Cocaine alone* days (6.0±1.6; $Z = 1.342$, $p = 0.180$), and thus significantly differed from CeA ChR2 rats ($F_{1,7} = 8.810$, $p = 0.021$).

Cocaine motivation unaffected by BNST CRF-containing neuron excitation.

In BNST, pairing laser excitation of CRF-containing neurons with one of two cocaine options in the 2-choice task potentially suppressed overall cocaine intake, but did not significantly alter preference among options (Figure 4.6A). Regarding overall cocaine consumption, BNST ChR2 rats took much less cocaine in total (*Laser+Cocaine* infusions plus *Cocaine alone* infusions combined) than NAc ChR2 rats or CeA ChR2 rats ($F_{2,14} = 5.002$, $p = 0.023$; Figure 4.7). Overall, BNST ChR2 rats also consumed only roughly 2/3 as much cocaine

as BNST eYFP control rats with inactive virus by the final day of testing (BNST ChR2: 5.5±0.4 total infusions on day 10; n=2 BNST eYFP: 9.0±1.0 infusions; t_6= 3.834, p = 0.009). Regarding choice, BNST ChR2 rats equally chose *Laser+Cocaine* and *Cocaine alone* options (n=5; $F_{1,4}$ = 0.435, p = 0.546), and responded for both options at very low rates. For example, BNST ChR2 rats made only 2.8±0.4 *Laser+Cocaine* nosepokes vs 3.6±0.6 *Cocaine alone* nosepokes on day 10. BNST ChR2 rats failed to escalate cocaine self-administration across days, earning a similar value of 5.5±0.4 *Laser+Cocaine* infusions on day 10 versus 7.7±2.0 *Cocaine alone* infusions on day 1; this was, if anything, higher than it was on day 10.

BNST eYFP control rats similarly chose equally between *Laser+Cocaine* (5.5±0.5 day 10 infusions) and *Cocaine alone* options (3.5±1.5; $F_{1,1}$ = 3.94, p = 0.643; Figure 4.7B).

In the progressive ratio task, BNST ChR2 laser stimulation of CRF-containing neurons failed to alter the breakpoint magnitude of motivation to work for cocaine rewards. BNST ChR2 rats reached effort breakpoints of 5.2±2.6 on *Laser+Cocaine* day and of 4.3±2.0 on *Cocaine alone* day (n=5 Wilcoxon Z = 0.921, p = 0.357; Figure 4.7C). BNST ChR2 rats similarly did not differ in number of nosepoke responses for cocaine infusions, whether or not laser was concurrently present (n=5; *Laser+Cocaine*: 9.8±7.4 responses, *Cocaine alone*: 6.4±4.5; Z = 1.095, p = 0.273). BNST eYFP controls rats also showed no laser effects on effort breakpoint, reaching ratios of 6.0±0.0 for *Laser+Cocaine* and 3.0±1.0 for *Cocaine alone* (n=2, Z = 1.342, p = 0.180).

Minimal CRF neuronal self-stimulation in NAc and CeA

In the spout-touch self-stimulation task, each instrumental touch on the designated empty *Laser-spout* earned 3-sec bins of laser excitation (10Hz). Touches on the other *Inactive spout* delivered nothing and were a control measure of exploration. Rats were categorized as *robust*

self-stimulators if they met the combined criteria of a) >50 *Laser spout* touches per session and b) twice as many *Laser spout* touches as *Inactive spout* touches. Rats were categorized as *low self-stimulator*s if they met the lesser combined criteria of a) >10 *Laser spout* touches (but <50), and b) twice as many *Laser spout* touches as *Inactive spout* touches. For NAc sites, no rats met the >50 *Laser spout* touches criterion for robust self-stimulation on day 1, but 5 out of 6 NAc ChR2 rats met the lesser >10 *Laser spout* criterion for low self-stimulation. Similarly, on days 2-3 of testing these NAc ChR2 rats self-stimulated NAc CRF neurons 39.8±5.2 times by touching the *Laser spout* per 30-min session, compared to 9.9±4.9 touches on the *Inactive spout*, and so made >400% more contacts on the *Laser spout* than the *Inactive spout* (n=5; $F_{1,4}$ = 22.305, p = 0.009; Figure 4.8A). In contrast, 1 control eYFP rat did initially meet low self-stimulation criteria on day 1 but failed to meet this criterion on days 2-3. Overall, NAc eYFP rats (n=4) touched equally on the *Laser spout* (11.6±5.8 touches) and *Inactive spout* (8.5±5.4 touches) across days 2-3, earning only one-third the number of laser illuminations as NAc ChR2 self-stimulators ($F_{1,7}$ = 13.092, p = 0.009).

For CeA sites, 2 out of 6 CeA ChR2 rats met criterion for robust self-stimulation, and 5 out of 6 met criterion for low self-stimulation. These CeA ChR2 rats self-stimulated by making 40.0±12.9 touches on the *Laser spout* per day versus only 8.3±2.2 touches on their *Inactive spout* on days 2-3 of testing, or 400% more touches on *Laser spout* as on *Inactive spout* that delivered nothing (n=5; $F_{1,4}$ = 7.713, p = 0.050; Figure 4.8B). eYFP CeA control rats made only 13.0±3.7 touches on the *Laser spout* versus 9.8±2.0 touches on the *Inactive spout,* which trended marginally toward fewer laser illuminations than CeA ChR2 rats on days 2-3 ($F_{1,7}$ = 4.101, p = 0.083).

By contrast, BNST ChR2 rats failed to self-stimulate CRF-containing neurons in BNST. BNST ChR2 rats touched the *Laser spout* (24.3±7.1 touches) and *Inactive spout* (17.4±3.8) roughly equally on days 2-3 of testing (n=5; $F_{1,4} = 0.811$, $p = 0.419$), failing to meet criteria for either robust or low levels of BNST CRF self-stimulation (Figure 4.8C).

Discussion

Pairing optogenetic excitation of CRF-containing neurons in NAc and CeA caused rats to selectively pursue and escalate self-administration of intrajugular cocaine infusions with concurrent ChR2 laser stimulation. Excitation of these CRF systems in NAc and CeA focused pursuit on the laser-paired cocaine infusion in the two-choice task, enhanced breakpoint effort in the progressive ratio task, and was even sought after by itself in the spout-touch self-stimulation task. In contrast, excitation of BNST CRF-containing neurons did not cause a focusing of cocaine pursuit on either the laser-paired or cocaine alone self-administration options, and if anything trended toward a suppression in escalation of cocaine intake. Together these findings provide insight into the mechanisms through which brain stress systems can mediate cocaine pursuit and consumption.

Motivation mechanisms for sucrose or cocaine

We have previously demonstrated that optogenetic ChR2 stimulation of CRF systems in NAc and CeA can bias and amplify incentive motivation for sucrose rewards, while BNST CRF systems caused only aversive motivation and avoidance of paired-sucrose rewards (Baumgartner et al. 2021). These sucrose incentive effects are in line with proposed neurobiological mechanisms through which stressors can lead to overconsumption and eating of "comfort foods" (Dallman et al. 2003). However, theories on drug reward and addiction-related brain CRF systems are largely associated with aversive and distress-related motivation. Our results provide evidence that drug pursuit and consumption can instead be driven by positively-valenced NAc and CeA CRF systems, similar to sucrose. This suggests that our demonstrated incentive

motivation roles for NAc and CeA CRF-containing neurons may be more of a comprehensive brain mechanism for stress-based motivation than previously thought.

In contrast, the present study found that excitation of BNST CRF-containing neurons did not bias drug motivation either toward or away from the laser-paired cocaine infusion. This result differs from previously demonstrated negative avoidance of a sucrose reward paired with laser excitation of BNST CRF-containing neurons, along with the patterns of distant Fos activation seen previously that were not recruited in the current study (Baumgartner et al. 2021). What could drive this difference between BNST CRF system control of sucrose versus cocaine motivation? One possibility is that BNST CRF systems may mediate aversive motivation for natural sucrose rewards, but there are other unknown mechanisms for motivation for cocaine rewards. This possibility would suggest that BNST CRF systems may actually be more important for natural rewards in comparison to drug motivation and addiction. Another possibility is that excitation of BNST CRF systems did in fact suppress cocaine motivation just like sucrose, and that suppression prevented any escalation of cocaine self-administration in general so that no avoidance could be detected. Indeed, BNST ChR2 animals showed an overall suppression in total number of cocaine infusions across days in comparison to NAc and CeA ChR2 groups, and even inactive control virus animals.

It is also possible that differences in life stress experiences could alter the control of BNST CRF systems on motivation. For example, the current experiment used rats on a restricted food diet during 2-choice cocaine operant tests, while previously rats that avoided laser-paired sucrose had *ad libitum* access to food in their home cages. Typically, food restriction is known to enhance drug-seeking and consumption (Carroll et al. 1979; Papasava and Singer 1985). However, as CRF signaling has been implicated in both suppression of food intake and also

excessive food consumption, including differentially across brain structures, it is possible that BNST CRF systems may have unique motivational roles for food-restricted versus non-restricted rats (Bernier and Peter 2001; Dunn and Berridge 1990; Epstein et al. 2016; Iemolo et al. 2013; Krahn et al. 1986). Another possible difference between this and previous sucrose experiments is that following catheter surgery, animals in the current study were single-housed to protect catheter patency, while previous sucrose rats were group-housed. This social isolation can conceivably cause chronic changes to brain stress systems like BNST CRF signaling, which could potentially explain the behavioral differences between sucrose and cocaine motivation experiments (Clark and Galef 1980; Manouze et al. 2019).

Individual differences in experienced valence

Some individuals may be more or less affected by stress-induced reward consumption, and the current study indicates that there may be individual differences in affective valence induced by CRF systems. The current work here, in line with previous findings (Baumgartner et al. 2021), demonstrates that some individual rats will self-stimulate for excitation of CRF-containing neurons in NAc or CeA, thus suggesting an induced positive state. However, this is not universally true for all rats, as a number of rats receiving the same NAc or CeA CRF-containing neuronal stimulation do not meet any criteria for self-stimulation. It is therefore possible that though CRF brain systems are able to guide and direct motivation for rewards, in a subset of individuals it can also mediate changes in affective valence, with no differences between these groups in cocaine pursuit and consumption. Future research should investigate whether there is a relationship between these individual differences and other specific aspects of motivation, as in the present study, positively experienced self-stimulations in NAc and CeA ChR2 groups did not predict motivation to pursue and consume cocaine rewards.

Motivational roles for CRF systems

CRF systems in the extended amygdala are traditionally thought to generate aversive *distress* states, mediating anxiety-like responses to natural stressors and enhancing "emotionality" (Dunn and Berridge 1990; Heinrichs and Joppa 2001; Hupalo et al. 2019; Koob and Bloom 1985). CRF-containing neuronal populations in CeA and BNST are linked to a wide spectrum of negatively-valenced states, including anxiety, pain, fear and fear learning, and drug withdrawal (Asok et al. 2018, 2016; Fadok et al. 2017; Funk et al. 2006; Minami 2019; Pomrenze et al. 2019b, 2019a; Sahuque et al. 2006; Takahashi et al. 2019; Tran et al. 2014). As predicted by the allostatic model of addiction, chronic drug use increases CRF activation in the extended amygdala to elicit aversive withdrawal effects, thus leading to addictive relapse and overconsumption as attempts at hedonic self-medication (Funk et al. 2006; Koob and Le Moal 1997, 2008; Koob and Schulkin 2019; Koob 2010, 2013; Olive et al. 2002; Park et al. 2013; Zorrilla et al. 2014).

However, our results support an alternate theory where CRF system activation increased drug seeking and escalation through incentive motivation, in contrast to hypothesized negative states induced by CRF. This adds to a growing body of literature supporting a range of positively-valenced roles for CRF systems, capable of initiating bio-behavioral responses to both positive and negative stimuli (Kim et al. 2017; Lemos and Alvarez 2020; Lemos et al. 2012, 2019; Merali et al. 1998, 2004; Schulkin 2017). For the present NAc and CeA ChR2 incentive effects, CRF system activation may amplify incentive salience or 'wanting' to pursue and self-administer cocaine drug rewards. Further, while it is possible that the present BNST CRF-containing neuronal stimulation may be neutral or aversive, we saw no evidence that activation of this BNST CRF system actually *enhanced* motivation for drug-seeking for either cocaine

reward, as would be predicted in hedonic-dysregulation theories. If anything, the lack of escalation in our BNST ChR2 group as compared to other groups suggests that activation of these BNST neurons may actually be capable of suppressing motivation for cocaine, or is at least inconsequential to cocaine pursuit and consumption.

Flexibility in valence

It is of course possible that the positive valence of CRF system stimulation in NAc or CeA may flip valence under specific circumstances, such as chronic stress (Lemos and Alvarez 2020; Lemos et al. 2012). Indeed, preliminary work from our lab suggests that activation of CeA CRF-containing neurons does not increase appetitive behaviors toward an aversive stimulus (unpublished data), that excitation of all CeA cell-types is capable of eliciting (Warlow et al. 2020). Therefore, the target of CRF-initiated motivation and attribution of salience also likely influences resulting affective valence. Given the range of bio-behavioral states and responses to stressors that CRF is capable of initiating, a role for CRF in motivation is likely flexible and equally expansive (Schulkin 2017).

CRF and addiction

Understanding the relationship between brain CRF systems and drug motivation is integral to understanding stress-induced addictive relapse. While the aversive distress of withdrawal or adverse life stressors is a plausible reason for relapse, addiction persists long after withdrawal states subside. Additionally, cue-triggered drug craving often occurs in the absence of any feelings of conditioned withdrawal (Childress et al. 1988; O'Brien et al. 1998). Here we demonstrate that the escalation of drug intake elicited by CRF systems is actually driven by incentive motivational mechanisms in NAc and CeA, while BNST CRF-containing systems if anything suppressed drug intake and escalation. This may explain how positively-valenced

emotions and stressful events (i.e., forming a new relationship, winning the lottery) are recognized triggers for relapse in treatment programs in addition to typical aversive stressors (Annis and Graham 1995; Carney et al. 2000; Kaundal et al. 2016; Larimer et al. 1999; Maisto et al. 1988b; Swendsen et al. 2000). Ultimately, while a role of CRF systems in aversive motivation is well defined, there is also a separable positive incentive role that we demonstrate here within the nucleus accumbens and central amygdala which may be integral to understanding substance abuse and addictive relapse (Lemos and Alvarez 2020).

Figures

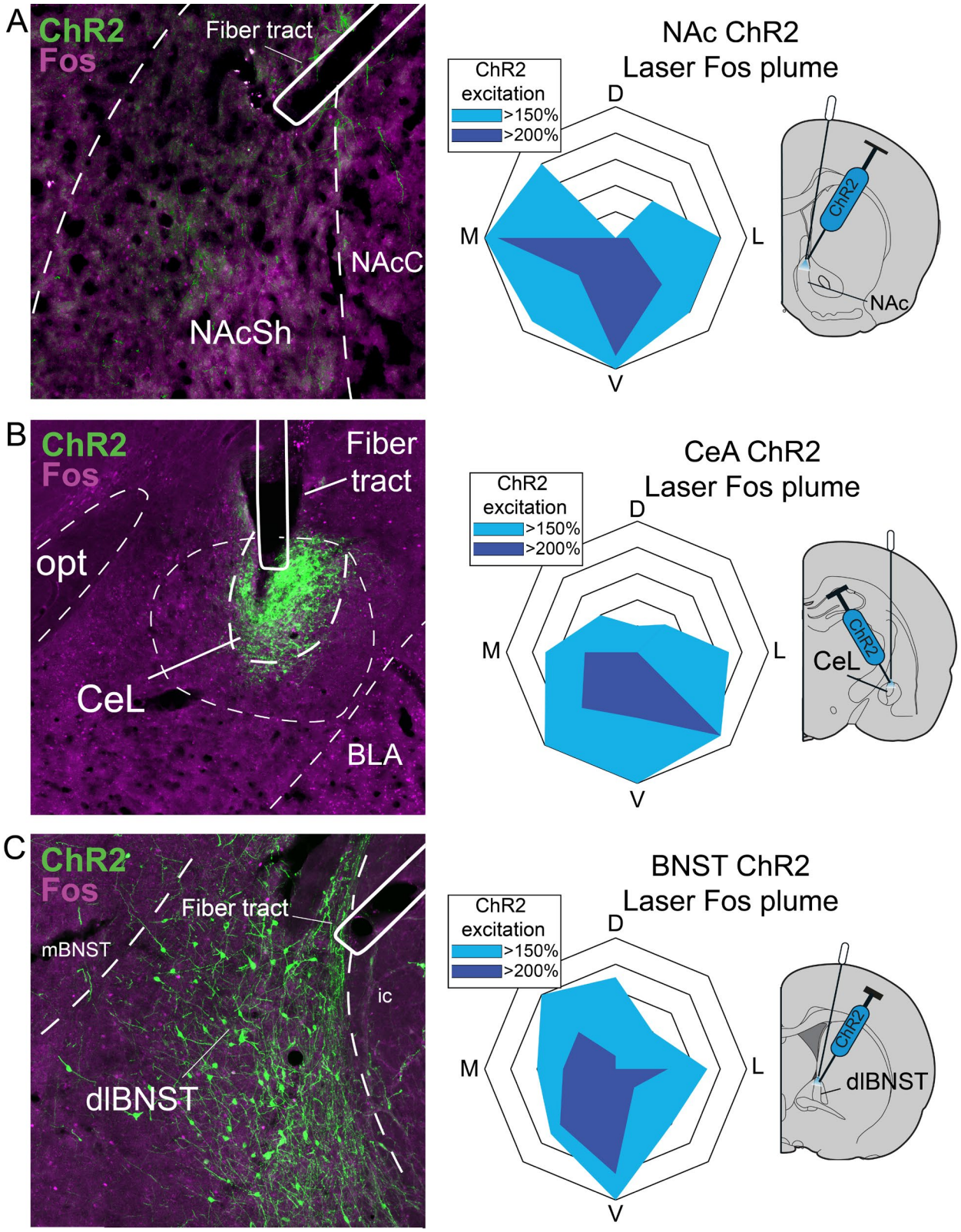
A
ChR2
Fos
Fiber tract
NAcC
NAcSh
NAc ChR2
Laser Fos plume
ChR2
excitation
>150%
>200%
D
M
L
V
ChR2
NAc
B
ChR2
Fos
Fiber
tract
opt
CeL
BLA
CeA ChR2
Laser Fos plume
ChR2
excitation
>150%
>200%
D
M
L
V
ChR2
CeL
C
ChR2
Fos
Fiber tract
mBNST
ic
dlBNST
BNST ChR2
Laser Fos plume
ChR2
excitation
>150%
>200%
D
M
L
V
ChR2
dlBNST

4.1 Photomicrograph of virus expression and local Fos plumes.
Photomicrographs display ChR2 virus expression (green) and Fos expression (purple) in *Crh*-Cre+ rats surrounding optogenetic fiber tips in **A**) nucleus accumbens (NAc) shell, **B**) central nucleus of the amygdala (CeA), and **C**) bed nucleus of the stria terminalis (BNST). Laser Fos plume diagrams at right show size and intensity of local Fos expression following ChR2 stimulation of CRF-containing neurons. Light blue reflects >150% Fos enhancement and dark blue reflects >200% Fos enhancement over baseline inactive virus control groups. NAcSh, nucleus accumbens shell; NAcC, nucleus accumbens core; opt, optic tract; CeL, lateral central amygdala; BLA, basolateral amygdala; mBNST, medial bed nucleus of stria terminalis; dlBNST, dorsolateral bed nucleus of stria terminalis.

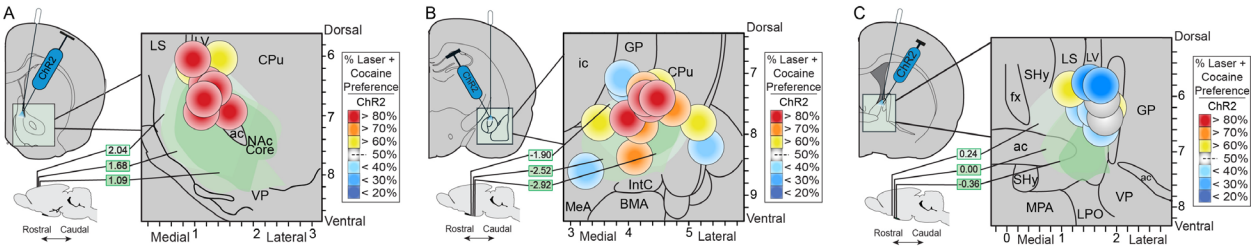

4.2 Localization of function maps

Functional maps show histological placements of ChR2 rats receiving CRF-containing neuronal excitation in the **A**) nucleus accumbens (NAc) medial shell, **B**) central nucleus of the amygdala (CeA), or **C**) dorsolateral bed nucleus of the stria terminalis (BNST). Symbol sizes show 0.7mm diameters to reflect measured radii of local Fos plumes. Colors indicate % preference for the laser-paired cocaine option in 2-choice test, with reds indicating stronger *Laser+Cocaine* preference and blues indicating avoidance of the laser-paired cocaine infusion. LS, lateral septum; LV, lateral ventricle; CPu, caudate putamen; NAc, nucleus accumbens; VP, ventral pallidum; ac, anterior commissure; ic, internal capsule; MeA, medial amygdala; GP, globus pallidus; IntC, intercalated amygdala; BMA, basomedial amygdala; BLA, basolateral amygdala; fx, fornix; SHy, septohypothalamic nucleus, MPA, medial preoptic area; LPO, lateral preoptic area

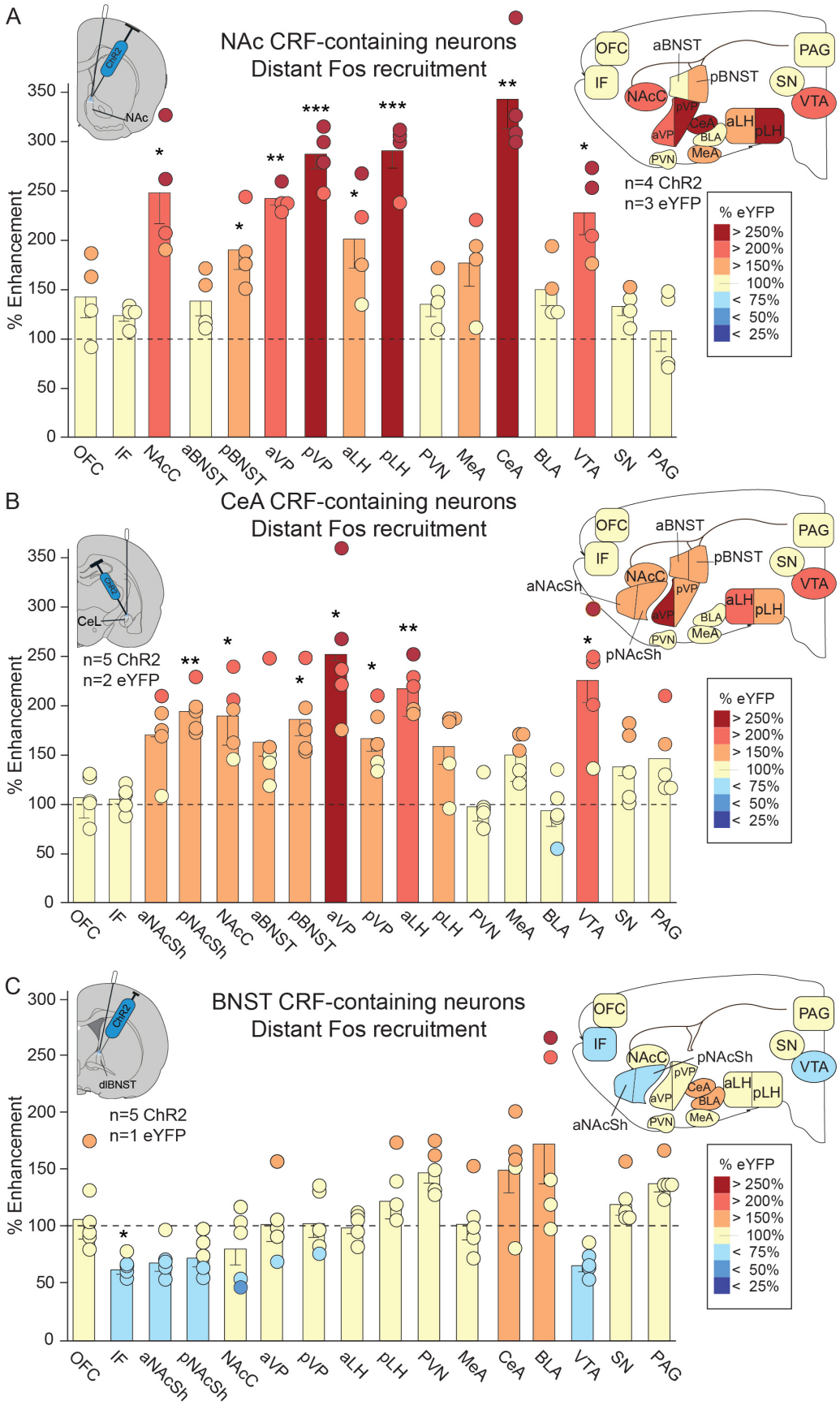
A
NAc CRF-containing neurons
Distant Fos recruitment
ChR2
NAc
% Enhancement
n=4 ChR2
n=3 eYFP
% eYFP
> 250%
> 200%
> 150%
100%
< 75%
< 50%
< 25%
OFC
IF
NAcC
aBNST
pBNST
aVP
pVP
aLH
pLH
PVN
MeA
CeA
BLA
VTA
SN
PAG
B
CeA CRF-containing neurons
Distant Fos recruitment
CeL
n=5 ChR2
n=2 eYFP
aNAcSh
pNAcSh
C
BNST CRF-containing neurons
Distant Fos recruitment
dlBNST
n=5 ChR2
n=1 eYFP

4.3 Distant Fos recruitment from NAc, CeA, or BNST CRF-containing neuron excitation
Enhanced Fos expression >150-300% over eYFP control levels in mesocorticolimbic structures following ChR2 excitation of CRF-containing neurons in **A**) nucleus accumbens (NAc): enhancing distant Fos expression in the nucleus accumbens core (NAcC), anterior and posterior ventral pallidum (aVP, pVP), posterior bed nucleus of stria terminalis (BNST), anterior and posterior lateral hypothalamus (aLH, pLH), central amygdala (CeA), and ventral tegmentum (VTA) and **B**) CeA: enhancing Fos expression in NAcC, posterior NAc shell (pNAcSh), pBNST, aVP, pVP, aLH, and VTA. **C)** Excitation of BNST CRF-containing neurons caused a suppression in distant Fos expression in the infralimbic cortex (IF). OFC, orbitofrontal cortex; aBNST, anterior bed nucleus of stria terminalis; PVN, paraventricular nucleus of the hypothalamus; MeA, medial amygdala; BLA, basolateral amygdala; SN, substantia nigra; PAG, midbrain periaqueductal grey area. Means and SEM shown. *$p<0.05$, **$p<0.01$, ***$p<0.001$

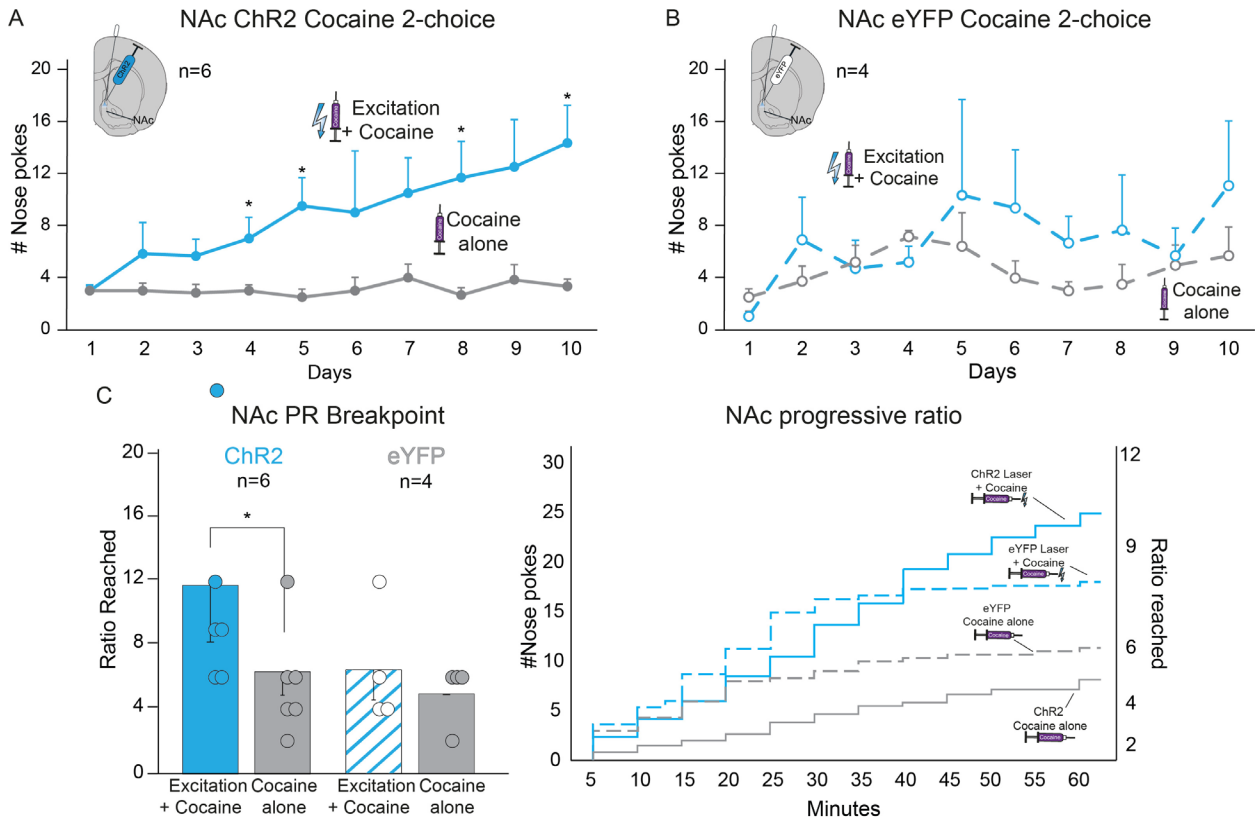

4.4 NAc CRF-containing neuronal stimulation biases and amplifies cocaine motivation
A) ChR2 excitation of CRF-containing neurons in NAc medial shell caused preference for the laser-paired cocaine infusion over *Cocaine alone* in the 2-choice test (n=6), reaching a 4:1 ratio by day 10. **B)** In comparison, control NAc eYFP rats chose equally between options (n=3). **C)** In progressive ratio (PR) breakpoint tests, NAc ChR2 CRF-containing neuron excitation enhanced incentive motivation breakpoint *Laser+Sucrose* over *Sucrose Alone* (n=6). Laser did not affect NAc eYFP control breakpoint between progressive ratio test days (n=3). Means and SEM reported. **p*<0.05

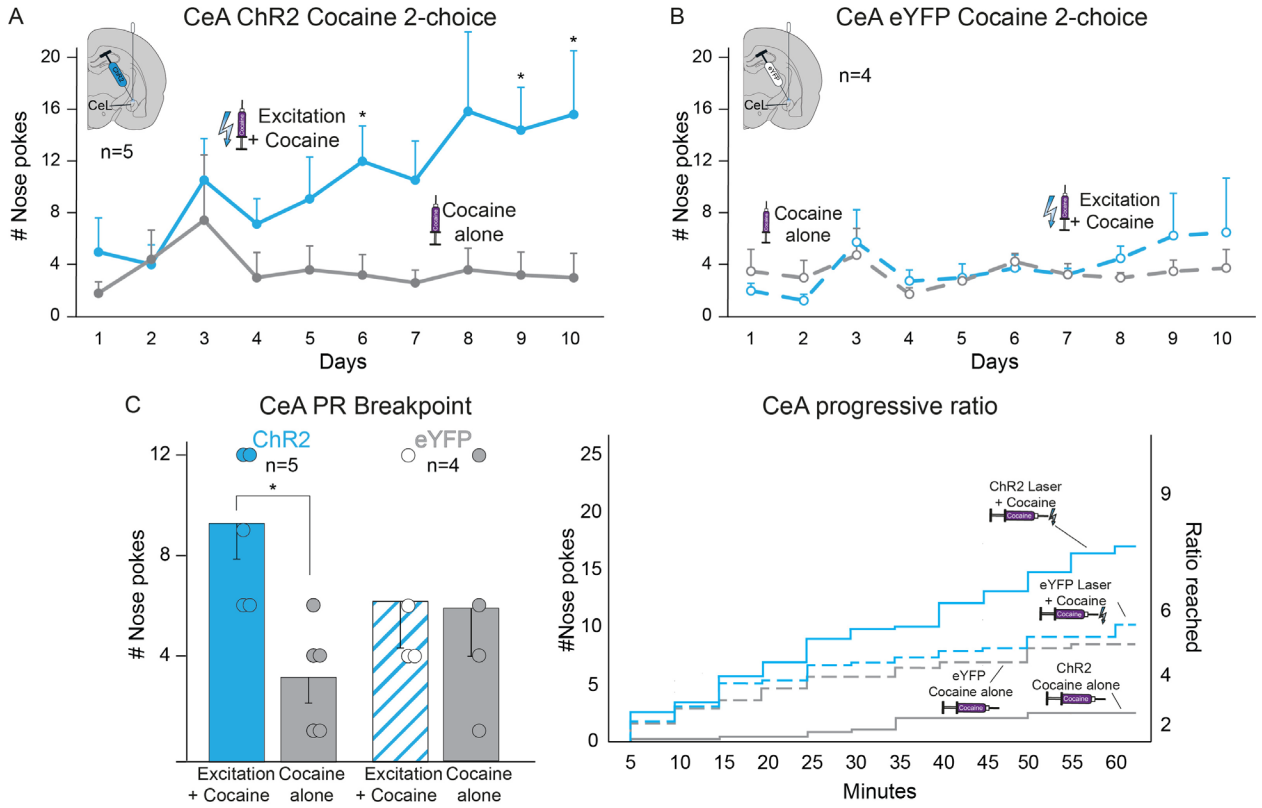

4.5 CeA CRF-containing neuronal stimulation biases and amplifies cocaine motivation
A) ChR2 excitation of CRF-containing neurons in the lateral CeA) caused preference for the laser-paired cocaine infusion over *Cocaine alone* in the 2-choice test (n=5), reaching a 4:1 ratio by day 10. **B)** In comparison, control CeA eYFP rats chose equally between options (n=4). **C)** In progressive ratio (PR) breakpoint tests, CeA ChR2 CRF-containing neuron excitation enhanced incentive motivation breakpoint for *Laser+Sucrose* over *Sucrose Alone* (n=5). Laser did not affect CeA eYFP control breakpoint (n=4) between progressive ratio test days. Means and SEM reported. *$p<0.05$

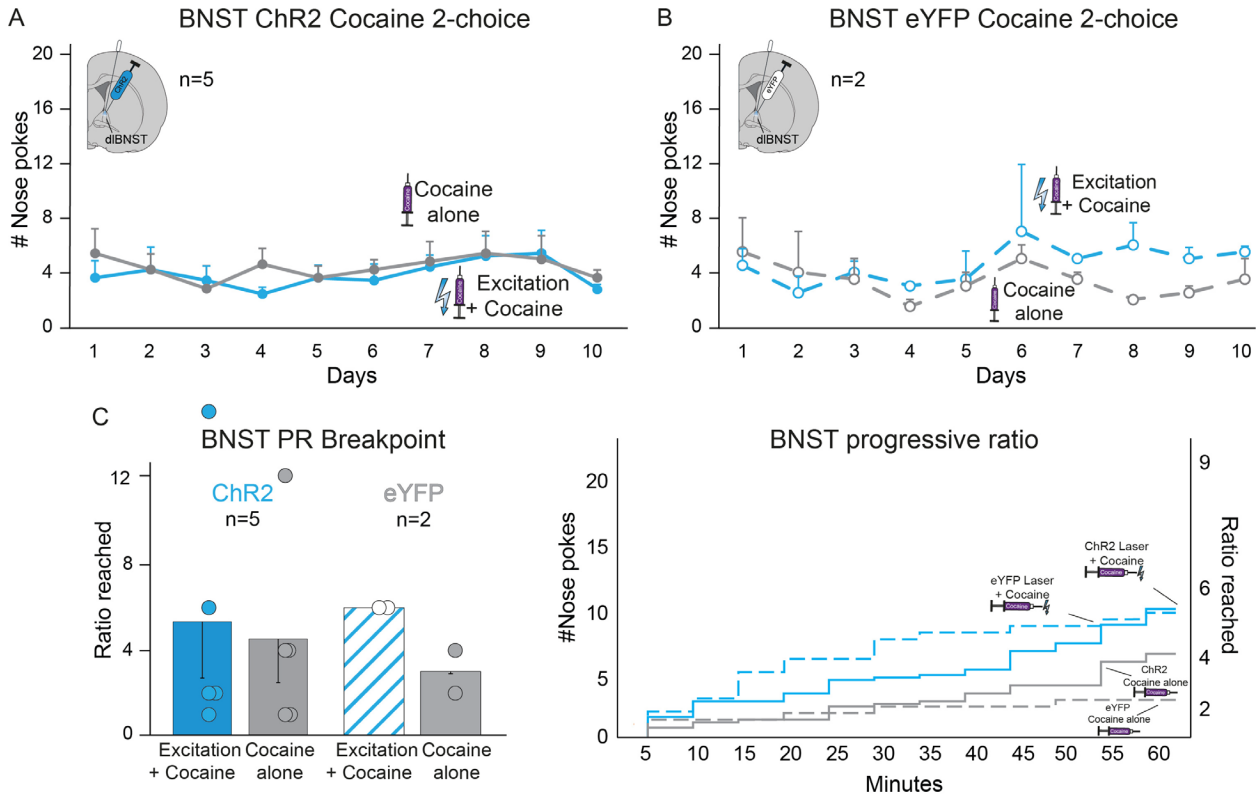

4.6 BNST CRF system stimulation fails to direct or enhance escalation of cocaine pursuit
ChR2 excitation of BNST CRF-containing neurons did not direct cocaine preference in the 2-choice self-administration task for either **A)** ChR2 BNST rats (n=5), or **B)** inactive eYFP control rats (n=2). **C)** In progressive ratio (PR) breakpoint tests of magnitude of motivation to pursue cocaine, neither ChR2 BNST (n=5) or eYFP control (n=2) groups showed any difference in effort breakpoint nor nose poke responses between *Laser+Cocaine* and *Cocaine alone* days. Means and SEM reported.

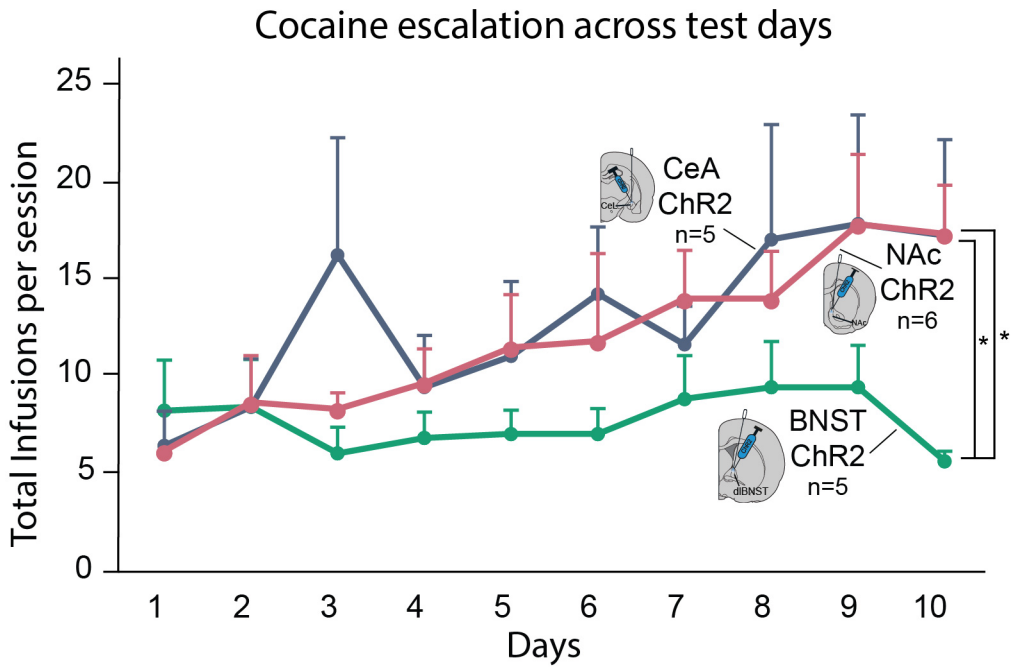

4.7 Differences in cocaine escalation for NAc and CeA versus BNST ChR2 groups
When evaluating the total number of cocaine infusions (*Laser+Cocaine* plus *Cocaine alone* infusions) rats received across testing days, rats that had the opportunity to receive CRF-containing neuron stimulation of BNST neurons (n=5) showed a suppressed escalation of cocaine intake in comparison to rats able to receive CRF-containing neuron stimulation in NAc (n=6) or CeA (n=5). Means±SEM shown. *$p<0.05$.

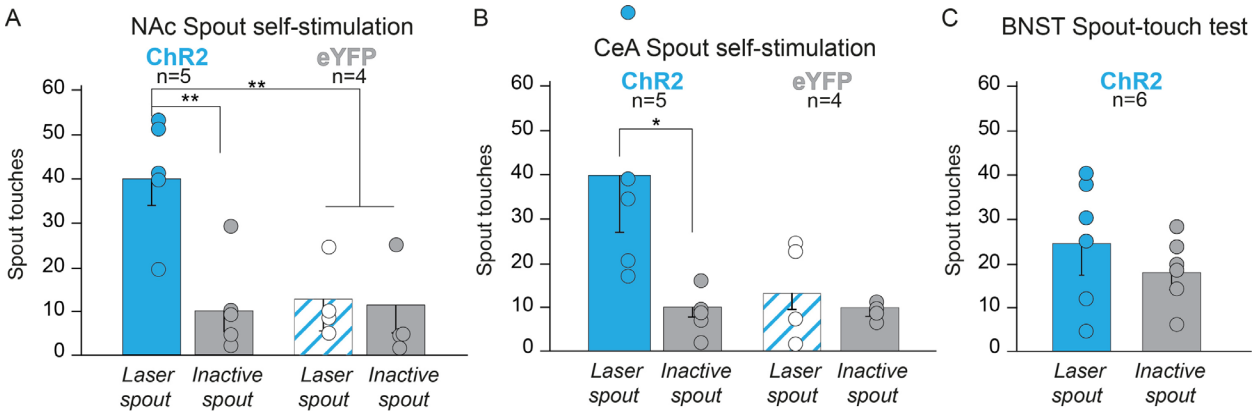

4.8 Spout self-stimulation of NAc and CeA CRF-containing neurons, not BNST
A) In the spout-touch self-stimulation task, NAc ChR2 rats (n=5) given the opportunity to self-stimulate CRF-containing neurons in NAc shell responded on average 4x more on the *Laser spout* in comparison to the *Inactive spout* that delivered nothing. These ChR2 NAc rats also responded at higher levels on the *Laser spout* than NAc inactive eYFP control rats (n=3). **B)** Rats given the opportunity to touch a *Laser spout* that delivered CeA CRF-containing neuron excitation (n=5) touched the *Laser spout* 4x more than the *Inactive spout*, while CeA eYFP rats (n=2) responded randomly between both spouts. **C)** Rats able to receive BNST CRF-containing neuron excitation showed no self-stimulation in the spout-touch task and responded randomly between the *Laser spout* and *Inactive spout.* Means and SEM reported. **p* <0.05, ***p*<0.01

Tables

Target	Confirmed placement ranges (mm from Bregma)			ChR2 N's		eYFP N's		Contralateral misses, locations
	A/P	M/L	D/V	Uni	Bil	Uni	Bil	
CeA	-1.92 to -3.12	± 3.8 to 4.6	-6.8 to -8.2	2	4	1	2	MeA, optic tract, BLA
NAc	+2.52 to 1.08	± 0.6 to 1.6	-6.0 to -7.0	2	2	1	2	NAcC
BNST	+0.36 to -0.36	±1.4 to 1.8	-6.1 to -6.5	1	4	0	1	LS

4.1 Histological placements of experimental animals
Coordinates and N's of ChR2 and eYFP *Crh*-Cre rats for central amygdala (CeA), nucleus accumbens (NAc), and bed nucleus of stria terminalis (BNST) target groups. MeA, medial amygdala; BLA, basolateral amygdala; NAcC, nucleus accumbens core; LS, lateral septum.

CHAPTER V. General Discussion

Synopsis

Incentive motivation and aversive motivation are controlled through interconnected limbic circuits capable of generating positively-valenced and negatively-valenced affective states. Interactions between traditional reward-related circuitry and brain stress systems can modulate affective valence and motivation in response to changing internal states and environmental contexts. Understanding these brain circuits and their ability to switch between positive and negative valence is critical to understanding the inappropriate attribution of salience and valence underlying neuropsychiatric disorders such as schizophrenia and addiction.

Nucleus accumbens drives incentive 'desire' and aversive 'dread' through disinhibition

While the NAc medial shell has long been implicated in both appetitive and fearful motivated behaviors, there is opposing evidence on the mechanisms through which these behaviors are initiated. On one side, decades of electrode self-stimulation and modern optogenetic studies have demonstrated that *excitation* of NAc shell elicits motivational effects (Cole et al. 2018; Koo et al. 2014; Lobo et al. 2010; Mogenson et al. 1979; Phillips 1984; Van Ree and Otte 1980; Rolls 1971). However, a large body of literature also implicates *inhibition* of NAc shell in generating these behaviors (Echo et al. 2001; Reynolds and Berridge 2008, 2003; Richard and Berridge 2011b, 2013; Stratford and Kelley 1997).

The NAc shell is therefore likely capable of multiple mechanisms for generating motivated behaviors, thus including both excitatory and inhibitory hypotheses. This inhibitory mechanism is posited to require the release of downstream structures such as lateral hypothalamus (LH) and ventral pallidum (VP) into excitation through disinhibition (Heimer et al. 1991; Humphries and Prescott 2010; Lu et al. 1998; Mogenson et al. 1983; Usuda et al. 1998; Zahm and Heimer 1990; Zhou et al. 2003). The disinhibition of NAc shell generating appetitive and fearful motivation aligns with pharmacological studies examining motivation elicited by DNQX or muscimol microinjections in NAc (Covelo et al. 2014; Faure et al. 2010; Reynolds and Berridge 2001, 2002, 2008; Richard and Berridge 2011b; Richard et al. 2013b; Stratford and Kelley 1997; Stratford and Wirtshafter 2012). However, there are cases where DNQX can alternatively act as an AMPA receptor *agonist* (Lee et al. 2010; Menuz et al. 2007), in which case the observed behavioral effects would actually align with the long demonstrated excitatory effects (Mogenson et al. 1979; Phillips 1984; Van Ree and Otte 1980; Rolls 1971). To my knowledge, this inhibition hypothesis has never been explicitly tested, and in Chapter 2 I sought to directly investigate this proposed mechanism.

The inhibition hypothesis was indeed supported in the current work, as simultaneous optogenetic excitation of NAc shell was capable of blocking the 'desire' and 'dread' behaviors elicited by DNQX microinjections. First, I was able to replicate previous flips between appetitive and fearful motivation along the rostro-caudal gradient by manipulating environmental ambience. Further, I demonstrated that both appetitive eating effects and fearful defensive-treading effects generated by DNQX microinjections were suppressed by concurrent optogenetic excitation. This importantly extends the inhibitory mode of motivation in NAc shell to both

incentive and aversive motivation, suggesting this disinhibition mechanism has a more expansive role in generating motivation.

Next, I examined whether the downstream effects of DNQX-elicited motivation aligned with an inhibitory hypothesis of motivation by analyzing Fos gene expression as a proxy for neuronal activation. As inhibiting NAc MSNs through DNQX AMPA receptor blockade is posited to release downstream structures into activation and release associated motivated behaviors, we in fact did demonstrate that DNQX microinjections both elicited appetitive motivation and enhanced Fos expression in downstream limbic structures such as LH, VP, and ventral tegmentum (VTA). Further, concurrent optogenetic excitation suppressed both the DNQX-induced behavioral and neural effects, as ChR2 laser paired with DNQX microinjections returned downstream structures LH, VTA, and VP to baseline levels of activation. Altogether, these experiments provide behavioral and neural evidence for an inhibitory mode of motivation in NAc medial shell that extends across positively- and negatively-valenced affective states.

CRF brain systems in NAc, CeA, and BNST mediate incentive and aversive motivation for sucrose rewards

Corticotropin releasing factor (CRF) neural systems are highly implicated in generating aversive motivation underlying negative stress states such as aversive drug withdrawal (Bruchas et al. 2009; de Guglielmo et al. 2019; Grieder et al. 2014; Henckens et al. 2016; Koob et al. 2014; Olive et al. 2002; Pomrenze et al. 2019b, 2019a). However, other research provides evidence for potential incentive motivational roles of CRF systems, particularly in NAc and CeA (Kim et al. 2017; Lemos and Alvarez 2020; Lemos et al. 2012, 2019; Peciña et al. 2006). Chapter 3 of this dissertation therefore investigated the potential incentive and aversive

motivational roles of CRF-containing neuronal populations in NAc, CeA, and BNST through optogenetic manipulations in *Crh*-Cre+ transgenic rats.

This work demonstrates that optogenetic excitation of CRF-containing neurons in NAc and CeA are capable of directing and amplifying incentive motivation for sucrose rewards and that it is inherently positively-valenced on its own. Excitation of CRF-containing neurons in NAc or CeA caused rats to almost exclusively prefer a sucrose pellet paired with laser illuminations in the two-choice operant task, caused increased effort breakpoint for a laser-paired sucrose pellet in progressive ratio tests, and was actively sought after in self-stimulation tasks. This excitation also recruited a number of mesocorticolimbic structures into activation including VP, LH, and VTA, as measured through distant Fos analysis. Further, halorhodopsin inhibition of NAc and CeA CRF-containing neurons produced oppositely-valenced effects, biasing motivation away from an inhibitory laser-paired sucrose reward and suppressing incentive motivation for inhibitory laser-paired sucrose in breakpoint tests. This implies that not only are NAc and CeA CRF-containing neuronal populations *sufficient* for causing incentive motivation effects, but they are also *necessary* for this incentive motivation direction and amplification.

In contrast, excitation of BNST CRF-containing neurons produced only aversive motivation and negative-valence. This CRF system activation caused strong avoidance of a laser paired-sucrose option in the two-choice task, suppressed incentive motivation for laser-paired sucrose through progressive ratio effort breakpoint tasks, and was avoided in self-stimulation tasks. Finally, excitation of these BNST CRF systems recruited distinct activation patterns from NAc or CeA stimulation, eliciting Fos enhancements in pain- or distress-related structures including paraventricular nucleus of the hypothalamus and midbrain periaqueductal gray area.

Altogether, these findings suggest that BNST CRF systems may play a more traditional role in fear and aversive motivation as posited by opponent-process theories.

One novel finding from Chapter 3 lies in the strong motivational effects elicited by sparse CRF-containing neurons in NAc, in comparison to better categorized and denser CRF-containing populations in CeA and BNST. Though little is known about CRF-expressing neurons in NAc, which may potentially act locally by activating acetylcholine interneurons and local dopamine release (Lemos et al. 2012, 2019), we were able to demonstrate their prevalence using fluorescent *in situ* hybridization (FISH). With RNAScope FISH (Wang et al. 2012), I was able to validate the co-expression of Cre-recombinase and *Crh* mRNAs in NAc medial shell, lateral CeA, and dorsolateral BNST with minimal non-specific binding in the new *Crh*-Cre+ BAC transgenic rat line. While CeA CRF-containing neuron populations have previously been validated using immunohistochemistry, potential Cre/CRF overlap in NAc cells in this rat line had not been previously evaluated (Pomrenze et al. 2015). Further, I was able to assess *Crh* and *Cre* mRNA co-expression with FISH to quantitatively compare Cre selectivity and penetrance across regions. This analysis showed that though they are less concentrated than CeA and BNST CRF neuronal populations, CRF-expressing neurons are prevalent throughout the rostro-caudal axis and dorsal/ventral portions of NAc medial shell. If anything, we are potentially undercounting NAc CRF-containing neurons, as penetrance of Cre-recombinase in neurons with *Crh* mRNAs was lowest within the NAc in comparison to CeA and BNST expressions. Future research should further categorize these NAc CRF-containing neurons, which though sparse are capable of greatly influencing incentive motivation.

Altogether, the set of findings from Chapter 3 highlights the range of affective valence capable of being generated by CRF-containing neuronal populations and suggests that incentive motivation mechanisms are possible from NAc and CeA CRF systems.

CRF-containing neurons in NAc and CeA mediate incentive motivation for cocaine rewards, ambivalence from BNST CRF systems

The influence of brain CRF systems on addictive behaviors and overconsumption has traditionally been posited to occur through negative *distress* states (Koob 2013; Roberto et al. 2017; Zorrilla et al. 2014). That is, increases in CRF expression in CeA and BNST are thought to drive the aversive feelings associated with drug withdrawal once use or consumption has ceased, and thus lead to addictive relapse in attempts to self-medicate this distressing state (de Guglielmo et al. 2017; Koob 2013; Koob et al. 2014; Olive et al. 2002; Roberto et al. 2017). This proposed mechanism of CRF systems in the extended amygdala is central to the prominent allostatic model of addiction, also known as opponent-process, hedonic homeostatic dysregulation, or hyperkatifeia theory theories. Stemming from original opponent-process theory from Solomon & Corbit (Solomon and Corbit 1978; Solomon 1980), the allostatic model hypothesizes that with continued drug use, the positive or euphoric state induced by drugs of abuse, or positive A-state, gradually decreases with tolerance. At the same time, continued drug use causes the opponent distressful B-state to increase over time, and this state is thought to be driven by upregulated CRF systems. Through this lens, addictive relapse and overconsumption are proposed to occur as attempts to self-medicate the aversive affective states caused by CRF systems in the extended amygdala, which includes the CeA, BNST, and posterior portions of the accumbens shell in this model (Koob and Le Moal 1997, 2008; Koob and Schulkin 2019; Koob and Volkow 2010).

However, addictive relapse can occur long after discontinued drug use or withdrawal subsides and positive stressors are also well known triggers for relapse, suggesting that aversive stress withdrawal states are likely not the only cause of addictive relapse or overconsumption (Childress et al. 1988; Grilo et al. 2012; Larimer et al. 1999; Maisto et al. 1988a, 1988b; O'Brien et al. 1998; Reyes et al. 2009). Further, while CRF has indeed been long implicated in addictive relapse or reinstatement in animal models, these CRF-induced effects do not require other stress molecules like corticosterone and instead mimic reinstatement in ways similar to heroin (Shaham and Stewart 1995; Shaham et al. 1997).

Given the incentive motivational effects following CRF-containing neuronal stimulation in NAc and CeA in Chapter 3, I next wanted to test whether this positively-valenced affective state from CRF system activation could also be directed toward drugs of abuse. Here the allostatic model of addiction would predict that pairing laser excitation of CRF-containing neurons with a cocaine reward would make that reward less valuable in comparison to a cocaine infusion without laser, since CRF system activation should create a negative distress state. However, we found that just as in Chapter 3 with sucrose rewards, laser excitation of NAc and CeA CRF-containing neurons was able to bias and amplify motivation for the paired cocaine reward. Interestingly, we found that BNST CRF-containing neuron excitation did not direct motivation toward either cocaine option in contrast to the negative avoidance of laser-paired sucrose rewards demonstrated in Chapter 3. However, while the aversive B-state caused by CRF activation is posited to cause escalation of intake to self-medicate the distress state, we saw no such evidence of escalation of cocaine self-administration in these BNST animals who if anything, demonstrated a suppression in cocaine escalation.

Incentive and aversive motivation through 'wanting' systems

It is critical to understand brain systems for incentive motivation and aversive motivation, particularly in cases where that motivation becomes pathological, such as addiction. However, as outlined above, the current experiments investigating CRF system activation do not align with the theory of addiction that usually evokes this system, the allostatic or hedonic dysregulation theory. Further, the Chapter 2 experiments do not align with this theory either, as the same inhibition of NAc, a region integral to addictive models, can cause both incentive and aversive motivation depending on the environment, thus suggesting more flexible mechanisms for affective valence rather that static motivational drives. Indeed, the overconsumption of food elicited by DNQX microinjections was not in response to an aversive distress state, as rats with increased appetitive motivation here displayed no fear related or aversive reactions. Further, the aversive motivation that was observed in rats following DNQX microinjections in the stressful environment did not coincide with appetitive effects, suggesting that these appetitive and distress behaviors are not dependent on one another. Altogether, if the current experiments do not support opponent-process theories, what psychological mechanism could lead to such pathological motivational states and also align with the current findings?

The ability of DNQX microinjections in NAc to elicit 'desire' and 'dread' are likely driven by directing endogenous mesolimbic dopamine and incentive salience systems. Psychologically, DNQX microinjections could elicit the demonstrated motivated behaviors by causing previously neutral cues (e.g., video camera and test room) to take on positive incentive salience in standard laboratory conditions or could cause these previously neutral cues to become more aversive and fearfully salient when tested in the stressful ambience. Indeed, NAc disinhibition from DNQX and associated motivated behaviors are blocked by concurrent dopamine D1 or D2 receptor antagonists, suggesting that local dopamine signaling is required to

generate these motivational effects (Richard and Berridge 2011b; Richard et al. 2013b). It would be interesting for future studies to test whether dopamine receptor antagonists would additionally block the recruitment of downstream mesocorticolimbic structures seen in the Fos analysis following DNQX microinjections, similar to concurrent optogenetic excitation.

Given the wide influence of 'wanting' systems in incentive motivation, mesocorticolimbic dopamine could also mediate the present positively-valenced motivational effects that are influenced by acute stress and CRF systems (Berridge 2019; Lemos and Alvarez 2020; Lemos et al. 2012; Peciña et al. 2006; Wang et al. 2005). Local CRF-containing neurons in NAc or connections between CeA CRF-containing neurons and mesocorticolimbic dopamine could therefore modulate the attribution and magnitude of incentive salience 'wanting' for natural and drug rewards. First, our distant Fos analyses did indicate that excitation of NAc or CeA CRF-containing neuronal populations recruits downstream mesolimbic structures such as VTA into activation, suggesting the recruitment of this incentive salience 'wanting' system. Further supporting this connectivity, NAc CRF microinjections elicit conditioned place-preference and local dopamine release in non-stressed mice (Lemos et al. 2012). However, chronic stress eliminates the ability of NAc CRF microinjections to stimulate local dopamine release, suggesting a mechanism through which stress experiences can cause flips between positively- and negatively-valenced affective states (Lemos et al. 2012). Still, it is likely that CRF systems, at least in NAc, act to modify the incentive salience of reward cues. In a Pavlovian Instrumental transfer (PIT) task, CRF microinjections in NAc shell amplify cue-triggered 'wanting' and pursuit of a sucrose reward when a cue embodied with incentive salience is presented, comparable to dopamine-stimulating amphetamine microinjections in the same test (Peciña et al. 2006). As these CRF-induced bursts in reward seeking are not triggered without

the presentation of the Pavlovian reward cue, NAc CRF systems are likely amplifying the attribution of incentive salience specifically. It would be interest for future research to test whether the incentive motivational effects caused by CeA and NAc CRF-containing neuronal excitation would be blocked by concurrent dopamine antagonist administration or to test whether excitation of these neurons could also preferentially induce bursts of incentive motivation following presentation of a Pavlovian reward cue during PIT.

Incentive sensitization theory

If CRF systems can influence 'wanting' and incentive motivation without requiring aversive states, there must still be a mechanism through which CRF systems and associated stress could lead to addictive relapse and overconsumption, given the large body of research implicating CRF in these behaviors (Mantsch et al. 2016; Shaham and Stewart 1995; Shaham et al. 1997). Indeed, the incentive sensitization theory (IST) of addiction provides both psychological and neurobiological explanations.

Most drugs of abuse directly or indirectly enhance dopamine release in NAc, thus activating incentive salience 'wanting' systems which can become sensitized with chronic use. Further, the sensitized dopaminergic response can coincide with sensitized incentive salience responses, or incentive sensitization, thus making drug-related cues more powerful and stronger 'motivational magnets' over chronic use (Berridge and Robinson 2016; Horger et al. 1990; Kalivas and Stewart 1991; Mendrek et al. 1998; Robinson et al. 2016; Robinson and Berridge 1993; Vezina et al. 2002). This powerful incentive sensitization can explain the phenomenon of "chasing ghosts", where some individuals with cocaine addiction report scouring the ground for and attempting to smoke tiny specks of white around them, despite rationally knowing that these are not cocaine but small pebbles (Rosse et al. 1993, 1994).

In particularly susceptible individuals, incentive sensitization can last many years, even after drug use subsides, as previous drug cues can long maintain their powerful incentive salience as a 'motivational magnet' (Robinson and Berridge 1993). With the high occurrence of relapse despite years of sobriety, such as that seen in alcohol addiction, incentive sensitization theory can explain how a susceptible individual may still maintain that heightened incentive salience and sensitized dopaminergic response to previous alcohol-related cues that they may encounter (Robinson and Berridge 1993). These powerful neurobiological and psychological effects therefore offer possible causes for addiction and escalating drug use, as well as relapse that occurs long after drug-use subsides. Further, incentive sensitization and accompanying dopamine system sensitization can occur even without drug use for very vulnerable individuals, which could lead to behavioral addictions such as eating disorders or gambling addictions (Davis and Carter 2009; Devoto et al. 2018; Gearhardt et al. 2011; Hartston 2012; Linnet et al. 2012; O'Sullivan et al. 2011; Olney et al. 2018; Pfaus et al. 1990; Ray et al. 2012; Stice et al. 2012; Voon et al. 2017; Zeeb et al. 2017).

These motivational mechanisms could underlie the surprising behavioral addictions that can be observed in some Parkinson's patients following treatment with dopamine direct agonists. For certain individuals receiving supplemental dopamine medications, who therefore produce heightened dopaminergic responses similar to incentive sensitization, intense addictive behaviors such as compulsive gambling, compulsive sex, or compulsive shopping can occur, even for individuals who never displayed these behaviors pre-treatment (Bostwick et al. 2009; O'Sullivan et al. 2011; Vela et al. 2016; Voon et al. 2017; Warren et al. 2017; Weintraub et al. 2010).

Sensitization of incentive salience for drug or reward cues can also be dynamic across different situations. For example, particular states such as stress, hunger, etc. are capable of

amplifying that peak of incentive salience elicited by cues, thus suggesting that momentary experiences of stress or heightened emotions can enhance 'wanting' (Lemos and Alvarez 2020; Lemos et al. 2012; Peciña et al. 2006). The current dissertation supports this notion, providing evidence that both external stressful environments and activation of CRF stress systems are capable of amplifying incentive motivation and aversive motivation. Stressful or emotional moments can also enhance mesolimbic dopamine release, providing a mechanism through which these stress states can magnify incentive salience (Boyson et al. 2014; Lemos and Alvarez 2020; Lemos et al. 2012; Rougé-Pont et al. 1993; Wanat et al. 2008).

Evidence for modes vs modules

The current experiments provide evidence for the coexistence of both excitatory and inhibitory mechanisms of motivation in NAc shell, and insight into the mechanisms through which the same limbic areas may be able to control both positively- and negatively-valenced effects. For instance, the same DNQX microinjections were able to elicit both 'desire' and 'dread' in NAc shell. Further, despite the large body of literature demonstrating the negatively-valenced effects of CeA CRF systems (Asok et al. 2018; Fadok et al. 2017; Jo et al. 2020; Partridge et al. 2016; Pomrenze et al. 2019b; Ventura-Silva et al. 2020), here I demonstrate that activation of these CeA CRF-containing neurons causes only positively-valenced effects in the current experiments. Thus, this dissertation ultimately prompts the question of how could opposing valences be elicited from the same brain manipulations even within the same brain structures?

One option is called the 'modules' hypothesis. This posits that there are actually *separate* brain units (e.g., cells, ensembles, or even brain areas) that control *separate* behaviors (Berridge 2019). For example, perhaps there are specific neurons in the accumbens that elicit

'desire' vs those that elicit 'dread' that make up the consistent rostro-caudal gradient or 'keyboard' of motivational valence. However, the modules hypothesis does not entirely explain the environmental tuning of the rostro-caudal axis in the generation of motivation, as these separate rostral and caudal modules would need to extend or shrink based on environmental conditions, such as in the stressful ambience condition. Instead, this change in behavioral effects induced by the same manipulations in the same target locations supports a 'modes' hypothesis.

In contrast to a 'modules' framework, the 'modes' hypothesis posits that the *same* brain units can control *separate* behaviors (Berridge 2019). Here, brain areas, neuronal ensembles, or general neurobiological units are capable of generating opposing valences. This framework aligns much more with the motivational effects elicited from central points in the rostro-caudal axis of the accumbens medial shell, which are capable of generating either appetitive or aversive motivation, or even a mix of the two, based on environmental ambience.

The current group of experiments provides evidence for the coexistence of both 'modes' and 'modules' motivational mechanisms across the limbic system. Specifically, we demonstrate potential 'modules' of incentive motivation through CRF systems in NAc and CeA, versus a 'module' of aversive motivation through BNST CRF systems that exists for both natural sucrose rewards and drug rewards such as cocaine. However, it is of course possible that the positive/negative valence of incentive motivation versus fearful motivation induced by optogenetic stimulation of these CRF systems may be switchable, depending on environmental conditions. Indeed, optogenetic stimulation of all neuronal cell-types in CeA has been found to flip depending on environmental situations and the types of stimuli laser is paired with (Warlow et al. 2020). Beyond immediate environmental tunings, NAc CRF microinjections in mice have been found to flip from positively-valenced to negatively-valenced following chronic stress

exposure (Lemos et al. 2012). Therefore, the valence of our specific CRF neuronal stimulation effects might also be capable of different 'modes' in different situations, so that CeA CRF or NAc CRF system valence might become negative in particular conditions, such as situations involving strong fear, aversive stress, or drug withdrawal. Overall, the novel positive 'modes' of CRF-containing neurons in NAc and CeA contrasted with the well-documented negative 'modes' of CRF systems, along with ambience-mediated 'modes' in accumbens medial shell for 'desire' and 'dread', may ultimately indicate that the ability to elicit flexible motivational valences is a specific feature of striatal-level structures.

Striatal-level generators of motivation

In a cortico-striatal-pallidal macrosystem, striatal-level structures NAc and CeA, which both generate incentive and aversive motivations, share unique anatomical characteristics that may particularly underlie their motivational strength (Alheid and Heimer 1988; Heimer and Van Hoesen 2006; Heimer et al. 2007; Swanson 2005; Zahm 2006). This anatomical framework identifies conserved cortical-striatal-pallidal structures that show high overlap in neuron types, connectivity patterns, and embryological origins. That is, NAc and CeA both receive descending glutamate inputs from cortical structures and send GABAergic outputs to pallidal targets, with loops to thalamus and back to cortical regions. For example, the NAc receives cortical inputs from prefrontal cortex and sends projects to ventral pallidum, closely resembling dorsal striatum connectivity (Alheid and Heimer 1988; Heimer et al. 1991; Mogenson et al. 1983; Swanson 2005; Zahm and Heimer 1990). The CeA additionally fits the striatal criteria when using a macrosystem framework that identifies the extended amygdala. Specifically, the CeA receives cortical-like glutamatergic input from basolateral amygdala and sends GABAerfic projections to the BNST as a pallidal-level structure (Alheid and Heimer 1988; Alheid 2003; Heimer and Van

Hoesen 2006; Heimer et al. 2007). These parallel macrosystems in NAc and CeA may therefore include special roles for striatal-level structures in generating motivation, likely through specific mesocorticolimbic dopamine connections (Alheid 2003; Carlezon and Thomas 2009; Fudge and Emiliano 2003; Heimer and Van Hoesen 2006; Kim et al. 2017; Mogenson et al. 1980; Richard et al. 2013a; Robinson et al. 2014; Warlow et al. 2020, 2017; Zahm 2006).

Conversely, the only structure in the current experiments that solely elicited aversive motivation is the BNST, a pallidal-level structure. Indeed, BNST mirrors other pallidal-level structures of ventral pallidum and globus pallidus in being composed of mostly GABAergic neurons receiving striatal-type inputs, with outputs sent primarily to effector targets in hypothalamus and brainstem and minor projections to re-entrant thalamo-cortico-striatal-pallidal loops (Alheid and Heimer 1988; Alheid 2003; Heimer and Van Hoesen 2006; Heimer et al. 2007; Zahm 2006). As a structure that has currently only demonstrated a negatively-valenced motivational 'mode' in the present dissertation, it is possible that differences in striatal- and pallidal-level structures underlie different incentive motivational capabilities.

Incentive and aversive motivation in clinical disorders

The present collection of results emphasizes the influence of brain stress systems and environmental stressors in the magnifying of incentive and fearful salience, thus resulting in powerful incentive motivation and aversive motivation. Such cases of extreme 'wanting' have major implications for clinical cases of excessive reward pursuit and consumption, such as addiction (Berridge and Robinson 2016; Olney et al. 2018; Robinson et al. 2016; Robinson and Berridge 1993). Given the prevalence of stress-induced relapse in both animal models and human experiences, understanding the brain mechanisms that drive this tuning of incentive salience are of critical importance for any therapeutic interventions (Hellberg et al. 2019; Reyes

et al. 2009; Shaham et al. 1997; Stewart 2000; Sureshkumar et al. 2017). This dissertation therefore offers a strong argument for stress-based tuning through an incentive sensitization theory addiction framework. The incentive motivation elicited by CRF systems in particular may explain why positive stressors are well-known triggers for relapse in rehabilitation programs, and in general can explain how relapse can occur long after consumption and withdrawal has subsided (Grilo et al. 2012; Kaundal et al. 2016; Larimer et al. 1999; Reyes et al. 2009; Stewart 2000; Sureshkumar et al. 2017). Positively-valenced stressors are much less studied in animal models of relapse in comparison to negatively-valenced stressors, and this work highlights the need for both in investigations into the neurobiology of addictive relapse.

Though the current set of experiments provide much insight into the incentive and aversive motivational mechanisms that may drive addiction, these findings have many further implications in neuropsychiatric disorders beyond substance use disorders. For example, the fearful negative salience elicited toward seemingly neutral environmental cues following DNQX administration could be a mechanism through which paranoia and fear may occur in schizophrenia. Indeed, elevated dopamine signaling is highly implicated in the neurobiological profile of schizophrenia, which is posited to contribute to psychosis through aberrant salience (Abi-Dargham et al. 1998; Breier et al. 1997; Ceaser and Barch 2015; Davis et al. 1991; Howes and Kapur 2009; Howes et al. 2009; Kapur 2003; Kapur et al. 2005). Given the bivalent motivation generated by accumbens inhibition, schizophrenia perhaps involves neural dysregulations in the rostro-caudal 'keyboard' gradient of 'desire' and 'dread', biasing toward the incorrect attribution of aberrant salience for stimuli that would be positive or neutral to neurotypical individuals (Faure et al. 2010; Olney et al. 2018; Richard and Berridge 2011a, 2013).

Dysregulations in brain CRF systems have additionally been implicated in a range of stress- and anxiety related neuropsychiatric disorders (Epstein et al. 2016; Hostetler and Ryabinin 2013; Piccin and Contarino 2020; Zorrilla and Koob 2004). Women are twice as likely to be diagnosed with anxiety-related disorders in general, which can include generalized anxiety disorder, obsessive-compulsive disorder, post-traumatic stress disorder, and depression (Kessler et al. 2012; Navarro-Mateu et al. 2015). Mounting evidence supports prominent sex-based differences in CRF systems in both animal and human models that could mediate these clinical presentations (Agoglia et al. 2020; Bangasser and Wiersielis 2018; Becker 2016; Dunlop et al. 2017; Malikowska-Racia and Salat 2019; O'Dell and Torres 2014; Piccin and Contarino 2020; Salvatore et al. 2018; Tollefson et al. 2017; Uchida et al. 2019; Uribe et al. 2020). However, recent clinical trials report that CRF antagonist administration does little to relieve symptoms of these and addictive disorders in women or men (Coric et al. 2010; Dunlop et al. 2017; Grillon et al. 2015; Kwako et al. 2015; Schwandt et al. 2016), suggesting that the expression of anxiety-related disorders and sex differences likely stems from an interaction of multiple neurobiological systems (Shaham and de Wit 2016).

Conclusion

In conclusion, the limbic system contains powerful mediators and generators of both incentive motivation and aversion motivation, particularly in striatal-level structures. This dissertation ultimately emphasizes the *flexibility* of these motivational brain circuits, which must adapt to constantly changing internal and external environments. While mesocorticolimbic dopamine may drive 'wanting' and incentive or fearful motivation directly, stress can greatly influence these motivational drives through activation of brain CRF systems and environmental tunings of the rostro-caudal 'keyboard' of the accumbens medial shell. Overall, further research

into the brain mechanisms underlying stress-mediated incentive motivation and aversion motivation would offer critical insights into various neuropsychiatric disorders of affective valence and motivation.

Appendix A: Chapter III Supplementary information

Chapter III Supplementary Methods

Stereotaxic surgery

Rats were anesthetized with isoflurane gas (4-5% induction, 1-2% maintenance) and placed in stereotaxic apparatuses (David Kopf, CA). Pre-surgery rats received atropine (0.05mg/kg; i.p.; Henry Schein) and post-surgery received cefazolin (75mg/kg, s.c.; Henry Schein) and carprofen, which was also provided for 2 days post-surgery (5mg/kg; s.c.; Henry Schein). Bilateral infusions in NAc, CeA, or BNST contained either active AAV-DIO-ChR2-eYFP virus (n=19 female, n=14 male), or optically-inactive control virus AAV-DIO-eYFP (n=10 female, n=9 male), both driven by EF1a promoters to infect only neurons containing Cre-recombinase. A separate group received halorhodopsin AAV-DIO-NpHR-eYFP (n=8 female, n=11 male) virus for CRF-containing neuronal inhibition (Fig. A.6). NAc shell coordinates were: flat skull, from bregma A/P: +1.0 to +2.0, M/L: ±2.5 to 3.3, D/V: -6.5 to -7.2 (10º-16º; n=13 female, n=11 male). Lateral CeA coordinates were: A/P: -2.2 to -2.8, M/L: ±4.2 to 4.7, D/V: -7.2 to -7.6 (n=12 female, n=12 male). Dorsolateral BNST coordinates were: A/P: +0.24 to -0.24, M/L: ±3.6, D/V: -6.9, (16º; n=12 female, n=11 male). Sites were bilaterally identical within individuals but staggered across rats (Fig. 3.1, Table 3.1). Rats received bilateral 1.0µl virus infusions (0.1µl/min) with 10min for diffusion, and optic fibers (200µm) 0.3mm above

virus were secured with surgical screws and acrylic. Rats were monitored 7 days post-surgery, with 3 weeks for viral incubation.

Two-choice sucrose

Rats underwent an instrumental two-choice task to evaluate whether associative pairing of CRF-containing neuronal stimulation with earning one sucrose reward made it more or less desirable than an identical sucrose reward received without laser (Robinson et al. 2014). Rats were first habituated to sucrose pellets in home cages and underwent 1 day where pellets were delivered to the operant box sucrose dish freely every minute for 25min. Next, rats received 5 days of Pavlovian lever training in ~45min sessions, where one of two levers appeared in alteration every minute for 8-sec paired with a distinct tone or white noise assigned to each lever, which was followed by a sucrose pellet for rats to associate these levers and rewards.

Next, one lever was permanently assigned *Laser+Sucrose* for each rat (counter-balanced) and the other was assigned the *Sucrose-alone*. Training included one day of fixed ratio 1 (FR1) reinforcement, where rats could freely choose between both available levers in 30min sessions. Each *Laser+Sucrose* lever press earned a sucrose pellet, assigned tone, and laser illumination (8-sec). Responses on *Sucrose alone* lever earned a sucrose pellet and assigned tone only. Rats next underwent 3 days of FR1 with each session now beginning with a forced-exposure to each lever: only one lever was presented (random order) until the rat pressed it, that lever was repeated a second time, and then it was withdrawn while the other lever was presented twice. This was to remind rats of each lever outcome daily before choosing freely. The remainder of the 30min session had both levers available for free choice. Levers retracted for an 8-sec time out period following each reward earned. On days 4-8, the beginning forced-exposure to both levers continued and the schedule of reinforcement escalated: FR4 (day 4), random ratio 4 (RR4, day 5), and RR6 (days 6-8). Three additional RR6 days followed at the alternate laser frequency for each rat (10Hz or 40Hz). The separate group with inhibitory halorhodopsin virus underwent identical procedures with constant yellow laser illumination.

Progressive ratio

Progressive ratio (PR) tests assessed whether ChR2 stimulation of CRF-expressing neurons changed the magnitude of incentive motivation to earn sucrose reward. Rats were tested one day with laser stimulation, using parameters identical to those in the two-choice task, and with only *Laser+Sucrose* lever available in a 30min session. A second test on a separate day

was run withonly *Sucrose-alone* lever available, and without laser (counter-balanced order). A third test on *Laser+Sucrose* day followed but used the alternate laser frequency (10Hz/40Hz). Within each session, the number of responses required to earn next reward increased after each reward received, following PR=$[5e^{(reward\ number \times 0.2)}] - 5$, rounded to the nearest integer (Robinson et al. 2014). Breakpoint or ratio-reached were compared between days. Separate halorhodopsin rats underwent similar PR tests with laser inhibition.

Spout-touch self-stimulation

Incentive properties of CRF-expressing neuronal stimulation alone without sucrose were tested in an instrumental spout-touch self-stimulation test. With two empty waterspouts available, each touch on a designated *Laser-spout* provided stimulation (3-sec; 10Hz/40Hz; 30min). Touches on the other *Inactive-spout* earned nothing, as a baseline exploration measure. Rats were classified on Day 1 as robust self-stimulators if they made 2x more touches on *Laser-spout* as on *Inactive-spout,* and made >50 *Laser-spout* touches (Warlow et al. 2020). Others were classified as low-level self-stimulators if they made at least 10 *Laser-spout* touches and 2x more *Laser-spout* than *Inactive-spout* touches. Days 2-3 evaluated the consistency of self-stimulation. MedPC programs recorded responses. Pilot NpHR groups underwent similar testing with inhibitory yellow laser (constant Hz, 8-sec stimulation; Fig. A.6)

Place-based self-stimulation

In another, relatively passive, place-based self-stimulation test, rats could earn laser self-stimulations by entering and remaining in a designated chamber within a 3-chamber apparatus (2 major, 1 smaller center). Rats started sessions in the center chamber. An initial session without laser evaluated baseline preference. Then for 3 test days, one side was designated the *Laser-delivering* chamber, with distinct contextual cues (dots/stripes, floor textures), and the opposite side was another no-laser chamber with distinct cues. Entry into the *Laser-delivering* chamber (>half-body) triggered onset of laser stimulation, which continued to cycle for as long as rats remained in that chamber (3-sec-on/4-sec-off; 10Hz/40Hz; triggered via MATLAB program), and terminated upon exit. Time spent in each chamber was scored by video (Noldus Observer XT 12). Difference-scores (*Laser-delivering* - *No-laser* seconds) were compared between groups. Pilot NpHR groups underwent similar testing with inhibitory yellow laser (constant Hz, cycling 8-sec-on, 4-sec-off; Fig. A.6)

Histology

Brains were sectioned into 40 micrometer slices using a cryostat (Leica, Wetzlar, Germany). Tissue was rinsed for 10min in 0.1M sodium phosphate buffer (NaPB) three times and blocked with 5% normal donkey serum (60 min). Tissue was incubated overnight at room temperature in rabbit anti-cFos (1:2500; Catalog#: 226 003; Lot #: 4-63; RRID: AB_2231974; Synaptic Systems, Göttingen, Germany) and chicken anti-GFP (1:2000; Catalog#: AB13970; Lot #: GR3190550-30; RRID:AB_300798; Abcam, Cambridge, MA). Slices were rinsed 3x for 10min in 0.1M NaPB before incubation with biotinylated donkey anti-rabbit secondary (1:300; Catalog #: AB2340593; Lot #: 128703; RRID: AB_2340593; Jackson Immunoresearch, West Grove, PA) and donkey anti-chicken Alexa Fluor 488 (1:300; Code #: AB2340375; Lot #: 144438; RRID:AB_2340375; Jackson Immunoresearch, West Grove, PA) for 120min. Tissue was rinsed 3x for 10min in 0.1M NaPB before incubation with Streptavidin Cy3 (1:300; Catalog #: AB2337244, Lot #: 141873, RRID: AB_2337244; Jackson Immunoresearch, West Grove, PA) for 90min. Tissue was rinsed 3x for 10min in 0.1M NaPB, mounted onto slides, and coverslipped with Pro-long gold (Invitrogen). Images were taken using a digital camera (Qimaging, Surrey, BC, Canada) attached to a fluorescence microscope (Leica, Wetzlar, Germany) at sites surrounding optic fibers. Immunoreactivity was visualized with filters with excitation bands 515-545 for Fos protein and 490-510 for virus. Adobe Photoshop was used to adjust contrast and brightness.

Local Fos plumes

Local Fos plumes were evaluated by counting Fos+ neurons in 15 successive blocks (50x50um) along eight radial arms surrounding the fiber tip (Baumgartner et al. 2020; Warlow et al. 2020). Neuron counting stopped once 2 consecutive blocks without Fos+ cells occurred, marking that arm's radius. Fos elevation was assessed as %change from levels of respective illuminated inactive-eYFP virus controls who underwent identical conditions.

RNAScope® Fluorescent In Situ Hybridization (ISH)

Brains were rapidly dissected, and flash frozen in dry ice. Brains were equilibrized for at least 1 hour in a Leica cryostat and sectioned into 17µm slices. A total of ~12-20 slices per rat (n=3 female, n=3 male) were collected from *Crh*-Cre+ rats. Sections across the three slides per rat included sections of 1) nucleus accumbens shell and dorsal striatum, 2) dorsolateral BNST and globus pallidum, and 3) central amygdala and nearby amygdala nuclei. Slices were thaw mounted on Superfrost plus slides (Fischer) and stored at -80 C with desiccators. Procedures for

ISH followed Advanced Cellular Diagnostics (ACD) manual for RNAscope® 2.0 assay and followed previous reports (Lemos et al. 2019; Wang et al. 2012).

Briefly, slides were fixed for 20 min (4º C) in 10% neutral buffered formalin and washed twice for 1 min each with PBS. Slides were dehydrated for 5 min with 50% ethanol, for 5 min with 70% ethanol, and twice for 5 min with 100% ethanol before overnight incubation at -20º C in 100% ethanol. The next day slides were first dried for 10 min (room temperature) and a hydrophobic barrier was drawn around the sections and dried for 15 min. Section were incubated with Protease Pretreat-4 for 20 min, washed twice for 1 min each with ddH20, and incubated with ACD probes Rn-Crem-03 (Catalogue# 530001) and Rn-Crh-C3 (Catalogue # 318931-C3) for 2 hours in the ACD HybEZ oven (40º C). Slides then underwent amplification steps in the HybEZ oven (40º C) with two 2 min washes between steps (at room temperature). These amplification (at 40º C) steps included 1) Amp 1 for 30 min, 2) Amp 2 for 15 min, 3) Amp 3 for 30 min, and 4) Amp 4-Alt A for 15 min. Sections were stained with a DAPI-containing solution at room temperature, coverslipped with ProLong Gold Antifade, and stored at 4º C until imaging.

Sections were imaged with a digital camera (Qimaging, Surrey, BC, Canada) attached to a fluorescence Leica DM microscope (Leica, Wetzlar, Germany). Images at 40x were taken of the NAc shell, CeA, and BNST with the same hardware and software settings for quantification, titrated for each probe. The number of cells expressing either Cre mRNA or *Crh* mRNA (containing >5 particles) were manually counted in core sample volumes (0.1mm x 0.1mm x 17µm boxes; placed to contain at least 1 *Crh*+ expressing cell) of tissue in CeA, NAc shell, and BNST (CeA: n=3 female, n=3 male; NAc: n=3 female, n=4 male; BNST: n=3 female, n=3 male) (Lemos et al. 2019).

Chapter III Supplementary Results

Local Fos plumes

Laser excitation of CRF-containing neurons in NAc ChR2 rats elevated local Fos expression surrounding optic fiber tips by 150-200% in Fos plumes of 0.22-0.36mm radius, over NAc eYFP control level at corresponding sites (Fig. 3.1). In CeA, ChR2 stimulation of CRF-containing neurons produced 150-200% elevated Fos plumes of 0.25–0.38mm radius, and in BNST produced 150-200% Fos plumes of 0.26-0.43mm radius (Fig. 3.2). These Fos plume sizes suggest that laser illumination of ChR2-infected CRF-containing neurons induced local zones of neural activation ~0.6-0.8mm in all three structures. Therefore 0.7mm diameter size was used for placement symbols in localization-of-function maps (Fig. 3.1).

Fluorescent in situ hybridization

The number of cells expressing either Cre+ mRNA or *Crh*+ mRNA (containing >5 particles) were counted in core sample volumes (0.1mm x 0.1mm x 17μm; placed to contain at least 1 *Crh*+ expressing cell) of tissue in CeA, NAc shell, and BNST (CeA: n=3 female, n=3 male; NAc: n=3 female, n=3 male; BNST: n=3 female, n=3 male) (Lemos et al. 2019). In CeA, CRF-containing neurons and Cre-expressing neurons were densely concentrated within the lateral division of CeA (CeL), with an average density of 10.1±0.9 co-labeled Cre+/CRF neurons in a 0.1mm x 0.1mm area. CRF-containing neurons made up 31.3% of neurons sampled within the CeL, with an average of 10.5±1.0 Cre+ and 10.6±1.0 CRF+ neurons per box. Similar densities were seen in females (34.0%) and in males (29.8%). Non-specific Cre+ expression was not typically observed as 96.4% of Cre+ neurons in CeA were co-labeled with *Crh* mrRNA, and Cre+ mRNA was present in 95.3% of CRF mRNA-containing neurons (Fig. 3.3).

In NAc, CRF-containing neurons were sparsely distributed throughout the rostro-caudal axis of medial shell (+2.52 to +1.08mm AP). The density of Cre+/CRF+ neurons in NAc shell was 6.0±0.7 cells per 0.1mm x 0.1mm box, or approximately half that of CeA density. NAc CRF-containing neurons made up 18.7% of neurons present in sample boxes, with an average of 6.3±0.7 Cre+ and 6.9±0.7 CRF+ neurons per box. Similar CRF+ mRNA expression was seen in the rostral (19.0% of neurons) and caudal (18.2%) accumbens shell. Similar densities were seen

in females (18.4%) and in males (19.0%). Significant non-specific Cre+ expression was not observed, with 95.3% of Cre mRNA+ neurons also containing CRF mRNA, and 87.1% of CRF mRNA+ neurons also were Cre mRNA+.

In BNST, neurons expressing CRF mRNA+ were distributed throughout the dorsolateral BNST 1-3 slices per rat) with an average density of 10.0±0.7 co-labeled Cre+/CRF neurons per 0.1x0.1mm box, similar as in CeA. BNST CRF-containing neurons made up 23.2% of neurons sampled within the dorsolateral BNST, with an average of 11.0±0.9 Cre+ and 10.4±0.7 CRF+ neurons per box. Substantial non-specific Cre+ expression was not observed as 90.1% of Cre+ neurons were co-labeled with CRF mrRNA, and Cre+ mRNA was present in 95.7% of CRF mRNA-containing neurons. Similar densities were seen in females (19.7%) and in males (27.6%).

Further analysis of potential sex differences for NAc & CeA groups

Females and males both showed similar stimulation-induced incentive effects in NAc & CeA ChR2 groups on sucrose two-choice, sucrose breakpoint, and laser self-stimulation tests, but the N's of sex groups within each structure were too small for statistical comparison. Therefore, it seemed of interest to further combine data from the two structures, and to statistically compare females vs males for combined CeA and NAc groups (n=9 *Crh*-Cre+ ChR2 females, n=11 *Crh*-Cre+ ChR2 males). A power analysis based on our observed laser CRF-containing neuron ChR2 incentive effect sizes of 0.379 – 0.865 (partial η^2) in two-choice, breakpoint, and self-stimulation results, indicated that groups of 2-4 of each sex would be required to achieve actual power of 0.97 – 0.99. Similarly, a related power analysis based CRF-related sex differences in a recent study (Piccin and Contarino 2020), indicated that groups of n=6 of each sex would be required for actual power of 0.98. Our combined CeA/NAc sex groups at least exceeded these minimum N sizes.

In the two-choice sucrose test (laser effect size, partial $\eta^2 = 0.865$), female (n=7) and male (n=10) ChR2 rats did not differ in their strength of laser-induced preference for *Laser+Sucrose* over *Sucrose-alone* ($F_{1,15} = 1.06$, $p = 0.319$; CeA & NAc females = 9:1±1 ratio preference for *Laser+Sucrose* (452 ± 55 presses) over *Sucrose-alone* (57 ± 18); males = 8:1±1 ratio preference for *Laser+Sucrose* (386 ± 46 responses) over *Sucrose-alone*: 46 ± 15). Female

and male ChR2 rats also did not differ in overall lever-pressing in the two-choice task ($F_{1,15}$ = 0.545, p = 0.472).

In the progressive ratio test of sucrose motivation for CeA/NAc ChR2 rats (laser effect size, partial η^2 = 0.832), females and males did not differ in magnitude of enhancement of incentive motivation, both showing roughly 200% laser-induced increases in effort breakpoint (*Laser+Sucrose* females: 91 ± 10 breakpoint, n=6; males: 113 ± 9, n=7; *Sucrose alone* females: 44 ± 10; males: 56 ± 9; $F_{1,11}$ = 0.837, p = 0.380). There was also no apparent sex difference in effort breakpoints achieved during progressive ratio regardless of laser effects ($F_{1,11}$ = 1.961, p = 0.189).

In the spout-touch self-stimulation task (laser effect size, partial η^2 = 0.830), female (n=7) and male (n=7) *Crh*-Cre+ ChR2 rats did not differ in their number of *Laser-spout* self-stimulations (female = 17 ± 4 self-stimulations; male = 18 ± 4; $F_{1,12}$ = 0.12, p = 0.915). Females and males also did not differ in their pattern of touches across the two spouts (*Inactive spout* touches: female = 7±3; male = 9±3; $F_{1,12}$ = 0.167, p = 0.690). In the place-based self-stimulation task laser effect size, partial η^2 = 0.379), female and male *Crh*-Cre+ ChR2 rats did not differ in their preference for the *Laser-delivering* chamber (females: 210% more time in *Laser-delivering* chamber than in *No-laser* chamber, n=7; males: 170%, n=7; $F_{1,12}$ = 0.269, p = 0.613). There were no sex differences in time spent in each chamber (females = 547±73 seconds in *Laser-delivering* chamber: 255±43 sec in *No-laser* chamber; males = 519±74 sec in *Laser-delivering* chamber, 301±43 in *No-laser* chamber; $F_{1,12}$ = 0.34, p = 0.857).

We recognize that anatomical and behavioral sex differences have been reported in CRF systems, for example in extended amygdala and NAc (Agoglia et al. 2020; Bale and Vale 2003; Bangasser and Wiersielis 2018; Connelly and Unterwald 2020; Piccin and Contarino 2020; Salvatore et al. 2018; Torres et al. 2015; Uchida et al. 2019; Uribe et al. 2020; Valentino et al. 2013; Weathington et al. 2014; Wiersielis et al. 2016). However, our current data suggest incentive enhancement effects of ChR2 laser stimulation for CeA *Crh*-Cre+ and NAc *Crh*-Cre+ groups were similar for both females and males here, with roughly comparable magnitudes in both sexes. We acknowledge that future studies with larger groups could potentially find subtle sex differences for these CRF ChR2 effects in future, but we conclude that the categorical effects for positively-valenced vs negatively-valenced motivation induced by CRF-containing neuronal stimulation in CeA, NAc and BNST described here appear robust and shared across sexes.

Figures

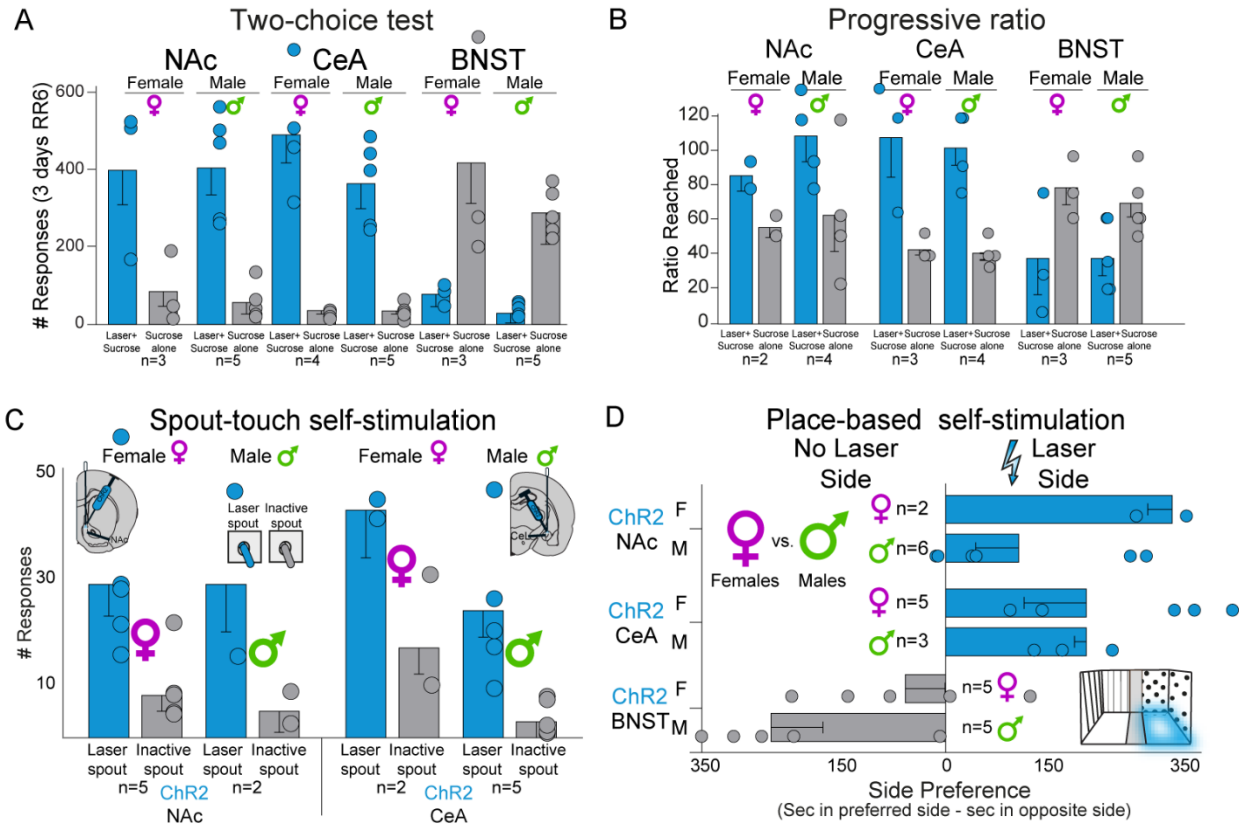

A.1 Female and male groups across behavioral tests
A) On average, male and female rats demonstrated similar levels of Laser+Sucrose preference in the two-choice test (NAc: n=3 female, 5:1 ratio preference; n=5 male, 7:1 ratio; CeA: n=4 female, 13:1 ratio; n=5 male, 10:1 ratio), while on average male BNST rats displayed a stronger opposite ratio preference for the Sucrose-alone option (n=5, 10:1 ratio) than female BNST rats (n=3 female, 5:1 ratio). **B)** On average in NAc (n=2 female, n=4 male) and CeA (n=3 female, n=4 male) groups, both female and male rats displayed ~200% increases in Laser+Sucrose breakpoint effort. In BNST groups, female (n=3) and male (n=5) rats showed similar ~50% suppression in Laser+Sucrose breakpoint effort. **C)** In the spout-touch task, laser self-stimulations were similar for NAc rats (n=5 female, n=2 male; days 2-3, 10Hz and 40Hz combined), though the small group of female CeA ChR2 rats (n=2) on average self-stimulated more than male CeA rats (n=5). **D)** On average, the small group of female NAc rats (n=2) displayed slightly higher levels of place-based self-stimulation than male NAc rats (n=6), and male BNST ChR2 rats showed a stronger laser-avoidance on average (n=5 female; n=5 male). However, these small samples are not properly powered to detect meaningful sex differences across regions. Means and SEM reported.

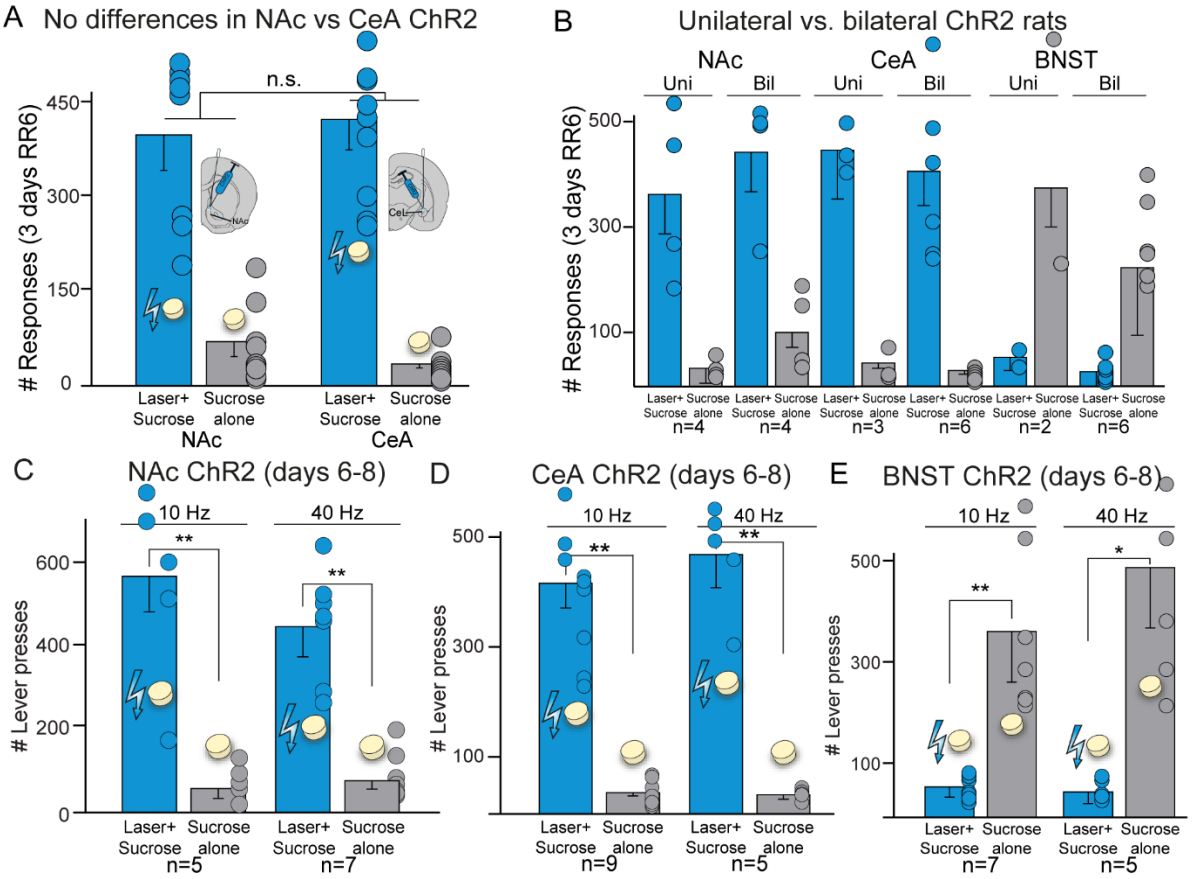

A.2 Two-choice extended data

A) When comparing incentive motivational effects on sucrose preference between brain regions, there was no difference in laser bias for NAc and CeA ChR2 rats in the two-choice task (mixed-model ANOVA, laser x group interaction, $F_{1,15} = 0.757$, $p = 0.398$) or total number of Laser+Sucrose lever presses induced by ChR2 pairings (two-way unpaired t-test, $t_{15} = 0.649$, $p = 0.526$). **B)** On average rats receiving unilateral ChR2 CRF-containing neuron excitation (NAc: n=4; CeA: n=3; BNST: n=2) demonstrated similar laser-preference as those receiving bilateral excitation (NAc: n=4; CeA: n=6; BNST: n=6), though groups were too small to detect possible differences. **C)** Both 10Hz and 40Hz ChR2 excitation caused similar preference for Laser+Sucrose with no differences between frequencies for NAc laser-effects (10Hz: $F_{1,4} = 24.540$, $p = 0.008$, n=5; 40Hz: $F_{1,6} = 39.209$, $p = 0.001$, n=7; frequency x laser interaction: $F_{1,10} = 1.186$, $p = 0.302$), or **D)** CeA ChR2 laser-preferences (10Hz: $F_{1,8} = 59.101$, $p<0.001$, n=9; 40Hz: $F_{1,4} = 90.572$, $p = 0.001$, n=5; frequency x laser interaction: $F_{1,12} = 0.534$, $p = 0.479$). **E)** BNST ChR2 excitation during 3 days of RR6 showed similar Laser+Sucrose avoidance at both 10Hz ($F_{1,6} = 30.241$, $p = 0.002$, n=7) and 40Hz ($F_{1,4} = 9.474$, $p = 0.037$, n=5), with no differences between frequencies ($F_{1,10} = 0.996$, $p = 0.342$). Means and SEM reported. n.s., nonsignificant

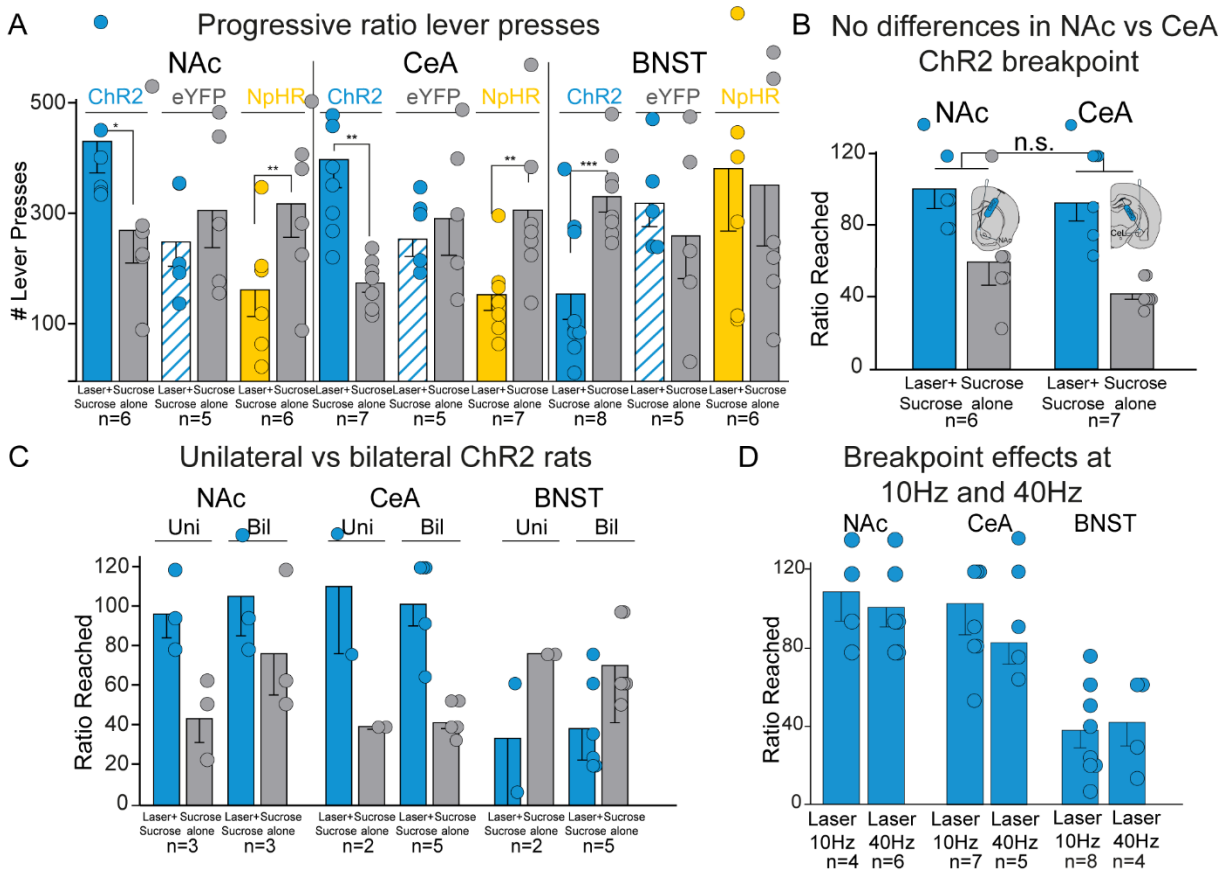

A.3 Progressive ratio extended data

A) NAc and CeA ChR2 animals pressed more for Laser+Sucrose than Sucrose-alone (two-way paired t-test, NAc: $t_5 = 4.015$, $p = 0.010$, 95% CI: [58,234], $d = 1.6$, n=6; CeA: $t_6 = 4.959$, $p = 0.003$, 95% CI: [113,333], $d = 2.48$, n=7), while BNST ChR2 rats responded at higher rates on the Sucrose alone day (two-way paired t-test, $t_7 = 6.178$, $p < 0.001$, 95% CI: [109,243], $d = 2.75$, n=8). eYFP rats responded equally between days across groups (two-way paired t-test, NAc: $t_4 = 0.788$, $p = 0.475$, n=5; CeA: $t_4 = 0.453$, $p = 0.673$, n=5; BNST: $t_4 = 0.506$, $p = 0.640$, n=5). CeA NpHR rats pressed less on the Laser+Sucrose day (two-way paired t-test, $t_6 = 4.631$, $p = 0.004$, 95% CI: [72,231], $d = 2.44$, n=7), as did NAc NpHR rats (two-way paired t-test, $t_5 = 4.659$, $p = 0.006$, 95% CI: [69,239], $d = 2.04$, n=6). BNST NpHR rats responded equally across PR days (two-way paired t-test, $t_5 = 0.365$, $p = 0.730$, n=6). **B)** When comparing incentive effects in sucrose motivation between brain regions, NAc and CeA ChR2 rats demonstrated comparable levels of breakpoint enhancement from CRF-containing neuron excitation (mixed-model ANOVA, laser x group interaction, $F_{1,11} = 0.010$, $p = 0.921$). **C)** On average rats that received unilateral ChR2 stimulation (NAc: n=3; CeA: n=2; BNST: n=2) demonstrated comparable laser-based effects on sucrose motivation as rats that bilateral ChR2 (NAc: n=3; CeA: n=5; BNST: n=5), though groups are too small to meaningfully compare effects. **D)** Both 10Hz ($t_3 = 4.841$, $p = 0.017$, n=4) and 40Hz ChR2 ($t_5 = 6.010$, $p = 0.002$, n=6) excitation in NAc caused ~200% enhancements of breakpoint effort for Laser+Sucrose. CeA ChR2 stimulation of CRF-containing neurons also caused ~200% increases in laser-paired breakpoint similarly at 10Hz ($t_6 = 4.992$, $p = 0.002$ n=7) or 40Hz ($t_4 = 4.3981$, $p = 0.012$, n=5). BNST ChR2 excitation during PR testing showed comparable ~50% reductions in laser-paired breakpoint at10Hz ($t_7 = 6.178$, $p<0.001$, n=8) and 40Hz ($t_3 = 5.333$, $p = 0.013$, n=4). Means and SEM reported. n.s., nonsignificant, *p<0.05, **p<0.01, ***p<0.001

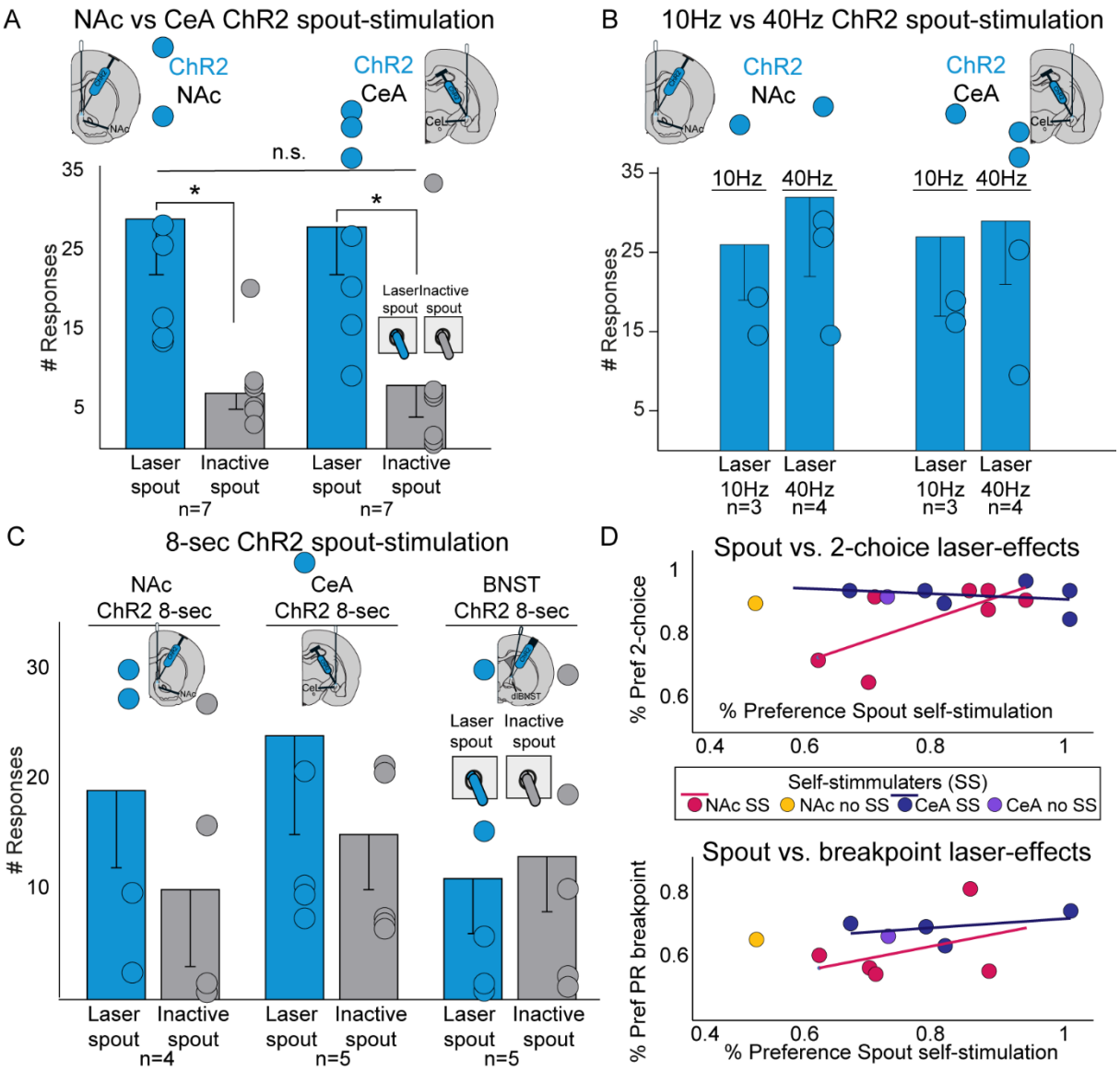

A.4 Spout self-stimulation extended data

A) There was no difference in the magnitude of self-stimulation between NAc (n=7) and CeA (n=7) ChR2 rats (days 2-3, 10Hz and 40Hz combined; laser x group interaction, $F_{1,12} = 0.002$, $p = 0.961$). **B)** Both 10Hz (NAc n=3; CeA n=3) and 40Hz (NAc n=4; CeA n=4) ChR2 excitation in NAc and CeA ChR2 self-stimulators caused similar self-stimulation for *Laser-spout* on average, though groups are underpowered to detect potential differences. **C)** A pilot experiment tested self-stimulation for 8-sec laser durations across ChR2 groups, though the present small pilot is not sufficiently powered to detect potential effects (10Hz and 40Hz, 2-3mW, 8-sec bins). **D)** Correlations between percent preference for *Laser-spout* in spout self-stimulation task and percent preference or percent enhancements for *Laser+Sucrose* lever in two-choice and progressive ratio tasks. Correlations and lines depict data only from rats designated as self-stimulators, while non-self-stimulating individuals are depicted for comparison. Means and SEM reported. n.s., nonsignificant *p<0.05

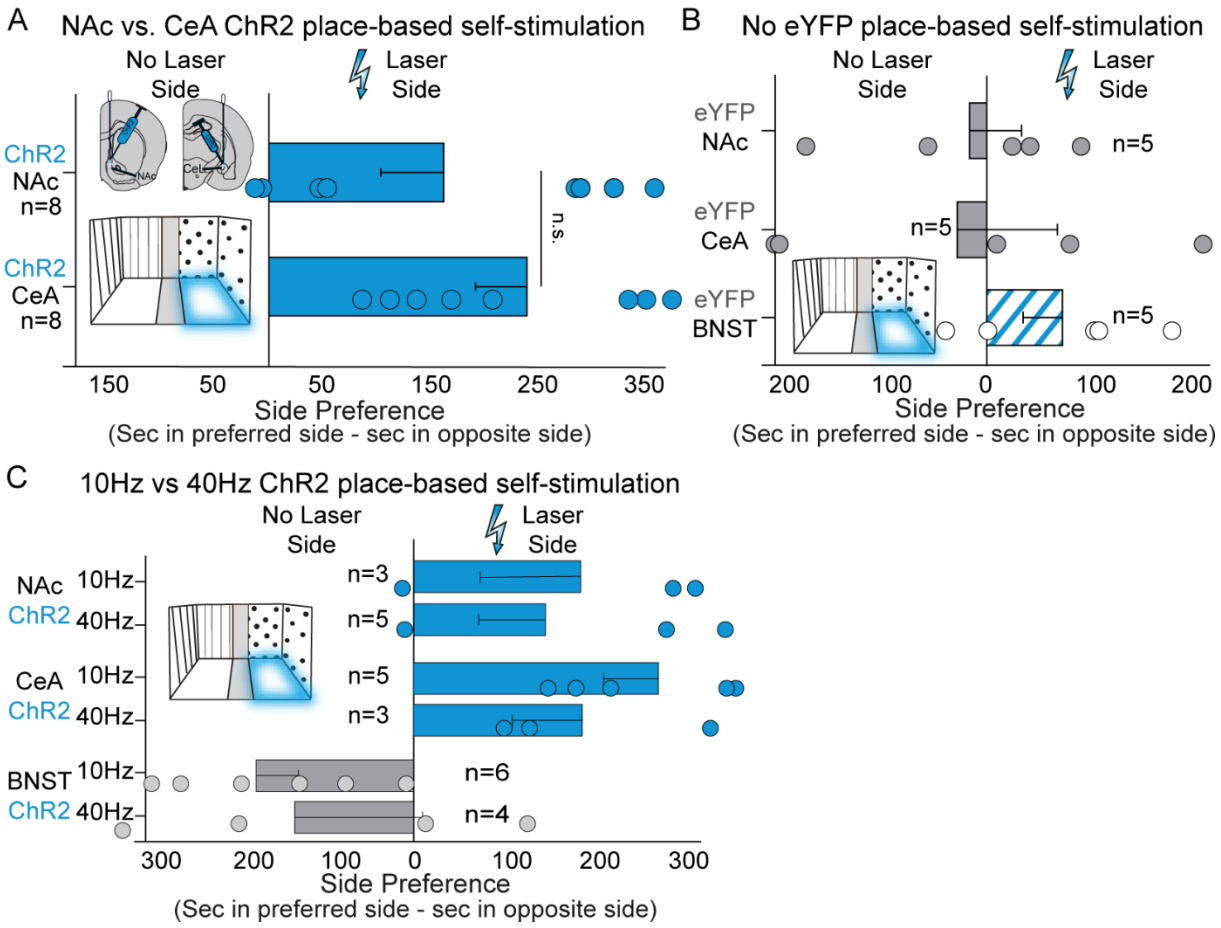

A.5 Place-based self-stimulation extended data

A) Both NAc ChR2 and CeA ChR2 sites supported comparable levels of place-based self-stimulation of CRF-containing neurons (laser x group, $F_{1,14} = 0.028$, $p = 0.871$). **B)** No significant laser-preference or avoidance was present for eYFP rats (main effect of laser, NAc: $F_{1,4} = 0.113$, $p = 0.754$, n=5; CeA: $F_{1,4} = 0.086$, $p = 0.784$, n=5; BNST: $F_{1,4} = 3.726$, $p = 0.126$, n=5). **C)** Both 10Hz and 40Hz ChR2 excitation in NAc caused similar levels of self-stimulation, causing ~150% increases on average in time spent in the *Laser-delivering* chamber at 10Hz (n=3) and 40Hz (n=5). CeA ChR2 self-stimulation across frequencies was on average stronger at 10Hz frequency (n=5; 200±10% increase) than 40Hz (n=3; 150±25% increase), though groups are not properly powered to detect meaningful differences. *Laser-delivering* chamber avoidance was present in rats receiving BNST CRF-neuron excitation at both laser frequencies tested (n=6 10Hz, n=4 40Hz) causing ~50% decrease in time spent in *Laser-delivering* side on average in the current sample. Means and SEM reported. n.s., nonsignificant

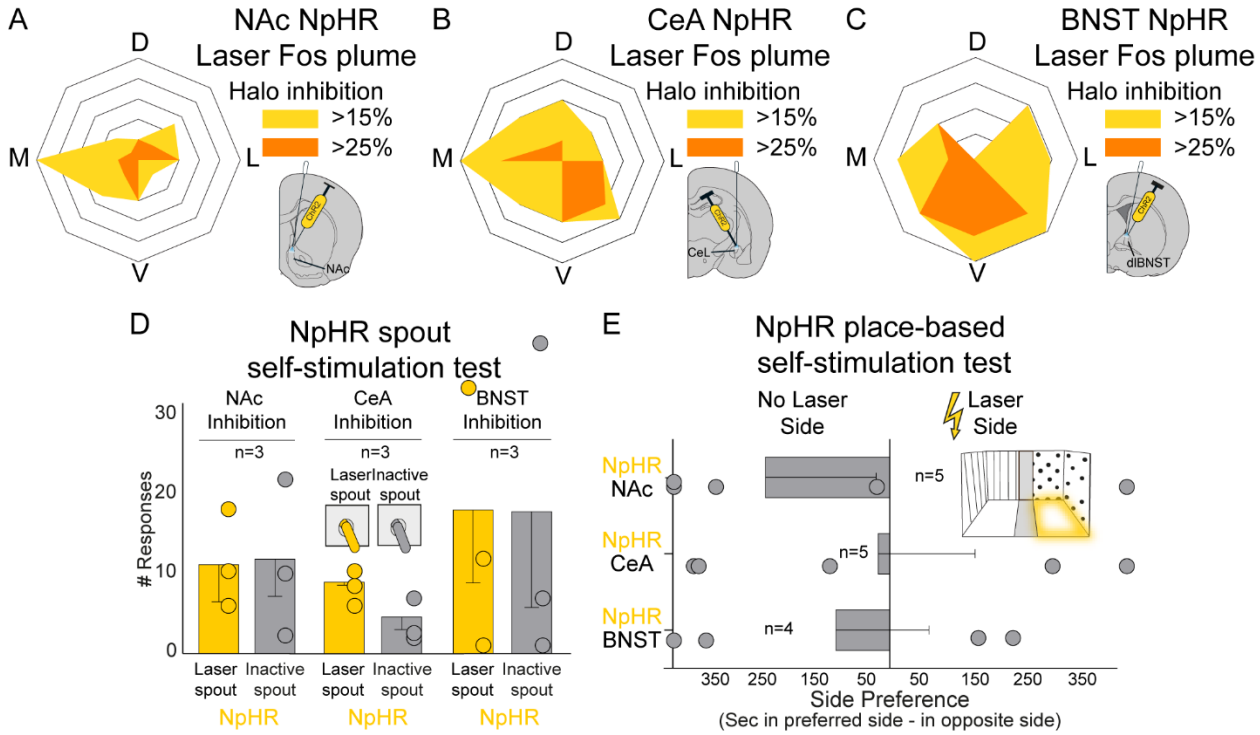

A.6 Halorhodopsin pilot data

A) Average Fos plume in *Crh*-Cre+ NpHR rats after laser inhibition targeting NAc CRF-expressing neurons (plumes of 0.11-0.22mm radius from fiber tip), **B)** CeA CRF-expressing neurons (plumes 0.08-0.16mm radius), and **C)** BNST CRF-expressing neurons (0.09-0.14mm radius; >15% suppression from eYFP control baseline: yellow; >25% suppression from eYFP: orange). D: dorsal, M: medial, L: lateral, V: ventral. **D)** NAc, CeA, and BNST NpHR pilot rats in the spout self-stimulation test responded minimally and equally between *Laser-spout* (8-10mW; constant; 8-sec) and *Inactive-spout*, though groups are underpowered to properly detect laser-effects (NAc n=3; CeA n=3; BNST n=3). **E)** Inhibition of CRF-expressing neurons in NAc (n=5), CeA (n=5), or BNST (n=4) NpHR rats does not support place-based self-stimulation or avoidance, at least in these current pilot groups. Means and SEM reported.

Tables

NAc CRF neurons	**Fos+ count**		**ChR2 vs. eYFP Unpaired t-test, p-value**		**Confidence Interval**	**Effect size**
Region	NAc ChR2 (n=6)	NAc eYFP (n=5)	*t*	*p*	95% CI	*d*
IF	58.5 ± 6.4	47.8 ± 2.7	0.68	*0.52*		
OFC	64.2 ± 1.8	54.2 ± 9.4	0.37	*0.72*		
NAcC	87.7 ± 3.8	49.4 ± 2.7	7.89	*<0.001**	27, 49	*5.06*
aVP	62.7 ± 1.4	36.4 ± 3.6	7.29	*<0.001**	18, 34	*4.61*
pVP	68.6± 1.7	28.0 ± 2.4	13.56	*<0.001**	34, 48	*8.73*
aBNST	60.0 ± 1.9	36.6 ± 2.7	6.66	*<0.001*	15, 31	*4.25*
pBNST	84.6 ± 3.4	39.4 ± 2.7	10.48	*<0.001**	35, 55	*6.45*
aLH	65.7 ± 2.9	36.2 ± 1.7	8.37	*<0.001**	21, 37	*5.46*
pLH	67.2 ± 3.3	30.4 ± 2.5	8.62	*<0.001**	27, 46	*5.41*
PVN	58.5 ± 3.5	49.6 ± 3.1	1.87	*0.10*		
MeA	66.8 ± 4.2	34.8 ± 3.8	5.58	*<0.001**	19, 45	*3.42*
CeA	65.2 ± 3.3	30.6 ± 1.3	9.00	*<0.001**	26, 43	*6.29*
BLA	44.8 ± 4.6	40.7 ± 4.3	0.34	*0.74*		
VTA	56.0 ± 1.2	27.8 ± 3.0	9.27	*<0.001**	21, 35	*5.76*
SN	32.2 ± 3.2	25.6 ± 5.0	1.15	*0.28*		
PAG	52.3 ± 3.6	40.6 ± 4.9	1.97	*0.08*		
CeA CRF neurons	**Fos+ count**		**ChR2 vs. eYFP Unpaired t-test, p-value**		**Confidence Interval**	**Effect size**
Region	CeA ChR2 (n=6)	CeA eYFP (n=5)	*t*	*p*	95% CI	*d*
IF	52.0 ± 4.9	39.4 ± 2.2	2.18	*0.057*		
OFC	71.2 ± 4.6	46.4 ± 2.1	4.52	*0.001*	12, 37	*3.12*
aNAcSh	63.3 ± 3.5	37.2 ± 1.7	6.28	*<0.001**	17, 36	*4.21*
pNAcSh	90.0 ± 8.7	35.2 ± 4.2	5.28	*0.001**	31, 78	*3.56*

NAcC	95.8 ± 9.6	25.8 ± 6.8	5.72	*<0.001**	43, 98	*3.62*
aVP	61.0 ± 2.3	28.2 ± 2.0	10.65	*<0.001**	36, 40	*6.62*
pVP	62.0 ± 2.4	29.2 ± 2.1	10.02	*<0.001**	25, 40	*6.19*
aBNST	85.7 ± 6.1	28.8 ± 2.0	8.17	*<0.001**	41, 73	*5.90*
pBNST	104.3± 7.0	41.6 ± 5.0	6.97	*<0.001**	42, 83	*4.41*
aLH	55.3 ± 2.7	27.6 ± 4.1	5.86	*<0.001**	17, 38	*4.20*
pLH	53.7 ± 2.0	30.6 ± 0.6	9.93	*<0.001**	18, 28	*7.33*
PVN	65.2± 10.3	51.4 ± 6.1	1.09	*0.30*		
MeA	60.5 ± 2.6	32.2 ± 3.3	6.82	*<0.001**	19, 38	*4.13*
BLA	54.5 ± 3.1	37.0 ± 6.3	2.65	*0.027**	3, 32	*1.62*
VTA	55.2 ± 7.0	33.6 ± 2.4	2.72	*0.023**	4, 40	*1.94*
SN	34.2 ± 4.2	29.6 ± 2.3	0.90	*0.39*		
PAG	47.7 ± 3.1	47.6 ± 2.0	0.02	*0.99*		

BNST CRF neurons	**Fos+ count**		**ChR2 vs. eYFP Unpaired t-test, p-value**		**Confidence Interval**	**Effect size**
Region	BNST ChR2 (n=5)	BNST eYFP (n=4)	*t*	*p*	95% CI	*d*
IF	53.6 ± 6.2	47.5 ± 3.1	0.81	*0.45*		
OFC	64.0 ± 7.7	49.5 ± 4.9	1.49	*0.18*		
aNAcSh	65.0 ± 5.0	47.5 ± 5.9	2.28	*0.056*		
pNAcSh	68.6 ± 7.2	47.8 ± 1.9	2.50	*0.041**	1, 41	*2.08*
NAcC	74.6 ± 5.6	43.3 ± 2.5	4.69	*0.002**	16, 47	*3.58*
aVP	47.8 ± 5.8	33.8 ± 4.6	1.69	*0.13*		
pVP	63.2 ± 2.5	37.8 ± 0.86	8.752	*<0.001**	19, 32	*7.06*
aLH	67.8 ± 1.2	34.3 ± 1.5	17.44	*<0.001**	29, 38	*11.6*
pLH	65.4 ± 2.5	34.5 ± 2,6	8.49	*<0.001**	22, 40	*5.72*
PVN	73.8 ± 2.8	36.5 ± 1.6	10.74	*<0.001**	29, 46	*7.94*
MeA	72.4 ± 6.3	45.0 ± 4.0	3.45	*0.011**	9, 46	*2.49*
CeA	42.6 ± 3.9	29.0 ± 2.5	2.79	*0.03**	2, 25	*1.95*
BLA	72.0 ± 2.8	38.3 ± 2.1	9.26	*<0.001**	25, 42	*6.48*

VTA	43.8 ± 5.4	41.8 ± 3.6	0.30	*0.77*		
SN	41.0 ± 1.9	34.5 ± 2.5	2.07	*0.077*		
PAG	71.0 ± 2.4	40.8 ± 5.0	5.84	*0.001**	18, 42	*3.92*

A.1 Brain-wide Fos activation from CRF system excitation in NAc, CeA, or BNST
Table shows Fos+ protein quantification in mesocorticolimbic regions after final exposure to ChR2 excitation in NAc (top; n=3 female, n=3 male ChR2 group), CeA (middle; n=3 female, n=3 male ChR2 group), or BNST (below; n=2 female, n=3 male ChR2 group). Fos+ protein quantification in mesocorticolimbic regions (left columns), for ChR2 rats and eYFP rats. "Fos+ Count" reflects mean of each group at each site ± standard error (SEM). Two-sided unpaired t-tests between ChR2 and eYFP rats were performed for each target group (NAc, CeA, or BNST). Also see Fig. 3.4. IF, infralimbic cortex; OFC, orbitofrontal cortex; aNAcSh, anterior nucleus accumbens shell; pNAcSh, posterior nucleus accumbens shell; NAcC, nucleus accumbens core; aVP, anterior ventral pallidum; pVP, posterior ventral pallidum; aBNST, anterior bed nucleus of stria terminalis; pBNST, posterior bed nucleus of stria terminalis; aLH, anterior lateral hypothalamus; pLH, posterior lateral hypothalamus; PVN, hypothalamic paraventricular nucleus; MeA, medial amygdala; CeA, central amygdala; BLA, basolateral amygdala; VTA, ventral tegmentum; SN, substantia nigra; PAG, midbrain periaqueductal gray. *p<0.05, **p<0.01, ***p<0.001

References

Abi-Dargham A, Gil R, Krystal J, Baldwin RM, Seibyl JP, Bowers M, et al. Increased striatal dopamine transmission in schizophrenia: confirmation in a second cohort. Am J Psychiatry. 1998 Jun;155(6):761–767.

Agoglia AE, Tella J, Herman MA. Sex differences in corticotropin releasing factor peptide regulation of inhibitory control and excitability in central amygdala corticotropin releasing factor receptor 1-neurons. Neuropharmacology. 2020 Dec 1;180:108296.

Alheid GF. Extended amygdala and basal forebrain. Ann N Y Acad Sci. 2003 Apr;985:185–205.

Alheid GF, Heimer L. New perspectives in basal forebrain organization of special relevance for neuropsychiatric disorders: the striatopallidal, amygdaloid, and corticopetal components of substantia innominata. Neuroscience. 1988 Oct;27(1):1–39.

Annis HM, Graham JM. Profile types on the Inventory of Drinking Situations: Implications for relapse prevention counseling. Psychol Addict Behav. 1995 Sep;9(3):176–182.

Asok A, Draper A, Hoffman AF, Schulkin J, Lupica CR, Rosen JB. Optogenetic silencing of a corticotropin-releasing factor pathway from the central amygdala to the bed nucleus of the stria terminalis disrupts sustained fear. Mol Psychiatry. 2018;23(4):914–922.

Asok A, Schulkin J, Rosen JB. Corticotropin releasing factor type-1 receptor antagonism in the dorsolateral bed nucleus of the stria terminalis disrupts contextually conditioned fear, but not unconditioned fear to a predator odor. Psychoneuroendocrinology. 2016 Apr 28;70:17–24.

Baldo BA, Gual-Bonilla L, Sijapati K, Daniel RA, Landry CF, Kelley AE. Activation of a subpopulation of orexin/hypocretin-containing hypothalamic neurons by GABAA receptor-mediated inhibition of the nucleus accumbens shell, but not by exposure to a novel environment. Eur J Neurosci. 2004 Jan;19(2):376–386.

Bale TL, Vale WW. Increased depression-like behaviors in corticotropin-releasing factor receptor-2-deficient mice: sexually dichotomous responses. J Neurosci. 2003 Jun 15;23(12):5295–5301.

Bals-Kubik R, Ableitner A, Herz A, Shippenberg TS. Neuroanatomical sites mediating the motivational effects of opioids as mapped by the conditioned place preference paradigm in rats. J Pharmacol Exp Ther. 1993 Jan;264(1):489–495.

Bangasser DA, Wiersielis KR. Sex differences in stress responses: a critical role for corticotropin-releasing factor. Hormones. 2018 Apr 16;

Baumgartner HM, Cole SL, Olney JJ, Berridge KC. Desire or Dread from Nucleus Accumbens Inhibitions: Reversed by Same-Site Optogenetic Excitations. J Neurosci. 2020 Mar 25;40(13):2737–2752.

Baumgartner HM, Schulkin J, Berridge KC. Activating corticotropin releasing factor (CRF) systems in nucleus accumbens, amygdala, and bed nucleus of stria terminalis: Incentive motivation or aversive motivation? Biol Psychiatry. 2021 Jan;

Becker JB. Sex differences in addiction. Dialogues Clin Neurosci. 2016;18(4):395–402.

Bernier NJ, Peter RE. Appetite-suppressing effects of urotensin I and corticotropin-releasing hormone in goldfish (Carassius auratus). Neuroendocrinology. 2001 Apr 1;73(4):248–260.

Berridge KC. Affective valence in the brain: modules or modes? Nat Rev Neurosci. 2019;20(4):225–234.

Berridge KC, Robinson TE. What is the role of dopamine in reward: hedonic impact, reward learning, or incentive salience? Brain Res Brain Res Rev. 1998 Dec 1;28(3):309–369.

Berridge KC, Robinson TE. Liking, wanting, and the incentive-sensitization theory of addiction. Am Psychol. 2016 Nov;71(8):670–679.

Bostwick JM, Hecksel KA, Stevens SR, Bower JH, Ahlskog JE. Frequency of new-onset pathologic compulsive gambling or hypersexuality after drug treatment of idiopathic Parkinson disease. Mayo Clin Proc. 2009 Apr;84(4):310–316.

Boyson CO, Holly EN, Shimamoto A, Albrechet-Souza L, Weiner LA, DeBold JF, et al. Social stress and CRF-dopamine interactions in the VTA: role in long-term escalation of cocaine self-administration. J Neurosci. 2014 May 7;34(19):6659–6667.

Breier A, Su TP, Saunders R, Carson RE, Kolachana BS, de Bartolomeis A, et al. Schizophrenia is associated with elevated amphetamine-induced synaptic dopamine concentrations: evidence from a novel positron emission tomography method. Proc Natl Acad Sci USA. 1997 Mar 18;94(6):2569–2574.

Broca P. Anatomie comparée des circonvolutions cérébrales. Le grand lobe limbique et la scissure limbique dans la série des mammifères. Rev Anthrop. 1978;

Bromberg-Martin ES, Hikosaka O. Midbrain dopamine neurons signal preference for advance information about upcoming rewards. Neuron. 2009 Jul 16;63(1):119–126.

Bruchas MR, Land BB, Lemos JC, Chavkin C. CRF1-R activation of the dynorphin/kappa opioid system in the mouse basolateral amygdala mediates anxiety-like behavior. PLoS One. 2009 Dec 31;4(12):e8528.

Carlezon WA, Thomas MJ. Biological substrates of reward and aversion: a nucleus accumbens activity hypothesis. Neuropharmacology. 2009;56 Suppl 1:122–132.

Carlezon WA, Wise RA. Rewarding actions of phencyclidine and related drugs in nucleus accumbens shell and frontal cortex. J Neurosci. 1996 May 1;16(9):3112–3122.

Carney MA, Armeli S, Tennen H, Affleck G, O'Neil TP. Positive and negative daily events, perceived stress, and alcohol use: a diary study. J Consult Clin Psychol. 2000 Oct;68(5):788–798.

Carroll ME, France CP, Meisch RA. Food deprivation increases oral and intravenous drug intake in rats. Science. 1979 Jul 20;205(4403):319–321.

Castro DC, Berridge KC. Opioid hedonic hotspot in nucleus accumbens shell: mu, delta, and kappa maps for enhancement of sweetness "liking" and "wanting". J Neurosci. 2014 Mar 19;34(12):4239–4250.

Castro DC, Berridge KC. Opioid and orexin hedonic hotspots in rat orbitofrontal cortex and insula. Proc Natl Acad Sci USA. 2017 Oct 24;114(43):E9125–E9134.

Castro DC, Bruchas MR. A Motivational and Neuropeptidergic Hub: Anatomical and Functional Diversity within the Nucleus Accumbens Shell. Neuron. 2019 May 8;102(3):529–552.

Ceaser AE, Barch DM. Striatal Activity is Associated with Deficits of Cognitive Control and Aberrant Salience for Patients with Schizophrenia. Front Hum Neurosci. 2015;9:687.

Cheer JF, Heien MLAV, Garris PA, Carelli RM, Wightman RM. Simultaneous dopamine and single-unit recordings reveal accumbens GABAergic responses: implications for intracranial self-stimulation. Proc Natl Acad Sci USA. 2005 Dec 27;102(52):19150–19155.

Childress AR, McLellan AT, Ehrman R, O'Brien CP. Classically conditioned responses in opioid and cocaine dependence: a role in relapse? NIDA Res Monogr. 1988;84:25–43.

Clark MM, Galef BG. Effects of rearing environment on adrenal weights, sexual development, and behavior in gerbils: an examination of Richter's domestication hypothesis. J Comp Physiol Psychol. 1980 Oct;94(5):857–863.

Cole SL, Robinson MJF, Berridge KC. Optogenetic self-stimulation in the nucleus accumbens: D1 reward versus D2 ambivalence. PLoS One. 2018 Nov 29;13(11):e0207694.

Connelly KL, Unterwald EM. Regulation of CRF mRNA in the Rat Extended Amygdala Following Chronic Cocaine: Sex Differences and Effect of Delta Opioid Receptor Agonism. Int J Neuropsychopharmacol. 2020 Feb 1;23(2):117–124.

Corbit LH, Muir JL, Balleine BW. The role of the nucleus accumbens in instrumental conditioning: Evidence of a functional dissociation between accumbens core and shell. J Neurosci. 2001 May 1;21(9):3251–3260.

Coric V, Feldman HH, Oren DA, Shekhar A, Pultz J, Dockens RC, et al. Multicenter, randomized, double-blind, active comparator and placebo-controlled trial of a corticotropin-releasing factor receptor-1 antagonist in generalized anxiety disorder. Depress Anxiety. 2010 May;27(5):417–425.

Covelo IR, Patel ZI, Luviano JA, Stratford TR, Wirtshafter D. Manipulation of GABA in the ventral pallidum, but not the nucleus accumbens, induces intense, preferential, fat consumption in rats. Behav Brain Res. 2014 Aug 15;270:316–325.

Dabrowska J, Hazra R, Guo J-D, Dewitt S, Rainnie DG. Central CRF neurons are not created equal: phenotypic differences in CRF-containing neurons of the rat paraventricular hypothalamus and the bed nucleus of the stria terminalis. Front Neurosci. 2013 Aug 30;7:156.

Dabrowska J, Martinon D, Moaddab M, Rainnie DG. Targeting Corticotropin-Releasing Factor Projections from the Oval Nucleus of the Bed Nucleus of the Stria Terminalis Using Cell-Type Specific Neuronal Tracing Studies in Mouse and Rat Brain. J Neuroendocrinol. 2016;28(12).

Dallman MF. Stress-induced obesity and the emotional nervous system. Trends Endocrinol Metab. 2010 Mar;21(3):159–165.

Dallman MF, Pecoraro N, Akana SF, La Fleur SE, Gomez F, Houshyar H, et al. Chronic stress and obesity: a new view of “comfort food”. Proc Natl Acad Sci USA. 2003 Sep 30;100(20):11696–11701.

Davis C, Carter JC. Compulsive overeating as an addiction disorder. A review of theory and evidence. Appetite. 2009 Aug;53(1):1–8.

Davis KL, Kahn RS, Ko G, Davidson M. Dopamine in schizophrenia: a review and reconceptualization. Am J Psychiatry. 1991 Nov;148(11):1474–1486.

de Boer SF, van der Vegt BJ, Koolhaas JM. Individual variation in aggression of feral rodent strains: a standard for the genetics of aggression and violence? Behav Genet. 2003 Sep;33(5):485–501.

de Guglielmo G, Kallupi M, Pomrenze MB, Crawford E, Simpson S, Schweitzer P, et al. Central amygdala CRF pathways in alcohol dependence. BioRxiv. 2017 May 5;

de Guglielmo G, Kallupi M, Pomrenze MB, Crawford E, Simpson S, Schweitzer P, et al. Inactivation of a CRF-dependent amygdalofugal pathway reverses addiction-like behaviors in alcohol-dependent rats. Nat Commun. 2019 Mar 18;10(1):1238.

Devoto F, Zapparoli L, Bonandrini R, Berlingeri M, Ferrulli A, Luzi L, et al. Hungry brains: A meta-analytical review of brain activation imaging studies on food perception and appetite in obese individuals. Neurosci Biobehav Rev. 2018 Jul 30;94:271–285.

DiFeliceantonio AG, Berridge KC. Dorsolateral neostriatum contribution to incentive salience: opioid or dopamine stimulation makes one reward cue more motivationally attractive than another. Eur J Neurosci. 2016 Apr 3;43(9):1203–1218.

DiFeliceantonio AG, Mabrouk OS, Kennedy RT, Berridge KC. Enkephalin surges in dorsal neostriatum as a signal to eat. Curr Biol. 2012 Oct 23;22(20):1918–1924.

Dunlop BW, Binder EB, Iosifescu D, Mathew SJ, Neylan TC, Pape JC, et al. Corticotropin-Releasing Factor Receptor 1 Antagonism Is Ineffective for Women With Posttraumatic Stress Disorder. Biol Psychiatry. 2017 Dec 15;82(12):866–874.

Dunn AJ, Berridge CW. Physiological and behavioral responses to corticotropin-releasing factor administration: is CRF a mediator of anxiety or stress responses? Brain Res Brain Res Rev. 1990 Aug;15(2):71–100.

Echo JA, Lamonte N, Christian G, Znamensky V, Ackerman TF, Bodnar RJ. Excitatory amino acid receptor subtype agonists induce feeding in the nucleus accumbens shell in rats: opioid antagonist actions and interactions with μ-opioid agonists. Brain Res. 2001 Dec;921(1-2):86–97.

Epstein DH, Kennedy AP, Furnari M, Heilig M, Shaham Y, Phillips KA, et al. Effect of the CRF1-receptor antagonist pexacerfont on stress-induced eating and food craving. Psychopharmacology. 2016 Dec;233(23-24):3921–3932.

Erb S, Brown ZJ. A role for corticotropin-releasing factor in the long-term expression of behavioral sensitization to cocaine. Behav Brain Res. 2006 Sep 25;172(2):360–364.

Erb S, Petrovic A, Yi D, Kayyali H. Central injections of CRF reinstate cocaine seeking in rats after postinjection delays of up to 3 h: an influence of time and environmental context. Psychopharmacology. 2006 Jul;187(1):112–120.

Erb S, Salmaso N, Rodaros D, Stewart J. A role for the CRF-containing pathway from central nucleus of the amygdala to bed nucleus of the stria terminalis in the stress-induced reinstatement of cocaine seeking in rats. Psychopharmacology. 2001 a Dec;158(4):360–365.

Erb S, Shaham Y, Stewart J. Stress-induced relapse to drug seeking in the rat: role of the bed nucleus of the stria terminalis and amygdala. Stress. 2001 b Dec;4(4):289–303.

Fadok JP, Krabbe S, Markovic M, Courtin J, Xu C, Massi L, et al. A competitive inhibitory circuit for selection of active and passive fear responses. Nature. 2017 Feb 2;542(7639):96–100.

Faure A, Richard JM, Berridge KC. Desire and dread from the nucleus accumbens: cortical glutamate and subcortical GABA differentially generate motivation and hedonic impact in the rat. PLoS One. 2010 Jun 18;5(6):e11223.

Fudge JL, Emiliano AB. The extended amygdala and the dopamine system: another piece of the dopamine puzzle. J Neuropsychiatry Clin Neurosci. 2003;15(3):306–316.

Funk CK, O'Dell LE, Crawford EF, Koob GF. Corticotropin-releasing factor within the central nucleus of the amygdala mediates enhanced ethanol self-administration in withdrawn, ethanol-dependent rats. J Neurosci. 2006 Nov 1;26(44):11324–11332.

Funk CK, Zorrilla EP, Lee M-J, Rice KC, Koob GF. Corticotropin-releasing factor 1 antagonists selectively reduce ethanol self-administration in ethanol-dependent rats. Biol Psychiatry. 2007 Jan 1;61(1):78–86.

Gearhardt AN, Yokum S, Orr PT, Stice E, Corbin WR, Brownell KD. Neural correlates of food addiction. Arch Gen Psychiatry. 2011 Aug;68(8):808–816.

Giardino WJ, Eban-Rothschild A, Christoffel DJ, Li S-B, Malenka RC, de Lecea L. Parallel circuits from the bed nuclei of stria terminalis to the lateral hypothalamus drive opposing emotional states. Nat Neurosci. 2018 Jul 23;21(8):1084–1095.

Gray TS, Magnuson DJ. Peptide immunoreactive neurons in the amygdala and the bed nucleus of the stria terminalis project to the midbrain central gray in the rat. Peptides. 1992 Jun;13(3):451–460.

Grieder TE, Herman MA, Contet C, Tan LA, Vargas-Perez H, Cohen A, et al. VTA CRF neurons mediate the aversive effects of nicotine withdrawal and promote intake escalation. Nat Neurosci. 2014 Dec;17(12):1751–1758.

Grillon C, Hale E, Lieberman L, Davis A, Pine DS, Ernst M. The CRH1 antagonist GSK561679 increases human fear but not anxiety as assessed by startle. Neuropsychopharmacology. 2015 Mar 13;40(5):1064–1071.

Grilo CM, Pagano ME, Stout RL, Markowitz JC, Ansell EB, Pinto A, et al. Stressful life events predict eating disorder relapse following remission: six-year prospective outcomes. Int J Eat Disord. 2012 Mar;45(2):185–192.

Haber SN, Knutson B. The reward circuit: linking primate anatomy and human imaging. Neuropsychopharmacology. 2010 Jan;35(1):4–26.

Hartston H. The case for compulsive shopping as an addiction. J Psychoactive Drugs. 2012 Mar;44(1):64–67.

Heimer L, Van Hoesen GW. The limbic lobe and its output channels: implications for emotional functions and adaptive behavior. Neurosci Biobehav Rev. 2006;30(2):126–147.

Heimer L, Van Hoesen GW, Trimble M, Zahm DS. Anatomy of Neuropsychiatry: The New Anatomy of the Basal Forebrain and Its Implications for Neuropsychiatric Illness. Academic Press; 2007.

Heimer L, Zahm DS, Churchill L, Kalivas PW, Wohltmann C. Specificity in the projection patterns of accumbal core and shell in the rat. Neuroscience. 1991;41(1):89–125.

Heinrichs SC, Joppa M. Dissociation of arousal-like from anxiogenic-like actions of brain corticotropin-releasing factor receptor ligands in rats. Behav Brain Res. 2001 Jul;122(1):43–50.

Heinrichs SC, Menzaghi F, Schulteis G, Koob GF, Stinus L. Suppression of corticotropin-releasing factor in the amygdala attenuates aversive consequences of morphine withdrawal. Behav Pharmacol. 1995 Jan;6(1):74???80.

Hellberg SN, Russell TI, Robinson MJF. Cued for risk: Evidence for an incentive sensitization framework to explain the interplay between stress and anxiety, substance abuse, and reward uncertainty in disordered gambling behavior. Cogn Affect Behav Neurosci. 2019;19(3):737–758.

Henckens MJAG, Deussing JM, Chen A. Region-specific roles of the corticotropin-releasing factor-urocortin system in stress. Nat Rev Neurosci. 2016 Sep 2;17(10):636–651.

Herdegen T, Leah JD. Inducible and constitutive transcription factors in the mammalian nervous system: control of gene expression by Jun, Fos and Krox, and CREB/ATF proteins. Brain Res Brain Res Rev. 1998 Dec;28(3):370–490.

Herrick CJ. Neurological' ' foundations of animal behavior. Brains' ' of rats and men. Chicago: University of Chicago Press; 1926. p. 382.

Horger BA, Shelton K, Schenk S. Preexposure sensitizes rats to the rewarding effects of cocaine. Pharmacology Biochemistry and Behavior. 1990 Dec;37(4):707–711.

Hostetler CM, Ryabinin AE. The CRF system and social behavior: a review. Front Neurosci. 2013 May 31;7:92.

Howes OD, Kapur S. The dopamine hypothesis of schizophrenia: version III--the final common pathway. Schizophr Bull. 2009 May;35(3):549–562.

Howes OD, Montgomery AJ, Asselin M-C, Murray RM, Valli I, Tabraham P, et al. Elevated striatal dopamine function linked to prodromal signs of schizophrenia. Arch Gen Psychiatry. 2009 Jan;66(1):13–20.

Hull CL. Essentials of behavior. 1951;

Humphries MD, Prescott TJ. The ventral basal ganglia, a selection mechanism at the crossroads of space, strategy, and reward. Prog Neurobiol. 2010 Apr;90(4):385–417.

Hupalo S, Bryce CA, Bangasser DA, Berridge CW, Valentino RJ, Floresco SB. Corticotropin-Releasing Factor (CRF) circuit modulation of cognition and motivation. Neurosci Biobehav Rev. 2019 Jun 15;103:50–59.

Iemolo A, Blasio A, St Cyr SA, Jiang F, Rice KC, Sabino V, et al. CRF-CRF1 receptor system in the central and basolateral nuclei of the amygdala differentially mediates excessive eating of palatable food. Neuropsychopharmacology. 2013 Nov;38(12):2456–2466.

Itoga CA, Chen Y, Fateri C, Echeverry PA, Lai JM, Delgado J, et al. New viral-genetic mapping uncovers an enrichment of corticotropin-releasing hormone-expressing neuronal inputs to the nucleus accumbens from stress-related brain regions. J Comp Neurol. 2019 Oct 15;527(15):2474–2487.

Jo YS, Namboodiri VMK, Stuber GD, Zweifel LS. Persistent activation of central amygdala CRF neurons helps drive the immediate fear extinction deficit. Nat Commun. 2020 Jan 22;11(1):422.

Jongen-Rělo AL, Groenewegen HJ, Voorn P. Evidence for a multi-compartmental histochemical organization of the nucleus accumbens in the rat. J Comp Neurol. 1993 Nov 8;337(2):267–276.

Kalivas PW, Duffy P. Effect of acute and daily cocaine treatment on extracellular dopamine in the nucleus accumbens. Synapse. 1990;5(1):48–58.

Kalivas PW, Stewart J. Dopamine transmission in the initiation and expression of drug- and stress-induced sensitization of motor activity. Brain Res Brain Res Rev. 1991 Dec;16(3):223–244.

Kapur S. Psychosis as a state of aberrant salience: a framework linking biology, phenomenology, and pharmacology in schizophrenia. Am J Psychiatry. 2003 Jan;160(1):13–23.

Kapur S, Mizrahi R, Li M. From dopamine to salience to psychosis--linking biology, pharmacology and phenomenology of psychosis. Schizophr Res. 2005 Nov 1;79(1):59–68.

Kaundal P, Sharma I, Jha T. Assessment of psychosocial factors associated with relapse in patients with alcohol dependence: a retrospective observational study. Int J Basic Clin Pharmacol. 2016;969–974.

Kelley AE. Neural integrative activities of nucleus accumbens subregions in relation to learning and motivation. Psychobiology. 1999;

Kelley AE, Swanson CJ. Feeding induced by blockade of AMPA and kainate receptors within the ventral striatum: a microinfusion mapping study. Behav Brain Res. 1997 Dec;89(1-2):107–113.

Kelly PH. Unilateral 6-hydroxydopamine lesions of nigrostriatal or mesolimbic dopamine-containing terminals and the drug-induced rotation of rats. Brain Res. 1975 Dec 12;100(1):163–169.

Kessler RC, Petukhova M, Sampson NA, Zaslavsky AM, Wittchen H-U. Twelve-month and lifetime prevalence and lifetime morbid risk of anxiety and mood disorders in the United States. Int J Methods Psychiatr Res. 2012 Sep;21(3):169–184.

Kim J, Zhang X, Muralidhar S, LeBlanc SA, Tonegawa S. Basolateral to central amygdala neural circuits for appetitive behaviors. Neuron. 2017 Mar 22;93(6):1464–1479.e5.

Koo JW, Lobo MK, Chaudhury D, Labonté B, Friedman A, Heller E, et al. Loss of BDNF signaling in D1R-expressing NAc neurons enhances morphine reward by reducing GABA inhibition. Neuropsychopharmacology. 2014 Oct;39(11):2646–2653.

Koob GF. The role of CRF and CRF-related peptides in the dark side of addiction. Brain Res. 2010 Feb 16;1314:3–14.

Koob GF. Addiction is a Reward Deficit and Stress Surfeit Disorder. Front Psychiatry. 2013 Aug 1;4:72.

Koob GF. Drug addiction: hyperkatifeia/negative reinforcement as a framework for medications development. Pharmacol Rev. 2021 Jan;73(1):163–201.

Koob GF, Bloom FE. Corticotropin-releasing factor and behavior. Fed Proc. 1985 Jan;44(1 Pt 2):259–263.

Koob GF, Buck CL, Cohen A, Edwards S, Park PE, Schlosburg JE, et al. Addiction as a stress surfeit disorder. Neuropharmacology. 2014 Jan;76 Pt B:370–382.

Koob GF, Le Moal M. Drug abuse: hedonic homeostatic dysregulation. Science. 1997 Oct 3;278(5335):52–58.

Koob GF, Le Moal M. Addiction and the brain antireward system. Annu Rev Psychol. 2008;59:29–53.

Koob GF, Schulkin J. Addiction and stress: An allostatic view. Neurosci Biobehav Rev. 2019;106:245–262.

Koob GF, Volkow ND. Neurocircuitry of addiction. Neuropsychopharmacology. 2010 Jan;35(1):217–238.

Koob GF, Volkow ND. Neurobiology of addiction: a neurocircuitry analysis. Lancet Psychiatry. 2016 Aug;3(8):760–773.

Krahn DD, Gosnell BA, Grace M, Levine AS. CRF antagonist partially reverses CRF- and stress-induced effects on feeding. Brain Res Bull. 1986 Sep;17(3):285–289.

Krause M, German PW, Taha SA, Fields HL. A pause in nucleus accumbens neuron firing is required to initiate and maintain feeding. J Neurosci. 2010 Mar 31;30(13):4746–4756.

Kwako LE, Spagnolo PA, Schwandt ML, Thorsell A, George DT, Momenan R, et al. The corticotropin releasing hormone-1 (CRH1) receptor antagonist pexacerfont in alcohol dependence: a randomized controlled experimental medicine study. Neuropsychopharmacology. 2015 Mar 13;40(5):1053–1063.

Larimer ME, Palmer RS, Marlatt GA. Relapse prevention. An overview of Marlatt's cognitive-behavioral model. Alcohol Res Health. 1999;23(2):151–160.

Ledoux J. Emotion and the limbic system concept. Concepts in neuroscience. 1991;

LeDoux JE. Emotional memory systems in the brain. Behav Brain Res. 1993 Dec 20;58(1-2):69–79.

Lee S-H, Govindaiah G, Cox CL. Selective excitatory actions of DNQX and CNQX in rat thalamic neurons. J Neurophysiol. 2010 Apr;103(4):1728–1734.

Lemos JC, Alvarez VA. The upside of stress: a mechanism for the positive motivational role of corticotropin releasing factor. Neuropsychopharmacology. 2020;45(1):219–220.

Lemos JC, Shin JH, Alvarez VA. Striatal cholinergic interneurons are a novel target of corticotropin releasing factor. J Neurosci. 2019 Jul 17;39(29):5647–5661.

Lemos JC, Wanat MJ, Smith JS, Reyes BAS, Hollon NG, Van Bockstaele EJ, et al. Severe stress switches CRF action in the nucleus accumbens from appetitive to aversive. Nature. 2012 Oct 18;490(7420):402–406.

Lex A, Hauber W. Dopamine D1 and D2 receptors in the nucleus accumbens core and shell mediate Pavlovian-instrumental transfer. Learn Mem. 2008 Jul 14;15(7):483–491.

Lim MM, Liu Y, Ryabinin AE, Bai Y, Wang Z, Young LJ. CRF receptors in the nucleus accumbens modulate partner preference in prairie voles. Horm Behav. 2007 Apr;51(4):508–515.

Linnet J, Mouridsen K, Peterson E, Møller A, Doudet DJ, Gjedde A. Striatal dopamine release codes uncertainty in pathological gambling. Psychiatry Res. 2012 Oct 30;204(1):55–60.

Ljungberg T, Apicella P, Schultz W. Responses of monkey midbrain dopamine neurons during delayed alternation performance. Brain Res. 1991 Dec 20;567(2):337–341.

Lobo MK, Covington HE, Chaudhury D, Friedman AK, Sun H, Damez-Werno D, et al. Cell type-specific loss of BDNF signaling mimics optogenetic control of cocaine reward. Science. 2010 Oct 15;330(6002):385–390.

Lu XY, Ghasemzadeh MB, Kalivas PW. Expression of D1 receptor, D2 receptor, substance P and enkephalin messenger RNAs in the neurons projecting from the nucleus accumbens. Neuroscience. 1998 Feb;82(3):767–780.

Maclean PD. Psychosomatic disease and the visceral brain; recent developments bearing on the Papez theory of emotion. Psychosom Med. 1949 Dec;11(6):338–353.

Maisto SA, O'Farrell TJ, Connors GJ, McKay JR, Pelcovits M. Alcoholics' attributions of factors affecting their relapse to drinking and reasons for terminating relapse episodes. Addict Behav. 1988 a;13(1):79–82.

Maisto SA, O'Farrell TJ, McKay JR, Connors GJ, Pelcovits M. Alcoholic and spouse concordance on attributions about relapse to drinking. J Subst Abuse Treat. 1988 b;5(3):179–181.

Makino S, Gold PW, Schulkin J. Corticosterone effects on corticotropin-releasing hormone mRNA in the central nucleus of the amygdala and the parvocellular region of the paraventricular nucleus of the hypothalamus. Brain Res. 1994 a Mar 21;640(1-2):105–112.

Makino S, Gold PW, Schulkin J. Effects of corticosterone on CRH mRNA and content in the bed nucleus of the stria terminalis; comparison with the effects in the central nucleus of the amygdala and the paraventricular nucleus of the hypothalamus. Brain Res. 1994 b Sep 19;657(1-2):141–149.

Maldonado-Irizarry CS, Swanson CJ, Kelley AE. Glutamate receptors in the nucleus accumbens shell control feeding behavior via the lateral hypothalamus. J Neurosci. 1995 Oct;15(10):6779–6788.

Malikowska-Racia N, Salat K. Recent advances in the neurobiology of posttraumatic stress disorder: A review of possible mechanisms underlying an effective pharmacotherapy. Pharmacol Res. 2019 Feb 8;142:30–49.

Manouze H, Ghestem A, Poillerat V, Bennis M, Ba-M'hamed S, Benoliel JJ, et al. Effects of single cage housing on stress, cognitive, and seizure parameters in the rat and mouse pilocarpine models of epilepsy. Eneuro. 2019 Aug 1;6(4).

Mantsch JR, Baker DA, Funk D, Lê AD, Shaham Y. Stress-Induced Reinstatement of Drug Seeking: 20 Years of Progress. Neuropsychopharmacology. 2016 Jan;41(1):335–356.

McEwen BS, Akil H. Revisiting the stress concept: implications for affective disorders. J Neurosci. 2020 Jan 2;40(1):12–21.

Mendrek A, Blaha CD, Phillips AG. Pre-exposure of rats to amphetamine sensitizes self-administration of this drug under a progressive ratio schedule. Psychopharmacology. 1998 Feb;135(4):416–422.

Menuz K, Stroud RM, Nicoll RA, Hays FA. TARP auxiliary subunits switch AMPA receptor antagonists into partial agonists. Science. 2007 Nov 2;318(5851):815–817.

Merali Z, McIntosh J, Anisman H. Anticipatory cues differentially provoke in vivo peptidergic and monoaminergic release at the medial prefrontal cortex. Neuropsychopharmacology. 2004 Aug;29(8):1409–1418.

Merali Z, McIntosh J, Kent P, Michaud D, Anisman H. Aversive and appetitive events evoke the release of corticotropin-releasing hormone and bombesin-like peptides at the central nucleus of the amygdala. J Neurosci. 1998 Jun 15;18(12):4758–4766.

Merchenthaler I. Corticotropin releasing factor (CRF)-like immunoreactivity in the rat central nervous system. Extrahypothalamic distribution. Peptides. 1984 Jan;5:53–69.

Merchenthaler I, Vigh S, Schally AV, Stumpf WE, Arimura A. Immunocytochemical localization of corticotropin releasing factor (CRF)-like immunoreactivity in the thalamus of the rat. Brain Res. 1984 Dec 3;323(1):119–122.

Meredith GE, Baldo BA, Andrezjewski ME, Kelley AE. The structural basis for mapping behavior onto the ventral striatum and its subdivisions. Brain Struct Funct. 2008 Sep 1;213(1-2):17–27.

Meredith GE, Blank B, Groenewegen HJ. The distribution and compartmental organization of the cholinergic neurons in nucleus accumbens of the rat. Neuroscience. 1989;31(2):327–345.

Merlo Pich E, Lorang M, Yeganeh M, Rodriguez de Fonseca F, Raber J, Koob GF, et al. Increase of extracellular corticotropin-releasing factor-like immunoreactivity levels in the amygdala of awake rats during restraint stress and ethanol withdrawal as measured by microdialysis. J Neurosci. 1995 Aug;15(8):5439–5447.

Miller NE. Neal E. Miller: selected papers. 1971;

Minami M. The role of the bed nucleus of the stria terminalis in pain-induced aversive motivation. Curr Opin Behav Sci. 2019 Apr;26:46–53.

Mogenson GJ, Jones DL, Yim CY. From motivation to action: functional interface between the limbic system and the motor system. Prog Neurobiol. 1980;14(2-3):69–97.

Mogenson GJ, Swanson LW, Wu M. Neural projections from nucleus accumbens to globus pallidus, substantia innominata, and lateral preoptic-lateral hypothalamic area: an anatomical and electrophysiological investigation in the rat. J Neurosci. 1983 Jan;3(1):189–202.

Mogenson GJ, Takigawa M, Robertson A, Wu M. Self-stimulation of the nucleus accumbens and ventral tegmental area of Tsai attenuated by microinjections of spiroperidol into the nucleus accumbens. Brain Res. 1979 Aug 3;171(2):247–259.

Navarro-Mateu F, Tormo MJ, Salmerón D, Vilagut G, Navarro C, Ruíz-Merino G, et al. Prevalence of Mental Disorders in the South-East of Spain, One of the European Regions Most Affected by the Economic Crisis: The Cross-Sectional PEGASUS-Murcia Project. PLoS One. 2015 Sep 22;10(9):e0137293.

O'Brien CP, Childress AR, Ehrman R, Robbins SJ. Conditioning factors in drug abuse: can they explain compulsion? J Psychopharmacol (Oxford). 1998;12(1):15–22.

O'Connor EC, Kremer Y, Lefort S, Harada M, Pascoli V, Rohner C, et al. Accumbal D1R neurons projecting to lateral hypothalamus authorize feeding. Neuron. 2015 Nov 4;88(3):553–564.

O'Dell LE, Torres OV. A mechanistic hypothesis of the factors that enhance vulnerability to nicotine use in females. Neuropharmacology. 2014 Jan;76 Pt B:566–580.

O'Donnell P, Grace AA. Synaptic interactions among excitatory afferents to nucleus accumbens neurons: hippocampal gating of prefrontal cortical input. J Neurosci. 1995 May;15(5 Pt 1):3622–3639.

O'Donnell P, Greene J, Pabello N, Lewis BL, Grace AA. Modulation of cell firing in the nucleus accumbens. Ann N Y Acad Sci. 1999 Jun 29;877:157–175.

O'Sullivan SS, Wu K, Politis M, Lawrence AD, Evans AH, Bose SK, et al. Cue-induced striatal dopamine release in Parkinson's disease-associated impulsive-compulsive behaviours. Brain. 2011 Apr;134(Pt 4):969–978.

Olive MF, Koenig HN, Nannini MA, Hodge CW. Elevated extracellular CRF levels in the bed nucleus of the stria terminalis during ethanol withdrawal and reduction by subsequent ethanol intake. Pharmacol Biochem Behav. 2002 May;72(1-2):213–220.

Olney JJ, Warlow SM, Naffziger EE, Berridge KC. Current perspectives on incentive salience and applications to clinical disorders. Curr Opin Behav Sci. 2018 Aug;22:59–69.

Owings DH, Coss RG. Snake mobbing by california ground squirrels: adaptive variation and ontogeny. Behaviour. 1977 Jan 1;62(1):50–68.

Papasava M, Singer G. Self-administration of low-dose cocaine by rats at reduced and recovered body weight. Psychopharmacology. 1985;85(4):419–425.

Papez JW. A proposed mechanism of emotion. 1937. J Neuropsychiatry Clin Neurosci. 1995;7(1):103–112.

Park PE, Vendruscolo LF, Schlosburg JE, Edwards S, Schulteis G, Koob GF. Corticotropin-releasing factor (CRF) and α 2 adrenergic receptors mediate heroin withdrawal-potentiated startle in rats. Int J Neuropsychopharmacol. 2013 Sep;16(8):1867–1875.

Parkinson JA, Olmstead MC, Burns LH, Robbins TW, Everitt BJ. Dissociation in effects of lesions of the nucleus accumbens core and shell on appetitive pavlovian approach

behavior and the potentiation of conditioned reinforcement and locomotor activity by D-amphetamine. J Neurosci. 1999 Mar 15;19(6):2401–2411.

Partridge JG, Forcelli PA, Luo R, Cashdan JM, Schulkin J, Valentino RJ, et al. Stress increases GABAergic neurotransmission in CRF neurons of the central amygdala and bed nucleus stria terminalis. Neuropharmacology. 2016 Mar 22;107:239–250.

Paxinos G, Watson C. The rat brain in stereotaxic coordinates, Ed 6. Amsterdam: Academic. 2007;

Peciña S, Berridge KC. Opioid site in nucleus accumbens shell mediates eating and hedonic "liking" for food: map based on microinjection Fos plumes. Brain Res. 2000 Apr 28;863(1-2):71–86.

Peciña S, Berridge KC. Hedonic hot spot in nucleus accumbens shell: where do mu-opioids cause increased hedonic impact of sweetness? J Neurosci. 2005 Dec 14;25(50):11777–11786.

Peciña S, Schulkin J, Berridge KC. Nucleus accumbens corticotropin-releasing factor increases cue-triggered motivation for sucrose reward: paradoxical positive incentive effects in stress? BMC Biol. 2006 Apr 13;4:8.

Peng J, Long B, Yuan J, Peng X, Ni H, Li X, et al. A quantitative analysis of the distribution of CRH neurons in whole mouse brain. Front Neuroanat. 2017 Jul 25;11:63.

Pennartz CM, Groenewegen HJ, Lopes da Silva FH. The nucleus accumbens as a complex of functionally distinct neuronal ensembles: an integration of behavioural, electrophysiological and anatomical data. Prog Neurobiol. 1994 Apr;42(6):719–761.

Pfaus JG, Damsma G, Nomikos GG, Wenkstern DG, Blaha CD, Phillips AG, et al. Sexual behavior enhances central dopamine transmission in the male rat. Brain Res. 1990 Oct 22;530(2):345–348.

Phillips AG. Brain reward circuitry: a case for separate systems. Brain Res Bull. 1984 Feb;12(2):195–201.

Piccin A, Contarino A. Sex-linked roles of the CRF1 and the CRF2 receptor in social behavior. J Neurosci Res. 2020 May 29;98(8):1561–1574.

Pomrenze MB, Giovanetti SM, Maiya R, Gordon AG, Kreeger LJ, Messing RO. Dissecting the Roles of GABA and Neuropeptides from Rat Central Amygdala CRF Neurons in Anxiety and Fear Learning. Cell Rep. 2019 a Oct 1;29(1):13–21.e4.

Pomrenze MB, Millan EZ, Hopf FW, Keiflin R, Maiya R, Blasio A, et al. A transgenic rat for investigating the anatomy and function of corticotrophin releasing factor circuits. Front Neurosci. 2015 Dec 24;9:487.

Pomrenze MB, Tovar-Diaz J, Blasio A, Maiya R, Giovanetti SM, Lei K, et al. A corticotropin releasing factor network in the extended amygdala for anxiety. J Neurosci. 2019 b Feb 6;39(6):1030–1043.

Ray NJ, Miyasaki JM, Zurowski M, Ko JH, Cho SS, Pellecchia G, et al. Extrastriatal dopaminergic abnormalities of DA homeostasis in Parkinson's patients with medication-induced pathological gambling: a [11C] FLB-457 and PET study. Neurobiol Dis. 2012 Dec;48(3):519–525.

Van Ree JM, Otte AP. Effects of (Des-Tyr1)-gamma-endorphin and alpha-endorphin as compared to haloperidol and amphetamine on nucleus accumbens self-stimulation. Neuropharmacology. 1980 May;19(5):429–434.

Reed SJ, Lafferty CK, Mendoza JA, Yang AK, Davidson TJ, Grosenick L, et al. Coordinated reductions in excitatory input to the nucleus accumbens underlie food consumption. Neuron. 2018 Sep 19;99(6):1260–1273.e4.

Refojo D, Schweizer M, Kuehne C, Ehrenberg S, Thoeringer C, Vogl AM, et al. Glutamatergic and dopaminergic neurons mediate anxiogenic and anxiolytic effects of CRHR1. Science. 2011 Sep 30;333(6051):1903–1907.

Reyes CD, Pagano ME, Ronis RJ. The Impact of Stressful Life Events on Alcohol Relapse: Findings from the Collaborative Longitudinal Personality Disorders Study. J Dual Diagn. 2009 Apr 1;5(2):226–232.

Reynolds SM, Berridge KC. Fear and feeding in the nucleus accumbens shell: rostrocaudal segregation of GABA-elicited defensive behavior versus eating behavior. J Neurosci. 2001 May 1;21(9):3261–3270.

Reynolds SM, Berridge KC. Positive and negative motivation in nucleus accumbens shell: bivalent rostrocaudal gradients for GABA-elicited eating, taste "liking"/"disliking" reactions, place preference/avoidance, and fear. J Neurosci. 2002 Aug 15;22(16):7308–7320.

Reynolds SM, Berridge KC. Glutamate motivational ensembles in nucleus accumbens: rostrocaudal shell gradients of fear and feeding. Eur J Neurosci. 2003 May 1;17(10):2187–2200.

Reynolds SM, Berridge KC. Emotional environments retune the valence of appetitive versus fearful functions in nucleus accumbens. Nat Neurosci. 2008 Apr;11(4):423–425.

Richard JM, Berridge KC. Metabotropic glutamate receptor blockade in nucleus accumbens shell shifts affective valence towards fear and disgust. Eur J Neurosci. 2011 a Feb;33(4):736–747.

Richard JM, Berridge KC. Nucleus accumbens dopamine/glutamate interaction switches modes to generate desire versus dread: D(1) alone for appetitive eating but D(1) and D(2) together for fear. J Neurosci. 2011 b Sep 7;31(36):12866–12879.

Richard JM, Berridge KC. Prefrontal cortex modulates desire and dread generated by nucleus accumbens glutamate disruption. Biol Psychiatry. 2013 Feb 15;73(4):360–370.

Richard JM, Castro DC, Difeliceantonio AG, Robinson MJF, Berridge KC. Mapping brain circuits of reward and motivation: in the footsteps of Ann Kelley. Neurosci Biobehav Rev. 2013 a Nov;37(9 Pt A):1919–1931.

Richard JM, Plawecki AM, Berridge KC. Nucleus accumbens GABAergic inhibition generates intense eating and fear that resists environmental retuning and needs no local dopamine. Eur J Neurosci. 2013 b Jun;37(11):1789–1802.

Rinker JA, Marshall SA, Mazzone CM, Lowery-Gionta EG, Gulati V, Pleil KE, et al. Extended Amygdala to Ventral Tegmental Area Corticotropin-Releasing Factor Circuit Controls Binge Ethanol Intake. Biol Psychiatry. 2017 Jun 1;81(11):930–940.

Roberto M, Spierling SR, Kirson D, Zorrilla EP. Corticotropin-Releasing Factor (CRF) and Addictive Behaviors. Int Rev Neurobiol. 2017 Aug 7;136:5–51.

Robinson MJF, Fischer AM, Ahuja A, Lesser EN, Maniates H. Roles of "wanting" and "liking" in motivating behavior: gambling, food, and drug addictions. Current topics in behavioral neurosciences. 2016;27:105–136.

Robinson MJF, Warlow SM, Berridge KC. Optogenetic excitation of central amygdala amplifies and narrows incentive motivation to pursue one reward above another. J Neurosci. 2014 Dec 10;34(50):16567–16580.

Robinson TE, Berridge KC. The neural basis of drug craving: an incentive-sensitization theory of addiction. Brain Res Brain Res Rev. 1993 Dec;18(3):247–291.

Rodaros D, Caruana DA, Amir S, Stewart J. Corticotropin-releasing factor projections from limbic forebrain and paraventricular nucleus of the hypothalamus to the region of the ventral tegmental area. Neuroscience. 2007 Nov 30;150(1):8–13.

Roitman MF, Wheeler RA, Carelli RM. Nucleus accumbens neurons are innately tuned for rewarding and aversive taste stimuli, encode their predictors, and are linked to motor output. Neuron. 2005 Feb 17;45(4):587–597.

Roitman MF, Wheeler RA, Tiesinga PHE, Roitman JD, Carelli RM. Hedonic and nucleus accumbens neural responses to a natural reward are regulated by aversive conditioning. Learn Mem. 2010 Nov;17(11):539–546.

Roitman MF, Wheeler RA, Wightman RM, Carelli RM. Real-time chemical responses in the nucleus accumbens differentiate rewarding and aversive stimuli. Nat Neurosci. 2008 Dec;11(12):1376–1377.

Rolls ET. Contrasting effects of hypothalamic and nucleus accumbens septi self-stimulation on brain stem single unit activity and cortical arousal. Brain Res. 1971 Aug 20;31(2):275–285.

Rosse RB, Fay-McCarthy M, Collins JP, Alim TN, Deutsch SI. The relationship between cocaine-induced paranoia and compulsive foraging: a preliminary report. Addiction. 1994 Sep;89(9):1097–1104.

Rosse RB, Fay-McCarthy M, Collins JP, Risher-Flowers D, Alim TN, Deutsch SI. Transient compulsive foraging behavior associated with crack cocaine use. Am J Psychiatry. 1993 Jan;150(1):155–156.

Rougé-Pont F, Piazza PV, Kharouby M, Le Moal M, Simon H. Higher and longer stress-induced increase in dopamine concentrations in the nucleus accumbens of animals predisposed to amphetamine self-administration. A microdialysis study. Brain Res. 1993 Jan 29;602(1):169–174.

Sahuque LL, Kullberg EF, Mcgeehan AJ, Kinder JR, Hicks MP, Blanton MG, et al. Anxiogenic and aversive effects of corticotropin-releasing factor (CRF) in the bed nucleus of the stria terminalis in the rat: role of CRF receptor subtypes. Psychopharmacology. 2006 May;186(1):122–132.

Salvatore M, Wiersielis KR, Luz S, Waxler DE, Bhatnagar S, Bangasser DA. Sex differences in circuits activated by corticotropin releasing factor in rats. Horm Behav. 2018;97:145–153.

Schmidt HD, Anderson SM, Pierce RC. Stimulation of D1-like or D2 dopamine receptors in the shell, but not the core, of the nucleus accumbens reinstates cocaine-seeking behaviour in the rat. Eur J Neurosci. 2006 Jan;23(1):219–228.

Schulkin J. The CRF Signal: Uncovering an Information Molecule. Oxford University Press; 2017.

Schwandt ML, Cortes CR, Kwako LE, George DT, Momenan R, Sinha R, et al. The CRF1 Antagonist Verucerfont in Anxious Alcohol-Dependent Women: Translation of Neuroendocrine, But not of Anti-Craving Effects. Neuropsychopharmacology. 2016 Apr 25;41(12):2818–2829.

Shaham Y, de Wit H. Lost in translation: CRF1 receptor antagonists and addiction treatment. Neuropsychopharmacology. 2016;41(12):2795–2797.

Shaham Y, Funk D, Erb S, Brown TJ, Walker CD, Stewart J. Corticotropin-releasing factor, but not corticosterone, is involved in stress-induced relapse to heroin-seeking in rats. J Neurosci. 1997 Apr 1;17(7):2605–2614.

Shaham Y, Stewart J. Stress reinstates heroin-seeking in drug-free animals: an effect mimicking heroin, not withdrawal. Psychopharmacology. 1995 Jun;119(3):334–341.

Shalev U, Erb S, Shaham Y. Role of CRF and other neuropeptides in stress-induced reinstatement of drug seeking. Brain Res. 2010 Feb 16;1314:15–28.

Shimada S, Inagaki S, Kubota Y, Ogawa N, Shibasaki T, Takagi H. Coexistence of peptides (corticotropin releasing factor/neurotensin and substance P/somatostatin) in the bed nucleus of the stria terminalis and central amygdaloid nucleus of the rat. Neuroscience. 1989;30(2):377–383.

Simms JA, Nielsen CK, Li R, Bartlett SE. Intermittent access ethanol consumption dysregulates CRF function in the hypothalamus and is attenuated by the CRF-R1 antagonist, CP-376395. Addict Biol. 2014 Jul;19(4):606–611.

Smith KS, Berridge KC, Aldridge JW. Disentangling pleasure from incentive salience and learning signals in brain reward circuitry. Proc Natl Acad Sci USA. 2011 Jul 5;108(27):E255–64.

Soares-Cunha C, Coimbra B, David-Pereira A, Borges S, Pinto L, Costa P, et al. Activation of D2 dopamine receptor-expressing neurons in the nucleus accumbens increases motivation. Nat Commun. 2016 Jun 23;7:11829.

Solomon RL. The opponent-process theory of acquired motivation: the costs of pleasure and the benefits of pain. Am Psychol. 1980 Aug;35(8):691–712.

Solomon RL, Corbit JD. An opponent-process theory of motivation. The American Economic Review. 1978;

Spierling SR, Zorrilla EP. Don't stress about CRF: assessing the translational failures of CRF1antagonists. Psychopharmacology. 2017 Mar 7;234(9-10):1467–1481.

Stewart J. Pathways to relapse: the neurobiology of drug- and stress-induced relapse to drug-taking. J Psychiatry Neurosci. 2000 Mar;25(2):125–136.

Stice E, Yokum S, Burger K, Epstein L, Smolen A. Multilocus genetic composite reflecting dopamine signaling capacity predicts reward circuitry responsivity. J Neurosci. 2012 Jul 18;32(29):10093–10100.

Stratford TR. Activation of feeding-related neural circuitry after unilateral injections of muscimol into the nucleus accumbens shell. Brain Res. 2005 Jun 28;1048(1-2):241–250.

Stratford TR, Kelley AE. GABA in the nucleus accumbens shell participates in the central regulation of feeding behavior. J Neurosci. 1997 Jun 1;17(11):4434–4440.

Stratford TR, Wirtshafter D. Evidence that the nucleus accumbens shell, ventral pallidum, and lateral hypothalamus are components of a lateralized feeding circuit. Behav Brain Res. 2012 Jan 15;226(2):548–554.

Sureshkumar K, Kailash S, Dalal PK, Reddy MM, Sinha PK. Psychosocial Factors Associated with Relapse in Patients with Alcohol Dependence. Indian J Psychol Med. 2017 Jun;39(3):312–315.

Sutton RE, Koob GF, Le Moal M, Rivier J, Vale W. Corticotropin releasing factor produces behavioural activation in rats. Nature. 1982 May 27;297(5864):331–333.

Swanson LW. Anatomy of the soul as reflected in the cerebral hemispheres: neural circuits underlying voluntary control of basic motivated behaviors. J Comp Neurol. 2005 Dec 5;493(1):122–131.

Swanson LW, Sawchenko PE, Rivier J, Vale WW. Organization of ovine corticotropin-releasing factor immunoreactive cells and fibers in the rat brain: an immunohistochemical study. Neuroendocrinology. 1983;36(3):165–186.

Swanson LW, Simmons DM. Differential steroid hormone and neural influences on peptide mRNA levels in CRH cells of the paraventricular nucleus: a hybridization histochemical study in the rat. J Comp Neurol. 1989 Jul 22;285(4):413–435.

Swendsen JD, Tennen H, Carney MA, Affleck G, Willard A, Hromi A. Mood and alcohol consumption: an experience sampling test of the self-medication hypothesis. J Abnorm Psychol. 2000 May;109(2):198–204.

Taha SA, Norsted E, Lee LS, Lang PD, Lee BS, Woolley JD, et al. Endogenous opioids encode relative taste preference. Eur J Neurosci. 2006 Aug 21;24(4):1220–1226.

Takahashi D, Asaoka Y, Kimura K, Hara R, Arakaki S, Sakasai K, et al. Tonic suppression of the mesolimbic dopaminergic system by enhanced corticotropin-releasing factor signaling within the bed nucleus of the stria terminalis in chronic pain model rats. J Neurosci. 2019 Aug 26;

Tarazi FI, Campbell A, Baldessarini RJ. Effects of hippocampal lesions on striatolimbic ionotropic glutamatergic receptors. Neurosci Lett. 1998 a Jun 26;250(1):13–16.

Tarazi FI, Campbell A, Yeghiayan SK, Baldessarini RJ. Localization of ionotropic glutamate receptors in caudate-putamen and nucleus accumbens septi of rat brain: comparison of NMDA, AMPA, and kainate receptors. Synapse. 1998 b Oct;30(2):227–235.

Thompson RH, Swanson LW. Hypothesis-driven structural connectivity analysis supports network over hierarchical model of brain architecture. Proc Natl Acad Sci USA. 2010 Aug 24;107(34):15235–15239.

Tindell AJ, Smith KS, Berridge KC, Aldridge JW. Dynamic computation of incentive salience: “wanting” what was never “liked”. J Neurosci. 2009 Sep 30;29(39):12220–12228.

Tollefson S, Himes M, Narendran R. Imaging corticotropin-releasing-factor and nociceptin in addiction and PTSD models. Int Rev Psychiatry. 2017 Dec 12;29(6):567–579.

Torres OV, Pipkin JA, Ferree P, Carcoba LM, O’Dell LE. Nicotine withdrawal increases stress-associated genes in the nucleus accumbens of female rats in a hormone-dependent manner. Nicotine Tob Res. 2015 Apr;17(4):422–430.

Torruella-Suárez ML, Vandenberg JR, Cogan ES, Tipton GJ, Teklezghi A, Dange K, et al. Manipulations of Central Amygdala Neurotensin Neurons Alter the Consumption of Ethanol and Sweet Fluids in Mice. J Neurosci. 2020 Jan 15;40(3):632–647.

Tran L, Schulkin J, Greenwood-Van Meerveld B. Importance of CRF receptor-mediated mechanisms of the bed nucleus of the stria terminalis in the processing of anxiety and pain. Neuropsychopharmacology. 2014 Oct;39(11):2633–2645.

Treit D, Pinel JP, Fibiger HC. Conditioned defensive burying: a new paradigm for the study of anxiolytic agents. Pharmacol Biochem Behav. 1981 Oct;15(4):619–626.

Trouche S, Koren V, Doig NM, Ellender TJ, El-Gaby M, Lopes-Dos-Santos V, et al. A Hippocampus-Accumbens Tripartite Neuronal Motif Guides Appetitive Memory in Space. Cell. 2019 Mar 7;176(6):1393–1406.e16.

Uchida K, Otsuka H, Morishita M, Tsukahara S, Sato T, Sakimura K, et al. Female-biased sexual dimorphism of corticotropin-releasing factor neurons in the bed nucleus of the stria terminalis. Biol Sex Differ. 2019 Jan 28;10(1):6.

Uribe KP, Correa VL, Pinales BE, Flores RJ, Cruz B, Shan Z, et al. Overexpression of corticotropin-releasing factor in the nucleus accumbens enhances the reinforcing effects of nicotine in intact female versus male and ovariectomized female rats. Neuropsychopharmacology. 2020;45(2):394–403.

Usuda I, Tanaka K, Chiba T. Efferent projections of the nucleus accumbens in the rat with special reference to subdivision of the nucleus: biotinylated dextran amine study. Brain Res. 1998 Jun 22;797(1):73–93.

Vale W, Spiess J, Rivier C, Rivier J. Characterization of a 41-residue ovine hypothalamic peptide that stimulates secretion of corticotropin and beta-endorphin. Science. 1981 Sep 18;213(4514):1394–1397.

Valentino RJ, Van Bockstaele E, Bangasser D. Sex-specific cell signaling: the corticotropin-releasing factor receptor model. Trends Pharmacol Sci. 2013 Aug;34(8):437–444.

Vela L, Martínez Castrillo JC, García Ruiz P, Gasca-Salas C, Macías Macías Y, Pérez Fernández E, et al. The high prevalence of impulse control behaviors in patients with early-onset Parkinson's disease: A cross-sectional multicenter study. J Neurol Sci. 2016 Sep 15;368:150–154.

Ventura-Silva AP, Borges S, Sousa N, Rodrigues AJ, Pêgo JM. Amygdalar corticotropin-releasing factor mediates stress-induced anxiety. Brain Res. 2020 Feb 15;1729:146622.

Vezina P, Lorrain DS, Arnold GM, Austin JD, Suto N. Sensitization of midbrain dopamine neuron reactivity promotes the pursuit of amphetamine. J Neurosci. 2002 Jun 1;22(11):4654–4662.

Voon V, Napier TC, Frank MJ, Sgambato-Faure V, Grace AA, Rodriguez-Oroz M, et al. Impulse control disorders and levodopa-induced dyskinesias in Parkinson's disease: an update. Lancet Neurol. 2017 Feb 15;16(3):238–250.

Voorn P, Gerfen CR, Groenewegen HJ. Compartmental organization of the ventral striatum of the rat: immunohistochemical distribution of enkephalin, substance P, dopamine, and calcium-binding protein. J Comp Neurol. 1989 Nov 8;289(2):189–201.

Voorn P, Jorritsma-Byham B, Van Dijk C, Buijs RM. The dopaminergic innervation of the ventral striatum in the rat: a light- and electron-microscopical study with antibodies against dopamine. J Comp Neurol. 1986 Sep 1;251(1):84–99.

Vranjkovic O, Van Newenhizen EC, Nordness ME, Blacktop JM, Urbanik LA, Mathy JC, et al. Enhanced CRFR1-Dependent Regulation of a Ventral Tegmental Area to Prelimbic Cortex Projection Establishes Susceptibility to Stress-Induced Cocaine Seeking. J Neurosci. 2018 Dec 12;38(50):10657–10671.

Wanat MJ, Hopf FW, Stuber GD, Phillips PEM, Bonci A. Corticotropin-releasing factor increases mouse ventral tegmental area dopamine neuron firing through a protein kinase C-dependent enhancement of Ih. J Physiol (Lond). 2008 Apr 15;586(8):2157–2170.

Wang B, Shaham Y, Zitzman D, Azari S, Wise RA, You Z-B. Cocaine experience establishes control of midbrain glutamate and dopamine by corticotropin-releasing factor: a role in stress-induced relapse to drug seeking. J Neurosci. 2005 Jun 1;25(22):5389–5396.

Wang F, Flanagan J, Su N, Wang L-C, Bui S, Nielson A, et al. RNAscope: a novel in situ RNA analysis platform for formalin-fixed, paraffin-embedded tissues. J Mol Diagn. 2012 Jan;14(1):22–29.

Wang KS, Smith DV, Delgado MR. Using fMRI to study reward processing in humans: past, present, and future. J Neurophysiol. 2016 Mar;115(3):1664–1678.

Warlow SM, Naffziger EE, Berridge KC. The central amygdala recruits mesocorticolimbic circuitry for pursuit of reward or pain. Nat Commun. 2020 Jun 1;11(1):2716.

Warlow SM, Robinson MJF, Berridge KC. Optogenetic central amygdala stimulation intensifies and narrows motivation for cocaine. J Neurosci. 2017 Aug 30;37(35):8330–8348.

Warren N, O'Gorman C, Lehn A, Siskind D. Dopamine dysregulation syndrome in Parkinson's disease: a systematic review of published cases. J Neurol Neurosurg Psychiatry. 2017 Oct 10;88(12):1060–1064.

Weathington JM, Hamki A, Cooke BM. Sex- and region-specific pubertal maturation of the corticotropin-releasing factor receptor system in the rat. J Comp Neurol. 2014 Apr 15;522(6):1284–1298.

Weintraub D, Koester J, Potenza MN, Siderowf AD, Stacy M, Voon V, et al. Impulse control disorders in Parkinson disease: a cross-sectional study of 3090 patients. Arch Neurol. 2010 May;67(5):589–595.

Wheeler RA, Twining RC, Jones JL, Slater JM, Grigson PS, Carelli RM. Behavioral and electrophysiological indices of negative affect predict cocaine self-administration. Neuron. 2008 Mar 13;57(5):774–785.

Wiersielis KR, Wicks B, Simko H, Cohen SR, Khantsis S, Baksh N, et al. Sex differences in corticotropin releasing factor-evoked behavior and activated networks. Psychoneuroendocrinology. 2016 Jul 28;73:204–216.

Záborszky L, Alheid GF, Beinfeld MC, Eiden LE, Heimer L, Palkovits M. Cholecystokinin innervation of the ventral striatum: a morphological and radioimmunological study. Neuroscience. 1985 Feb;14(2):427–453.

Zahm DS. An electron microscopic morphometric comparison of tyrosine hydroxylase immunoreactive innervation in the neostriatum and the nucleus accumbens core and shell. Brain Res. 1992 Mar 20;575(2):341–346.

Zahm DS. The evolving theory of basal forebrain functional-anatomical “macrosystems”. Neurosci Biobehav Rev. 2006;30(2):148–172.

Zahm DS, Heimer L. Two transpallidal pathways originating in the rat nucleus accumbens. J Comp Neurol. 1990 Dec 15;302(3):437–446.

Zahm DS, Parsley KP, Schwartz ZM, Cheng AY. On lateral septum-like characteristics of outputs from the accumbal hedonic “hotspot” of Peciña and Berridge with commentary on the transitional nature of basal forebrain “boundaries”. J Comp Neurol. 2013 Jan 1;521(1):50–68.

Zeeb FD, Li Z, Fisher DC, Zack MH, Fletcher PJ. Uncertainty exposure causes behavioural sensitization and increases risky decision-making in male rats: toward modelling gambling disorder. J Psychiatry Neurosci. 2017 Nov;42(6):404–413.

Zhou L, Furuta T, Kaneko T. Chemical organization of projection neurons in the rat accumbens nucleus and olfactory tubercle. Neuroscience. 2003;120(3):783–798.

Zorrilla EP, Koob GF. The therapeutic potential of CRF1 antagonists for anxiety. Expert Opin Investig Drugs. 2004 Jul;13(7):799–828.

Zorrilla EP, Logrip ML, Koob GF. Corticotropin releasing factor: a key role in the neurobiology of addiction. Front Neuroendocrinol. 2014 Apr;35(2):234–244.